

**Part I: NUMERICAL EXPERIMENTS FOR THE COMPUTATION
OF INVARIANT CURVES IN DYNAMICAL SYSTEMS**

**PART II: NUMERICAL CONVERGENCE RESULTS FOR A ONE-
DIMENSIONAL STEFAN PROBLEM**

Thesis by
Anne Chantal Morlet

In Partial Fulfillment of the Requirements
for the Degree of
Doctor of Philosophy

California Institute of Technology
Pasadena, California

1990
(Submitted February 8, 1990)

ACKNOWLEDGMENTS

I want to thank my thesis advisor Professor Jens Lorenz for his support, for his guidance and his numerous suggestions during my stay at Caltech. His challenging and great ideas helped me to get my projects moving forward.

I am very grateful to Dr. David Brown for suggesting the very interesting problem on dendritic growth to me and for all the helpful discussions we have had. I am very thankful for the time he spent reading this manuscript and improving the English.

I thank Professor Heinz-Otto Kreiss for all of his remarks and comments when I worked on the dendrite growth problem. Without his help, I would have been unable to carry out the analysis of the problem.

I thank all the applied mathematicians from the Computer Research and Applications Group at Los Alamos National Laboratory for the interesting discussions we have had and for financial support in the form of Graduate Research Assitanship during the summers 1987, 1988, and 1989.

ABSTRACT

Part I

We derive a model equation for the linearized equation of an invariant curve for a Poincaré map. We discretize the model equation with a second-order and third-order finite difference schemes, and with a cubic spline interpolation scheme. We also approximate the solution of the model equation with a truncated Fourier expansion. We derive error estimates for the second-order and third-order finite difference schemes and for the cubic spline interpolation scheme. We numerically implement the four schemes we consider and plot some error curves.

Part II

We show for a one-dimensional Stefan problem, that the numerical solution converges to the solution of the continuous equations in the limit of zero meshsize and timestep. We discretize the continuous equations with a second-order finite difference scheme in space and Crank-Nicholson scheme in time. We derive error equations and we use L_2 estimates to bound the error in terms of the truncation errors of the finite difference scheme. We confirm the analysis with numerical computations. We numerically prove that we have fourth-order convergence in space if we discretize the partial differential equations with a fourth-order scheme in space.

TABLE OF CONTENTS

Acknowledgments	iii
Abstract	iv
Table of Figures	vii
Table of Tables	xv

Part I

I Introduction	3
II The Linear Problem Analytical Results	7
II.1 Existence and Uniqueness of the Solution	8
II.2 Regularity of the Solution	9
II.3 Error Analysis	11
II.3.1 Second-Order Finite Difference	11
II.3.2 Third-Order Finite Difference	14
II.3.3 Spline Interpolant	19
II.3.4 Fourier Method	29
III The Linear Problem Numerical Results	33
III.1 The Second-Order Finite Difference	34
III.2 The Third-Order Finite Difference	50
III.3 Spline Interpolation Scheme	56
III.4 Fourier Method	70
III.5 Comparison of the second-order finite difference, of the third-order finite difference, and of cubic spline interpolation schemes	74
IV Conclusions and Discussion	81
References	85

Part II

I On Some Convergence Results for a One-Dimensional Stefan Problem	88
I.1 Introduction	88
I.2 The Discrete Equations	94
I.3 Estimates for the Continuous Problem - Existence and Uniqueness of the Solution of the Continuous Problem	98

I.4 Estimates for the Linearized Continuous Error Equation	113
I.5 Estimates for the Linearized Semi-Discrete Error Equations	118
I.6 Estimates for the Linearized Discrete Error Equations	131
I.7 Estimates for the Discrete Equations	144
I.8 Numerical Example	153
I.9 Conclusion and Discussion	162
AI Basic Results on L_2 Estimates for Continuous Equations	165
AII Basic Results on L_2 Estimates for Semi-Discrete Equations	169
AIII Generalization to the Two-Phase One-Dimensional Stefan Problem	173
AIV Generalization to a Centered Fourth-Order Finite Difference Scheme in Space	204
AV Numerical Example: The Stefan Problem Solved in a Fixed Frame of Reference	211
References	220

TABLE OF FIGURES

Part I

III.1.1 Numerical solution of $R(x) = H(x)(R \circ \alpha)(x) + Q(x)$, discretized with 40 meshpoints and a second-order finite difference scheme. $H = .1$, $\alpha = x + .11$, and $Q = 1 + .5 \sin(2\pi x) + .5 \sin(4\pi x) + .5 \sin(6\pi x) + .1 \sin(10\pi x)$. . .	36
III.1.2 Numerical solution of $R(x) = H(x)(R \circ \alpha)(x) + Q(x)$, discretized with 640 meshpoints and a second-order finite difference scheme. $H = .1$, $\alpha = x + .11$, and $Q = 1 + .5 \sin(2\pi x) + .5 \sin(4\pi x) + .5 \sin(6\pi x) + .1 \sin(10\pi x)$. . .	36
III.1.3 Numerical solution of $R(x) = H(x)(R \circ \alpha)(x) + Q(x)$, discretized with 40 meshpoints and a second-order finite difference scheme. $H = .1$, $\alpha = x + .11 + .15 \sin(2\pi x)$, and $Q = 1 + .5 \sin(2\pi x) + .5 \sin(4\pi x) + .5 \sin(6\pi x) + .1 \sin(10\pi x)$	37
III.1.4 Numerical solution of $R(x) = H(x)(R \circ \alpha)(x) + Q(x)$, discretized with 640 meshpoints and a second-order finite difference scheme. $H = .1$, $\alpha = x + .11 + .15 \sin(2\pi x)$, and $Q = 1 + .5 \sin(2\pi x) + .5 \sin(4\pi x) + .5 \sin(6\pi x) + .1 \sin(10\pi x)$	37
III.1.5 Numerical solution of $R(x) = H(x)(R \circ \alpha)(x) + Q(x)$, discretized with 40 meshpoints and a second-order finite difference scheme. $H = .1$, $\alpha = x + .11 + .5 \sin(2\pi x)$, and $Q = 1 + .5 \sin(2\pi x) + .5 \sin(4\pi x) + .5 \sin(6\pi x) + .1 \sin(10\pi x)$	38
III.1.6 Numerical solution of $R(x) = H(x)(R \circ \alpha)(x) + Q(x)$, discretized with 640 meshpoints and a second-order finite difference scheme. $H = .1$, $\alpha = x + .11 + .5 \sin(2\pi x)$, and $Q = 1 + .5 \sin(2\pi x) + .5 \sin(4\pi x) + .5 \sin(6\pi x) + .1 \sin(10\pi x)$	38
III.1.7 Numerical solution of $R(x) = H(x)(R \circ \alpha)(x) + Q(x)$, discretized with 40 meshpoints and a second-order finite difference scheme. $H = .1$, $\alpha = x + .11 + .75 \sin(2\pi x)$, and $Q = 1 + .5 \sin(2\pi x) + .5 \sin(4\pi x) + .5 \sin(6\pi x) + .1 \sin(10\pi x)$	39
III.1.8 Numerical solution of $R(x) = H(x)(R \circ \alpha)(x) + Q(x)$, discretized with 640 meshpoints and a second-order finite difference scheme. $H = .1$, $\alpha = x + .11 + .75 \sin(2\pi x)$, and $Q = 1 + .5 \sin(2\pi x) + .5 \sin(4\pi x) + .5 \sin(6\pi x) + .1 \sin(10\pi x)$	39
III.1.9 Numerical solution of $R(x) = H(x)(R \circ \alpha)(x) + Q(x)$, discretized with 40 meshpoints and a second-order finite difference scheme. $H = .1$, $\alpha = x + .11 + 1.5 \sin(2\pi x)$, and $Q = 1 + .5 \sin(2\pi x) + .5 \sin(4\pi x) + .5 \sin(6\pi x) + .1 \sin(10\pi x)$	40

III.1.10 Numerical solution of $R(x) = H(x)(R \circ \alpha)(x) + Q(x)$, discretized with 640 meshpoints and a second-order finite difference scheme. $H = .1$, $\alpha = x + .11 + 1.5 \sin(2\pi x)$, and $Q = 1 + .5 \sin(2\pi x) + .5 \sin(4\pi x) + .5 \sin(6\pi x) + .1 \sin(10\pi x)$ 40

III.1.11 Numerical solution of $R(x) = H(x)(R \circ \alpha)(x) + Q(x)$, discretized with 40 meshpoints and a second-order finite difference scheme. $H = .1$, $\alpha = x + .11 + 2 \sin(2\pi x)$, and $Q = 1 + .5 \sin(2\pi x) + .5 \sin(4\pi x) + .5 \sin(6\pi x) + .1 \sin(10\pi x)$ 41

III.1.12 Numerical solution of $R(x) = H(x)(R \circ \alpha)(x) + Q(x)$, discretized with 640 meshpoints and a second-order finite difference scheme. $H = .1$, $\alpha = x + .11 + 2 \sin(2\pi x)$, and $Q = 1 + .5 \sin(2\pi x) + .5 \sin(4\pi x) + .5 \sin(6\pi x) + .1 \sin(10\pi x)$ 41

III.1.13 Numerical solution of $R(x) = H(x)(R \circ \alpha)(x) + Q(x)$, discretized with 640 meshpoints and a second-order finite difference scheme. $H = .7$, $\alpha = x + .11$, and $Q = 1 + .5 \sin(2\pi x) + .5 \sin(4\pi x) + .5 \sin(6\pi x) + .1 \sin(10\pi x)$. . . 42

III.1.14 Numerical solution of $R(x) = H(x)(R \circ \alpha)(x) + Q(x)$, discretized with 640 meshpoints and a second-order finite difference scheme. $H = .7$, $\alpha = x + .11 + .15 \sin(2\pi x)$, and $Q = 1 + .5 \sin(2\pi x) + .5 \sin(4\pi x) + .5 \sin(6\pi x) + .1 \sin(10\pi x)$ 42

III.1.15 Numerical solution of $R(x) = H(x)(R \circ \alpha)(x) + Q(x)$, discretized with 640 meshpoints and a second-order finite difference scheme. $H = .7$, $\alpha = x + .11 + .5 \sin(2\pi x)$, and $Q = 1 + .5 \sin(2\pi x) + .5 \sin(4\pi x) + .5 \sin(6\pi x) + .1 \sin(10\pi x)$ 43

III.1.16 Numerical solution of $R(x) = H(x)(R \circ \alpha)(x) + Q(x)$, discretized with 640 meshpoints and a second-order finite difference scheme. $H = .7$, $\alpha = x + .11 + .75 \sin(2\pi x)$, and $Q = 1 + .5 \sin(2\pi x) + .5 \sin(4\pi x) + .5 \sin(6\pi x) + .1 \sin(10\pi x)$ 43

III.1.17 Numerical solution of $R(x) = H(x)(R \circ \alpha)(x) + Q(x)$, discretized with 640 meshpoints and a second-order finite difference scheme. $H = .7$, $\alpha = x + .11 + 1.5 \sin(2\pi x)$, and $Q = 1 + .5 \sin(2\pi x) + .5 \sin(4\pi x) + .5 \sin(6\pi x) + .1 \sin(10\pi x)$ 44

III.1.18 Numerical solution of $R(x) = H(x)(R \circ \alpha)(x) + Q(x)$, discretized with 640 meshpoints and a second-order finite difference scheme. $H = .7$, $\alpha = x + .11 + 2 \sin(2\pi x)$, and $Q = 1 + .5 \sin(2\pi x) + .5 \sin(4\pi x) + .5 \sin(6\pi x) + .1 \sin(10\pi x)$ 44

III.1.19 The logarithm of the maximum norm of the error for different values of n , $n = 5, 10, 20, 40, 80, 120, 160, 200, 240, 280, 320, 360, 400, 440, 480, 520, 560, 600, 640, 680$, for $\alpha = x + .11 + c \sin(2\pi x)$, for $c = .001, .01, .05, .1, .14, 1/(2\pi), .5, .75, 1, 1.5, 2, 3, 4$, for $H = .1$, and for $Q = 1 + .5 \sin(2\pi x) + .5 \sin(4\pi x) + .5 \sin(6\pi x) + .1 \sin(10\pi x)$ 45

III.1.20 Log-Log plot of the maximum norm of the error vs. the number of meshpoints n , $n = 5, 10, 20, 40, 80, 120, 160, 200, 240, 280, 320, 360, 400, 440, 480$,

520, 560, 600, 640, 680, for $\alpha = x + .11 + c \sin(2\pi x)$, for $c = .001, .01, .05, .1, .14, 1/(2\pi), .5, .75, 1, 1.5, 2, 3, 4$, for $H = .1$, and for $Q = 1 + .5 \sin(2\pi x) + .5 \sin(4\pi x) + .5 \sin(6\pi x) + .1 \sin(10\pi x)$ 46

III.1.21 The logarithm of the L_2 norm of the error for different values of n , $n = 5, 10, 20, 40, 80, 120, 160, 200, 240, 280, 320, 360, 400, 440, 480, 520, 560, 600, 640, 680$, for $\alpha = x + .11 + c \sin(2\pi x)$, for $c = .001, .01, .05, .1, .14, 1/(2\pi), .5, .75, 1, 1.5, 2, 3, 4$, for $H = .1$, and for $Q = 1 + .5 \sin(2\pi x) + .5 \sin(4\pi x) + .5 \sin(6\pi x) + .1 \sin(10\pi x)$ 47

III.1.22 Log-Log plot of the L_2 norm of the error vs. the number of meshpoints n $n = 5, 10, 20, 40, 80, 120, 160, 200, 240, 280, 320, 360, 400, 440, 480, 520, 560, 600, 640, 680$, for $\alpha = x + .11 + c \sin(2\pi x)$, for $c = .001, .01, .05, .1, .14, 1/(2\pi), .5, .75, 1, 1.5, 2, 3, 4$, for $H = .1$, and for $Q = 1 + .5 \sin(2\pi x) + .5 \sin(4\pi x) + .5 \sin(6\pi x) + .1 \sin(10\pi x)$ 47

III.1.23 The logarithm of the maximum norm of the error for different values of n , $n = 5, 10, 20, 40, 80, 120, 160, 200, 240, 280, 320, 360, 400, 440, 480, 520, 560, 600, 640, 680$, for $\alpha = x + .11 + c \sin(2\pi x)$, for $c = .001, .01, .05, .1, 1/(2\pi), .25, .5, .75, 1$, for $H = .7$, and for $Q = 1 + .5 \sin(2\pi x) + .5 \sin(4\pi x) + .5 \sin(6\pi x) + .1 \sin(10\pi x)$ 48

III.1.24 Log-Log plot of the maximum norm of the error vs. the number of meshpoints n , $n = 5, 10, 20, 40, 80, 120, 160, 200, 240, 280, 320, 360, 400, 440, 480, 520, 560, 600, 640, 680$, for $\alpha = x + .11 + c \sin(2\pi x)$, for $c = .001, .01, .05, .1, 1/(2\pi), .25, .5, .75, 1$, for $H = .7$, and for $Q = 1 + .5 \sin(2\pi x) + .5 \sin(4\pi x) + .5 \sin(6\pi x) + .1 \sin(10\pi x)$ 49

III.1.25 The logarithm of L_2 norm of the error for different values of n , $n = 5, 10, 20, 40, 80, 120, 160, 200, 240, 280, 320, 360, 400, 440, 480, 520, 560, 600, 640, 680$, for $\alpha = x + .11 + c \sin(2\pi x)$, for $c = .001, .01, .05, .1, 1/(2\pi), .25, .5, .75, 1$, for $H = .7$, and for $Q = 1 + .5 \sin(2\pi x) + .5 \sin(4\pi x) + .5 \sin(6\pi x) + .1 \sin(10\pi x)$ 49

III.1.26 Log-Log plot of the L_2 norm of the error vs. the number of meshpoints n $n = 5, 10, 20, 40, 80, 120, 160, 200, 240, 280, 320, 360, 400, 440, 480, 520, 560, 600, 640, 680$, for $\alpha = x + .11 + c \sin(2\pi x)$, for $c = .001, .01, .05, .1, 1/(2\pi), .25, .5, .75, 1$, for $H = .7$, and for $Q = 1 + .5 \sin(2\pi x) + .5 \sin(4\pi x) + .5 \sin(6\pi x) + .1 \sin(10\pi x)$ 50

III.2.1 The logarithm of the maximum norm of the error for different values of n , $n = 5, 10, 20, 40, 80, 120, 160, 200, 240, 280, 320, 360, 400, 440, 480, 520, 560, 600, 640, 680$, for $\alpha = x + .11 + c \sin(2\pi x)$, for $c = .001, .01, .05, .1, .14, 1/(2\pi), .5, .75, 1, 1.5, 2, 3, 4$, for $H = .1$, and for $Q = 1 + .5 \sin(2\pi x) + .5 \sin(4\pi x) + .5 \sin(6\pi x) + .1 \sin(10\pi x)$ 51

III.2.2 Log-Log plot of the maximum norm of the error vs. the number of meshpoints n , $n = 5, 10, 20, 40, 80, 120, 160, 200, 240, 280, 320, 360, 400, 440, 480, 520, 560, 600, 640, 680$, for $\alpha = x + .11 + c \sin(2\pi x)$, for $c = .001, .01, .05, .1, .14, 1/(2\pi), .5, .75, 1, 1.5, 2, 3, 4$, for $H = .1$, and for $Q = 1 + .5 \sin(2\pi x) + .5 \sin(4\pi x) + .5 \sin(6\pi x) + .1 \sin(10\pi x)$ 51

.5 sin (4 π x) + .5 sin (6 π x) + .1 sin (10 π x) 52

III.2.3 The logarithm of the L₂ norm of the error for different values of n, n = 5, 10, 20, 40, 80, 120, 160, 200, 240, 280, 320, 360, 400, 440, 480, 520, 560, 600, 640, 680, for α = x + .11 + c sin (2 π x), for c = .001, .001, .05, .1, .14, 1/(2 π), .5, .75, 1, 1.5, 2, 3, 4, for H = .1, and for Q = 1 + .5 sin (2 π x) + .5 sin (4 π x) + .5 sin (6 π x) + .1 sin (10 π x) 53

III.2.4 Log-Log plot of the L₂ norm of the error vs. the number of meshpoints n n = 5, 10, 20, 40, 80, 120, 160, 200, 240, 280, 320, 360, 400, 440, 480, 520, 560, 600, 640, 680, for α = x + .11 + c sin (2 π x), for c = .001, .01, .05, .1, .14, 1/(2 π), .5, .75, 1, 1.5, 2, 3, 4, for H = .1, and for Q = 1 + .5 sin (2 π x) + .5 sin (4 π x) + .5 sin (6 π x) + .1 sin (10 π x) 53

III.2.5 The logarithm of the maximum norm of the error for different values of n, n = 5, 10, 20, 40, 80, 120, 160, 200, 240, 280, 320, 360, 400, 440, 480, 520, 560, 600, 640, 680, for α = x + .11 + c sin (2 π x), for c = .001, .01, .05, .1, 1/(2 π), .25, .5, .75, 1, for H = .7, and for Q = 1 + .5 sin (2 π x) + .5 sin (4 π x) + .5 sin (6 π x) + .1 sin (10 π x) 54

III.2.6 Log-Log plot of the maximum norm of the error vs. the number of meshpoints n, n = 5, 10, 20, 40, 80, 120, 160, 200, 240, 280, 320, 360, 400, 440, 480, 520, 560, 600, 640, 680, for α = x + .11 + c sin (2 π x), for c = .001, .01, .05, .1, 1/(2 π), .25, .5, .75, 1, for H = .7, and for Q = 1 + .5 sin (2 π x) + .5 sin (4 π x) + .5 sin (6 π x) + .1 sin (10 π x) 55

III.2.7 The logarithm of L₂ norm of the error for different values of n, n = 5, 10, 20, 40, 80, 120, 160, 200, 240, 280, 320, 360, 400, 440, 480, 520, 560, 600, 640 680, for α = x + .11 + c sin (2 π x), for c = .001, .01, .05, .1, 1/(2 π), .25, .5, .75, 1, for H = .7, and for Q = 1 + .5 sin (2 π x) + .5 sin (4 π x) + .5 sin (6 π x) + .1 sin (10 π x) 55

III.2.8 Log-Log plot of the L₂ norm of the error vs. the number of meshpoints n n = 5, 10, 20, 40, 80, 120, 160, 200, 240, 280, 320, 360, 400, 440, 480, 520, 560, 600, 640, 680, for α = x + .11 + c sin (2 π x), for c = .001, .01, .05, .1, 1/(2 π), .25, .5, .75, 1, for H = .7, and for Q = 1 + .5 sin (2 π x) + .5 sin (4 π x) + .5 sin (6 π x) + .1 sin (10 π x) 56

III.3.1 Numerical solution of (R ◦ α) (x) = H (x) R (x) + Q (x) discretized with 640 meshpoints and a cubic spline interpolation scheme. H = 10, α = x + .11 and Q = 1 + .5 sin (2 π x) + .5 sin (4 π x) + .5 sin (6 π x) + .1 sin (10 π x) 57

III.3.2 Numerical solution of (R ◦ α) (x) = H (x) R (x) + Q (x) discretized with 640 meshpoints and a cubic spline interpolation scheme. H = 10, α = x + .11 + .15 sin (2 π x), and Q = 1 + .5 sin (2 π x) + .5 sin (4 π x) + .5 sin (6 π x) + .1 sin (10 π x) 58

III.3.3 Numerical solution of (R ◦ α) (x) = H (x) R (x) + Q (x) discretized with 640 meshpoints and a cubic spline interpolation scheme. H = 10, α = x + .11 + .5 sin (2 π x), and Q = 1 + .5 sin (2 π x) + .5 sin (4 π x) + .5 sin (6 π x) + .1 sin (10 π x) 58

III.3.4 Numerical solution of $(R \circ \alpha)(x) = H(x) R(x) + Q(x)$ discretized with 640 meshpoints and a cubic spline interpolation scheme. $H = 10$, $\alpha = x + .11 + .75 \sin(2\pi x)$, and $Q = 1 + .5 \sin(2\pi x) + .5 \sin(4\pi x) + .5 \sin(6\pi x) + .1 \sin(10\pi x)$ 59

III.3.5 Numerical solution of $(R \circ \alpha)(x) = H(x) R(x) + Q(x)$ discretized with 640 meshpoints and a cubic spline interpolation scheme. $H = 10$, $\alpha = x + .11 + 1.5 \sin(2\pi x)$, and $Q = 1 + .5 \sin(2\pi x) + .5 \sin(4\pi x) + .5 \sin(6\pi x) + .1 \sin(10\pi x)$ 59

III.3.6 Numerical solution of $(R \circ \alpha)(x) = H(x) R(x) + Q(x)$ discretized with 640 meshpoints and a cubic spline interpolation scheme. $H = 10$, $\alpha = x + .11 + 2 \sin(2\pi x)$, and $Q = 1 + .5 \sin(2\pi x) + .5 \sin(4\pi x) + .5 \sin(6\pi x) + .1 \sin(10\pi x)$ 60

III.3.7 The logarithm of the maximum norm of the error for different values of n , $n = 5, 10, 20, 40, 80, 120, 160, 200, 240, 280, 320, 360, 400, 440, 480, 520, 560, 600, 640, 680$, for $\alpha = x + .11 + c \sin(2\pi x)$, for $c = .001, .01, .05, .1, .15, .25, .5, .75, 1, 1.25, 1.5, 1.75, 2$, for $H = 10$, and for $Q = 1 + .5 \sin(2\pi x) + .5 \sin(4\pi x) + .5 \sin(6\pi x) + .1 \sin(10\pi x)$ 61

III.3.8 Log-Log plot of the maximum norm of the error vs. the number of meshpoints n , $n = 5, 10, 20, 40, 80, 120, 160, 200, 240, 280, 320, 360, 400, 440, 480, 520, 560, 600, 640, 680$, for $\alpha = x + .11 + c \sin(2\pi x)$, for $c = .001, .01, .05, .1, .15, .25, .5, .75, 1, 1.25, 1.5, 1.75, 2$, for $H = 10$, and for $Q = 1 + .5 \sin(2\pi x) + .5 \sin(4\pi x) + .5 \sin(6\pi x) + .1 \sin(10\pi x)$ 61

III.3.9 The logarithm of the L_2 norm of the error for different values of n , $n = 5, 10, 20, 40, 80, 120, 160, 200, 240, 280, 320, 360, 400, 440, 480, 520, 560, 600, 640, 680$, for $\alpha = x + .11 + c \sin(2\pi x)$, for $c = .001, .01, .05, .1, .14, .5, .75, 1, 1.25, 1.5, 1.75, 2$, for $H = 10$, and for $Q = 1 + .5 \sin(2\pi x) + .5 \sin(4\pi x) + .5 \sin(6\pi x) + .1 \sin(10\pi x)$ 62

III.3.10 Log-Log plot of the L_2 of the error vs. the number of meshpoints n $n = 5, 10, 20, 40, 80, 120, 160, 200, 240, 280, 320, 360, 400, 440, 480, 520, 560, 600, 640, 680$, for $\alpha = x + .11 + c \sin(2\pi x)$, for $c = .001, .01, .05, .1, .15, .25, .5, .75, 1, 1.25, 1.5, 1.75, 2$, for $H = 10$, and for $Q = 1 + .5 \sin(2\pi x) + .5 \sin(4\pi x) + .5 \sin(6\pi x) + .1 \sin(10\pi x)$ 63

III.3.11 Numerical solution of $(R \circ \alpha)(x) = H(x) R(x) + Q(x)$ discretized with 640 meshpoints and a cubic spline interpolation scheme. $H = 10/7$, $\alpha = x + .11$, and $Q = 1 + .5 \sin(2\pi x) + .5 \sin(4\pi x) + .5 \sin(6\pi x) + .1 \sin(10\pi x)$ 64

III.3.12 Numerical solution of $(R \circ \alpha)(x) = H(x) R(x) + Q(x)$ discretized with 640 meshpoints and a cubic spline interpolation scheme. $H = 10/7$, $\alpha = x + .11 + .15 \sin(2\pi x)$, and $Q = 1 + .5 \sin(2\pi x) + .5 \sin(4\pi x) + .5 \sin(6\pi x) + .1 \sin(10\pi x)$ 64

III.3.13 Numerical solution of $(R \circ \alpha)(x) = H(x) R(x) + Q(x)$ discretized with 640 meshpoints and a cubic spline interpolation scheme. $H = 10/7$, $\alpha = x + .11 + .5 \sin(2\pi x)$, and $Q = 1 + .5 \sin(2\pi x) + .5 \sin(4\pi x) + .5 \sin(6\pi x)$

+ .1 sin (10 π x) 65

III.3.14 Numerical solution of $(R \circ \alpha)(x) = H(x)R(x) + Q(x)$ discretized with 640 meshpoints and a cubic spline interpolation scheme. $H = 10/7$, $\alpha = x + .11 + .75 \sin(2\pi x)$, and $Q = 1 + .5 \sin(2\pi x) + .5 \sin(4\pi x) + .5 \sin(6\pi x)$.1 sin (10 π x) 66

III.3.15 Numerical solution of $(R \circ \alpha)(x) = H(x)R(x) + Q(x)$ discretized with 640 meshpoints and a cubic spline interpolation scheme. $H = 10/7$, $\alpha = x + .11 + 1.5 \sin(2\pi x)$, and $Q = 1 + .5 \sin(2\pi x) + .5 \sin(4\pi x) + .5 \sin(6\pi x)$ + .1 sin (10 π x) 66

III.3.16 Numerical solution of $(R \circ \alpha)(x) = H(x)R(x) + Q(x)$ discretized with 640 meshpoints and a cubic spline interpolation scheme. $H = 10/7$, $\alpha = x + .11 + 2 \sin(2\pi x)$, and $Q = 1 + .5 \sin(2\pi x) + .5 \sin(4\pi x) + .5 \sin(6\pi x)$ + .1 sin (10 π x) 67

III.3.17 The logarithm of the maximum norm of the error for different values of n , $n = 5, 10, 20, 40, 80, 120, 160, 200, 240, 280, 320, 360, 400, 440, 480, 520, 560, 600, 640, 680$, for $\alpha = x + .11 + c \sin(2\pi x)$, for $c = .001, .01, .05, .1, .15, .25, .5, .75, 1, 1.25, 1.5, 1.75, 2$, for $H = 10/7$, and for $Q = 1 + .5 \sin(2\pi x) + .5 \sin(4\pi x) + .5 \sin(6\pi x) + .1 \sin(10\pi x)$ 67

III.3.18 Log-Log plot of the maximum norm of the error vs. the number of meshpoints n , $n = 5, 10, 20, 40, 80, 120, 160, 200, 240, 280, 320, 360, 400, 440, 480, 520, 560, 600, 640, 680$, for $\alpha = x + .11 + c \sin(2\pi x)$, for $c = .001, .01, .05, .1, .15, .25, .5, .75, 1, 1.25, 1.5, 1.75, 2$, for $H = 10/7$, and for $Q = 1 + .5 \sin(2\pi x) + .5 \sin(4\pi x) + .5 \sin(6\pi x) + .1 \sin(10\pi x)$ 68

III.3.19 The logarithm of the L_2 norm of the error for different values of n , $n = 5, 10, 20, 40, 80, 120, 160, 200, 240, 280, 320, 360, 400, 440, 480, 520, 560, 600, 640, 680$, for $\alpha = x + .11 + c \sin(2\pi x)$, for $c = .001, .01, .05, .1, .14, .5, .75, 1, 1.25, 1.5, 1.75, 2$, for $H = 10/7$, and for $Q = 1 + .5 \sin(2\pi x) + .5 \sin(4\pi x) + .5 \sin(6\pi x) + .1 \sin(10\pi x)$ 69

III.3.20 Log-Log plot of the L_2 of the error vs. the number of meshpoints n $n = 5, 10, 20, 40, 80, 120, 160, 200, 240, 280, 320, 360, 400, 440, 480, 520, 560, 600, 640, 680$, for $\alpha = x + .11 + c \sin(2\pi x)$, for $c = .001, .01, .05, .1, .15, .25, .5, .75, 1, 1.25, 1.5, 1.75, 2$, for $H = 10/7$, and for $Q = 1 + .5 \sin(2\pi x) + .5 \sin(4\pi x) + .5 \sin(6\pi x) + .1 \sin(10\pi x)$ 70

III.4.1 The logarithm of the maximum norm of the error for different values of n , for $\alpha = x + .11 + c \sin(2\pi x)$, for $c = .001, .01, .05, .1, .14, 1/(2\pi), .5, 1, 2$, for $H = .1$ and for $Q = 1 + .5 \sin(2\pi x) + .5 \sin(4\pi x) + .5 \sin(6\pi x) + .1 \sin(10\pi x)$ 71

III.4.2 Log-Log plot of the maximum norm of the error vs. the number of modes n for $\alpha = x + .11 + c \sin(2\pi x)$, $c = .001, .01, .05, .1, .14, 1/(2\pi), .5, 1, 2$, for $H = .1$, and for $Q = 1 + .5 \sin(2\pi x) + .5 \sin(4\pi x) + .5 \sin(6\pi x) + .1 \sin(10\pi x)$ 72

III.4.3 The logarithm of the L_2 norm of the error for different values of n , for

$\alpha = x + .11 + c \sin(2 \pi x)$, for $c = .001, .01, .05, .1, .14, 1/(2 \pi), .5, 1, 2$, for $H = .1$, and for $Q = 1 + .5 \sin(2 \pi x) + .5 \sin(4 \pi x) + .5 \sin(6 \pi x) + .1 \sin(10 \pi x)$ 73

III.4.4 Log-Log plot of the L_2 norm of the error vs. the number of modes n , for $\alpha = x + .11 + c \sin(2 \pi x)$, $c = .001, .01, .05, .1, .14, 1/(2 \pi), .5, 1, 2$, for $H = .1$, and for $Q = 1 + .5 \sin(2 \pi x) + .5 \sin(4 \pi x) + .5 \sin(6 \pi x) + .1 \sin(10 \pi x)$ 73

III.5.1 The logarithm of the maximum norm of the error for different values of n , $n = 5, 10, 20, 40, 80, 120, 160, 200, 240, 280, 320, 360, 400, 480, 520, 560, 600, 640, 680$ for a second-order finite difference, for a third-order finite difference, and for cubic spline interpolation schemes. $\alpha = x + .11 + .001 \sin(2 \pi x)$, $H = .1$ or $H = 10$, and $Q = 1 + .5 \sin(2 \pi x) + .5 \sin(4 \pi x) + .5 \sin(6 \pi x) + .1 \sin(10 \pi x)$ 75

III.5.2 The logarithm of the L_2 norm of the error for different values of n , $n = 5, 10, 20, 40, 80, 120, 160, 200, 240, 280, 320, 360, 400, 480, 520, 560, 600, 640, 680$ for a second-order finite difference, for a third-order finite difference, and for cubic spline interpolation schemes. $\alpha = x + .11 + .001 \sin(2 \pi x)$, $H = .1$ or $H = 10$, and $Q = 1 + .5 \sin(2 \pi x) + .5 \sin(4 \pi x) + .5 \sin(6 \pi x) + .1 \sin(10 \pi x)$ 75

III.5.3 The logarithm of the maximum norm of the error for different values of n , $n = 5, 10, 20, 40, 80, 120, 160, 200, 240, 280, 320, 360, 400, 480, 520, 560, 600, 640, 680$ for a second-order finite difference, for a third-order finite difference, and for cubic spline interpolation schemes. $\alpha = x + .11 + .001 \sin(2 \pi x)$, $H = .1$ or $H = 10$, and $Q = 1 + .5 \sin(2 \pi x) + .5 \sin(4 \pi x) + .5 \sin(6 \pi x) + .1 \sin(10 \pi x)$ 76

III.5.4 The logarithm of the L_2 norm of the error for different values of n , $n = 5, 10, 20, 40, 80, 120, 160, 200, 240, 280, 320, 360, 400, 480, 520, 560, 600, 640, 680$ for a second-order finite difference, for a third-order finite difference, and for cubic spline interpolation schemes. $\alpha = x + .11 + .001 \sin(2 \pi x)$, $H = .1$ or $H = 10$, and $Q = 1 + .5 \sin(2 \pi x) + .5 \sin(4 \pi x) + .5 \sin(6 \pi x) + .1 \sin(10 \pi x)$ 77

III.5.5 The logarithm of the maximum norm of the error for different values of n , $n = 5, 10, 20, 40, 80, 120, 160, 200, 240, 280, 320, 360, 400, 480, 520, 560, 600, 640, 680$ for a second-order finite difference, for a third-order finite difference, and for cubic spline interpolation schemes. $\alpha = x + .11 + .001 \sin(2 \pi x)$, $H = .1$ or $H = 10$, and $Q = 1 + .5 \sin(2 \pi x) + .5 \sin(4 \pi x) + .5 \sin(6 \pi x) + .1 \sin(10 \pi x)$ 78

III.5.6 The logarithm of the L_2 norm of the error for different values of n , $n = 5, 10, 20, 40, 80, 120, 160, 200, 240, 280, 320, 360, 400, 480, 520, 560, 600, 640, 680$ for a second-order finite difference, for a third-order finite difference, and for cubic spline interpolation schemes. $\alpha = x + .11 + .001 \sin(2 \pi x)$, $H = .1$ or $H = 10$, and $Q = 1 + .5 \sin(2 \pi x) + .5 \sin(4 \pi x) + .5 \sin(6 \pi x) + .1 \sin(10 \pi x)$

.1 $\sin(10 \pi x)$ 79

III.5.7 The logarithm of the maximum norm of the error for different values of n , $n = 5, 10, 20, 40, 80, 120, 160, 200, 240, 280, 320, 360, 400, 480, 520, 560, 600, 640, 680$ for a second-order finite difference, for a third-order finite difference, and for cubic spline interpolation schemes. $\alpha = x + .11 + .001 \sin(2 \pi x)$, $H = .1$ or $H = 10$, and $Q = 1 + .5 \sin(2 \pi x) + .5 \sin(4 \pi x) + .5 \sin(6 \pi x) +$
.1 $\sin(10 \pi x)$ 79

III.5.8 The logarithm of the L_2 norm of the error for different values of n , $n = 5, 10, 20, 40, 80, 120, 160, 200, 240, 280, 320, 360, 400, 480, 520, 560, 600, 640, 680$ for a second-order finite difference, for a third-order finite difference, and for cubic spline interpolation schemes. $\alpha = x + .11 + .001 \sin(2 \pi x)$, $H = .1$ or $H = 10$, and $Q = 1 + .5 \sin(2 \pi x) + .5 \sin(4 \pi x) + .5 \sin(6 \pi x) +$
.1 $\sin(10 \pi x)$ 80

Part II

I.1.1 Geometry of the interface for a two-dimensional problem 91

I.8.1 Solution of the equation for the solid and the liquid at the times
 $t = 1 + .1 n, n = 0, 1, \dots, 50$ 156

I.8.2 Position of the interface between the times $t = 1$ and $t = 6$ 157

I.8.3 Log-Log plot of the position of the interface vs. time 158

Appendix V

AV.1 Solution of the equation for the solid and the liquid at the times
 $t = 1 + .1 n, n = 0, 1, \dots, 50$ 214

AV.2 Position of the interface between the times $t = 1$ and $t = 6$ 215

AV.3 Log-Log plot of the position of the interface vs. time 216

TABLE OF TABLES

Part I

III.0.1 Table of the estimated regularity of the analytical solution of (II.0.1) for different values of c and for $H = .1$	34
III.0.2 Table of the estimated regularity of the analytical solution of (II.0.1) for different values of c and for $H = .1$	34

Part II

I.8.1 Table of errors at the time $t = 3.5$ for a fixed timestep $\tau = .00001$ and different meshsizes	158
I.8.2 Table of exponents at the time $t = 3.5$ for a fixed timestep $\tau = .00001$ and different meshsizes	159
I.8.3 Table of errors at the time $t = 6$ for a fixed timestep $\tau = .00001$ and different meshsizes	159
I.8.4 Table of exponents at the time $t = 6$ for a fixed timestep $\tau = .00001$ and different meshsizes	159
I.8.5 Table of errors at the time $t = 3.5$ for a fixed meshsize $h_1 = h_2 = .008368$ and different timesteps	160
I.8.6 Table of exponents at the time $t = 3.5$ for a fixed meshsize $h_1 = h_2 = .008368$ and different timesteps	160
I.8.7 Table of errors at the time $t = 6$ for a fixed meshsize $h_1 = h_2 = .008368$ and different timesteps	160
I.8.8 Table of exponents at the time $t = 6$ for a fixed meshsize $h_1 = h_2 = .008368$ and different timesteps	161

Appendix V

AV.1 Table of errors at the time $t = 3.5$ for a fixed timestep $\tau = .00001$ and different meshsizes	213
AV.2 Table of exponents at the time $t = 3.5$ for a fixed timestep $\tau = .00001$ and different meshsizes	216
AV.3 Table of errors at the time $t = 6$ for a fixed timestep $\tau = .00001$ and different meshsizes	217
AV.4 Table of exponents at the time $t = 6$ for a fixed timestep $\tau = .00001$ and different meshsizes	217

AV.5 Table of errors at the time $t = 3.5$ for a fixed meshsize $h_1 = h_2 = .005$ and different timesteps	217
AV.6 Table of exponents at the time $t = 3.5$ for a fixed meshsize $h_1 = h_2 = .005$ and different timesteps	218
AV.7 Table of errors at the time $t = 6$ for a fixed meshsize $h_1 = h_2 = .005$ and different timesteps	218
AV.8 Table of exponents at the time $t = 6$ for a fixed meshsize $h_1 = h_2 = .005$ and different timesteps	218

**Part I: NUMERICAL EXPERIMENTS FOR THE COMPUTATION
OF INVARIANT CURVES IN DYNAMICAL SYSTEMS**

CHAPTER I

INTRODUCTION

In this work we use both analytical and numerical methods to investigate the functional equation

$$(I.1) \quad R(x) = H(x) (R \circ \alpha)(x) + Q(x) \quad x \in S^1.$$

Here α is a given, smooth, 1-1 and onto function from the unit circle S^1 onto itself, H and Q are given smooth functions from S^1 to $(-\infty, \infty)$, and the function R is defined from S^1 to $(-\infty, \infty)$ and is unknown. The unit circle S^1 is the quotient space of the set of reals by the set of integers.

Before analyzing (I.1), we would like to point out how this functional equation arises from the system of ordinary differential equations

$$(I.2a) \quad \frac{d}{dt} \theta = a(\theta, t),$$

$$(I.2b) \quad \frac{d}{dt} r = -b(\theta, t) r + c(\theta, t),$$

where a , b , and c are smooth and given functions from $S^1 \times S^1$ to $(-\infty, \infty)$.

Consider the manifold $M = \{(\theta, t, u(\theta, t)), (\theta, t) \in T^2\}$, where u is defined from T^2 to $(-\infty, \infty)$ with $T^2 = S^1 \times S^1$. We would like to know the conditions under which M is an invariant manifold under (I.2). One can show that M is invariant under the flow of the differential system (I.2) if and only if the function u satisfies

$$(I.3) \quad \frac{\partial}{\partial t} u + a(\theta, t) \frac{\partial}{\partial \theta} u + b(\theta, t) u = c(\theta, t).$$

However, instead of computing the invariant manifold M under the flow of (I.2), we will compute an invariant curve of the Poincaré map with respect to the time variable t . Once such a curve is known, an invariant manifold M is easily obtained.

To compute such a curve, we need to integrate system (I.2) with respect to time. Consider the initial condition $\theta(0) = \theta_0$ and $r(0) = r_0$. The solution at time t of (I.2) with the initial condition (θ_0, r_0) is given by $(\theta(\theta_0, t), r(\theta_0, r_0, t))$. Once we have an expression for $\theta(\theta_0, t)$, we can use the r equation to obtain an explicit expression for $r(\theta_0, r_0, t)$,

$$(I.4) \quad r(\theta_0, r_0, t) = \tilde{H}(\theta_0, t) r_0 + \tilde{Q}(\theta_0, t),$$

with $\theta_0 \in S^1$, and with

$$\begin{aligned}\tilde{H}(\theta_0, t) &= \exp\left(-\int_0^t b(\theta(\theta_0, \tau), \tau) d\tau\right), \\ \tilde{Q}(\theta_0, t) &= \int_0^t \exp\left(-\int_s^t b(\theta(\theta_0, \tau), \tau) d\tau\right) c(\theta(\theta_0, s), s) ds.\end{aligned}$$

Because the time variable t is in S^1 , we can define the Poincaré map \mathbf{P} by

$$\mathbf{P} : \begin{cases} S^1 \times (-\infty, \infty) \rightarrow S^1 \times (-\infty, \infty) \\ (\theta_0, r_0) \rightarrow (\theta(\theta_0, 1), r(\theta_0, r_0, 1)) \end{cases}$$

We would like to find an expression for an invariant curve under the Poincaré map \mathbf{P} , that has the form $\Gamma = \{(x, R(x)), x \in S^1\}$, where the function R is an unknown function from S^1 to $(-\infty, \infty)$. The curve Γ is invariant under the Poincaré map \mathbf{P} if the point $\mathbf{P}(x, R(x))$ is on the curve Γ for all $x \in S^1$. Thus, for the point $(\theta(x, 1), r(x, R(x), 1))$ to belong to Γ , we require $\mathbf{P}(x, R(x)) = (\theta(x, 1), \hat{H}(x)R(x) + \hat{Q}(x))$ to satisfy

$$(I.5) \quad R(\theta(x, 1)) = \hat{H}(x)R(x) + \hat{Q}(x),$$

with $\hat{H}(x) = \tilde{H}(x, 1)$ and $\hat{Q}(x) = \tilde{Q}(x, 1)$.

Because the function a from (I.2a) is smooth, we know that the function

$$\begin{cases} S^1 \rightarrow S^1 \\ x \rightarrow \theta(x, 1) \end{cases}$$

is 1-1 and onto, and therefore, this function has a unique inverse α . Applying the inverse α to the arguments of the equation (I.5), we then deduce (I.1) with the functions H and Q given by

$$\begin{aligned}H(\theta_1) &= \hat{H}(\alpha(\theta_1)), \\ Q(\theta_1) &= \hat{Q}(\alpha(\theta_1)).\end{aligned}$$

To investigate the functional equation (I.1), we begin in chapter 2 by showing the existence and uniqueness of the solution of the functional equation using a contraction mapping argument on a complete normed space. We then show that the solution is k -times continuously differentiable if the functions H and α defined above satisfy the condition $\|H\|_\infty \|\alpha'\|_\infty^k < 1$. Once again a contraction mapping argument is used to prove this result. In particular, we note that the solution will not necessarily be smooth even if all the functions defining the functional equation (I.1) are

smooth. Because we have shown that, under certain conditions, the solution of the functional equation exists, is unique, and possesses k continuous derivatives, we can study the behavior of the error when the continuous equation is approximated by different discretization schemes. In particular, we study the error that occurs with second-order and third-order finite difference schemes, a cubic spline interpolation scheme, and with a truncated Fourier expansion. We first derive error estimates when the functional equation is discretized with a second-order finite difference scheme. We consider the cases of the solution of the continuous problem being at least twice continuously differentiable, being continuously differentiable, and being only continuous. We next derive error estimates when the functional equation is discretized with a third-order finite difference scheme. As before, we consider the cases of the solution of the continuous problem being at least three-times continuously differentiable, being twice continuously differentiable, being continuously differentiable, and being only continuous. We also study the behavior of the error when the functional equation is discretized with a cubic spline interpolation scheme. The cubic spline interpolation scheme is of interest, not because we want to have a higher-order scheme, but because we know that the numerical solution has a continuous second derivative on the whole domain of definition. This is of importance for nonlinear problems. For this scheme, we consider the cases of the solution of the continuous problem being at least four-times continuously differentiable, being three-times continuously differentiable, being twice continuously differentiable, being continuously differentiable, and being only continuous. We finally, because the solution of the continuous problem is defined on the unit circle S^1 , approximate the solution by a truncated Fourier expansion. For the Fourier expansion case, we derive an estimate (in L_2 norm) for the continuous operator L defined by

$$L: \begin{cases} C \rightarrow C \\ R \rightarrow R \circ \alpha \end{cases}.$$

Here C is the space of continuous functions defined on the unit circle S^1 .

In chapter 3, we plot the solution of a specific functional equation discretized with both a second-order finite difference scheme and a cubic spline interpolation scheme. There we also plot the error curves obtained by discretizing the functional equation with a second-order finite difference, with a third-order finite difference scheme, with a cubic spline interpolation scheme, and with a truncated Fourier series. We also study the influence of certain parameters in the equation on the smoothness of the solution. We do this by graphing the error curves as a function of the parameter in the function α for the second-order and third-order finite difference schemes, for the cubic spline interpolation scheme, and for the truncated Fourier series. We also fix all the parameters in the functional equation and compare these

error curves when the equation is discretized with three different schemes: a second-order finite difference scheme, a third-order finite difference scheme, and a cubic spline interpolation scheme.

CHAPTER II

THE LINEAR PROBLEM ANALYTICAL RESULTS

We consider the functional equation given by either

$$(II.0.1) \quad R(x) = H(x) (R \circ \alpha)(x) + Q(x),$$

or the equivalent form

$$(II.0.2) \quad (R \circ \alpha)(x) = \tilde{H}(x) R(x) + \tilde{Q}(x),$$

where H and \tilde{H} , Q and \tilde{Q} are related to each other by

$$\tilde{H}(x) = \frac{1}{H(x)}, \quad \tilde{Q}(x) = -\frac{Q(x)}{H(x)},$$

assuming $H(x) \neq 0 \forall x \in S^1$. Because (II.0.1) and (II.0.2) are equivalent, we will study the properties of the solution of (II.0.1) and the solution of various discrete equivalents of (II.0.1).

In this chapter we will assume that H , Q , and α are smooth functions defined on the unit circle S^1 . The functions H and Q map the unit circle S^1 to the real line. The function α maps the unit circle onto itself. In most of the sections of the error analysis part, we will not assume any monotonicity assumption on the function α . Only in section 4 of the error analysis part, we will assume that the function α is a bijection from the unit circle S^1 onto itself.

We first will study the existence and uniqueness of the solution of (II.0.1), and then study the conditions under which the solution $R(x)$ is smooth and possesses k continuous derivatives. Assuming some regularity on the solution of the continuous equation (II.0.1), we will derive error bounds for the solution \tilde{R} of the discrete version of (II.0.1). The equation (II.0.1) will be discretized using a second-order finite difference scheme, using a third-order finite difference scheme, using a cubic spline interpolation scheme, and using a Fourier expansion. A spectral method is a

natural approach because the solution R is a function defined on the unit circle S^1 .

II.1 Existence and Uniqueness of the Solution

Before computing any solution of (II.0.1), we would like to know under which conditions (II.0.1) has a unique solution. As before, H , Q , and α are smooth. We call a function R from S^1 to $(-\infty, \infty)$ a solution of (II.0.1) if (II.0.1) holds at each $x \in S^1$ and R is bounded. Thus we excluded explicitly all unbounded functions as solutions. The following theorem summarizes the results:

Theorem II.1.1.

Consider the equation

$$(II.1.1) \quad R(x) = H(x) (R \circ \alpha)(x) + Q(x), \quad x \in S^1.$$

Assume that the functions H , Q , and α are continuous and defined on the unit circle S^1 . If $|H|_\infty < 1$, then a solution of (II.1.1) exists, is unique, and is continuous.

Proof of Theorem II.1.1:

We first will show the uniqueness of the solution. Consider two solutions R_1 and R_2 of (II.0.1). The function $R_1 - R_2$ satisfies

$$(II.1.2) \quad (R_1 - R_2)(x) = H(x) [(R_1 - R_2) \circ \alpha](x), \quad x \in S^1.$$

By assumption, the function $R_1 - R_2$ is bounded. Because α maps the unit circle S^1 into itself, we know that

$$(II.1.3) \quad |(R_1 - R_2) \circ \alpha|_\infty \leq |R_1 - R_2|_\infty.$$

By taking absolute values of (II.1.2) and using (II.1.3), we deduce

$$(II.1.4) \quad |R_1 - R_2|_\infty \leq |H|_\infty |R_1 - R_2|_\infty.$$

From (II.1.4), we see that $R_1 = R_2$ because we have assumed $|H|_\infty < 1$. So the solutions of both (II.0.1) and (II.0.2) are unique.

We now want to show that there exists a continuous solution to (II.1.1). Define the operator L as

$$L: \begin{cases} C \rightarrow C \\ R \rightarrow H R \circ \alpha \end{cases},$$

where C is the set of continuous functions defined on the unit circle S^1 .

Showing that a solution to (II.1.1) exists is equivalent to showing that a solution to the equation

$$(II.1.5) \quad (I - L) R = Q,$$

exists. Because the function α maps the unit circle S^1 onto itself and because $|L|_\infty < 1$, the operator $I - L$ possesses an inverse. There exists a unique solution to (II.1.5). The solution to the equation (II.1.5) can be given explicitly by a uniformly convergent series, because the functions H and Q are known

$$(II.1.6) \quad R(x) = \sum_{k=0}^{\infty} \left(\left[\prod_{l=0}^{k-1} (H \circ \alpha^l)(x) \right] Q \circ \alpha^k(x) \right), \quad x \in S^1.$$

This series is uniformly convergent because the function α maps the unit circle S^1 onto itself and because $|H|_\infty < 1$. The solution exists and is uniformly bounded by the constant

$$\frac{|Q|_\infty}{1 - |H|_\infty}.$$

So a solution to (II.1.1) exists and is unique if $|H|_\infty < 1$. In a similar fashion, we can show that if $|\tilde{H}|_\infty > 1$, a solution to (II.0.2) exists and is unique.

II.2 Regularity of the Solution

In the previous section we have seen that there exists a unique solution to (II.0.1) if $|H|_\infty < 1$. We would like to know the regularity of the continuous solution as well, under the assumptions already given. The result, already presented in [2], can be summarized as

Theorem II.2.1.

Consider the equation

$$(II.2.1) \quad R(x) = H(x) (R \circ \alpha)(x) + Q(x), \quad x \in S^1.$$

Assume that the functions H , Q , and α are k -times continuously differentiable on the unit circle S^1 . If $|H|_\infty < 1$ and if $|H|_\infty |\alpha'|_\infty^k < 1$, then the solution R

of (II.2.1), is defined on the unit circle S^1 and possesses k continuous derivatives. Here $'$ denotes the first derivative of the function.

Proof of Theorem II.2.1:

We will prove this result using a fixed point theorem. We need to show that on a complete normed space, we can define an operator that will define a contraction mapping for the norm. We choose the same norm as in [2],

$$\|R\|_k = \epsilon \|R^{(k)}\|_\infty + \|R\|_\infty,$$

with $\epsilon > 0$ to be determined below. Here the function $R^{(k)}$ is the k -th derivative of R .

We define the operator L by

$$L R (x) = H (x) (R \circ \alpha) (x) + Q (x). \quad x \in S^1$$

The operator L will be defined on the space C^k of k -times continuously differentiable functions defined on the unit circle S^1 . The space C^k with the norm $\|\cdot\|_k$ is complete. We then have to prove that the operator L is a contraction mapping on the given space with respect to the norm $\|\cdot\|_k$. Once we have done this, the Banach fixed point theorem implies that the solution R of (II.2.1) possesses k continuous derivatives.

From the Leibnitz formula, we know that

$$(L R (x))^{(k)} = \sum_{l=0}^k \binom{k}{l} H^{(k-l)} (x) (R \circ \alpha)^{(l)} (x) + Q^{(k)} (x), \quad x \in S^1. \tag{II.2.2}$$

We would like to bound the difference $L R_1 - L R_2$ in the norm $\|\cdot\|_k$ in terms of $\|R_1^{(k)} - R_2^{(k)}\|_\infty$ and $\|R_1 - R_2\|_\infty$ first. From (II.2.2), we see that we need to consider Sobolev's inequality

$$\|R^{(j)}\|_\infty \leq \epsilon_0 \|R^{(k)}\|_\infty + C(\epsilon_0) \|R\|_\infty,$$

for $j = 1, \dots, k - 1$.

In (II.2.2) we can isolate the term $H (x) (\alpha')^k (x) (R^{(k)} \circ \alpha) (x)$ from the rest, and bound the other terms using Sobolev's inequality. We are lead to

$$\|L R_1 - L R_2\|_k \leq \left(\|H\|_\infty \|\alpha'\|_\infty^k + M \epsilon_0 \right) \epsilon \|R_1^{(k)} - R_2^{(k)}\|_\infty + (\epsilon M C(\epsilon_0) + \|H\|_\infty) \|R_1 - R_2\|_\infty, \tag{II.2.3}$$

where M is a constant that bounds the sum of the terms of the type $|H^{(k-1)}|_\infty |\alpha^{(m)}|_\infty^n$. Such a constant exists because the functions $H^{(k-1)}$ and $\alpha^{(m)}$ are continuous on the unit circle S^1 .

We first choose ϵ_0 such that $|H|_\infty |\alpha'|_\infty^k + M \epsilon_0 < 1$. Then we choose ϵ such that $\epsilon M C(\epsilon_0) + |H|_\infty < 1$. We choose Q_0 to be the maximum of $|H|_\infty |\alpha'|_\infty^k + M \epsilon_0$ and $\epsilon M C(\epsilon_0) + |H|_\infty$. This maximum is strictly smaller than 1. We then obtain

$$(II.2.4) \quad |L R_1 - L R_2|_k \leq Q_0 |R_1 - R_2|_k.$$

This proves that the operator L is a contraction mapping with respect to the norm $|\cdot|_k$, on a complete normed space. Thus, we can apply the Banach fixed point theorem that ensures us that there exists a unique solution $R \in C^k$ to the equation $R(x) = L R(x)$. So we deduce that the solution to (II.2.1) possesses k continuous derivatives.

II.3 Error Analysis

Because we can compute an analytical solution of (II.0.1), we can compare the numerical solution with the solution given by the infinite series (II.1.6). We would like to see how the discretization error behaves and what happens when the exact solution has lost the smoothness required by the numerical scheme. We will study four different kinds of schemes: a second-order finite difference scheme, a third-order finite difference scheme, a cubic spline interpolation scheme, and a Fourier expansion. We will also show that a solution to those discrete equations exists.

We will denote the infinity norm for the vector e by $|e|$. The vector e has as components the values of the grid function \tilde{e} on the grid.

II.3.1 Second-Order Finite Difference Scheme

As mentioned earlier, we assume that H , Q , and α are smooth on the unit circle S^1 . The scheme enforces the periodicity of the discrete solution by identifying the meshpoints $x_m, 1 + x_m, x_m - 1, 2 + x_m, x_m - 2$, and so on. Define \tilde{R} as a solution of (II.0.1) discretized with a second-order finite difference scheme

$$(II.3.1.1) \quad \tilde{R}_i = \tilde{H}_i \left(\theta_i \tilde{R}_{j+1} + (1 - \theta_i) \tilde{R}_j \right) + \tilde{Q}_i \quad i = 1, \dots, n.$$

Here \tilde{R}_i is an approximation of $R(x_i)$, $\tilde{Q}_i = Q(x_i)$, $\tilde{H}_i = H(x_i)$, and $\theta_i h = \alpha(x_i) - x_j$ with $0 \leq \theta_i < 1$. The term $\theta_i \tilde{R}_{j+1} + (1 - \theta_i) \tilde{R}_j$ is a second-order finite difference approximation of $(R \circ \alpha)(x_i)$. The position of the meshpoint x_j depends on the function α . It is the nearest meshpoint from $\alpha(x_i)$ such that $0 \leq \alpha(x_i) - x_j < h$ modulo 1. We Taylor expand $(R \circ \alpha)(x_i)$ about x_j up to its second-order term and we replace the first derivative of R at x_j by its first-order finite difference approximation to get the above expression. The result can be summarized as

Theorem II.3.1.1.

Discretize (II.0.1) with the second-order finite difference scheme (II.3.1.1).

Assume that H , Q , and α are smooth functions defined on the unit circle S^1 . Also let $|H|_\infty < 1$. The discrete system set up with the equations (II.3.1.1) has a unique solution for $|H|_\infty < 1$.

If the solution R of (II.0.1) is at least twice continuously differentiable, the error $\tilde{e}_i = R(x_i) - \tilde{R}_i$ satisfies

$$(II.3.1.2) \quad |\tilde{e}|_\infty \leq \frac{|H|_\infty}{1 - |H|_\infty} h^2 |R''|_\infty.$$

If the solution R of (II.0.1) is continuously differentiable, the error $\tilde{e}_i = R(x_i) - \tilde{R}_i$ satisfies

$$(II.3.1.3) \quad |\tilde{e}|_\infty \leq 2 \frac{|H|_\infty}{1 - |H|_\infty} h |R'|_\infty.$$

If the solution R of (II.0.1) is continuous, the error $\tilde{e}_i = R(x_i) - \tilde{R}_i$ satisfies

$$(II.3.1.4) \quad |\tilde{e}|_\infty \leq 2 \frac{|H|_\infty}{1 - |H|_\infty} |R|_\infty.$$

Proof of Theorem II.3.1.1:

From the Taylor expansion of $(R \circ \alpha)(x_i)$ at the meshpoint x_j , with x_j the meshpoint such that $0 \leq \alpha(x_i) - x_j < h$ modulo 1, up to the second-order term $R(x_j) + \theta_i h R'(x_j) + \theta_i^2 h^2 R''(\tau_i)/2$ and by replacing $R'(x_j)$ by its first-order approximation $(R(x_{j+1}) - R(x_j))/h - h R''(\chi_i)/2$, $\tau_i \in [x_j, \alpha(x_i)]$, $\chi_i \in [x_j, x_{j+1}]$, we obtain

$$(II.3.1.5) \quad (R \circ \alpha)(x_i) = (1 - \theta_i) R(x_j) + \theta_i R(x_{j+1}) + \frac{h^2}{2} (\theta_i^2 R''(\tau_i) - \theta_i R''(\chi_i)) \quad i = 1, \dots, n.$$

Thus the error $\tilde{e}_i = R(x_i) - \tilde{R}_i$ satisfies

$$(II.3.1.6) \quad \begin{aligned} \tilde{e}_i &= \tilde{H}_i \left(\theta_i \tilde{e}_{j+1} + (1 - \theta_i) \tilde{e}_j \right) \\ &+ \frac{1}{2} h^2 \tilde{H}_i \left(\theta_i^2 R''(\tau_i) - \theta_i R''(\chi_i) \right) \quad i = 1, \dots, n. \end{aligned}$$

If we define the discrete operator \tilde{L}_2 operating on the grid function $(v_i)_{i=1, \dots, n}$ as

$$\left(\tilde{L}_2 v \right)_i = \theta_i v_{j+1} + (1 - \theta_i) v_j \quad i = 1, \dots, n,$$

with j such that $0 \leq \alpha(x_i) - x_j < h$ modulo 1, we see that \tilde{L}_2 is of maximum norm 1, because $0 \leq \theta_i < 1$. If we consider all the equations (II.3.1.6), $i = 1, \dots, n$ and set up a system with them, we see that the vector \tilde{e}_2 , $\tilde{e}_2 = [\tilde{e}_i]^T$, satisfies the system

$$(II.3.1.7) \quad \left(I - \tilde{H} \tilde{L}_2 \right) \tilde{e}_2 = \frac{1}{2} h^2 \tilde{g}_2,$$

where $\tilde{g}_2 = [\tilde{g}_i]^T$, with $\tilde{g}_i = \tilde{H}_i \left(\theta_i^2 R''(\tau_i) - \theta_i R''(\chi_i) \right)$.

Because $\|H\|_\infty < 1$ and $\|\tilde{L}_2\|_\infty \leq 1$, the operator $I - \tilde{H} \tilde{L}_2$ is invertible and

$$(II.3.1.8) \quad \|\tilde{e}_2\| \leq \frac{1}{2} \frac{1}{1 - \|H\|_\infty} h^2 \|\tilde{g}_2\|.$$

Because $\|\tilde{H}_i \left(\theta_i^2 R''(\tau_i) - \theta_i R''(\chi_i) \right)\|$ is bounded by $2 \|H\|_\infty \|R''\|_\infty$, we get (II.3.1.2).

Because the operator $I - \tilde{H} \tilde{L}_2$ is invertible for $\|H\|_\infty < 1$, we easily show that there exists a unique solution to system set-up with the equations (II.3.1.1).

If the function R is only continuously differentiable, then (II.3.1.5) is no longer true. From the Taylor expansion of $(R \circ \alpha)(x_i)$ at x_j we know

$$(II.3.1.9) \quad \begin{aligned} (R \circ \alpha)(x_i) &= \theta_i R(x_{j+1}) + (1 - \theta_i) R(x_j) \\ &+ \theta_i h \left(R'(\mu_i) - R'(\tau_j) \right) \quad i = 1, \dots, n, \end{aligned}$$

because $(R \circ \alpha)(x_i) = R(x_j) + \theta_i h R'(\mu_i)$, $\mu_i \in [x_j, \alpha(x_i)]$, and $R(x_{j+1}) - R(x_j) = h R'(\tau_j)$, $\tau_j \in [x_j, x_{j+1}]$. So the error $\tilde{e}_i = R(x_i) - \tilde{R}_i$ satisfies

$$(II.3.1.10) \quad \begin{aligned} \tilde{e}_i &= \tilde{H}_i \left(\theta_i \tilde{e}_{j+1} + (1 - \theta_i) \tilde{e}_j \right) \\ &+ \theta_i h \tilde{H}_i \left(R'(\mu_i) - R'(\tau_j) \right) \quad i = 1, \dots, n. \end{aligned}$$

If we proceed as in the derivation of (II.3.1.2), we have to solve a system equivalent to (II.3.1.7) with a different right-hand side,

$$(II.3.1.11) \quad (I - \tilde{H} \tilde{L}_2) \tilde{e}_1 = h \tilde{g}_1,$$

where $\tilde{e}_1 = [\tilde{e}_i]^T$ and $\tilde{g}_1 = [\tilde{g}_i]^T$, with $\tilde{g}_i = \tilde{H}_i \theta_i (R'(\mu_i) - R'(\tau_j))$. So

$$(II.3.1.12) \quad |\tilde{e}_1| \leq \frac{1}{1 - |H|_\infty} h |\tilde{g}_1|.$$

Because we can bound the term $|R'(\mu_i) - R'(\tau_j)|$ by $2 |R'|_\infty$, we get (II.3.1.3).

If the analytical solution R is just continuous, neither (II.3.1.5) nor (II.3.1.9) are true. Instead we get the identity

$$(II.3.1.13) \quad \begin{aligned} (R \circ \alpha)(x_i) &= \theta_i R(x_{j+1}) + (1 - \theta_i) R(x_j) + (R \circ \alpha)(x_i) \\ &- \theta_i R(x_{j+1}) - (1 - \theta_i) R(x_j) \quad i = 1, \dots, n. \end{aligned}$$

So the error $\tilde{e}_i = R(x_i) - \tilde{R}_i$ satisfies

$$(II.3.1.14) \quad \begin{aligned} \tilde{e}_i &= \tilde{H}_i \left(\theta_i \tilde{e}_{j+1} + (1 - \theta_i) \tilde{e}_j \right) \\ &+ \tilde{H}_i \left((R \circ \alpha)(x_i) - \theta_i R(x_{j+1}) - (1 - \theta_i) R(x_j) \right) \quad i = 1, \dots, n. \end{aligned}$$

If we proceed as in the derivation of (II.3.1.2), we again have to solve a system equivalent to (II.3.1.7) with a different right-hand side,

$$(II.3.1.15) \quad (I - \tilde{H} \tilde{L}_2) \tilde{e}_0 = \tilde{g}_0,$$

where $\tilde{e}_0 = [\tilde{e}_i]^T$ and $\tilde{g}_0 = [\tilde{g}_i]^T$, with $\tilde{g}_i = \tilde{H}_i ((R \circ \alpha)(x_i) - \theta_i R(x_{j+1}) - (1 - \theta_i) R(x_j))$. So

$$(II.3.1.16) \quad |\tilde{e}_0| \leq \frac{1}{1 - |H|_\infty} |\tilde{g}_0|.$$

Because we can bound the term $|(R \circ \alpha)(x_i) - \theta_i R(x_{j+1}) - (1 - \theta_i) R(x_j)|$ by $2 |R|_\infty$, we obtain (II.3.1.4).

II.3.2 Third-Order Finite Difference Scheme

Define \hat{R} as a solution of (II.0.1) discretized with a third-order finite difference

$$(II.3.2.1) \quad \widehat{R}_i = \widetilde{H}_i \left(\frac{1}{2} (\theta_i^2 + \theta_i) \widehat{R}_{j+1} + (1 - \theta_i^2) \widehat{R}_j + \frac{1}{2} (\theta_i^2 - \theta_i) \widehat{R}_{j-1} \right) + \widetilde{Q}_i \quad i = 1, \dots, n.$$

Here \widehat{R}_i is an approximation of $R(x_i)$, where $\theta_i h = \alpha(x_i) - x_j$ with $0 \leq \theta_i < 1$, and where $x_m = (m-1)h$ are the discrete points, $m = 1, \dots, n$ with $h = 1/n$. Also let $\widetilde{H}_i = H(x_i)$ and $\widetilde{Q}_i = Q(x_i)$. The term $(\theta_i^2 + \theta_i) \widehat{R}_{j+1}/2 + (1 - \theta_i^2) \widehat{R}_j + (\theta_i^2 - \theta_i) \widehat{R}_{j-1}/2$ is a third-order finite difference approximation of $(R \circ \alpha)(x_i)$. We Taylor expand $(R \circ \alpha)(x_i)$ up to its third-order term, replace the first derivative of R at x_j by its second-order finite difference approximation, and replace the second derivative of R at x_j by its first-order finite difference approximation to get the above expression. The position of the meshpoint x_j depends on the function α . It is the nearest meshpoint from $\alpha(x_i)$ such that $0 \leq \alpha(x_i) - x_j < h$ modulo 1. The result can be summarized as

Theorem II.3.2.1.

Discretize (II.0.1) with the third-order finite difference scheme (II.3.2.1).

Assume that H, Q, α are smooth functions defined on the unit circle S^1 . If $|H|_\infty < 8/17$, the discrete system set up with the equations (II.3.2.1) has a unique solution.

If the solution R of (II.0.1) is at least three-times continuously differentiable and if $|H|_\infty < 8/17$, then the error $\hat{e}_i = R(x_i) - \widehat{R}_i$ satisfies

$$(II.3.2.2) \quad |\hat{e}|_\infty \leq \frac{17}{48} \frac{|H|_\infty}{1 - \frac{17}{8} |H|_\infty} h^3 |R^{(3)}|_\infty.$$

If the solution R of (II.0.1) is twice continuously differentiable and if $|H|_\infty < 8/17$, then the error $\hat{e}_i = R(x_i) - \widehat{R}_i$ satisfies

$$(II.3.2.3) \quad |\hat{e}|_\infty \leq \frac{17}{16} \frac{|H|_\infty}{1 - \frac{17}{8} |H|_\infty} h^2 |R''|_\infty.$$

If the solution R of (II.0.1) is continuously differentiable and if $|H|_\infty < 8/17$, then the error $\hat{e}_i = R(x_i) - \widehat{R}_i$ satisfies

$$(II.3.2.4) \quad |\hat{e}|_\infty \leq 3 \frac{|H|_\infty}{1 - \frac{17}{8} |H|_\infty} h |R'|_\infty.$$

If the solution R of (II.0.1) is continuous and if $|H|_\infty < 8/17$, then the error $\hat{e}_i = R(x_i) - \widehat{R}_i$ satisfies

$$(II.3.2.5) \quad |\hat{e}|_\infty \leq \frac{25}{8} \frac{|H|_\infty}{1 - \frac{17}{8} |H|_\infty} |R|_\infty.$$

Proof of Theorem II.3.2.1:

We proceed as in the proof of theorem II.3.1.1 for the second-order finite difference scheme.

We Taylor expand of $(R \circ \alpha)(x_i)$ at the meshpoint x_j , with x_j the meshpoint such that $0 \leq \alpha(x_i) - x_j < h$, modulo 1 up to the third-order term $R(x_j) + \theta_i h R'(x_j) + \theta_i^2 h^2 R''(x_j)/2 + \theta_i^3 h^3 R^{(3)}(\tau_i)/6$ and by replacing $R'(x_j)$ by its second-order approximation $(R(x_{j+1}) - R(x_{j-1}))/(2h) - h^2(R^{(3)}(\xi_{j+1}) - R^{(3)}(\xi_{j-1}))/12$, and $R''(x_j)$ by its first-order approximation $(R(x_{j+1}) - 2R(x_j) + R(x_{j-1}))/h^2 - h(R^{(3)}(\xi_{j+1}) + R^{(3)}(\xi_{j-1}))/6$. Here $\xi_{j+1} \in [x_j, x_{j+1}]$, $\xi_{j-1} \in [x_{j-1}, x_j]$, and $\tau_i \in [x_j, \alpha(x_i)]$, we obtain

$$(II.3.2.6) \quad \begin{aligned} (R \circ \alpha)(x_i) &= \frac{1}{2} (\theta_i^2 + \theta_i) R(x_{j+1}) + (1 - \theta_i^2) R(x_j) \\ &\quad + \frac{1}{2} (\theta_i^2 - \theta_i) R(x_{j-1}) + \frac{1}{12} h^3 \left(2 \theta_i^3 R^{(3)}(\tau_i) \right. \\ &\quad \left. - (\theta_i^2 + \theta_i) R^{(3)}(\xi_{j+1}) - (\theta_i^2 - \theta_i) R^{(3)}(\xi_{j-1}) \right) \quad i = 1, \dots, n. \end{aligned}$$

So the error $\hat{e}_i = R(x_i) - \hat{R}_i$ satisfies

$$(II.3.2.7) \quad \begin{aligned} \hat{e}_i &= \tilde{H}_i \left(\frac{1}{2} (\theta_i^2 + \theta_i) \hat{e}_{j+1} + (1 - \theta_i^2) \hat{e}_j + \frac{1}{2} (\theta_i^2 - \theta_i) \hat{e}_{j-1} \right) \\ &\quad + \frac{1}{12} h^3 \tilde{H}_i \left(2 \theta_i^3 R^{(3)}(\tau_i) - (\theta_i^2 + \theta_i) R^{(3)}(\xi_{j+1}) \right. \\ &\quad \left. - (\theta_i^2 - \theta_i) R^{(3)}(\xi_{j-1}) \right) \quad i = 1, \dots, n. \end{aligned}$$

Define the discrete operator \hat{L}_3 operating on the grid function $(v_i)_{i=1, \dots, n}$ as

$$\left(\hat{L}_3 v \right)_i = \frac{1}{2} (\theta_i^2 + \theta_i) v_{j+1} + (1 - \theta_i^2) v_j + \frac{1}{2} (\theta_i^2 - \theta_i) v_{j-1} \quad i = 1, \dots, n,$$

with j such that $0 \leq \alpha(x_i) - x_j < h$, modulo 1. We see that the operator \hat{L}_3 is of maximum norm $17/8$, because the maximum of $x^2 + x$ is 2 on the interval $[0, 1]$, the maximum of $1 - x^2$ is 1, and the maximum of $x - x^2$ is $1/4$. If we consider all the equations (II.3.2.7), $i = 1, \dots, n$, and if we set up a system with them, we see that the vector \hat{e}_3 satisfies the system

$$(II.3.2.8) \quad \left(I - \tilde{H} \hat{L}_3 \right) \hat{e}_3 = \frac{1}{12} h^3 \hat{g}_3,$$

where $\hat{e}_3 = [\hat{e}_i]^T$ and $\hat{g}_3 = [\hat{g}_i]^T$, with $\hat{g}_i = \tilde{H}_i (2 \theta_i^3 R^{(3)}(\tau_i) - (\theta_i^2 + \theta_i) R^{(3)}(\xi_{j+1}) - (\theta_i^2 - \theta_i) R^{(3)}(\xi_{j-1}))$. So if $|H|_\infty < 8/17$, the operator $I - \tilde{H} \hat{L}_3$ has an inverse and

$$(II.3.2.9) \quad |\hat{e}_3| \leq \frac{1}{12} \frac{1}{1 - \frac{17}{8} |H|_\infty} h^3 |\hat{g}_3|.$$

Because $|\hat{g}_3| \leq 17 |H|_\infty |R^{(3)}|_\infty / 4$, we obtain (II.3.2.2).

Because the operator $I - \tilde{H} \hat{L}_3$ has an inverse for $|H|_\infty < 8/17$, we easily show that the system set up with the equations (II.3.2.1) has a unique solution.

If R is only twice continuously differentiable, then (II.3.2.6) is no longer true. From Taylor expansion of $(R \circ \alpha)(x_i)$ at x_j we know

$$(II.3.2.10) \quad \begin{aligned} (R \circ \alpha)(x_i) &= \frac{1}{2} (\theta_i^2 + \theta_i) R(x_{j+1}) + (1 - \theta_i^2) R(x_j) \\ &\quad + (\theta_i^2 - \theta_i) R(x_{j-1}) + \frac{1}{4} h^2 (2 \theta_i^2 R''(\tau_i) \\ &\quad - (\theta_i^2 + \theta_i) R''(\xi_{j+1}) - (\theta_i^2 - \theta_i) R''(\xi_{j-1})) \quad i = 1, \dots, n, \end{aligned}$$

because $(R \circ \alpha)(x_i) = R(x_j) + \theta_i h R'(x_j) + \theta_i^2 h^2 R''(\tau_i)/2$, because $R'(x_j) = (R(x_{j+1}) - R(x_{j-1})) / (2h) - h(R''(\xi_{j+1}) - R''(\xi_{j-1})) / 4$, and because $(R(x_{j+1}) - 2R(x_j) + R(x_{j-1})) / h^2 = (R''(\xi_{j+1}) + R''(\xi_{j-1})) / 2$. Here $\tau_i \in [x_j, \alpha(x_i)]$, $\xi_{j+1} \in [x_j, x_{j+1}]$, and $\xi_{j-1} \in [x_{j-1}, x_j]$. So the error $\hat{e}_i = R(x_i) - \hat{R}_i$ satisfies

$$(II.3.2.11) \quad \begin{aligned} \hat{e}_i &= \tilde{H}_i \left(\frac{1}{2} (\theta_i^2 + \theta_i) \hat{e}_{j+1} + (1 - \theta_i^2) \hat{e}_j + \frac{1}{2} (\theta_i^2 - \theta_i) \hat{e}_{j-1} \right) \\ &\quad + \frac{1}{4} h^2 \tilde{H}_i \left(2 \theta_i^2 R''(\tau_i) - (\theta_i^2 + \theta_i) R''(\xi_{j+1}) \right. \\ &\quad \left. - (\theta_i^2 - \theta_i) R''(\xi_{j-1}) \right) \quad i = 1, \dots, n. \end{aligned}$$

If we proceed as in the derivation of (II.3.2.2), we have to solve a system equivalent to (II.3.2.8) with a different right-hand side

$$(II.3.2.12) \quad (I - \tilde{H} \hat{L}_3) \hat{e}_2 = \frac{1}{4} h^2 \hat{g}_2,$$

where $\hat{e}_2 = [\hat{e}_i]^T$ and $\hat{g}_2 = [\hat{g}_i]^T$, with $\hat{g}_i = \tilde{H}_i (2 \theta_i^2 R''(\tau_i) - (\theta_i^2 + \theta_i) R''(\xi_{j+1}) - (\theta_i^2 - \theta_i) R''(\xi_{j-1}))$. So

$$(II.3.2.13) \quad |\hat{e}_2| \leq \frac{1}{4} \frac{1}{1 - \frac{17}{8} |H|_\infty} h^2 |\hat{g}_2|.$$

Because $|\hat{g}_i|$ is bounded by $17 |H|_\infty |R''|_\infty / 4$, we deduce (II.3.2.3).

If R is only continuously differentiable, then (II.3.2.6) and (II.3.2.10) are no longer true. In this case we know from the Taylor expansion of $(R \circ \alpha)(x_i)$ at x_j that

$$(II.3.2.14) \quad \begin{aligned} (R \circ \alpha)(x_i) &= \frac{1}{2} (\theta_i^2 + \theta_i) R(x_{j+1}) + (1 - \theta_i^2) R(x_j) \\ &\quad + (\theta_i^2 - \theta_i) R(x_{j-1}) + h \left(\theta_i R'(\tau_i) \right. \\ &\quad \left. - \frac{1}{2} \theta_i^2 (R'(\chi_{j+1}) - R'(\chi_{j-1})) - \theta_i R'(\chi_j) \right) \quad i = 1, \dots, n, \end{aligned}$$

because $R \circ \alpha(x_i) = R(x_j) + \theta_i h R'(\tau_i)$, $R(x_{j+1}) - R(x_j) = h R'(\chi_{j+1})$, because $R(x_j) - R(x_{j-1}) = h R'(\chi_{j-1})$, and because $R(x_{j+1}) - R(x_{j-1}) = 2h R'(\chi_j)$. Here $\tau_i \in [x_j, \alpha(x_i)]$, $\chi_{j+1} \in [x_j, x_{j+1}]$, $\chi_j \in [x_{j-1}, x_{j+1}]$, and $\chi_{j-1} \in [x_{j-1}, x_j]$. So the error $\hat{e}_i = R(x_i) - \hat{R}_i$ satisfies

$$(II.3.2.15) \quad \begin{aligned} \hat{e}_i &= \tilde{H}_i \left(\frac{1}{2} (\theta_i^2 + \theta_i) \hat{e}_{j+1} + (1 - \theta_i^2) \hat{e}_j + (\theta_i^2 - \theta_i) \hat{e}_{j-1} \right) \\ &\quad + \tilde{H}_i h \left(\theta_i R'(\tau_i) - \frac{1}{2} \theta_i^2 (R'(\chi_{j+1}) \right. \\ &\quad \left. - R'(\chi_{j-1})) - \theta_i R'(\chi_j) \right) \quad i = 1, \dots, n. \end{aligned}$$

If we proceed as in the derivation of (II.3.2.2), we have to solve a system equivalent to (II.3.2.8) with a different right-hand side

$$(II.3.2.16) \quad (I - \tilde{H} \hat{L}_3) \hat{e}_1 = h \hat{g}_1,$$

where $\hat{e}_1 = [\hat{e}_i]^T$ and $\hat{g}_1 = [\hat{g}_i]^T$, with $\hat{g}_i = \tilde{H}_i (\theta_i (R'(\tau_i) - R'(\chi_j)) - \theta_i^2 (R'(\chi_{j+1}) - R'(\chi_{j-1}))/2)$. So

$$(II.3.2.17) \quad |\hat{e}_1| \leq \frac{1}{1 - \frac{17}{8} \|\tilde{H}\|_\infty} h |\hat{g}_1|.$$

Because $|\hat{g}_i|$ is bounded by $3 \|\tilde{H}\|_\infty \|R'\|_\infty$, we deduce (II.3.2.4).

If R is only continuous, then (II.3.2.6), (II.3.2.10), and (II.3.2.14) are no longer valid. For this case we have the identity

$$(II.3.2.18) \quad \begin{aligned} (R \circ \alpha)(x_i) &= \frac{1}{2} (\theta_i^2 + \theta_i) R(x_{j+1}) + (1 - \theta_i^2) R(x_j) \\ &\quad + \frac{1}{2} (\theta_i^2 - \theta_i) R(x_{j-1}) + (R \circ \alpha)(x_i) \\ &\quad - \frac{1}{2} (\theta_i^2 + \theta_i) R(x_{j+1}) - (1 - \theta_i^2) R(x_j) \\ &\quad - \frac{1}{2} (\theta_i^2 - \theta_i) R(x_{j-1}) \quad i = 1, \dots, n. \end{aligned}$$

So the error $\hat{e}_i = R(x_i) - \hat{R}_i$ satisfies

$$(II.3.2.19) \quad \begin{aligned} \hat{e}_i = & \tilde{H}_i \left(\frac{1}{2} (\theta_i^2 + \theta_i) \hat{e}_{j+1} + (1 - \theta_i^2) \hat{e}_j + \frac{1}{2} (\theta_i^2 - \theta_i) \hat{e}_{j-1} \right) \\ & + \tilde{H}_i \left((R \circ \alpha)(x_i) - \frac{1}{2} (\theta_i^2 + \theta_i) R(x_{j+1}) - (1 - \theta_i^2) R(x_j) \right. \\ & \left. - \frac{1}{2} (\theta_i^2 - \theta_i) R(x_{j-1}) \right) \quad i = 1, \dots, n. \end{aligned}$$

If we proceed as in the derivation of (II.3.2.2), we have to solve a system equivalent to (II.3.2.8) with a different right-hand side

$$(II.3.2.20) \quad (I - \tilde{H} \hat{L}_3) \hat{e}_0 = \hat{g}_0,$$

where $\hat{e}_0 = [\hat{e}_i]^T$ and $\hat{g}_0 = [\hat{g}_i]^T$ with $\hat{g}_i = \tilde{H}_i \left((R \circ \alpha)(x_i) - (\theta_i^2 + \theta_i) R(x_{j+1})/2 - (1 - \theta_i^2) R(x_j) - (\theta_i^2 - \theta_i) R(x_{j-1})/2 \right)$. So

$$(II.3.2.21) \quad |\hat{e}_0| \leq \frac{1}{1 - \frac{17}{8} |H|_\infty} |\hat{g}_0|.$$

Because $|\hat{g}_i|$ is bounded by $25 |H|_\infty |R|_\infty/8$, we deduce (II.3.2.5).

II.3.3 Spline Interpolation Scheme

We would like to know the behavior of the error when the equation (II.0.1) is discretized with cubic splines. The advantage of this method compared to the two finite difference methods studied previously is that the spline solution R^* will have a second derivative continuous everywhere on the unit circle S^1 . The disadvantage is that it will require more storage for the computation. Some of the results presented in this section have already been proven in [11], for the case of a cubic spline with the first derivative of the spline prescribed at the end points of the interval of study. Define S to be the cubic spline approximating the function R and satisfying $S(x_i) = R(x_i)$, and S^* to be the cubic spline satisfying $S^*(x_i) = R_i^*$, where R_i^* is a numerical approximation of $R(x_i)$. In order to simplify the algebra in this section, it will be assumed that the mesh is uniform. The results can be extended without difficulty to the case of a non-uniform mesh with the ratio of h_{max}/h_{min} bounded by a finite constant as presented in [11]. Discretize (II.0.1) with the scheme

$$(II.3.3.1) \quad R_i^* = H_i^* (S^* \circ \alpha)(x_i) + Q_i^* \quad i = 1, \dots, n,$$

where R_i^* is an approximation of $R(x_i)$, $H_i^* = H(x_i)$, $Q_i^* = Q(x_i)$, and where S^* is a cubic spline passing through the points R_i^* . Here $x_m = (m-1)h$ are the discrete points, $m = 1, \dots, n$, with $h = 1/n$. The following theorem summarizes the results:

Theorem II.3.3.1.

Discretize (II.0.1) with the scheme (II.3.3.1).

Assume that H , Q , and α are smooth functions defined on the unit circle S^1 . If $|H|_\infty < 18/(18 + \sqrt{3})$, the solution of the discrete system exists and is unique.

If the solution R of (II.0.1) is at least four-times continuously differentiable and if $|H|_\infty < 18/(18 + \sqrt{3})$, then the error $e_i^* = R(x_i) - R_i^*$ satisfies

$$(II.3.3.2) \quad |e^*|_\infty \leq 2 \frac{|H|_\infty}{1 - \frac{18+\sqrt{3}}{18} |H|_\infty} h^4 |R^{(4)}|_\infty.$$

If the solution R of (II.0.1) is three-times continuously differentiable and if $|H|_\infty < 18/(18 + \sqrt{3})$, then the error $e_i^* = R(x_i) - R_i^*$ satisfies

$$(II.3.3.3) \quad |e^*|_\infty \leq 5 \frac{|H|_\infty}{1 - \frac{18+\sqrt{3}}{18} |H|_\infty} h^3 |R^{(3)}|_\infty.$$

If the solution R of (II.0.1) is twice continuously differentiable and if $|H|_\infty < 18/(18 + \sqrt{3})$, then the error $e_i^* = R(x_i) - R_i^*$ satisfies

$$(II.3.3.4) \quad |e^*|_\infty \leq 10 \frac{|H|_\infty}{1 - \frac{18+\sqrt{3}}{18} |H|_\infty} h^2 |R^{(2)}|_\infty.$$

If the solution R of (II.0.1) is continuously differentiable and if $|H|_\infty < 18/(18 + \sqrt{3})$, then the error $e_i^* = R(x_i) - R_i^*$ satisfies

$$(II.3.3.5) \quad |e^*|_\infty \leq \frac{11}{2} \frac{|H|_\infty}{1 - \frac{18+\sqrt{3}}{18} |H|_\infty} h |R'|_\infty.$$

If the solution R of (II.0.1) is continuous and if $|H|_\infty < 18/(18 + \sqrt{3})$, then the error $e_i^* = R(x_i) - R_i^*$ satisfies

$$(II.3.3.6) \quad |e^*|_\infty \leq \frac{21}{2} \frac{|H|_\infty}{1 - \frac{18+\sqrt{3}}{18} |H|_\infty} |R|_\infty.$$

Before proving these error bounds, we have to compute the maximum norm of the cubic spline operator. To do that, we first will show that the inverse of the

matrix relating the moments to the values of the function through which we want to fit the spline at the discretization points is, at most, of maximum norm 1.

Lemma II.3.3.2.

Consider the matrix

$$(II.3.3.7) \quad M = \begin{bmatrix} 2 & \frac{1}{2} & 0 & \dots & 0 & \frac{1}{2} \\ \frac{1}{2} & 2 & \frac{1}{2} & \dots & 0 & 0 \\ 0 & \frac{1}{2} & 2 & \frac{1}{2} & \dots & 0 \\ \vdots & \ddots & \ddots & \ddots & \ddots & \vdots \\ 0 & \dots & \frac{1}{2} & 2 & \frac{1}{2} & 0 \\ 0 & \dots & 0 & \frac{1}{2} & 2 & \frac{1}{2} \\ \frac{1}{2} & 0 & \dots & 0 & \frac{1}{2} & 2 \end{bmatrix}.$$

This matrix M has the following property,

$$M z = w \implies | z | \leq | w |,$$

where $| z |$ means the maximum norm of the vector z .

Proof of Lemma II.3.3.2:

Suppose that the component of maximum absolute value is the r -th one for the vector z . Then, we have $| z | = | z_r |$. From the structure of the matrix M we deduce that

$$\frac{1}{2} z_{r-1} + 2 z_r + \frac{1}{2} z_{r+1} = w_r$$

So we know from the triangle inequality that

$$(II.3.3.8a) \quad | w | \geq | w_r | \geq 2 | z_r | - \frac{1}{2} | z_{r+1} | - \frac{1}{2} | z_{r-1} |,$$

$$(II.3.3.8b) \quad \geq | z_r |.$$

Because we have shown that the matrix M^{-1} is at most of maximum norm 1, we can estimate the maximum norm of the cubic spline operator. The following lemma summarizes the result:

Lemma II.3.3.3.

The maximum norm of the cubic spline operator is smaller than or equal to $(18 + \sqrt{3})/18$.

Proof of Lemma II.3.3.3:

From [11], we know that

$$(II.3.3.9) \quad S(x) = M_j \frac{(x_{j+1} - x)^3}{6h} + M_{j+1} \frac{(x - x_j)^3}{6h} + A_j (x - x_j) + B_j,$$

for $x \in [x_j, x_{j+1}]$, where A_j and B_j are given by

$$(II.3.3.10) \quad A_j = \frac{y_{j+1} - y_j}{h} - \frac{h}{6} (M_{j+1} - M_j),$$

$$(II.3.3.11) \quad B_j = y_j - M_j \frac{h^2}{6},$$

and the moments M_j are the solution of the system $M \underline{M} = \underline{F}$, with

$$(II.3.3.12) \quad F_j = \frac{3}{h} \left(\frac{y_{j+1} - y_j}{h} - \frac{y_j - y_{j-1}}{h} \right).$$

The vector $\underline{y} = [y_i]^T$ is the vector of data through which we would fit the cubic spline.

Because the problem is defined on the unit circle S^1 , we identify $j - 1$ and $n - 1$ for $j = 0$, and we identify $j + 1$ and 0 for $j = n - 1$.

From Lemma II.3.3.2 and (II.3.3.12), we deduce that

$$(II.3.3.13) \quad |M_j| \leq \frac{12}{h^2} \|y\|_\infty.$$

Because we have bounded the moments M_j in terms of the data y_j , we can estimate the maximum norm of the cubic spline operator from the expressions (II.3.3.9), (II.3.3.10), and (II.3.3.11). We have

$$(II.3.3.14) \quad S(x) = -\frac{(x_{j+1} - x)(x - x_j)}{6h} (M_j (2x_{j+1} - x - x_j) + M_{j+1} (x_{j+1} + x - 2x_j)) + \frac{y_{j+1}}{h} (x - x_j) + \frac{y_j}{h} (x_{j+1} - x),$$

for $x \in [x_j, x_{j+1}]$.

From there, we will bound the cubic terms in terms of the moments and the linear terms in terms of the data. The polynomial $(x_{j+1} - x)(x - x_j)(x_{j+1} + x - 2x_j)$ keeps a constant sign on the subintervals $[x_j, (x_j + x_{j+1})/2]$ and $[(x_j + x_{j+1})/2, x_{j+1}]$. An upper bound for the polynomial on each subinterval is $\sqrt{3} h^3/36$. We are lead to

$$(II.3.3.15a) \quad |S(x)| \leq \frac{\sqrt{3} h^2}{216} |\underline{M}| + \|y\|_\infty,$$

$$(II.3.3.15b) \quad \leq \frac{18 + \sqrt{3}}{18} \|y\|_\infty.$$

From (II.3.3.15b), we deduce that

$$|S|_{\infty} \leq \frac{18 + \sqrt{3}}{18}$$

Because we have shown that the cubic spline operator is at most of maximum norm $(18 + \sqrt{3})/18$, we easily show that for $|H|_{\infty} < 18/(18 + \sqrt{3})$, the discrete system set up with the equations (II.3.3.1) has a unique solution.

Proof of Theorem II.3.3.1:

We would like to derive the equation that the error function $e_i^* = R(x_i) - R_i^*$ satisfies. Define S to be the cubic spline passing through the points $R(x_i)$. We then have using (II.0.1)

$$(II.3.3.16) \quad S(x_i) = R(x_i) = H_i^* (R \circ \alpha)(x_i) + Q(x_i) \quad i = 1, \dots, n.$$

If we subtract (II.3.3.1) from (II.3.3.16), we get

$$(II.3.3.17) \quad e_i^* = H_i^* (A e^*)_i + H_i^* ((R \circ \alpha)(x_i) - (S \circ \alpha)(x_i)) \quad i = 1, \dots, n,$$

where A is the cubic spline operator defined by $(A R^*)_i = (S^* \circ \alpha)(x_i)$. From the expression (II.3.3.12) for F_j and from (II.3.3.9), we see that the cubic spline operator is a linear operator. So we deduce (II.3.3.17) by adding and subtracting the term $(S \circ \alpha)(x_i)$ from

$$(II.3.3.18) \quad R(x_i) - R_i^* = H_i^* ((R \circ \alpha)(x_i) - (S^* \circ \alpha)(x_i)) \quad i = 1, \dots, n.$$

We will consider the operator $I - \tilde{H} A$ defined as

$$(II.3.3.19) \quad (I - \tilde{H} A) e^* = \tilde{H} z^*.$$

We obtain (II.3.3.19) by considering all the equations (II.3.3.17), $i = 1, \dots, n$ and setting up a system with them. The vectors e^* and z^* are given by $e^* = [e_i^*]^T$ and $z^* = [(R \circ \alpha)(x_i) - (S \circ \alpha)(x_i)]^T$ respectively.

If we assume that R is at least four-times continuously differentiable, and proceed as in [11] with minor changes because we consider periodic splines, we get

$$(II.3.3.20) \quad |R - S|_{\infty} \leq 2 h^4 |R^{(4)}|_{\infty},$$

because the constant C in [11] is less than or equal to 2 in our case.

From Lemma II.3.3.3, it is known that if $|H| < 18/(18+\sqrt{3})$, then the operator $I - \tilde{H} A$ is invertible. From the expression that the error $e_{\frac{1}{2}}^*$ satisfies and (II.3.3.20), we easily deduce (II.3.3.2).

In order to prove error bounds in the case that the function R is either three-times continuously differentiable or twice continuously differentiable, we have to bound the vector

$$\underline{r} = \underline{F} - M \underline{f} = M (\underline{M} - \underline{f}),$$

where

$$\underline{f} = \begin{bmatrix} R^{(2)}(x_0) \\ R^{(2)}(x_1) \\ \cdot \\ R^{(2)}(x_j) \\ \cdot \\ R^{(2)}(x_{n-1}) \end{bmatrix}.$$

The result can be summarized as follows

Lemma II.3.3.4.

If the solution R of (II.0.1) is three-times continuously differentiable, then

$$(II.3.3.21) \quad |\underline{M} - \underline{f}| \leq |\underline{r}| \leq 2 h |R^{(3)}|_{\infty}.$$

If the solution R of (II.0.1) is twice continuously differentiable, then

$$(II.3.3.22) \quad |\underline{M} - \underline{f}| \leq |\underline{r}| \leq 6 |R^{(2)}|_{\infty}.$$

Proof of Lemma II.3.3.4:

The first inequalities in (II.3.3.21) and in (II.3.3.22) are immediately deduced from Lemma II.3.3.2.

If the function R is three-times continuously differentiable, we know that

$$(II.3.3.23) \quad r_j = 3 \frac{y_{j+1} - 2 y_j + y_{j-1}}{h^2} - \frac{1}{2} R^{(2)}(x_{j-1}) - 2 R^{(2)}(x_j) - \frac{1}{2} R^{(2)}(x_{j+1}).$$

From the Taylor expansions of $R(x_{j-1})$ and $R(x_{j+1})$ around x_j up to the third-order term, of $R^{(2)}(x_{j-1})$ and $R^{(2)}(x_{j+1})$ around x_j up to the first-order term, we deduce that

$$(II.3.3.24) \quad r_j = \frac{h}{2} (R^{(3)}(\mu_{j+1}) - R^{(3)}(\mu_{j-1}) + R^{(3)}(\tau_{j-1}) - R^{(3)}(\tau_{j+1})),$$

where $\mu_{j-1} \in [x_{j-1}, x_j]$, $\mu_{j+1} \in [x_j, x_{j+1}]$, $\tau_{j-1} \in [x_{j-1}, x_j]$, and $\tau_{j+1} \in [x_j, x_{j+1}]$. We get the second inequality of (II.3.3.21) by replacing $R^{(3)}(x)$ by $|R^{(3)}|_\infty$ in (II.3.3.24).

If the function R is twice continuously differentiable, we know that

$$(II.3.3.25) \quad r_j = \frac{3}{2} (R^{(2)}(\xi_{j+1}) + R^{(2)}(\xi_{j-1})) - \frac{1}{2} R^{(2)}(x_{j-1}) - 2 R^{(2)}(x_j) - \frac{1}{2} R^{(2)}(x_{j+1}),$$

where $\xi_{j-1} \in [x_{j-1}, x_j]$ and $\xi_{j+1} \in [x_j, x_{j+1}]$. We get (II.3.3.25) by expanding $R(x_{j-1})$ and $R(x_{j+1})$ about x_j up to the second-order term. We obtain the second inequality of (II.3.3.22) by replacing $R^{(2)}(x)$ by $|R^{(2)}|_\infty$ in (II.3.3.25).

Because we have bounded $|\underline{M} - \underline{f}|_\infty$, we can derive (II.3.3.3). To do that, we first have to bound $|S^{(3)} - R^{(3)}|_\infty$. From (II.3.3.9), we know that

$$\begin{aligned} S^{(3)}(x) - R^{(3)}(x) &= \frac{M_j - M_{j-1}}{h} - R^{(3)}(x), \\ &= \frac{(x_j - x) R^{(3)}(\xi_j) - (x_{j-1} - x) R^{(3)}(\xi_{j-1})}{h} - R^{(3)}(x) \\ &\quad + \frac{M_j - R^{(2)}(x_j)}{h} - \frac{M_{j-1} - R^{(2)}(x_{j-1})}{h}, \end{aligned}$$

where $\xi_j \in [x, x_j]$, $\xi_{j-1} \in [x_{j-1}, x]$, and $x \in [x_{j-1}, x_j]$. We have to use the Taylor expansions of $R^{(2)}(x_{j-1})$ and of $R^{(2)}(x_j)$ about x . Because $|x_j - x| \leq h$, $|x_{j-1} - x| \leq h$, because $x_j - x \geq 0$ and $x - x_{j-1} \geq 0$, from the expression (II.3.3.21) of Lemma II.3.3.4, we obtain

$$(II.3.3.26) \quad |S^{(3)} - R^{(3)}|_\infty \leq 6 |R^{(3)}|_\infty.$$

Because we have estimated $|S^{(3)} - R^{(3)}|_\infty$, we can bound $|S^{(2)} - R^{(2)}|_\infty$. Assuming that x belongs to the interval $[x_i, x_{i+1}]$, we have

$$(II.3.3.27) \quad S^{(2)}(x) - R^{(2)}(x) = S^{(2)}(x_i(x)) - R^{(2)}(x_i(x)) + \int_{x_i(x)}^x (S^{(3)}(t) - R^{(3)}(t)) dt.$$

From (II.3.3.21) of Lemma II.3.3.4, from (II.3.3.26), and from the fact that $|x_i(x) - x| \leq h/2$, we obtain

$$(II.3.3.28) \quad |S^{(2)} - R^{(2)}|_\infty \leq 5 h |R^{(3)}|_\infty,$$

because from the cubic splines properties, we have $S^{(2)}(x_i(x)) = M_i$.

We now want to bound $|S' - R'|_\infty$. Because $S(x_i) = R(x_i)$ by hypothesis, because the function R is three-times continuously differentiable and because the spline function S is twice continuously differentiable, from Rolle's theorem we know that on each interval $[x_i, x_{i+1}]$, there exists a point ν_i such that $R'(\nu_i) = S'(\nu_i)$. So we get

$$(II.3.3.29) \quad S'(x) - R'(x) = \int_{\nu_i(x)}^x (S^{(2)}(t) - R^{(2)}(t)) dt.$$

So from (II.3.3.28), (II.3.3.29), and the fact that $|\nu_i(x) - x| \leq h$, we deduce

$$(II.3.3.30) \quad |S' - R'|_\infty \leq 5 h^2 |R^{(3)}|_\infty.$$

Because we have estimated $|S' - R'|_\infty$, we immediately obtain a bound for $|S - R|_\infty$, because

$$(II.3.3.31) \quad S(x) - R(x) = \int_{x_i(x)}^x (S'(t) - R'(t)) dt.$$

So from (II.3.3.30) and (II.3.3.31), we obtain

$$(II.3.3.32) \quad |S - R|_\infty \leq 5 h^3 |R^{(3)}|_\infty.$$

From Lemma II.3.3.3, it is known that if $|H|_\infty < 18/(18 + \sqrt{3})$, then the operator $I - \tilde{H}A$ is invertible. From the expression that the error e_i^* satisfies and (II.3.3.32), we easily deduce (II.3.3.3).

We want to bound the error when the function R is twice continuously differentiable. To do that, we first estimate $|S^{(2)} - R^{(2)}|_\infty$. From (II.3.3.9) we know that

$$(II.3.3.33) \quad S^{(2)}(x) - R^{(2)}(x) = M_j \frac{x_{j+1} - x}{h} + M_{j+1} \frac{x - x_j}{h} - R^{(2)}(x),$$

with $x \in [x_j, x_{j+1}]$.

After a few algebraic manipulations, from (II.3.3.33) we obtain

$$(II.3.3.34) \quad \begin{aligned} S^{(2)}(x) - R^{(2)}(x) &= (R^{(2)}(x_j) - R^{(2)}(x)) \frac{x_{j+1} - x}{h} \\ &\quad + (R^{(2)}(x_{j+1}) - R^{(2)}(x)) \frac{x - x_j}{h} \\ &\quad + (M_j - R^{(2)}(x_j)) \frac{x_{j+1} - x}{h} \\ &\quad + (M_{j+1} - R^{(2)}(x_{j+1})) \frac{x - x_j}{h}. \end{aligned}$$

So using (II.3.3.22) from Lemma II.3.3.4 and (II.3.3.34), we deduce

$$(II.3.3.35) \quad |S^{(2)} - R^{(2)}|_{\infty} \leq 10 |R^{(2)}|_{\infty}.$$

We now want to bound $|S' - R'|_{\infty}$. Because the functions R and S are twice continuously differentiable, (II.3.3.29) still holds. From (II.3.3.34) and (II.3.3.29), we obtain

$$(II.3.3.37) \quad |S' - R'|_{\infty} \leq 10 h |R^{(2)}|_{\infty}.$$

Because (II.3.3.36) gives a bound for $|S' - R'|_{\infty}$ we can now estimate $|S - R|_{\infty}$. If we use (II.3.3.31) and (II.3.3.36), we get

$$(II.3.3.37) \quad |S - R|_{\infty} \leq 10 h^2 |R^{(2)}|_{\infty}.$$

From Lemma II.3.3.3, it is known that if $|H|_{\infty} < 18/(18 + \sqrt{3})$, then the operator $I - \tilde{H} A$ is invertible. From the expression satisfied by the error e_i^* and (II.3.3.37), we easily deduce (II.3.3.4).

Finally, we want to bound the error when the function R is continuously differentiable. We can not proceed exactly as before, because the vector \underline{r} introduced in Lemma II.3.3.4 cannot be defined. Instead, we will try to bound the vector \underline{F} in terms of h and R' . In Lemma II.3.3.2 we have shown that the matrix M^{-1} is at most of maximum norm 1. We will be able to bound the moments with the bound on $|\underline{F}|$.

If the function R is continuously differentiable, we know that

$$F_j = \frac{3}{h} (R'(\tau_{j+1}) + R'(\tau_{j-1})),$$

with $\tau_{j-1} \in [x_{j-1}, x_j]$ and $\tau_{j+1} \in [x_j, x_{j+1}]$. So $|\underline{F}| < 6 |R'|_{\infty}/h$. Because the matrix M^{-1} is at most of maximum norm 1, we have

$$(II.3.3.38) \quad |\underline{M}| \leq \frac{6}{h} |R'|_{\infty}.$$

Because we have a bound for the moments, we can estimate $|S' - R'|_{\infty}$ using brute force estimates. If we differentiate (II.3.3.9) once, we obtain

$$(II.3.3.39) \quad S'(x) = -M_j \frac{(x_{j+1} - x)^2}{2h} + M_{j+1} \frac{(x - x_j)^2}{2h} + \frac{y_{j+1} - y_j}{h} - \frac{h}{6} (M_{j+1} - M_j).$$

If we use (II.3.3.38), the fact that $x \in [x_j, x_{j+1}]$, and the continuous differentiability of R , we get

$$(II.3.3.40) \quad |S' - R'|_{\infty} \leq \frac{11}{2} |R'|_{\infty}.$$

To bound $|S - R|_{\infty}$, we use (II.3.3.31) and (II.3.3.40). This yields

$$(II.3.3.41) \quad |S - R|_{\infty} \leq \frac{11}{2} h |R'|_{\infty}.$$

Lemma II.3.3.3 shows that if $|H|_{\infty} < 18/(18 + \sqrt{3})$, then the operator $I - \tilde{H} A$ is invertible. From the expression satisfied by the error and from (II.3.3.41), we can now easily deduce (II.3.3.5).

To bound $|S - R|_{\infty}$ when the function R is only continuous, we first bound the moments M_j in terms of h and $|R|_{\infty}$. Once we have bounded the moments, then we can use (II.3.3.9) to obtain a brute force estimate.

If the function R is only continuous, the components of the vector \underline{F} satisfy

$$|\underline{F}| \leq \frac{12}{h^2} |R|_{\infty}.$$

So the moments M_j satisfy

$$(II.3.3.42) \quad |\underline{M}| \leq \frac{12}{h^2} |R|_{\infty},$$

because the matrix M^{-1} is at most of maximum norm 1.

After a few algebraic manipulations on $S(x) - R(x)$ and using (II.3.3.42), we obtain

$$(II.3.3.43) \quad |S - R|_{\infty} \leq \frac{36 + \sqrt{3}}{18} |R|_{\infty}.$$

Lemma II.3.3.3 shows that if $|H|_{\infty} < 18/(18 + \sqrt{3})$, then the operator $I - \tilde{H} A$ is invertible. From the equation satisfied by the error e_i^* and from (II.3.3.43), we now easily deduce (II.3.3.6).

If we do not work with a uniform mesh, we will have to change the results from lemmas II.3.3.2, II.3.3.3, and II.3.3.4. The results from Lemma II.3.3.2 can be easily extended to the case of non-uniform mesh because we have assumed in the non-uniform mesh case that $\lambda_i \geq 0$, $\mu_i \geq 0$, $\lambda_i + \mu_i = 1$, $i = 1, \dots, n$. From there, all the other results and estimates can be deduced easily. In theorem II.3.3.1, we

will have to replace the meshsize h by the maximum length of the partition of the interval h_{max} and change certain constants.

II.3.4 Fourier Method

As already mentioned, the solution of (II.0.1) is defined on the unit circle S^1 . So a spectral method is an obvious method for discretizing equation (II.0.1). This time, we assume that the function α is a bijection from the unit circle S^1 onto itself. We will derive estimates for the continuous operator L defined as

$$L: \begin{cases} C \rightarrow C \\ R \rightarrow R \circ \alpha \end{cases},$$

where C is the set of continuously differentiable functions defined on the unit circle S^1 . The result is summarized by the following theorem

Theorem II.3.4.1.

The L_2 norm of the continuous operator L defined above is at most

$$(II.3.4.1) \quad \left(\|(\alpha^{-1})'\|_1 + \frac{\|(\alpha^{-1})^{(3)}\|_1}{12} \right)^{\frac{1}{2}},$$

if α is a bijection from the unit circle into itself and if α is at least three-times continuously differentiable. Here the norm $\| \cdot \|_1$ is the L_1 norm given by

$$\| u \|_1 = \int_0^1 | u(x) | dx$$

Proof of Theorem II.3.4.1:

Because the solution of (II.0.1) is defined on the unit circle S^1 and is by assumption at least continuously differentiable, there exists a convergent Fourier expansion for the function R . The convergence, because the solution is continuously differentiable, holds pointwise. It is given by

$$(II.3.4.2) \quad R(x) = \sum_{j=-\infty}^{\infty} \hat{R}_j e^{i 2 \pi j x}.$$

To obtain a bound for the operator L in L_2 norm, we must bound the expression $\|R \circ \alpha\|$ in terms of $\|R\|$. We can do this, by using Parseval's relation,

$$(II.3.4.3) \quad \|R\|^2 = \sum_{j=-\infty}^{\infty} |\widehat{R}_j|^2.$$

From the L_2 scalar product, we have

$$(II.3.4.4) \quad \|R \circ \alpha\|^2 = \sum_{j=-\infty}^{\infty} \sum_{l=-\infty}^{\infty} \widehat{R}_j \overline{\widehat{R}_l} \left(e^{i 2 \pi j \alpha(x)}, e^{i 2 \pi l \alpha(x)} \right),$$

where \bar{u} denotes the complex conjugate of u .

We want to estimate the scalar product $(e^{i 2 \pi j \alpha(x)}, e^{i 2 \pi l \alpha(x)})$ in terms of bounds on the function α and its derivatives. By definition, the scalar product is

$$(II.3.4.5) \quad \left(e^{i 2 \pi j \alpha(x)}, e^{i 2 \pi l \alpha(x)} \right) = \int_0^1 e^{i 2 \pi (j-l) \alpha(x)} dx.$$

Because the function α is a bijection from the unit circle onto itself, after a change of variables the relation (II.3.4.5) becomes

$$(II.3.4.6a) \quad \left(e^{i 2 \pi j \alpha(x)}, e^{i 2 \pi l \alpha(x)} \right) = \int_{\alpha(0)}^{\alpha(1)} e^{i 2 \pi (j-l) y} (\alpha^{-1})'(y) dy,$$

$$(II.3.4.6b) \quad = \int_0^1 e^{i 2 \pi (j-l) y} (\alpha^{-1})'(y) dy,$$

$$(II.3.4.6c) \quad = (\widehat{(\alpha^{-1})}')_{j-l},$$

where prime means the first derivative and where $(\widehat{(\alpha^{-1})}')_{j-l}$ is the $j-l$ Fourier coefficient of the function $(\alpha^{-1})'$. We have used the fact that the function α is a bijection from the unit circle S^1 onto itself. Using (II.3.4.6c), the equality (II.3.4.4) becomes

$$(II.3.4.7a) \quad \|R \circ \alpha\|^2 = \sum_{j=-\infty}^{\infty} \sum_{l=-\infty}^{\infty} \widehat{R}_j \overline{\widehat{R}_l} (\widehat{(\alpha^{-1})}')_{j-l},$$

$$\leq \left(\sum_{j=-\infty}^{\infty} \sum_{l=-\infty}^{\infty} |\widehat{R}_j|^2 |(\widehat{(\alpha^{-1})}')_{j-l}| \right)^{\frac{1}{2}}$$

$$(II.3.4.7b) \quad \left(\sum_{j=-\infty}^{\infty} \sum_{l=-\infty}^{\infty} |\widehat{R}_l|^2 |(\widehat{(\alpha^{-1})}')_{j-l}| \right)^{\frac{1}{2}},$$

$$(II.3.4.7c) \quad = \left(\sum_{j=-\infty}^{\infty} |(\widehat{(\alpha^{-1})}')_j| \right) \|R\|^2.$$

In the above, (II.3.4.7b) was obtained by applying the discrete Cauchy-Schwartz's inequality

$$(II.3.4.8) \quad \sum_{j=0}^{\infty} | a_j b_j | \leq \left(\sum_{j=0}^{\infty} a_j^2 \right)^{\frac{1}{2}} \left(\sum_{j=0}^{\infty} b_j^2 \right)^{\frac{1}{2}},$$

to (II.3.4.7a).

Because we have assumed that α is at least three-times differentiable, we will bound

$$(II.3.4.9) \quad \sum_{j=-\infty}^{\infty} | (\widehat{\alpha^{-1}})'_j |,$$

in terms of the L_1 norm of the third derivative of α . By definition, if $k \neq 0$ we have

$$(II.3.4.10a) \quad (\widehat{\alpha^{-1}})'_k = \int_0^1 e^{i 2 \pi k y} (\alpha^{-1})'(y) dy,$$

$$(II.3.4.10b) \quad = -\frac{1}{2 \pi i k} \int_0^1 e^{i 2 \pi k y} (\alpha^{-1})^{(2)}(y) dy,$$

$$(II.3.4.10c) \quad = -\frac{1}{4 \pi^2 k^2} \int_0^1 e^{i 2 \pi k y} (\alpha^{-1})^{(3)}(y) dy.$$

Because the last integral is bounded by $\| (\alpha^{-1})^{(3)} \|_1$, we deduce that

$$(II.3.4.11) \quad | (\widehat{\alpha^{-1}})'_k | \leq \frac{\| (\alpha^{-1})^{(3)} \|_1}{4 \pi^2 k^2},$$

if $k \neq 0$. If $k = 0$, then $| (\widehat{\alpha^{-1}})'_0 | \leq \| (\alpha^{-1})' \|_1$ from the definition of the scalar product. So using (II.3.4.10), we get the following bound for (II.3.4.9) in terms of the L_1 norm of $(\alpha^{-1})^{(3)}$:

$$(II.3.4.12a) \quad \sum_{j=-\infty}^{\infty} | (\widehat{\alpha^{-1}})'_j | \leq \| (\alpha^{-1})' \|_1 + \frac{\| (\alpha^{-1})^{(3)} \|_1}{2 \pi^2} \sum_{j=1}^{\infty} \frac{1}{k^2},$$

$$(II.3.4.12b) \quad = \| (\alpha^{-1})' \|_1 + \frac{\| (\alpha^{-1})^{(3)} \|_1}{12}.$$

(II.3.4.1) follows immediately from the bound (II.3.4.12b).

We would like to derive an estimate for the discrete equivalent of L. By discrete equivalent of L, we mean the operator obtained by replacing all the integrals needed to define the Fourier expansion of R and $R \circ \alpha$ by discrete sums. We have been

unable to do that because there is no obvious equivalent to the change of variable used in the continuous case for the discrete sums.

In the next chapter, we will describe the scheme we use to numerically solve the functional equation when the solution is approximated with a truncated Fourier expansion.

Because we have been unable to derive bounds for the discrete equivalent of the operator L defined in this section, we are unable to derive error estimates as done in the three previous sections, for the finite difference schemes and for the cubic spline interpolation scheme.

CHAPTER III

THE LINEAR PROBLEM NUMERICAL RESULTS

We would like to numerically investigate different properties of the solution of (II.0.1) and confirm the analytical results and error estimates that were obtained in the previous chapter, when the numerous assumptions on the function α are satisfied. We would also like to know what happens when these assumptions are violated, and whether the numerical solution still exists or not. In all the problems we have solved numerically, from theorem II.1.1, we know that there exists a solution to the continuous problem. We always will choose $\|H\|_\infty < 1$ for the equation (II.0.1) or $\|\tilde{H}\|_\infty > 1$ for (II.0.2) so that the solution to the continuous problem exists.

To simplify the computations in this section, we will take the function H to be constant and the function α to be $x + .11 + c \sin(2\pi x)$. The parameter c will range from 0 to 2 in most of the cases, except for the second-order and third-order finite difference schemes where it ranges from 0 to 4 if $H = .1$ and from 0 to 1 if $H = .7$. If $c < 1/(2\pi)$, the function α is a bijection from the unit circle S^1 onto itself. For $c > 1/(2\pi)$, however, some of the theorems proven in the previous chapter, like theorem II.3.4.1, which assumes the existence of an inverse, no longer apply.

As in the previous chapter, we will study the numerical solution when (II.0.1) is discretized with a second-order finite difference scheme, with a third-order finite difference scheme, with a cubic spline interpolation scheme, and with a discrete Fourier expansion. We will compare the behavior of those different schemes and try to find which one is the best to use, depending on the value of $\|H\|_\infty$ and the parameter c . One other important factor in our choice is whether we need a continuous first derivative for the interpolated discrete solution or not.

We can predict the regularity of the solution from theorem II.2.1. From this theorem we know that the solution is C^k if $\|H\|_\infty \|\alpha'\|_\infty^k < 1$. From this relation, we deduce that approximatively,

$$(III.0.1) \quad k = -\frac{\log(\|H\|_\infty)}{\log(\|\alpha'\|_\infty)}.$$

We use this relation to obtain the estimated value of k for two different constant

H, $H = .1$ and $H = .7$, with the function α given above. Table III.0.1 shows the estimated k for $H = .1$ with c ranging between 0 and 2. Table III.0.2 shows the estimated k for $H = .7$.

c	k
0	∞
.001	367
.005	74
.01	37
.05	8
.1	4
.15	3
.2	2
.3	2
.35	1
1.4	1
1.45	0
2	0

Table III.0.1 Table of the estimated regularity of the analytical solution of (II.0.1) for different values of c and for $H = .1$.

c	k
0	∞
.001	56
.005	11
.01	5
.05	1
.1	0
2	0

Table III.0.2 Table of the estimated regularity of the analytical solution of (II.0.1) for different values of c and for $H = .7$.

III.1 The Second-Order Finite Difference Scheme

In the previous chapter we have shown that the solution to

$$(III.1.1) \quad R(x) = H(x) (R \circ \alpha)(x) + Q(x), \quad x \in S^1$$

exists and is unique if the functions H , Q , and α are continuous and defined on the unit circle S^1 .

We have discretized (III.1.1) with the second-order finite difference scheme

$$(III.1.2) \quad \tilde{R}_i = \tilde{H}_i \left(\theta_i \tilde{R}_{j+1} + (1 - \theta_i) \tilde{R}_j \right) + \tilde{Q}_i \quad i = 1, \dots, n.$$

Here \tilde{R}_i is an approximation of $R(x_i)$, $\tilde{Q}_i = Q(x_i)$, $\tilde{H}_i = H(x_i)$, and $\theta_i h = \alpha(x_i) - x_j$ with $0 \leq \theta_i < 1$. Here $x_m = (m - 1)h$ are the discrete points, $m = 1, \dots, n$, and $h = 1/n$. We enforce the periodicity by equating the points x_m , x_{m+n} , x_{m-n} , x_{m+2n} , ... The term $\theta_i \tilde{R}_{j+1} + (1 - \theta_i) \tilde{R}_j$ is a second-order finite difference approximation of $(R \circ \alpha)(x_i)$. The position of the meshpoint x_j depends on the function α . It is the nearest point to $\alpha(x_i)$ such that $0 \leq \alpha(x_i) - x_j < h$ modulo 1. We Taylor expand $(R \circ \alpha)(x_i)$ about x_j up to its second-order term and replace the first derivative of R at x_j by its first-order finite difference approximation to get the above expression.

We have run numerical experiments for different values of the parameter c . Some values were chosen so that the function α is a bijection from the unit circle S^1 onto itself; other values were chosen so that the function α has no monotonicity properties. The estimates in tables III.0.1 and III.0.2 also show that the solution loses its smoothness in certain cases.

We have noticed that in order to have a good approximation to the solution, we need to have a good discrete approximation to the function Q . For example, we have run the code with

$$(III.1.3) \quad Q(x) = 1 + \frac{1}{2} \sin(2\pi x) + \frac{1}{2} \sin(4\pi x) + \frac{1}{2} \sin(6\pi x) + \frac{1}{10} \sin(10\pi x),$$

with both 40 and 640 meshpoints. Even if the contribution of the term $\sin(10\pi x)$ is smaller than that of the other terms in Q , a small number of meshpoints cannot represent the solution accurately. We can easily see this by comparing plots with 40 and 640 meshpoints, which have the same value of c .

In figure III.1.1, we plot the numerical solution of (III.1.1) discretized with the scheme (III.1.2) and $n = 40$. The function Q is given by the expression (III.1.3), $\alpha = x + .11$, and $H = .1$. In figure III.1.2, we plot the numerical solution of (III.1.1) with 640 meshpoints and the same functions Q , α , and H as in figure III.1.1.

In figure III.1.3, we plot the numerical solution of (III.1.1) discretized with the scheme (III.1.2) and $n = 40$ as before. The function Q is given by the expression

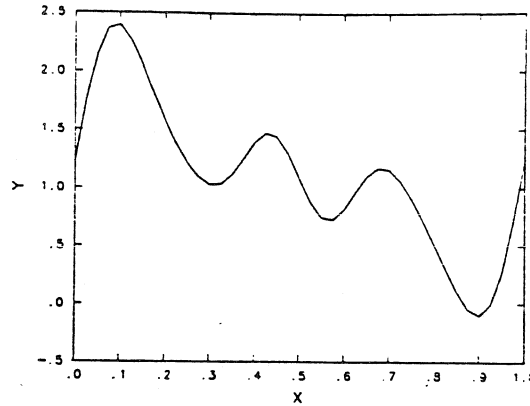


Figure III.1.1 Numerical solution of $R(x) = H(x)(R \circ \alpha)(x) + Q(x)$, discretized with 40 meshpoints and a second-order finite difference scheme. $H = .1$, $\alpha = x + .11$, and $Q = 1 + .5 \sin(2\pi x) + .5 \sin(4\pi x) + .5 \sin(6\pi x) + .1 \sin(10\pi x)$.

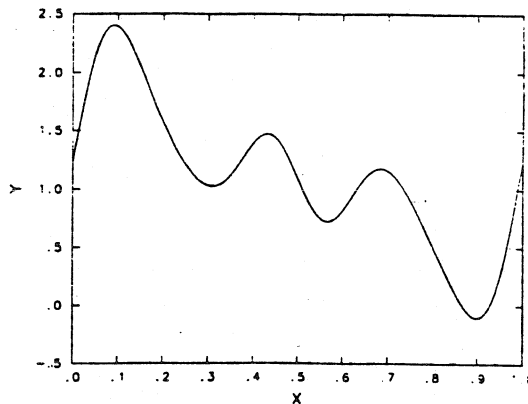


Figure III.1.2 Numerical solution of $R(x) = H(x)(R \circ \alpha)(x) + Q(x)$, discretized with 640 meshpoints and a second-order finite difference scheme. $H = .1$, $\alpha = x + .11$, and $Q = 1 + .5 \sin(2\pi x) + .5 \sin(4\pi x) + .5 \sin(6\pi x) + .1 \sin(10\pi x)$.

(III.1.3), $\alpha = x + .11 + .15 \sin(2\pi x)$, and $H = .1$. In figure III.1.4, we plot the numerical solution of (III.1.1) with 640 meshpoints and the same functions Q , α , and H as in figure III.1.3.

In figures III.1.1, III.1.2, III.1.3, and III.1.4, the parameter c is smaller than $1/(2\pi)$, so the function α is a bijection from the unit circle S^1 onto itself. From table III.0.1, we know that the solution of the continuous problem is at least twice continuously differentiable. The plots seem to confirm these estimates.

In figure III.1.5, we plot the numerical solution of (III.1.1) discretized with the

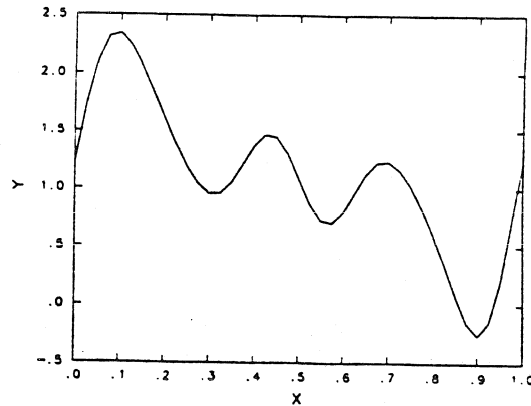


Figure III.1.3 Numerical solution of $R(x) = H(x)(R \circ \alpha)(x) + Q(x)$, discretized with 40 meshpoints and a second-order finite difference scheme. $H = .1$, $\alpha = x + .11 + .15 \sin(2\pi x)$, and $Q = 1 + .5 \sin(2\pi x) + .5 \sin(4\pi x) + .5 \sin(6\pi x) + .1 \sin(10\pi x)$.

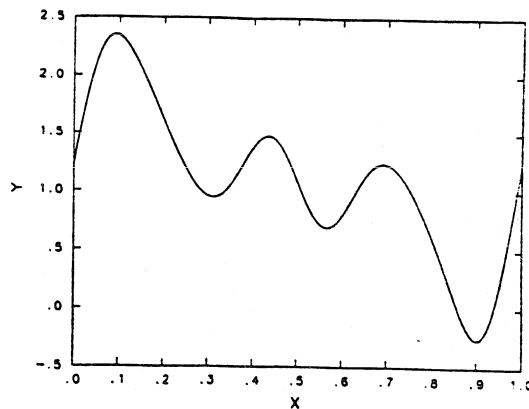


Figure III.1.4 Numerical solution of $R(x) = H(x)(R \circ \alpha)(x) + Q(x)$, discretized with 640 meshpoints and a second-order finite difference scheme. $H = .1$, $\alpha = x + .11 + .15 \sin(2\pi x)$, and $Q = 1 + .5 \sin(2\pi x) + .5 \sin(4\pi x) + .5 \sin(6\pi x) + .1 \sin(10\pi x)$.

scheme (III.1.2) and $n = 40$. The function Q is given by the expression (III.1.3), $\alpha = x + .11 + .5 \sin(2\pi x)$, and $H = .1$. In figure III.1.6, we plot the numerical solution of (III.1.1) with 640 meshpoints and the same functions Q , α , and H as in figure III.1.5.

In figure III.1.7, we plot the numerical solution of (III.1.1) discretized with the scheme (III.1.2) and $n = 40$. The function Q is given by the expression (III.1.3),

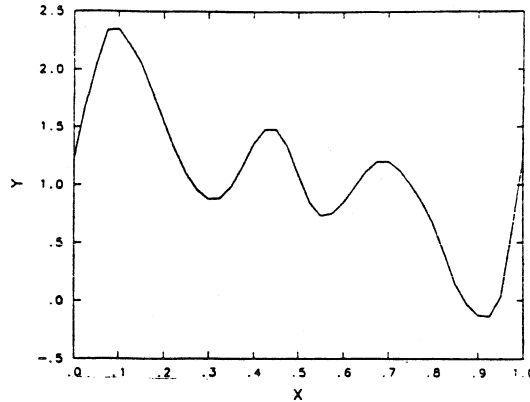


Figure III.1.5 Numerical solution of $R(x) = H(x)(R \circ \alpha)(x) + Q(x)$, discretized with 40 meshpoints and a second-order finite difference scheme. $H = .1$, $\alpha = x + .11 + .5 \sin(2\pi x)$, and $Q = 1 + .5 \sin(2\pi x) + .5 \sin(4\pi x) + .5 \sin(6\pi x) + .1 \sin(10\pi x)$.

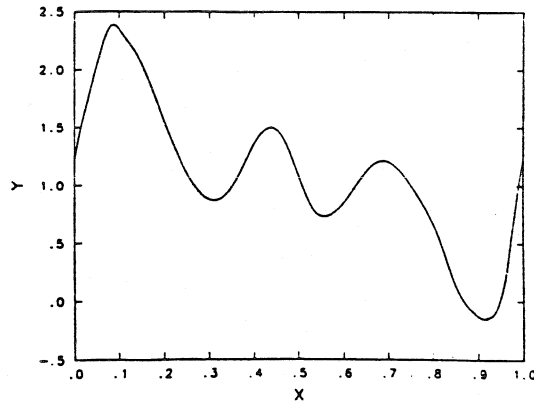


Figure III.1.6 Numerical solution of $R(x) = H(x)(R \circ \alpha)(x) + Q(x)$, discretized with 640 meshpoints and a second-order finite difference scheme. $H = .1$, $\alpha = x + .11 + .5 \sin(2\pi x)$, and $Q = 1 + .5 \sin(2\pi x) + .5 \sin(4\pi x) + .5 \sin(6\pi x) + .1 \sin(10\pi x)$.

$\alpha = x + .11 + .75 \sin(2\pi x)$, and $H = .1$. In figure III.1.8, we plot the numerical solution of (III.1.1) with 640 meshpoints and the same functions Q , α , and H as in figure III.1.7.

For figures III.1.5, III.1.6, III.1.7, and III.1.8, the estimates of table III.0.1 only show that the continuous solution is continuously differentiable. We see that the solution becomes less and less smooth, and from the plot of $c = .75$, we notice that

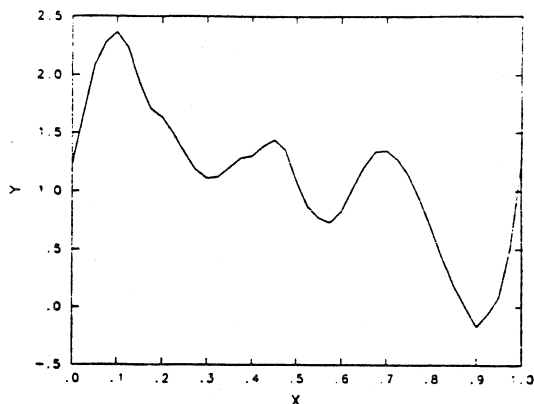


Figure III.1.7 Numerical solution of $R(x) = H(x)(R \circ \alpha)(x) + Q(x)$, discretized with 40 meshpoints and a second-order finite difference scheme. $H = .1$, $\alpha = x + .11 + .75 \sin(2\pi x)$, and $Q = 1 + .5 \sin(2\pi x) + .5 \sin(4\pi x) + .5 \sin(6\pi x) + .1 \sin(10\pi x)$.

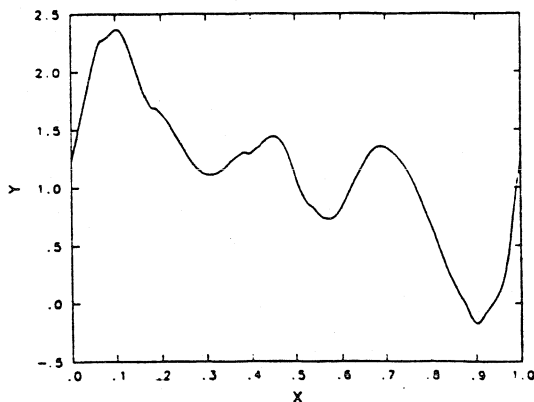


Figure III.1.8 Numerical solution of $R(x) = H(x)(R \circ \alpha)(x) + Q(x)$, discretized with 640 meshpoints and a second-order finite difference scheme. $H = .1$, $\alpha = x + .11 + .75 \sin(2\pi x)$, and $Q = 1 + .5 \sin(2\pi x) + .5 \sin(4\pi x) + .5 \sin(6\pi x) + .1 \sin(10\pi x)$.

the function is only continuously differentiable.

In figure III.1.9, we plot the numerical solution of (III.1.1) discretized with the scheme (III.1.2) and $n = 40$. For this figure, the function Q is given by the expression (III.1.3), $\alpha = x + .11 + 1.5 \sin(2\pi x)$, and $H = .1$. In figure III.1.10, we plot the numerical solution of (III.1.1) with 640 meshpoints and the same functions Q , α , and H as in figure III.1.9.

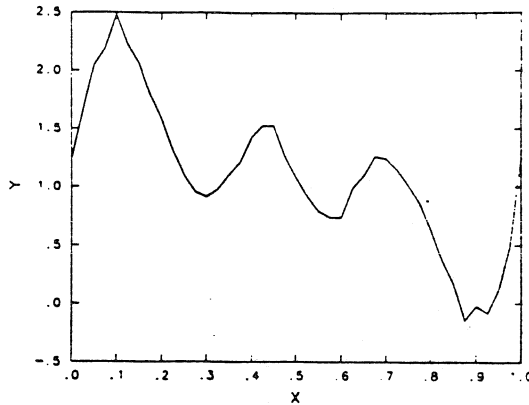


Figure III.1.9 Numerical solution of $R(x) = H(x)(R \circ \alpha)(x) + Q(x)$, discretized with 40 meshpoints and a second-order finite difference scheme. $H = .1$, $\alpha = x + .11 + 1.5 \sin(2\pi x)$, and $Q = 1 + .5 \sin(2\pi x) + .5 \sin(4\pi x) + .5 \sin(6\pi x) + .1 \sin(10\pi x)$.

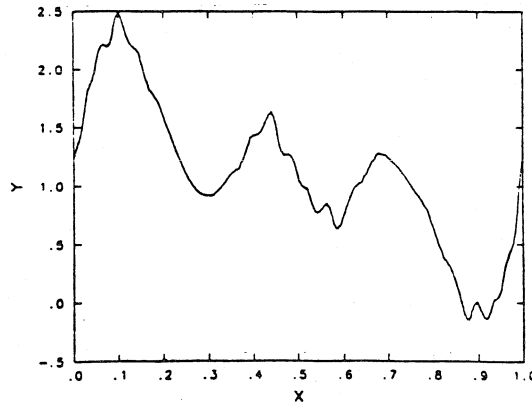


Figure III.1.10 Numerical solution of $R(x) = H(x)(R \circ \alpha)(x) + Q(x)$, discretized with 640 meshpoints and a second-order finite difference scheme. $H = .1$, $\alpha = x + .11 + 1.5 \sin(2\pi x)$, and $Q = 1 + .5 \sin(2\pi x) + .5 \sin(4\pi x) + .5 \sin(6\pi x) + .1 \sin(10\pi x)$.

In figure III.1.11, we plot the numerical solution of (III.1.1) discretized with the scheme (III.1.2) and $n = 40$. The function Q is given by the expression (III.1.3), $\alpha = x + .11 + 2 \sin(2\pi x)$, and $H = .1$. In figure III.1.12, we plot the numerical solution of (III.1.1) with 640 meshpoints and the same functions Q , α , and H as in figure III.1.11.

For figures III.1.9, III.1.10, III.1.11, and III.1.12, the solution of the continuous

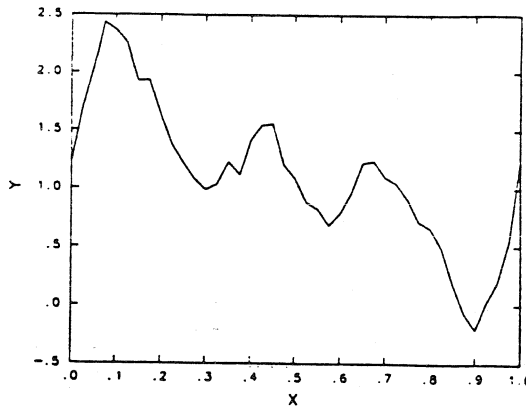


Figure III.1.11 Numerical solution of $R(x) = H(x)(R \circ \alpha)(x) + Q(x)$, discretized with 40 meshpoints and a second-order finite difference scheme. $H = .1$, $\alpha = x + .11 + 2 \sin(2\pi x)$, and $Q = 1 + .5 \sin(2\pi x) + .5 \sin(4\pi x) + .5 \sin(6\pi x) + .1 \sin(10\pi x)$.

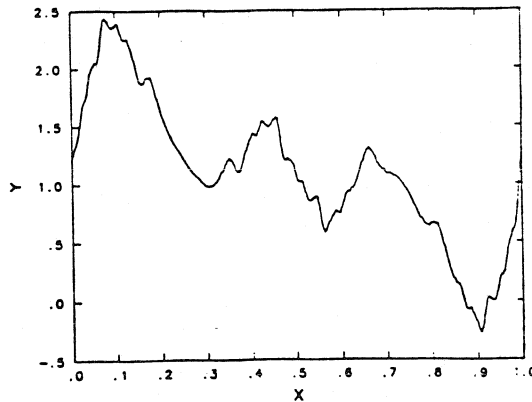


Figure III.1.12 Numerical solution of $R(x) = H(x)(R \circ \alpha)(x) + Q(x)$, discretized with 640 meshpoints and a second-order finite difference scheme. $H = .1$, $\alpha = x + .11 + 2 \sin(2\pi x)$, and $Q = 1 + .5 \sin(2\pi x) + .5 \sin(4\pi x) + .5 \sin(6\pi x) + .1 \sin(10\pi x)$.

problem is only supposed to be continuous. The estimates from table III.0.1 and the plots agree.

We want to see the influence of H on the solution of (III.1.1). To do that, we compute the numerical solution of (III.1.1) discretized with the scheme (III.1.2) and 640 meshpoints, with Q given by (III.1.3) and $H = .7$. As before, we compute it for different values of c .

In figure III.1.13, we plot the numerical solution of (III.1.1) discretized with the scheme (III.1.2) and $n = 640$. The function Q is given by the expression (III.1.3), $\alpha = x + .11$, and $H = .7$.

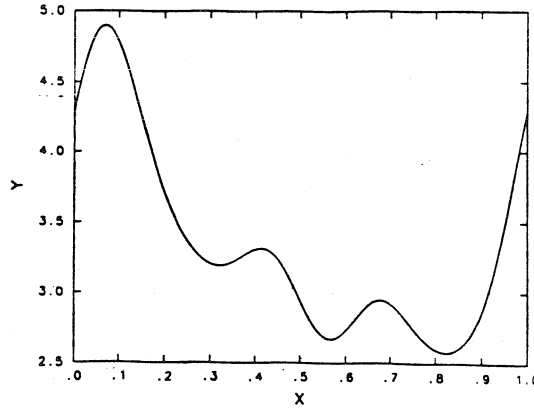


Figure III.1.13 Numerical solution of $R(x) = H(x)(R \circ \alpha)(x) + Q(x)$, discretized with 640 meshpoints and a second-order finite difference scheme. $H = .7$, $\alpha = x + .11$, and $Q = 1 + .5 \sin(2\pi x) + .5 \sin(4\pi x) + .5 \sin(6\pi x) + .1 \sin(10\pi x)$.

In figure III.1.14, we plot the numerical solution of (III.1.1) discretized with the scheme (III.1.2) and $n = 640$. The function Q is given by the expression (III.1.3), $\alpha = x + .11 + .15 \sin(2\pi x)$, and $H = .7$.

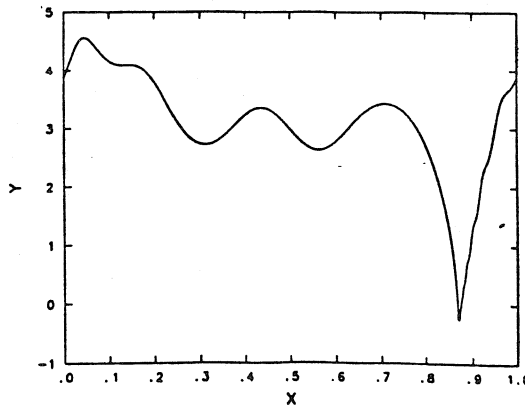


Figure III.1.14 Numerical solution of $R(x) = H(x)(R \circ \alpha)(x) + Q(x)$, discretized with 640 meshpoints and a second-order finite difference scheme. $H = .7$, $\alpha = x + .11 + .15 \sin(2\pi x)$, and $Q = 1 + .5 \sin(2\pi x) + .5 \sin(4\pi x) + .5 \sin(6\pi x) + .1 \sin(10\pi x)$.

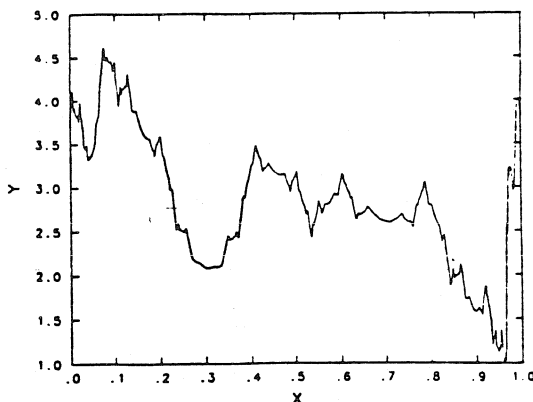


Figure III.1.15 Numerical solution of $R(x) = H(x) (R \circ \alpha)(x) + Q(x)$, discretized with 640 meshpoints and a second-order finite difference scheme. $H = .7$, $\alpha = x + .11 + .5 \sin(2\pi x)$, and $Q = 1 + .5 \sin(2\pi x) + .5 \sin(4\pi x) + .5 \sin(6\pi x) + .1 \sin(10\pi x)$.

In figure III.1.15, we plot the numerical solution of (III.1.1) discretized with the scheme (III.1.2) and $n = 640$. The function Q is given by the expression (III.1.3), $\alpha = x + .11 + .5 \sin(2\pi x)$, and $H = .7$.

In figure III.1.16, we plot the numerical solution of (III.1.1) discretized with the scheme (III.1.2) and $n = 640$. The function Q is given by the expression (III.1.3), $\alpha = x + .11 + .75 \sin(2\pi x)$, and $H = .7$.

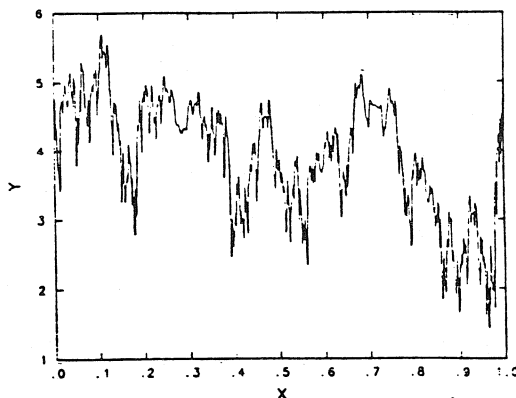


Figure III.1.16 Numerical solution of $R(x) = H(x) (R \circ \alpha)(x) + Q(x)$, discretized with 640 meshpoints and a second-order finite difference scheme. $H = .7$, $\alpha = x + .11 + .75 \sin(2\pi x)$, and $Q = 1 + .5 \sin(2\pi x) + .5 \sin(4\pi x) + .5 \sin(6\pi x) + .1 \sin(10\pi x)$.

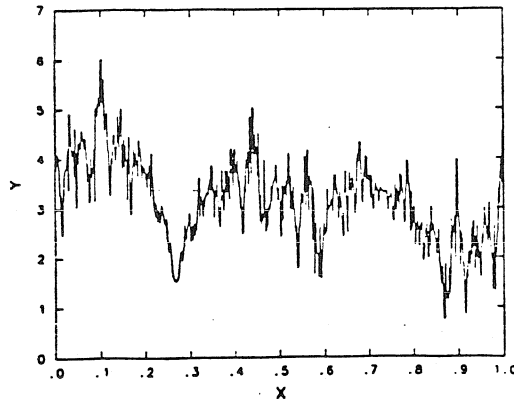


Figure III.1.17 Numerical solution of $R(x) = H(x)(R \circ \alpha)(x) + Q(x)$, discretized with 640 meshpoints and a second-order finite difference scheme. $H = .7$, $\alpha = x + .11 + 1.5 \sin(2\pi x)$, and $Q = 1 + .5 \sin(2\pi x) + .5 \sin(4\pi x) + .5 \sin(6\pi x) + .1 \sin(10\pi x)$.

In figure III.1.17, we plot the numerical solution of (III.1.1) discretized with the scheme (III.1.2) and $n = 640$. The function Q is given by the expression (III.1.3), $\alpha = x + .11 + 1.5 \sin(2\pi x)$, and $H = .7$.

In figure III.1.18, we plot the numerical solution of (III.1.1) discretized with the scheme (III.1.2) and $n = 640$. The function Q is given by the expression (III.1.3), $\alpha = x + .11 + 2 \sin(2\pi x)$, and $H = .7$.

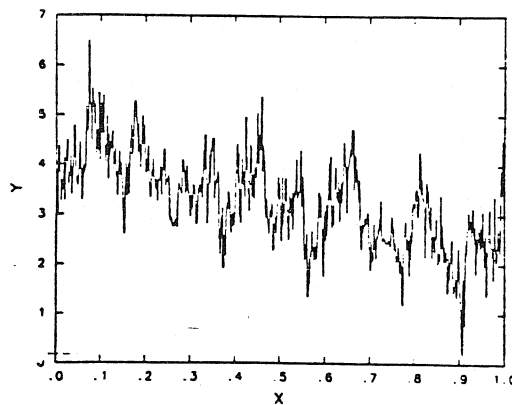


Figure III.1.18 Numerical solution of $R(x) = H(x)(R \circ \alpha)(x) + Q(x)$, discretized with 640 meshpoints and a second-order finite difference scheme. $H = .7$, $\alpha = x + .11 + 2 \sin(2\pi x)$, and $Q = 1 + .5 \sin(2\pi x) + .5 \sin(4\pi x) + .5 \sin(6\pi x) + .1 \sin(10\pi x)$.

From the different plots, we see that as $\|H\|_{\infty}$ gets larger, the solution becomes less smooth for the same value of the parameter c . This confirms the estimates from tables III.0.1 and III.0.2. We see that for values of c larger than 1, the solution for $H = .7$ is wilder than for $H = .1$.

Now we want to check the effect of the regularity of the continuous solution on the convergence of the finite difference scheme. We want to see whether the theoretical results of theorem II.3.1.1 are confirmed numerically. To do that, we have discretized (III.1.1) with the scheme (III.1.2), for $H = .1$, and for Q given by (III.1.3). We study numerically the error because we can get an explicit analytical expression for the solution of (II.0.1) or (II.0.2). The expression is given by the infinite series (II.1.6). (One only has to sum finitely many terms and can rigorously estimate the rest.)

In figure III.1.19, we plot the logarithm of the maximum norm of the error for different values of n , for $\alpha = x + .11 + c \sin(2\pi x)$, for $c = .001, .01, .05, .1, .14, 1/(2\pi), .5, .75, 1, 1.5, 2, 3, 4$, and for $H = .1$.

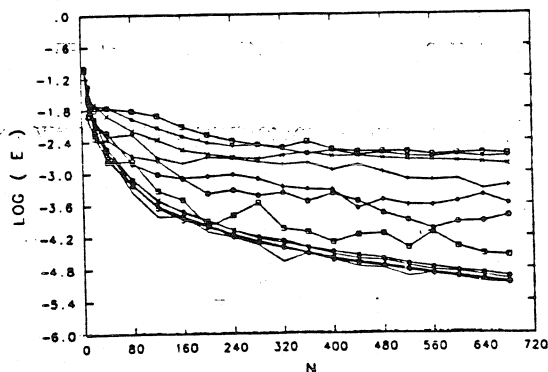


Figure III.1.19 The logarithm of the maximum norm of the error for different values of n , $n = 5, 10, 20, 40, 80, 120, 160, 200, 240, 280, 320, 360, 400, 440, 480, 520, 560, 600, 640, 680$, for $\alpha = x + .11 + c \sin(2\pi x)$, for $c = .001, .01, .05, .1, .14, 1/(2\pi), .5, .75, 1, 1.5, 2, 3, 4$, for $H = .1$, and for $Q = 1 + .5 \sin(2\pi x) + .5 \sin(4\pi x) + .5 \sin(6\pi x) + .1 \sin(10\pi x)$.

From figure III.1.19, we see that for $c = .001, .01, .05, .1, .14, 1/(2\pi)$, the envelope of the error curves is like $1/n^2$. So the error behaves like h^2 . For $c = .5, .75, 1$, we see that the envelope of the error curves is a hyperbola $1/n$. So the error behaves like h . For the other values of c the error is constant, independent of the number of meshpoints used. Moreover, table III.0.1 predicts that for $c = .001, .01, .05, .1, .14, 1/(2\pi)$, the solution of the continuous system is twice continuously

differentiable. For $c = .5, .75, 1$, it predicts that the solution of the continuous problem is only continuously differentiable. For the other values of the parameter c , it predicts that the solution is only continuous. Thus the theoretical results from theorem II.3.1.1 are confirmed by the numerical solutions.

In figure III.1.20, we have a Log-Log plot of the maximum norm of the error versus the number of meshpoints n , for $\alpha = x + .11 + c \sin(2\pi x)$, for $c = .001, .01, .05, .1, .14, 1/(2\pi), .5, .75, 1, 1.5, 2, 3, 4$, and for $H = .1$.

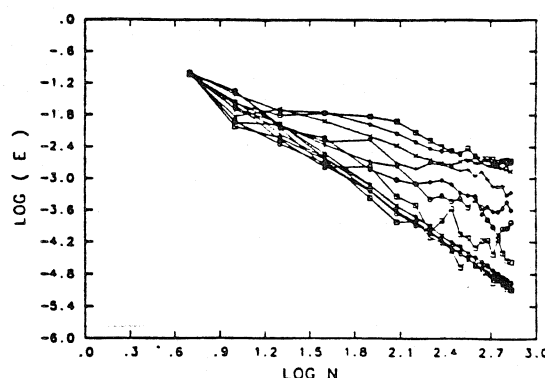


Figure III.1.20 Log-Log plot of the maximum norm of the error vs. the number of meshpoints n , $n = 5, 10, 20, 40, 80, 120, 160, 200, 240, 280, 320, 360, 400, 440, 480, 520, 560, 600, 640, 680$, for $\alpha = x + .11 + c \sin(2\pi x)$, for $c = .001, .01, .05, .1, .14, 1/(2\pi), .5, .75, 1, 1.5, 2, 3, 4$, for $H = .1$, and for $Q = 1 + .5 \sin(2\pi x) + .5 \sin(4\pi x) + .5 \sin(6\pi x) + .1 \sin(10\pi x)$.

From figure III.1.20, we see that for $c = .001, .01, .05, .1, .14, 1/(2\pi)$, the slope of the error curves is 2. So the scheme is second-order accurate. For $c = .5, .75, 1$, we see that the slope of the error curves is smaller than 2 and bigger than 1. For the other values of the parameter c , the slope is smaller than 1. Once again, the theoretical results of theorem II.3.1.1 are confirmed numerically.

In figure III.1.21, we plot the logarithm of the L_2 norm of the error for different values of n , for $\alpha = x + .11 + c \sin(2\pi x)$, for $c = .001, .01, .05, .1, .14, 1/(2\pi), .5, .75, 1, 1.5, 2, 3, 4$, and for $H = .1$.

Studying the L_2 norm of the error, we notice from figure III.1.21, that for $c = .001, .01, .05, .1, .14, 1/(2\pi)$, the error behaves like h^2 . For $c = .5, .75, 1$, the error behaves like h . For the other values of c , the error is constant and independent of the number of the meshpoints. Comparing figure III.1.19 and figure III.1.21, we see that when the solution is no longer twice continuously differentiable, there are less oscillations in the L_2 norm of the error than in the maximum norm.

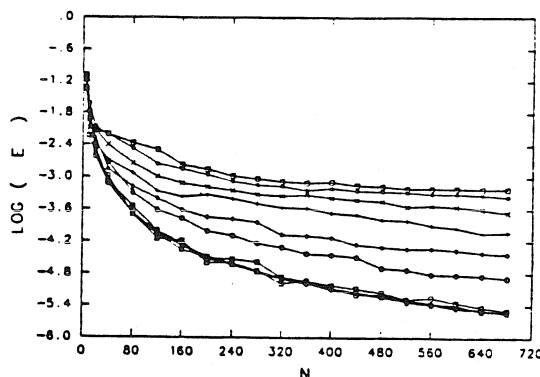


Figure III.1.21 The logarithm of the L_2 norm of the error for different values of n , $n = 5, 10, 20, 40, 80, 120, 160, 200, 240, 280, 320, 360, 400, 440, 480, 520, 560, 600, 640, 680$, for $\alpha = x + .11 + c \sin(2\pi x)$, for $c = .001, .01, .05, .1, .14, 1/(2\pi), .5, .75, 1, 1.5, 2, 3, 4$, for $H = .1$, and $Q = 1 + .5 \sin(2\pi x) + .5 \sin(4\pi x) + .5 \sin(6\pi x) + .1 \sin(10\pi x)$.

In figure III.1.22, we have a Log-Log plot of the L_2 norm of the error versus the number of meshpoints for different values of n , for $\alpha = x + .11 + c \sin(2\pi x)$, for $c = .001, .01, .05, .1, .14, 1/(2\pi), .5, .75, 1, 1.5, 2, 3, 4$, and for $H = .1$.

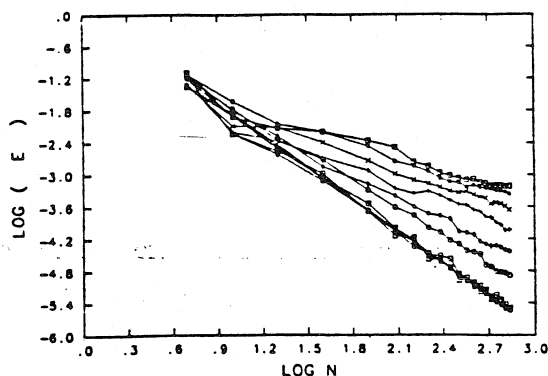


Figure III.1.22 Log-Log plot of the L_2 norm of the error vs. the number of meshpoints n , $n = 5, 10, 20, 40, 80, 120, 160, 200, 240, 280, 320, 360, 400, 440, 480, 520, 560, 600, 640, 680$, for $\alpha = x + .11 + c \sin(2\pi x)$, for $c = .001, .1, .05, .1, .14, 1/(2\pi), .5, .75, 1, 1.5, 2, 3, 4$, for $H = .1$, and for $Q = 1 + .5 \sin(2\pi x) + .5 \sin(4\pi x) + .5 \sin(6\pi x) + .1 \sin(10\pi x)$.

Studying the L_2 norm of the error, from figure III.1.22 we observe that for

$c = .001, .01, .05, .1, .14, 1/(2\pi)$, the slope of the curves is 2. For $c = .5, .75, 1$, the slope is smaller than 2 and bigger than 1. In the other cases, the slope is bigger than 1. As said before, when the solution is no longer twice continuously differentiable, the L_2 norm of the error oscillates less than the maximum norm.

In figure III.1.23, we plot the logarithm of the maximum norm of the error for different values of n , for $\alpha = x + .11 + c \sin(2\pi x)$, for $c = .001, .01, .05, .1, 1/(2\pi), .25, .5, .75, 1$, and for $H = .7$.

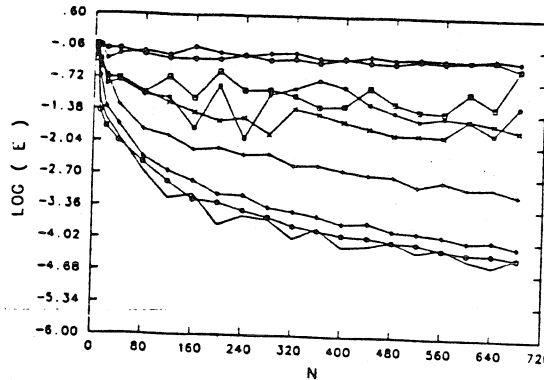


Figure III.1.23 The logarithm of the maximum norm of the error for different values of n , $n = 5, 10, 20, 40, 80, 120, 160, 200, 240, 280, 320, 360, 400, 440, 480, 520, 560, 600, 640, 680$, for $\alpha = x + .11 + c \sin(2\pi x)$, for $c = .001, .01, .05, .1, 1/(2\pi), .25, .5, .75, 1$, for $H = .7$, and for $Q = 1 + .5 \sin(2\pi x) + .5 \sin(4\pi x) + .5 \sin(6\pi x) + .1 \sin(10\pi x)$.

We see that for $c = .001, .01$, and $.05$, the error behaves like h^2 . For $c = .1, 1/(2\pi)$, it seems to behave like h . For the other values of c , the error looks independent of h and there is loss of convergence.

Figure III.1.24, exhibits a Log-Log plot of the maximum norm of the error versus the number of meshpoints n , for $\alpha = x + .11 + c \sin(2\pi x)$, for $c = .001, .01, .05, .1, 1/(2\pi), .25, .5, .75, 1$, and for $H = .7$.

This figure confirms the analytical results of table III.0.2. We note that for $c = .001, .01, .05$, the slope of the curve is 2. For $c = .1$, the slope is 1. For the other values of c , the envelope of the error curves is a line of slope 0.

In figure III.1.25, we plot the logarithm of the L_2 norm of the error for different values of n , for $\alpha = x + .11 + c \sin(2\pi x)$, for $c = .001, .01, .05, .1, 1/(2\pi), .25, .5, .75, 1$, and for $H = .7$.

From figure III.1.25, as in figure III.1.23, we observe that for $c = .001, .01, .05$, the L_2 norm of the error behaves like h^2 . For $c = .1, 1/(2\pi)$, the L_2 norm of the

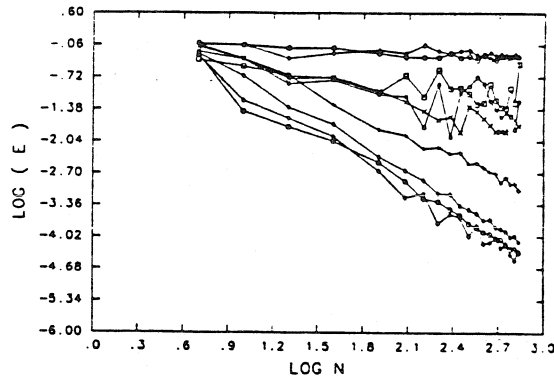


Figure III.1.24 Log-Log plot of the maximum norm of the error vs. the number of meshpoints n , $n = 5, 10, 20, 40, 80, 120, 160, 200, 240, 280, 320, 360, 400, 440, 480, 520, 560, 600, 640, 680$, for $\alpha = x + .11 + c \sin(2\pi x)$, $c = .001, .01, .05, .1, 1/(2\pi), .25, .5, .75, 1$, for $H = .7$, and for $Q = 1 + .5 \sin(2\pi x) + .5 \sin(4\pi x) + .5 \sin(6\pi x) + .1 \sin(10\pi x)$.

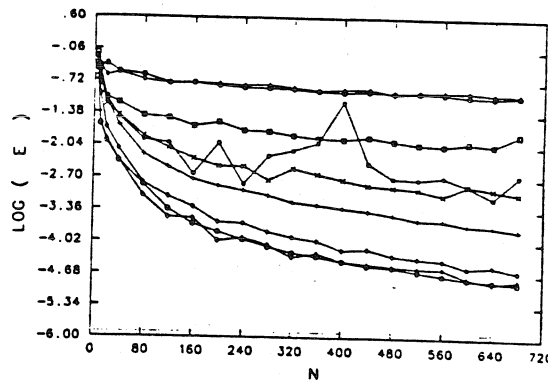


Figure III.1.25 The logarithm of the L_2 norm of the error for different values of n , $n = 5, 10, 20, 40, 80, 120, 160, 200, 240, 280, 320, 360, 400, 440, 480, 520, 560, 600, 640, 680$, for $\alpha = x + .11 + c \sin(2\pi x)$, for $c = .001, .01, .05, .1, 1/(2\pi), .25, .5, .75, 1$, for $H = .7$, and for $Q = 1 + .5 \sin(2\pi x) + .5 \sin(4\pi x) + .5 \sin(6\pi x) + .1 \sin(10\pi x)$.

error behaves like h . For larger values of c , it seems independent of the meshsize. As in the case $H = .1$, we notice that there are less oscillations in the L_2 norm of the error than in the maximum norm.

Figure III.1.26 shows a Log-Log plot of the L_2 norm of the error versus the

number of meshpoints n , for $\alpha = x + .11 + c \sin (2 \pi x)$, for $c = .001, .01, .05, .1, 1/(2 \pi), .25, .5, .75, 1$, and for $H = .7$.

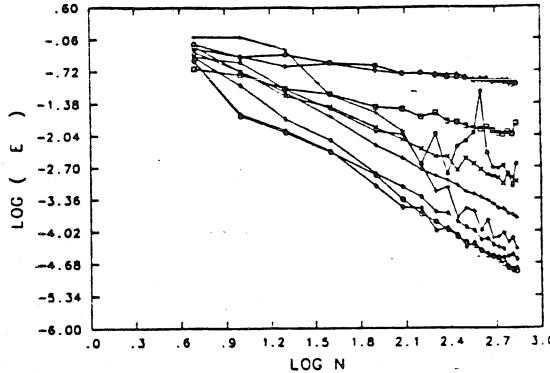


Figure III.1.26 Log-Log plot of the L_2 norm of the error vs. the number of meshpoints n , $n = 5, 10, 20, 40, 80, 120, 160, 200, 240, 280, 320, 360, 400, 440, 480, 520, 560, 600, 640, 680$, for $\alpha = x + .11 + c \sin (2 \pi x)$, for $c = .001, .01, .05, .1, 1/(2 \pi), .25, .5, .75, 1$, for $H = .7$, and for $Q = 1 + .5 \sin (2 \pi x) + .5 \sin (4 \pi x) + .5 \sin (6 \pi x) + .1 \sin (10 \pi x)$.

The results of figure III.1.26 confirm those of figure III.1.25.

If we compare the influence of the function H on the error, we see that as $|H|_\infty$ increases, the solution becomes less and less smooth and the magnitude of the error increases. For $c = 1$ and $H = .7$, we see that the computed solution is really wild, which is not the case for $c = 1$ and $H = .1$.

III.2 Third-Order Finite Difference Scheme

We have discretized (III.1.1) with the third-order finite difference scheme

$$(III.2.1) \quad \hat{R}_i = \tilde{H}_i \left(\frac{1}{2} (\theta_i^2 + \theta_i) \hat{R}_{j+1} + (1 - \theta_i^2) \hat{R}_j + \frac{1}{2} (\theta_i^2 - \theta_i) \hat{R}_{j-1} \right) + \tilde{Q}_i \quad i = 1, \dots, n.$$

Here \hat{R}_i is an approximation of $R(x_i)$, $\tilde{Q}_i = Q(x_i)$, $\tilde{H}_i = H(x_i)$, and $\theta_i h = \alpha(x_i) - x_j$ with $0 \leq \theta_i < 1$. As always, $x_m = (m - 1) h$ are the discrete points,

$m = 1, \dots, n$ and $h = 1/n$. As for the second-order finite difference scheme, the periodicity is enforced by identifying $j + n$ with j . The term $(\theta_i^2 + \theta_i) \widehat{R}_{j+1}/2 + (1 - \theta_i^2) \widehat{R}_j + (\theta_i^2 - \theta_i) \widehat{R}_{j-1}/2$ is a third-order finite difference approximation of $(R\alpha)(x_i)$. We Taylor expand $(R\alpha)(x_i)$ up to its third-order term, replace the first derivative of R at x_j by its second-order finite difference approximation, and replace the second derivative of R at x_j by its first-order finite difference approximation to get the above expression. The position of the meshpoint x_j depends on the function α . It is the nearest point from $\alpha(x_i)$ such that $0 \leq \alpha(x_i) - x_j < h$ modulo 1.

We have computed the numerical solution of (III.2.1) for two different values of H , one smaller than $8/17$ and the other larger. From these graphs, we conclude that the error bounds that were derived under the assumption $|H|_\infty < 8/17$, are still valid if $|H|_\infty > 8/17$.

In figure III.2.1, we plot the logarithm of the maximum norm of the error for different values of n , for $\alpha = x + .11 + c \sin(2\pi x)$, for $c = .001, .01, .05, .1, .14, 1/(2\pi), .5, .75, 1, 1.5, 2, 3, 4$, and for $H = .1$.

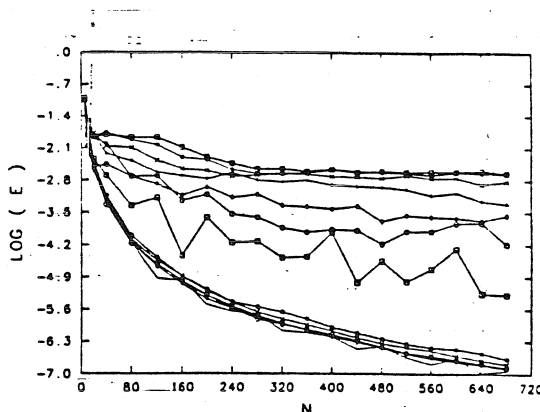


Figure III.2.1 The logarithm of the maximum norm of the error for different values of n , $n = 5, 10, 20, 40, 80, 120, 160, 200, 240, 280, 320, 360, 400, 440, 480, 520, 560, 600, 640, 680$, for $\alpha = x + .11 + c \sin(2\pi x)$, for $c = .001, .01, .05, .1, .14, 1/(2\pi), .5, .75, 1, 1.5, 2, 3, 4$, for $H = .1$, and for $Q = 1 + .5 \sin(2\pi x) + .5 \sin(4\pi x) + .5 \sin(6\pi x) + .1 \sin(10\pi x)$.

From figure III.2.1, we see that for $c = .001, .01, .05, .1, .14, 1/(2\pi)$, the envelope of the error curve goes like $1/n^3$. So the error behaves like h^3 . For $c = .5, .75, 1$, we see that the envelope of the error is a hyperbola $1/n$. So the error behaves like h . For the other values of c , the error is nearly constant, independent of the number of meshpoints used. From the results of table III.0.1, it seems that theoretical results agree with the numerical ones.

Figure III.2.2 shows a Log-Log plot of the maximum norm of the error versus the number of meshpoints n , for $\alpha = x + .11 + c \sin(2\pi x)$, for $c = .001, .01, .05, .1, .14, 1/(2\pi), .5, .75, 1, 1.5, 2, 3, 4$, and for $H = .1$.

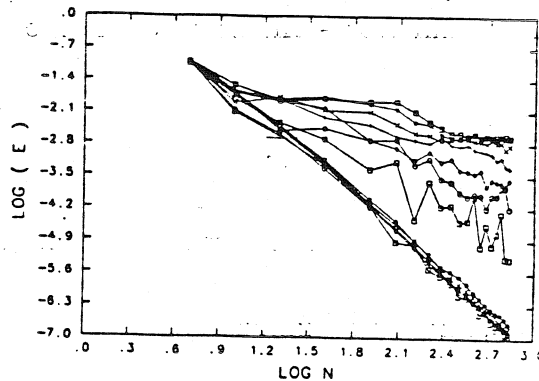


Figure III.2.2 Log-Log plot of the maximum norm of the error vs. the number of meshpoints n , $n = 5, 10, 20, 40, 80, 120, 160, 200, 240, 280, 320, 360, 400, 440, 480, 520, 560, 600, 640, 680$, for $\alpha = x + .11 + c \sin(2\pi x)$, for $c = .001, .01, .05, .1, .14, 1/(2\pi), .5, .75, 1, 1.5, 2, 3, 4$, for $H = .1$, and for $Q = 1 + .5 \sin(2\pi x) + .5 \sin(4\pi x) + .5 \sin(6\pi x) + .1 \sin(10\pi x)$.

From figure III.2.2, we see that the slope of the error curve is 3 when $c = .001, .01, .05, .1$, and $1/(2\pi)$. So the scheme is third-order accurate. For $c = .5, .75, 1$, we see that the slope of the error curve is smaller than 2 and bigger than 1. For the other values of the parameter c , the slope is smaller than 1. The theoretical results from theorem II.3.2.1 are thus confirmed numerically.

In figure III.2.3, we plot the logarithm of the L_2 norm of the error for different values of n , for $\alpha = x + .11 + c \sin(2\pi x)$, for $c = .001, .01, .05, .1, .14, 1/(2\pi), .5, .75, 1, 1.5, 2, 3, 4$, and for $H = .1$.

Studying the L_2 norm of the error, from figure III.2.3 we note that for $c = .001, .01, .05, .1$, and $1/(2\pi)$, the error behaves like h^3 . For $c = .5$, the error behaves like h^2 . For $c = .75$ and 1, the error behaves like h . For the other values of c , the error is constant and independent of the number of meshpoints. As for the second-order case, there are less oscillations in the L_2 norm of the error than in its maximum norm.

Figure III.2.4 exhibits a Log-Log plot of the L_2 norm of the error versus the number of meshpoints n , for $\alpha = x + .11 + c \sin(2\pi x)$, for $c = .001, .01, .05, .1, .14, 1/(2\pi), .5, .75, 1, 1.5, 2, 3, 4$, and for $H = .1$.

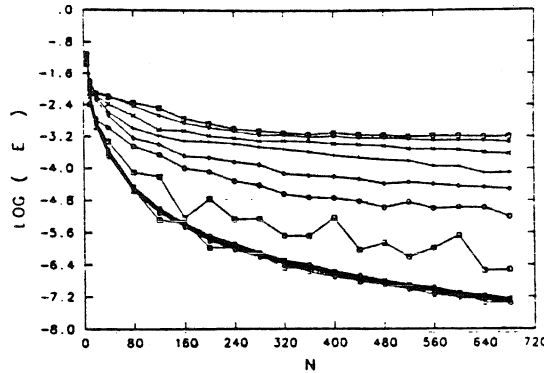


Figure III.2.3 The logarithm of the L_2 norm of the error for different values of n , $n = 5, 10, 20, 40, 80, 120, 160, 200, 240, 280, 320, 360, 400, 440, 480, 520, 560, 600, 640, 680$, for $\alpha = x + .11 + c \sin(2\pi x)$, for $c = .001, .01, .05, .1, .14, 1/(2\pi), .5, .75, 1, 1.5, 2, 3, 4$, for $H = .1$, and for $Q = 1 + .5 \sin(2\pi x) + .5 \sin(4\pi x) + .5 \sin(6\pi x) + .1 \sin(10\pi x)$.

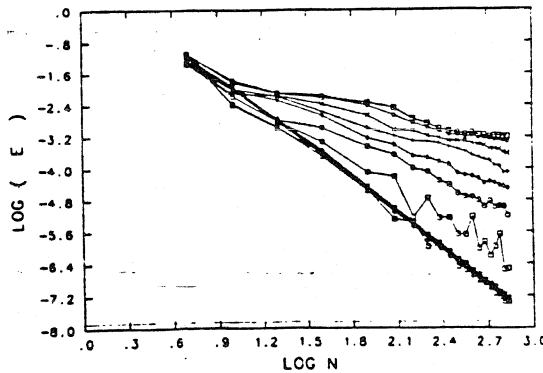


Figure III.2.4 Log-Log plot of the L_2 norm of the error vs. the number of mesh-points n , $n = 5, 10, 20, 40, 80, 120, 160, 200, 240, 280, 320, 360, 400, 440, 480, 520, 560, 600, 640, 680$, for $\alpha = x + .11 + c \sin(2\pi x)$, for $c = .001, .01, .05, .1, .14, 1/(2\pi), .5, .75, 1, 1.5, 2, 3, 4$, for $H = .1$, and for $Q = 1 + .5 \sin(2\pi x) + .5 \sin(4\pi x) + .5 \sin(6\pi x) + .1 \sin(10\pi x)$.

Studying the L_2 norm of the error, from figure III.2.4 we observe that the slope of the error curve is 3 for $c = .001, .01, .05, .1, .14$, and $1/(2\pi)$. For $c = .5$, the slope is smaller than 3 and bigger than 2. For $c = .75$ and 1, the slope is smaller than 2 and bigger than 1. In the other cases, the slope is smaller than 1. As

in the second-order case, when the solution is no longer three-times continuously differentiable, the L_2 norm of the error oscillates less than its maximum norm.

In figure III.2.5, we plot the logarithm of the maximum norm of the error for different values of n , for $\alpha = x + .11 + c \sin(2\pi x)$, for $c = .001, .01, .05, .1, 1/(2\pi), .25, .5, .75, 1$, and for $H = .7$.

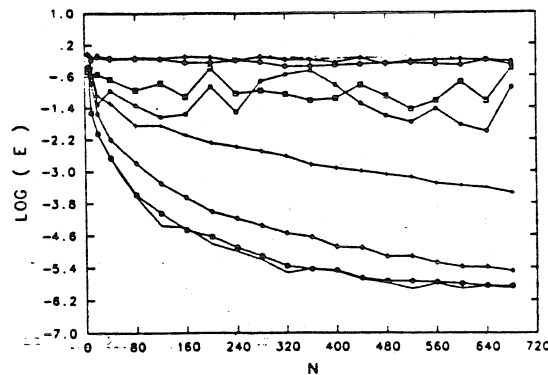


Figure III.2.5 The logarithm of the maximum norm of the error for different values of n , $n = 5, 10, 20, 40, 80, 120, 160, 200, 240, 280, 320, 360, 400, 440, 480, 520, 560, 600, 640, 680$, for $\alpha = x + .11 + c \sin(2\pi x)$, for $c = .001, .01, .05, .1, 1/(2\pi), .25, .5, .75, 1$, for $H = .7$, and for $Q = 1 + .5 \sin(2\pi x) + .5 \sin(4\pi x) + .5 \sin(6\pi x) + .1 \sin(10\pi x)$.

In figure III.2.5, we see that for $c = .001, .01$, and $.05$, the maximum norm of the error behaves like h^3 . For $c = .1$ and $1/(2\pi)$ it seems to behave like h . For the other values of c , the error looks independent of h and there is loss of convergence.

Figure III.2.6 shows a Log-Log plot of the maximum norm of the error versus the number of meshpoints n , for $\alpha = x + .11 + c \sin(2\pi x)$, for $c = .001, .01, .05, .1, 1/(2\pi), .25, .5, .75, 1$, and for $H = .7$.

Figure III.2.6 confirms the analytical results of table III.0.2. For $c = .001, .01$, and $.05$, the slope of the error curve is 2. For $c = .1$ the slope is 1. For the other values of c , the envelope of the error curve is a line of slope 0.

In figure III.2.7, we plot the logarithm of the L_2 norm of the error for different values of n , for $\alpha = x + .11 + c \sin(2\pi x)$, for $c = .001, .01, .05, .1, 1/(2\pi), .25, .5, .75, 1$, and for $H = .7$.

From figure III.2.7, we notice that for $c = .001, .01$, and $.05$, the L_2 norm of the error behaves like h^3 . For $c = .1$ and $1/(2\pi)$, it behaves like h . For larger values of the parameter c , it seems independent of the meshsize.

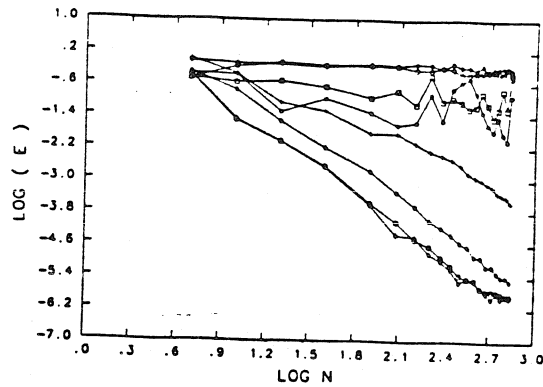


Figure III.2.6 Log-Log plot of the maximum norm of the error vs. the number of meshpoints n , $n = 5, 10, 20, 40, 80, 120, 160, 200, 240, 280, 320, 360, 400, 440, 480, 520, 560, 600, 640, 680$, for $\alpha = x + .11 + c \sin (2 \pi x)$, for $c = .001, .01, .05, .1, 1/(2 \pi), .25, .5, .75, 1$, for $H = .7$, and for $Q = 1 + .5 \sin (2 \pi x) + .5 \sin (4 \pi x) + .5 \sin (6 \pi x) + .1 \sin (10 \pi x)$.

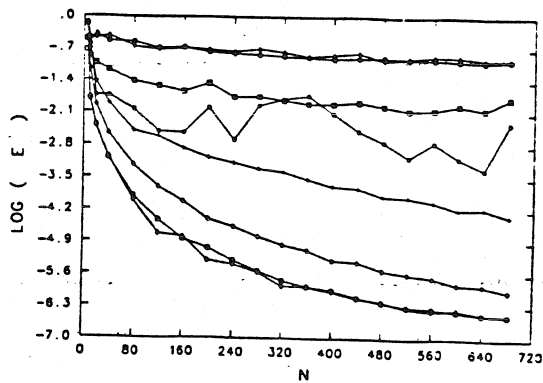


Figure III.2.7 The logarithm of the L_2 norm of the error for different values of n , $n = 5, 10, 20, 40, 80, 120, 160, 200, 240, 280, 320, 360, 400, 440, 480, 520, 560, 600, 640, 680$, for $\alpha = x + .11 + c \sin (2 \pi x)$, for $c = .001, .01, .05, .1, 1/(2 \pi), .25, .5, .75, 1$, for $H = .7$, and for $Q = 1 + .5 \sin (2 \pi x) + .5 \sin (4 \pi x) + .5 \sin (6 \pi x) + .1 \sin (10 \pi x)$.

Figure III.2.8 shows a Log-Log plot of the L_2 norm of the error versus the number of meshpoints n , for $\alpha = x + .11 + c \sin (2 \pi x)$, for $c = .001, .01, .05, .1, 1/(2 \pi), .25, .5, .75, 1$, and for $H = .7$.

The results from figure III.2.8 confirm those of figure III.2.7.

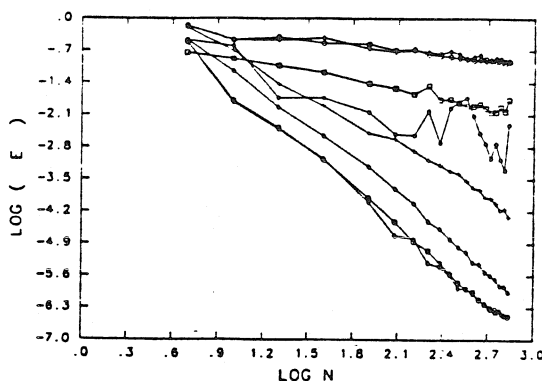


Figure III.2.8 Log-Log plot of the L_2 norm of the error vs. the number of mesh-points n , $n = 5, 10, 20, 40, 80, 120, 160, 200, 240, 280, 320, 360, 400, 440, 480, 520, 560, 600, 640, 680$, for $\alpha = x + .11 + c \sin (2 \pi x)$, for $c = .001, .01, .05, .1, 1/(2 \pi), .25, .5, .75, 1$, for $H = .7$, and for $Q = 1 + .5 \sin (2 \pi x) + .5 \sin (4 \pi x) + .5 \sin (6 \pi x) + .1 \sin (10 \pi x)$.

We remark that as in the second-order case, as $|H|_\infty$ increases, the solution becomes less and less smooth and the magnitude of the error increases.

III.3 Spline Interpolation Scheme

We numerically want to solve the equivalent of the system constituted of the equations

$$(III.3.1) \quad (S^* \circ \alpha)(x_i) = H_i^* R_i^* + Q_i^* \quad i = 1, \dots, n.$$

We are lead to the system of equations

$$(III.3.2) \quad (A R^*)_i = H_i^* R_i^* + Q_i^* \quad i = 1, \dots, n,$$

where R_i^* is an approximation of $R(x_i)$, $H_i^* = H(x_i)$, and $Q_i^* = Q(x_i)$. The spline operator A is such that $(A R^*)_i = (S^* \circ \alpha)(x_i)$, with S^* a 1-periodic cubic spline passing through the points R_j^* , $j = 1, \dots, n$. Here $x_m = (m - 1)h$ are the discrete points, $m = 1, \dots, n$, with $h = 1/n$.

We in fact want a numerical representation of the operator A defined in chapter II. We first set up the matrix F . This matrix F gives the right-hand-side \underline{F} in terms

of the data points R_i^* , such that $F \underline{R} = \underline{F}$. Then we set up the matrix M^{-1} , giving the vector of the moments \underline{M} in terms of the components of the vector \underline{F} and indirectly in terms of the data points R_i^* . Once we have these two matrices, we can have a representation of the spline operator A using the formulae (II.3.3.9) of chapter II for $i = 1, \dots, n$. Once we have a known expression for the moments M_j , we can compute the coefficients A_j and B_j for $j = 1, \dots, n$.

We have computed the numerical solution of (III.3.2) for two different values of H . Here we deal with a discrete equivalent of (II.0.2) instead of a discrete equivalent of (II.0.1).

In figure III.3.1, we plot the numerical solution of (II.0.2) discretized with the scheme (III.3.2) and 640 meshpoints. The function Q is given by the expression (III.1.3), $\alpha = x + .11$, and $H = 10$.

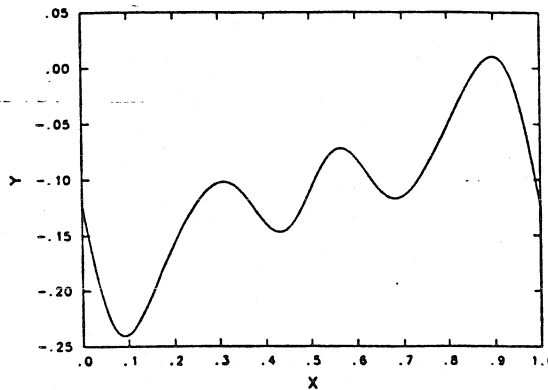


Figure III.3.1 Numerical solution of $(R \circ \alpha)(x) = H(x)R(x) + Q(x)$, discretized with 640 meshpoints and a cubic spline interpolation scheme. $H = 10$, $\alpha = x + .11$, and $Q = 1 + .5 \sin(2\pi x) + .5 \sin(4\pi x) + .5 \sin(6\pi x) + .1 \sin(10\pi x)$.

In figure III.3.2, we plot the numerical solution of (II.0.2) discretized with the scheme (III.3.2) and 640 meshpoints. The function Q is given by the expression (III.1.3), $\alpha = x + .11 + .15 \sin(2\pi x)$, and $H = 10$.

From figures III.3.1 and III.3.2, we notice that the plotted solution is smooth. The estimates from table III.0.1 are confirmed, even though these estimates were derived for the solution of (II.0.1). The equation (II.0.2) with $H = 10$ is equivalent to (II.0.1) with $H = .1$ if we choose the appropriate functions Q and \tilde{Q} for the equations (II.0.1) and (II.0.2) respectively.

In figure III.3.3, we plot the numerical solution of (II.0.2) discretized with the scheme (III.3.2) and 640 meshpoints. The function Q is given by the expression (III.1.3), $\alpha = x + .11 + .5 \sin(2\pi x)$, and $H = 10$.

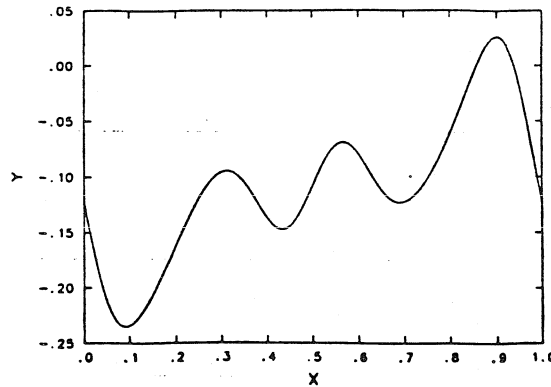


Figure III.3.2 Numerical solution of $(R \circ \alpha)(x) = H(x)R(x) + Q(x)$, discretized with 640 meshpoints and a cubic spline interpolation scheme. $H = 10$, $\alpha = x + .11 + .15 \sin(2\pi x)$, and $Q = 1 + .5 \sin(2\pi x) + .5 \sin(4\pi x) + .5 \sin(6\pi x) + .1 \sin(10\pi x)$.

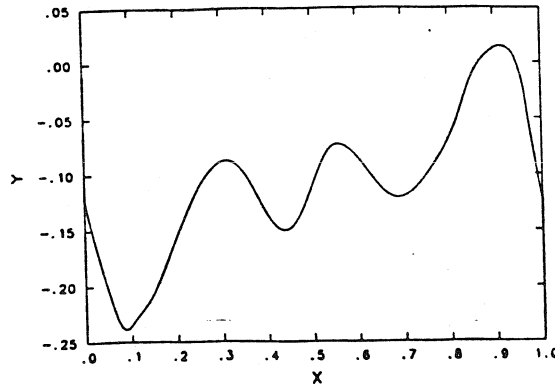


Figure III.3.3 Numerical solution of $(R \circ \alpha)(x) = H(x)R(x) + Q(x)$, discretized with 640 meshpoints and a cubic spline interpolation scheme. $H = 10$, $\alpha = x + .11 + .5 \sin(2\pi x)$, and $Q = 1 + .5 \sin(2\pi x) + .5 \sin(4\pi x) + .5 \sin(6\pi x) + .1 \sin(10\pi x)$.

In figure III.3.4, we plot the numerical solution of (II.0.2) discretized with the scheme (III.3.2) and 640 meshpoints. The function Q is given by the expression (III.1.3), $\alpha = x + .11 + .75 \sin(2\pi x)$, and $H = 10$.

From figures III.3.3 and III.3.4, we observe that the plotted solution is not as smooth as before. It is not obvious from figure III.3.3 that the solution is only continuously differentiable. From figure III.3.4, the estimates from table III.0.1 are

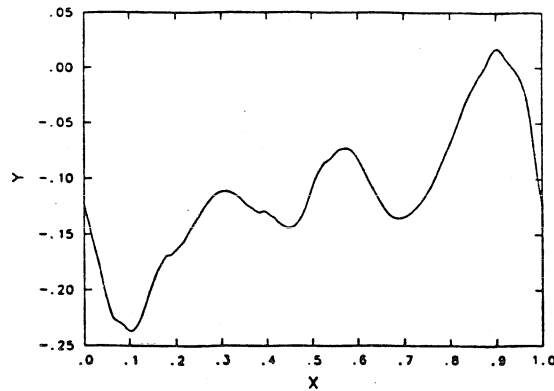


Figure III.3.4 Numerical solution of $(R \circ \alpha)(x) = H(x) R(x) + Q(x)$, discretized with 640 meshpoints and a cubic spline interpolation scheme. $H = 10$, $\alpha = x + .11 + .75 \sin(2\pi x)$, and $Q = 1 + .5 \sin(2\pi x) + .5 \sin(4\pi x) + .5 \sin(6\pi x) + .1 \sin(10\pi x)$.

confirmed.

In figure III.3.5, we plot the numerical solution of (II.0.2) discretized with the scheme (III.3.2) and 640 meshpoints. The function Q is given by the expression (III.1.3), $\alpha = x + .11 + 1.5 \sin(2\pi x)$, and $H = 10$.

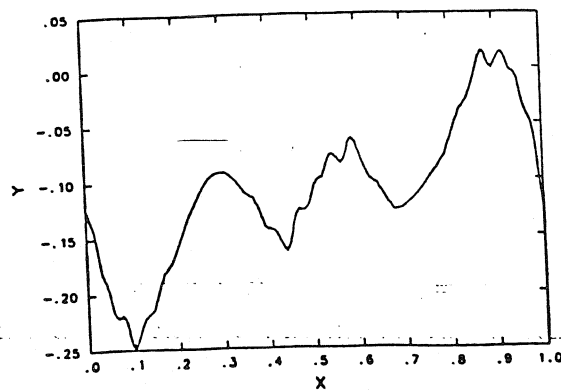


Figure III.3.5 Numerical solution of $(R \circ \alpha)(x) = H(x) R(x) + Q(x)$, discretized with 640 meshpoints and a cubic spline interpolation scheme. $H = 10$, $\alpha = x + .11 + 1.5 \sin(2\pi x)$, and $Q = 1 + .5 \sin(2\pi x) + .5 \sin(4\pi x) + .5 \sin(6\pi x) + .1 \sin(10\pi x)$.

In figure III.3.6, we plot the numerical solution of (II.0.2) discretized with the scheme (III.3.2) and 640 meshpoints. The function Q is given by the expression

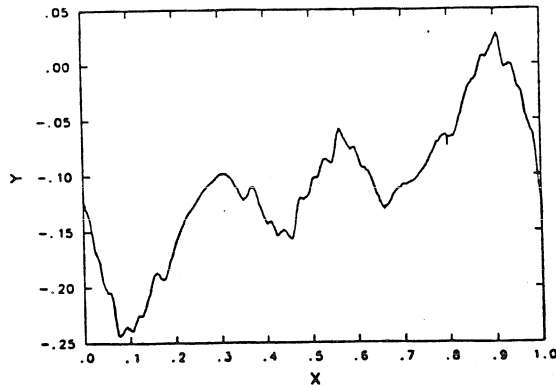


Figure III.3.6 Numerical solution of $(R \circ \alpha)(x) = H(x)R(x) + Q(x)$, discretized with 640 meshpoints and a cubic spline interpolation scheme. $H = 10$, $\alpha = x + .11 + 2 \sin(2\pi x)$, and $Q = 1 + .5 \sin(2\pi x) + .5 \sin(4\pi x) + .5 \sin(6\pi x) + .1 \sin(10\pi x)$.

(III.1.3), $\alpha = x + .11 + 2 \sin(2\pi x)$, and $H = 10$.

For figures III.3.5 and III.3.6, the solution of the continuous problem is only supposed to be continuous. The estimates from table III.0.1 and the plots agree.

In figure III.3.7, we plot the logarithm of the maximum norm of the error for different values of n , for $\alpha = x + .11 + c \sin(2\pi x)$, for $c = .001, .01, .05, .1, .15, .25, .5, .75, 1, 1.25, 1.5, 1.75, 2$, and for $H = 10$.

From figure III.3.7, we see that for $c = .001, .01, .05, .1$, and $.15$, the error behaves like h^4 . We see that for $c = .001, .01, .05$, and $.1$, this result was expected. For $c = .15$, the table III.0.1 tells us that the solution of the continuous problem is only three-times continuously differentiable. For $c = .25$, the error behaves nearly like h^4 , even though the estimates tell us that the solution of the continuous problem is only twice continuously differentiable. For $c = .5, .75, 1$, and 1.25 , the envelope of the error curves seems to behave like h . We see that as the value of the parameter c increases, the error gets larger. We notice that for $c = .5$, there are a lot of oscillations compared to the error curves for a smaller value of the parameter c . For $c = .75, 1$, and 1.25 , these oscillations have nearly disappeared but the envelope of the error curves is in $1/n$. For $c = 1.5, 1.75$, and 2 , the error seems constant and independent of the number of meshpoints.

In figure III.3.8, we have a Log-Log plot of the maximum norm of the error versus the number of meshpoints n , for $\alpha = x + .11 + c \sin(2\pi x)$, for $c = .001, .01, .05, .1, .15, .25, .5, .75, 1, 1.25, 1.5, 1.75, 2$, and for $H = 10$.

From figure III.3.8, we see that for $c = .001, .01, .05, .1$, and $.15$, the slope of the

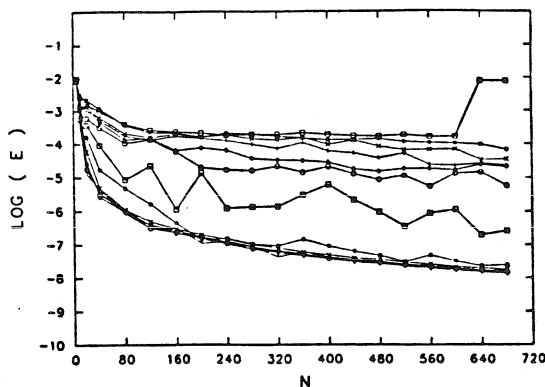


Figure III.3.7 The logarithm of the maximum norm of the error for different values of n , $n = 5, 10, 20, 40, 80, 120, 160, 200, 240, 280, 320, 360, 400, 440, 480, 520, 560, 600, 640, 680$, for $\alpha = x + .11 + c \sin(2\pi x)$, for $c = .001, .01, .05, .1, .15, .25, .5, .75, 1, 1.25, 1.5, 1.75, 2$, for $H = 10$, and for $Q = 1 + .5 \sin(2\pi x) + .5 \sin(4\pi x) + .5 \sin(6\pi x) + .1 \sin(10\pi x)$.

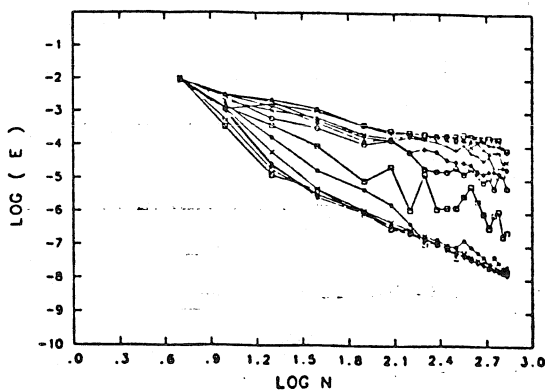


Figure III.3.8 Log-Log plot of the maximum norm of the error vs. the number of meshpoints n , $n = 5, 10, 20, 40, 80, 120, 160, 200, 240, 280, 320, 360, 400, 440, 480, 520, 560, 600, 640, 680$, for $\alpha = x + .11 + c \sin(2\pi x)$, for $c = .001, .01, .05, .1, .15, .25, .5, .75, 1, 1.25, 1.5, 1.75, 2$, for $H = 10$, and for $Q = 1 + .5 \sin(2\pi x) + .5 \sin(4\pi x) + .5 \sin(6\pi x) + .1 \sin(10\pi x)$.

error curve is 4. For $c = .25$, the slope of the error curve seems to be smaller than 4 but larger than 3 for small values of n then are the same as the error curves of slope 4. For $c = .5$, it is very difficult to determine a slope for the error curve because the error oscillates. The envelope seems to be a straight line of slope greater than

3 and lower than 2. For $c = .75, 1,$ and 1.25 , the slope of the error curve is greater than 2 and smaller than 1. For the other larger values of the parameter c , the slope is smaller than 1.

In figure III.3.9, we plot the logarithm of the L_2 norm of the error for different values of n , for $\alpha = x + .11 + c \sin(2\pi x)$, for $c = .001, .01, .05, .1, .15, .25, .5, .75, 1, 1.25, 1.5, 1.75, 2$, and for $H = 10$.

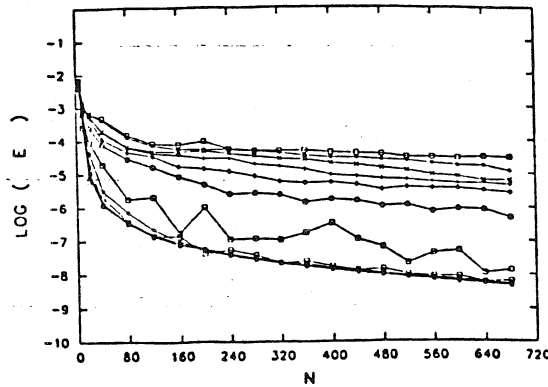


Figure III.3.9 The logarithm of the L_2 norm of the error for different values of n , $n = 5, 10, 20, 40, 80, 120, 160, 200, 240, 280, 320, 360, 400, 440, 480, 520, 560, 600, 640, 680$, for $\alpha = x + .11 + c \sin(2\pi x)$, for $c = .001, .01, .05, .1, .15, .25, .5, .75, 1, 1.25, 1.5, 1.75, 2$, for $H = 10$, and for $Q = 1 + .5 \sin(2\pi x) + .5 \sin(4\pi x) + .5 \sin(6\pi x) + .1 \sin(10\pi x)$.

From figure III.3.9, we see that for $c = .001, .01, .05, .1,$ and $.15$, the error behaves like h^4 . It is surprising to notice that the error behaves like h^4 for $c = .15$ because the solution of the continuous problem is only three-times continuously differentiable. For $c = .25$, the error is behaving nearly like h^4 . For $c = .5$, the error is still rather small but it oscillates a lot. From table III.0.1, for $c = .5$, the solution of the continuous problem is only continuously differentiable but the error curve shows it looks like h^2 at least. For $c = .75, 1,$ and 1.25 , the error behaves like h^2 . For the other larger values of the parameter considered, the error behaves nearly like h even though from the estimates of table III.0.1, we see that it should be independent of the number of meshpoints because the solution of the continuous problem is only continuous.

In figure III.3.10, we have a Log-Log plot of the L_2 norm of the error versus the number of meshpoints n , for $\alpha = x + .11 + c \sin(2\pi x)$, for $c = .001, .01, .05, .1, .15, .25, .5, .75, 1, 1.25, 1.5, 1.75, 2$, and for $H = 10$.

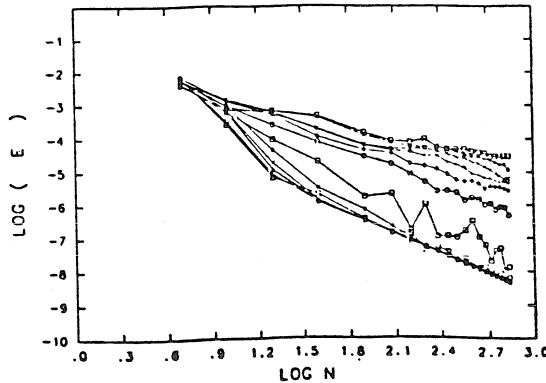


Figure III.3.10 Log-Log plot of the L_2 norm of the error vs. the number of meshpoints n , $n = 5, 10, 20, 40, 80, 120, 160, 200, 240, 280, 320, 360, 400, 440, 480, 520, 560, 600, 640, 680$, for $\alpha = x + .11 + c \sin(2\pi x)$, for $c = .001, .01, .05, .1, .15, .25, .5, .75, 1, 1.25, 1.5, 1.75, 2$, for $H = 10$, and for $Q = 1 + .5 \sin(2\pi x) + .5 \sin(4\pi x) + .5 \sin(6\pi x) + .1 \sin(10\pi x)$.

From figure III.3.10, we see that for $c = .001, .01, .05, .1$, and $.15$, the slope of the error curve is 4. For $c = .25$, the slope of the error curve is smaller than 4 for small values of n and is 4 for large values of n . The numerical error is smaller than expected for $c = .15$ and $.25$. From the theoretical results, we expected the error curves for $c = .15$ and $.25$ to have slope 3. For $c = .5$, the slope of the error curve is smaller than 4 but greater than 3. We notice that for $c = .5$ the error oscillates. For $c = .75$, the slope of the error curve is smaller than 3 but greater than 2. For $c = 1$ and 1.25 , the slope of the error curves is smaller than 2 and greater than 1. For the other larger values of the parameter c considered, the slope is smaller than 1 and greater than 0. For the other larger values of the parameter c considered, the behavior of the error is unexpected because from the theoretical results, we were supposed to get an error independent of the meshsize.

In figure III.3.11, we plot the numerical solution of (II.0.2) discretized with the scheme (III.3.2) and 640 meshpoints. The function Q is given by the expression (III.1.3), $\alpha = x + .11$, and $H = 10/7$.

From figure III.3.11, we notice that the plotted solution is smooth. The estimates from table III.0.2 are confirmed even though those estimates were derived for the solution of (II.0.1). The equation (II.0.2) with $H = 10/7$ is equivalent to (II.0.1) with $H = .7$ if we choose the appropriate functions Q and \tilde{Q} .

In figure III.3.12, we plot the numerical solution of (II.0.2) discretized with the scheme (III.3.2) and 640 meshpoints. The function Q is given by the expression

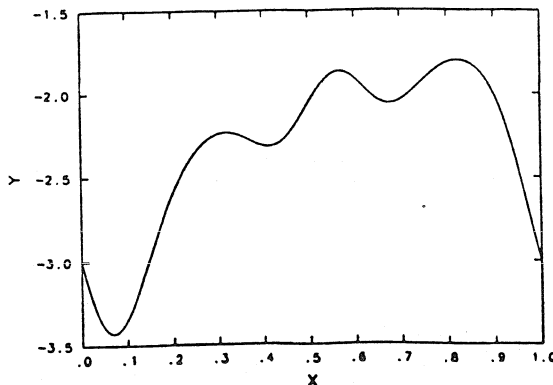


Figure III.3.11 Numerical solution of $(R \circ \alpha)(x) = H(x)R(x) + Q(x)$, discretized with 640 meshpoints and a cubic spline interpolation scheme. $H = 10/7$, $\alpha = x + .11$, and $Q = 1 + .5 \sin(2\pi x) + .5 \sin(4\pi x) + .5 \sin(6\pi x) + .1 \sin(10\pi x)$.

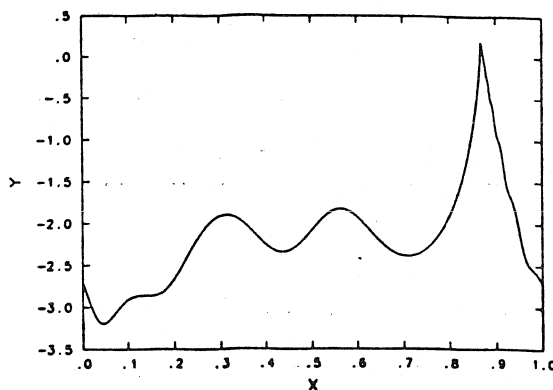


Figure III.3.12 Numerical solution of $(R \circ \alpha)(x) = H(x)R(x) + Q(x)$, discretized with 640 meshpoints and a cubic spline interpolation scheme. $H = 10/7$, $\alpha = x + .11 + .15 \sin(2\pi x)$, and $Q = 1 + .5 \sin(2\pi x) + .5 \sin(4\pi x) + .5 \sin(6\pi x) + .1 \sin(10\pi x)$.

(III.1.3), $\alpha = x + .11 + .15 \sin(2\pi x)$, and $H = 10/7$.

From figure III.3.12, we notice that the plotted solution has an infinite first derivative on the unit interval $[0, 1]$. From the estimates of table III.0.2, we know that the solution of the continuous problem (II.0.2) is only continuous. Away from the point where the first derivative is infinite, the plot shows that the solution is rather smooth. To get a better understanding of the behavior of the solution near the point where the first derivative becomes infinite, we could use local refinement.

We would like to know whether the loss of smoothness of the solution for $x \in [x_0, 1]$, x_0 the point where the first derivative seems to become infinite, is a numerical effect or not.

In figure III.3.13, we plot the numerical solution of (II.0.2) discretized with the scheme (III.3.2) and 640 meshpoints. The function Q is given by the expression (III.1.3), $\alpha = x + .11 + .5 \sin(2\pi x)$, and $H = 10/7$.

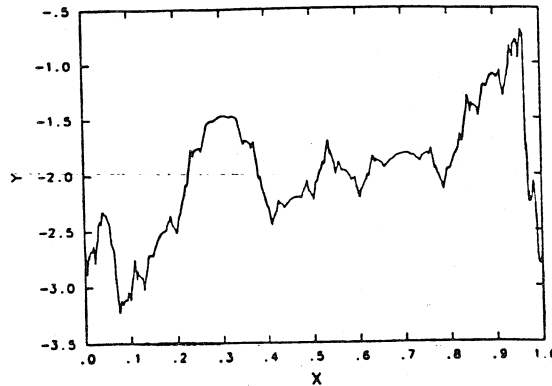


Figure III.3.13 Numerical solution of $(R \circ \alpha)(x) = H(x)R(x) + Q(x)$, discretized with 640 meshpoints and a cubic spline interpolation scheme. $H = 10/7$, $\alpha = x + .11 + .5 \sin(2\pi x)$, and $Q = 1 + .5 \sin(2\pi x) + .5 \sin(4\pi x) + .5 \sin(6\pi x) + .1 \sin(10\pi x)$.

In figure III.3.14, we plot the numerical solution of (II.0.2) discretized with the scheme (III.3.2) and 640 meshpoints. The function Q is given by the expression (III.1.3), $\alpha = x + .11 + .75 \sin(2\pi x)$, and $H = 10/7$.

In figure III.3.15, we plot the numerical solution of (II.0.2) discretized with the scheme (III.3.2) and 640 meshpoints. The function Q is given by the expression (III.1.3), $\alpha = x + .11 + 1.5 \sin(2\pi x)$, and $H = 10/7$.

In figure III.3.16, we plot the numerical solution of (II.0.2) discretized with the scheme (III.3.2) and 640 meshpoints. The function Q is given by the expression (III.1.3), $\alpha = x + .11 + 2 \sin(2\pi x)$, and $H = 10/7$.

From figures III.3.13, III.3.14, III.3.15, and III.3.16, we see that the solution is only continuous and it becomes wilder and wilder as the value of the parameter c increases. From these plots, we see that there is no point in trying local refinement because the local refinement criterion on such wild solutions will get us to refine everywhere on the unit interval $[0, 1]$. These plots confirm the estimates from table III.0.2.

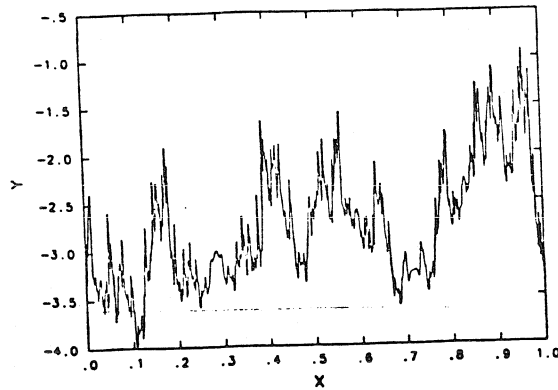


Figure III.3.14 Numerical solution of $(R \circ \alpha)(x) = H(x)R(x) + Q(x)$, discretized with 640 meshpoints and a cubic spline interpolation scheme. $H = 10/7$, $\alpha = x + .11 + .75 \sin(2\pi x)$, and $Q = 1 + .5 \sin(2\pi x) + .5 \sin(4\pi x) + .5 \sin(6\pi x) + .1 \sin(10\pi x)$.

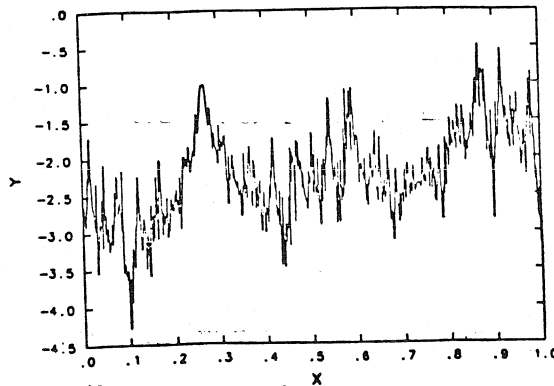


Figure III.3.15 Numerical solution of $(R \circ \alpha)(x) = H(x)R(x) + Q(x)$, discretized with 640 meshpoints and a cubic spline interpolation scheme. $H = 10/7$, $\alpha = x + .11 + 1.5 \sin(2\pi x)$, and $Q = 1 + .5 \sin(2\pi x) + .5 \sin(4\pi x) + .5 \sin(6\pi x) + .1 \sin(10\pi x)$.

In figure III.3.17, we plot the logarithm of the maximum norm of the error for different values of n , for $\alpha = x + .11 + c \sin(2\pi x)$, for $c = .001, .01, .05, .1, .15, .25, .5, .75, 1, 1.25, 1.5, 1.75, 2$, and for $H = 10/7$.

From figure III.3.17, we see that for $c = .001$, and $.01$ the error seems to behave like $1/n^4$. This result was expected. For $c = .05$, the error curve is not exactly like $1/n^4$ but is underneath the curve $1/n^3$. This result was far from being expected

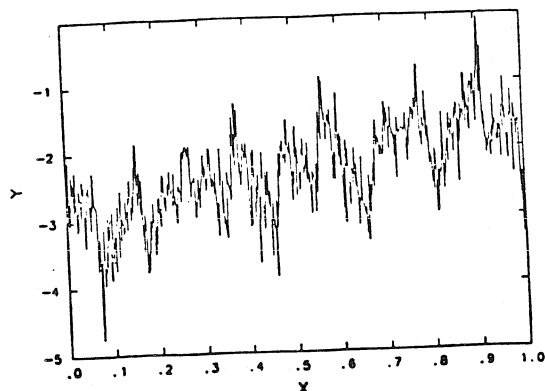


Figure III.3.16 Numerical solution of $(R\alpha)(x) = H(x)R(x) + Q(x)$, discretized with 640 meshpoints and a cubic spline interpolation scheme. $H = 10$, $\alpha = x + .11 + 2 \sin(2\pi x)$, and $Q = 1 + .5 \sin(2\pi x) + .5 \sin(4\pi x) + .5 \sin(6\pi x) + .1 \sin(10\pi x)$.

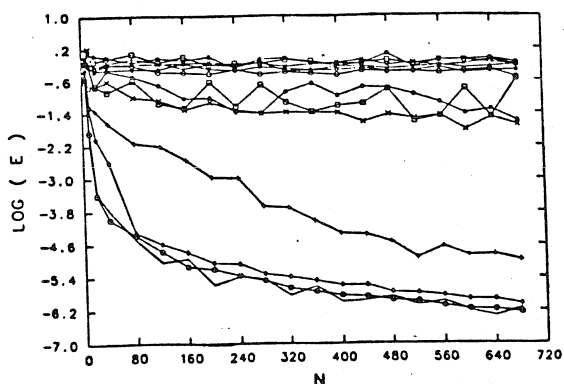


Figure III.3.17 The logarithm of the maximum norm of the error for different values of n , $n = 5, 10, 20, 40, 80, 120, 160, 200, 240, 280, 320, 360, 400, 440, 480, 520, 560, 600, 640, 680$, for $\alpha = x + .11 + c \sin(2\pi x)$, for $c = .001, .01, .05, .1, .15, .25, .5, .75, 1, 1.25, 1.5, 1.75, 2$, for $H = 10/7$, and for $Q = 1 + .5 \sin(2\pi x) + .5 \sin(4\pi x) + .5 \sin(6\pi x) + .1 \sin(10\pi x)$.

because the estimate from table III.0.2 tells us that the solution of the continuous problem for $c = .05$ is only continuously differentiable. For $c = .15$, the error curve behaves like $1/n^2$. Once more, this result is unexpected because the estimate from table III.0.2 tells us that for $c = .15$ the solution of the continuous problem is only continuous. For $c = .25, .5$, and $.75$, the envelope of the error curves seems to be

a hyperbola $1/n$. We notice in these cases that the error oscillates. For the other larger values of the parameter c considered, the error is constant and is independent of the meshsize.

In figure III.3.18, we have a Log-Log plot of the maximum norm of the error versus the number of meshpoints n , for $\alpha = x + .11 + c \sin(2\pi x)$, for $c = .001, .01, .05, .1, .15, .25, .5, .75, 1, 1.25, 1.5, 1.75, 2$, and for $H = 10/7$.

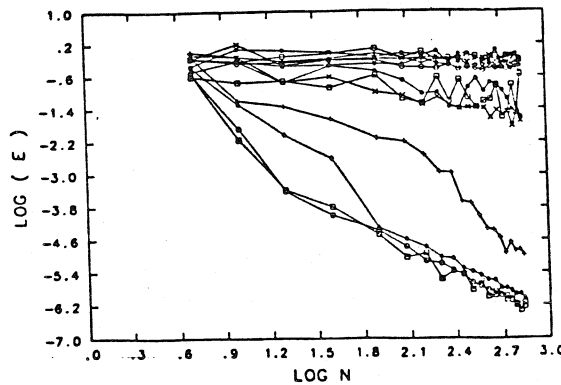


Figure III.3.18 Log-Log plot of the maximum norm of the error vs. the number of meshpoints n , $n = 5, 10, 20, 40, 80, 120, 160, 200, 240, 280, 320, 360, 400, 440, 480, 520, 560, 600, 640, 680$, for $\alpha = x + .11 + c \sin(2\pi x)$, for $c = .001, .01, .05, .1, .15, .25, .5, .75, 1, 1.25, 1.5, 1.75, 2$, for $H = 10/7$, and for $Q = 1 + .5 \sin(2\pi x) + .5 \sin(4\pi x) + .5 \sin(6\pi x) + .1 \sin(10\pi x)$.

From figure III.3.18, we see that for $c = .001$ and $.01$, the slope of the error curves is 4. For $c = .05$, the slope of the error curve seems to be smaller than 4 but larger than 3 for small values of n then are the same as the error curves of slope 4. For $c = .15$, the envelope of the error curve is a straight line of slope 2 even though for large values of n it seems to behave more like a straight line of slope 3. For $c = .25, .5$, and $.75$, the error curves seem to have as an envelope a straight line of slope smaller than 1 but larger than $.5$. For larger values of the parameter c considered, the error seems to be constant and independent of the number of meshpoints.

In figure III.3.19, we plot the logarithm of the L_2 norm of the error for different values of n , for $\alpha = x + .11 + c \sin(2\pi x)$, for $c = .001, .01, .05, .1, .15, .25, .5, .75, 1, 1.25, 1.5, 1.75, 2$, and for $H = 10/7$.

From figure III.3.19, we see that for $c = .001$, and $.01$ the error seems to behave like $1/n^4$. This result was expected. For $c = .05$, the error curve is not exactly like $1/n^4$ but is well underneath the curve $1/n^3$. This result was far from being

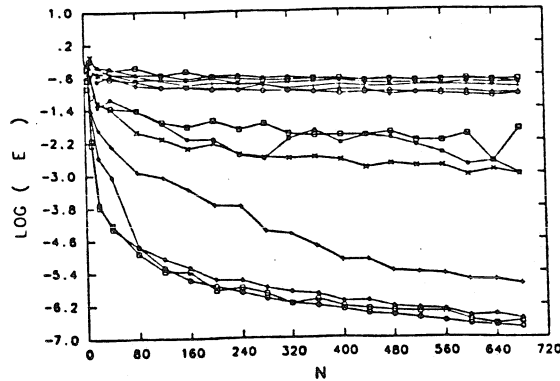


Figure III.3.19 The logarithm of the L_2 norm of the error for different values of n , $n = 5, 10, 20, 40, 80, 120, 160, 200, 240, 280, 320, 360, 400, 440, 480, 520, 560, 600, 640, 680$, for $\alpha = x + .11 + c \sin (2 \pi x)$, for $c = .001, .01, .05, .1, .15, .25, .5, .75, 1, 1.25, 1.5, 1.75, 2$, for $H = 10/7$, and for $Q = 1 + .5 \sin (2 \pi x) + .5 \sin (4 \pi x) + .5 \sin (6 \pi x) + .1 \sin (10 \pi x)$.

expected because the estimate from table III.0.2 tells us that the solution of the continuous problem for $c = .05$ is only continuously differentiable. For $c = .15$, the error curve behaves like $1/n^2$. Once more, this result is unexpected because the estimate from table III.0.2 tells us that for $c = .15$ the solution of the continuous problem is only continuous. For $c = .25, .5$, and $.75$, the envelope of the error curves seems to be a hyperbola $1/n$. We notice in these cases that the error oscillates. For the other larger values of the parameter c considered, the error is constant and is independent of the meshsize. As in previous cases, we notice that the L_2 norm of the error oscillates less than its maximum norm.

In figure III.3.20, we have a Log-Log plot of the L_2 norm of the error versus the number of meshpoints n , for $\alpha = x + .11 + c \sin (2 \pi x)$, for $c = .001, .01, .05, .1, .15, .25, .5, .75, 1, 1.25, 1.5, 1.75, 2$, and for $H = 10/7$.

From figure III.3.20, we see that for $c = .001$ and $.01$, the slope of the error curves is 4. For $c = .05$, the slope of the error curve seems to be smaller than 4 but larger than 3 for small values of n then are the same as the error curves of slope 4. For $c = .15$, the envelope of the error curve is a straight line of slope 2 even though for large values of n it seems to behave more like a straight line of slope 3. For $c = .25, .5$, and $.75$, the error curves seem to have as an envelope a straight line of slope smaller than 1 but larger than $.5$. For larger values of the parameter c considered, the error seems to be constant and independent of the number of meshpoints.

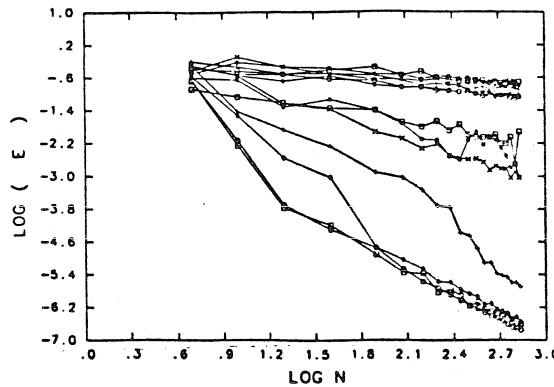


Figure III.3.20 Log-Log plot of the L_2 norm of the error vs. the number of meshpoints n , $n = 5, 10, 20, 40, 80, 120, 160, 200, 240, 280, 320, 360, 400, 440, 480, 520, 560, 600, 640, 680$, for $\alpha = x + .11 + c \sin(2\pi x)$, for $c = .001, .01, .05, .1, .15, .25, .5, .75, 1, 1.25, 1.5, 1.75, 2$, for $H = 10/7$, and for $Q = 1 + .5 \sin(2\pi x) + .5 \sin(4\pi x) + .5 \sin(6\pi x) + .1 \sin(10\pi x)$.

As already noticed for the second-order and third-order finite difference schemes, as \tilde{H} in (II.0.2) gets smaller but always larger than 1 or as H in (II.0.1) gets larger but always smaller than 1, the solution gets wilder and wilder.

III.4 Fourier Method

From theorem II.1.1, we know that the solution to (II.0.1) is defined on the unit circle S^1 . So we can approximate the solution to (II.0.1) by a truncated Fourier series,

$$(III.4.1) \quad R(x) = \sum_{l=-m}^n \hat{R}_l \exp(2\pi l x).$$

We use a fast Fourier transform method to compute the matrix and the right-hand-side of the system we want to solve to obtain the Fourier modes \hat{R}_l . We could have chosen the trapezoidal rule instead of a fast Fourier transform but the fast Fourier method is less costly. It is of the order $O(N \log(N))$ instead of $O(N^2)$ for the trapezoidal rule. The main work comes from the computation of the Fourier modes for the functions $H(x) \exp(2\pi l \alpha(x))$, $l = -m, \dots, n$. In the case we

have considered, we compute the Fourier modes for the functions $\exp(2\pi l \alpha(x))$ because we have chosen the function H to be constant. So we solve the system

$$(III.4.2) \quad (I - H A) \hat{R} = \hat{Q},$$

where \hat{R} is the vector of components $\hat{R}_l, l = -m, \dots, n$ and \hat{Q} , the vector of components $\hat{Q}_l, l = -m, \dots, n, \hat{Q}_l$ being the l -Fourier mode of the function Q . The matrix A is the matrix whose columns are the Fourier modes of the function $\exp(2\pi j \alpha(x))$.

We have computed a numerical solution of (II.0.1) for one value of $H, H = .1$. We have not done it for H larger because from the error curve we obtain and from the time spent computing the solution, we have realized that unless the analytical solution is extremely smooth, the Fourier method is not good.

In figure III.4.1, we plot the logarithm of the maximum norm of the error for different values of n , for $\alpha = x + .11 + c \sin(2\pi x)$, for $c = .001, .01, .05, .1, .14, 1/(2\pi), .5, 1, 2$, and for $H = .1$.

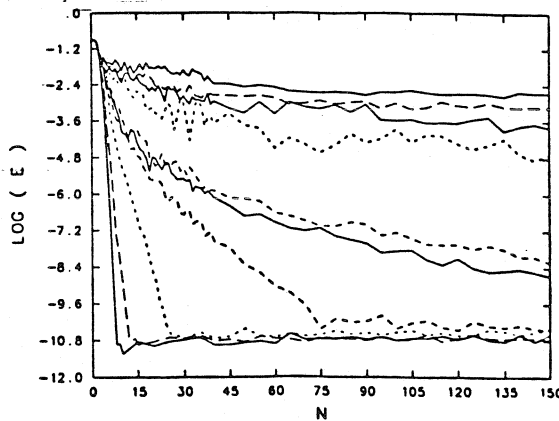


Figure III.4.1 The logarithm of the maximum norm of the error for different values of n , for $\alpha = x + .11 + c \sin(2\pi x)$, for $c = .001, .01, .05, .1, .14, 1/(2\pi), .5, 1, 2$, for $H = .1$, and for $Q = 1 + .5 \sin(2\pi x) + .5 \sin(4\pi x) + .5 \sin(6\pi x) + .1 \sin(10\pi x)$.

We see from figure III.4.1, that the larger parameter c gets, the more Fourier modes we need to reach machine precision for computations done in double precision on a sun workstation. As in the previous cases, we notice that we loose smoothness of the solution as the parameter c increases because for $c = .001$ and $c = .01$, we nearly have exponential convergence. For larger values of the parameter c , the convergence is no longer exponential. For $c = .05$, the error curve seems to behave like $1/n^k$, with $k = 6.77$. If we look at the curve for $c = .1$, the curve looks like $1/n^k$ with $k = 5.33$. For $c = .14$ and $c = 1/(2\pi)$, it looks like $1/n^k$ with $k = 3.5$.

For $c = .5$, the error curve behaves like $1/n^k$ with $k = 1.75$. For $c = 1$ and $c = 2$, the error curves look like $1/n^k$ with k respectively .92 and .69. For $c = 1$ or $c = 2$, we have lost convergence because the exponent k is smaller than 1.

In figure III.4.2, we have a Log-Log plot of the maximum norm of the error versus the number of modes n , for $\alpha = x + .11 + c \sin(2\pi x)$, for $c = .001, .01, .05, .1, .14, 1/(2\pi), .5, 1, 2$, and for $H = .1$.

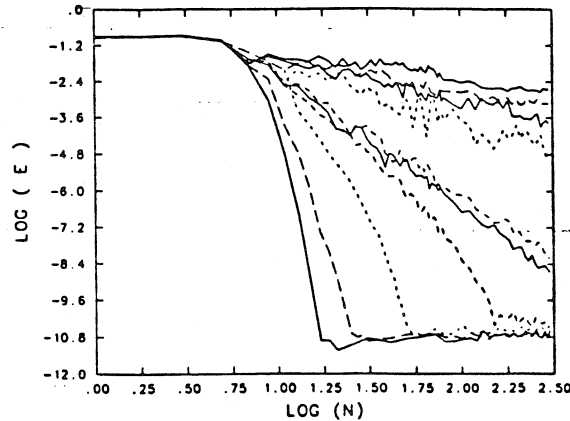


Figure III.4.2 Log-Log plot of the maximum norm of the error vs. the number of modes n , for $\alpha = x + .11 + c \sin(2\pi x)$, for $c = .001, .01, .05, .1, .14, 1/(2\pi), .5, 1, 2$, for $H = .1$, and for $Q = 1 + .5 \sin(2\pi x) + .5 \sin(4\pi x) + .5 \sin(6\pi x) + .1 \sin(10\pi x)$.

As from figure III.4.2, we notice that as the parameter c gets larger we need more and more Fourier modes to reach machine precision. We also notice the loss of smoothness of the analytical solution because the convergence is no longer exponential for $c > .01$. For $c = .05$, the slope of the error curve is 9.5. For $c = .1$ it is 6.7. For $c = .14$ and $c = 1/(2\pi)$, it is 3. For $c = .5$, it is 2.1. For $c = 1$, it is 1. For $c = 2$, it is smaller than 1, .8. For $c = 1$ and $c = 2$, we notice that the error is nearly independent of the number of modes used for the computation.

In figure III.4.3, we plot the logarithm of the L_2 norm of the error for different values of n , for $\alpha = x + .11 + c \sin(2\pi x)$, for $c = .001, .01, .05, .1, .14, 1/(2\pi), .5, 1, 2$, for $H = .1$.

Figure III.4.3 as in figure III.4.1 shows that as parameter c gets larger, we need more and more Fourier modes to reach machine precision. We notice that there are less oscillations in the L_2 norm of the error than in maximum norm. As for the maximum norm of the error, we see that for $c \leq .01$, the error decreases exponentially. For $c > .01$, the error doesn't behave exponentially. For $c = .05$ the error curve seems to behave like $1/n^k$ with $k = 7.5$. For $c = .1$, it looks like $1/n^k$

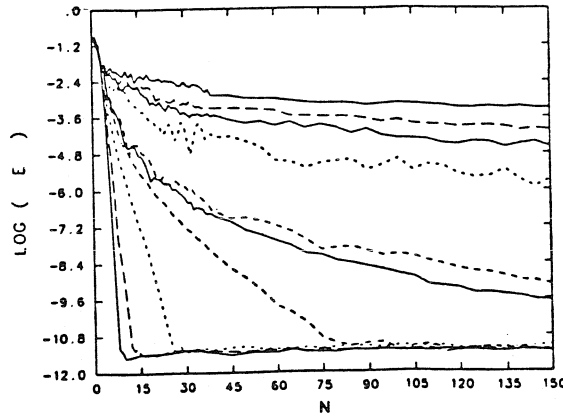


Figure III.4.3 The logarithm of the L_2 norm of the error for different values of n , for $\alpha = x + .11 + c \sin(2\pi x)$, for $c = .001, .01, .05, .1, .14, 1/(2\pi), .5, 1, 2$, for $H = .1$, and for $Q = 1 + .5 \sin(2\pi x) + .5 \sin(4\pi x) + .5 \sin(6\pi x) + .1 \sin(10\pi x)$.

with $k = 5.6$. For $c = .14$, it looks like $1/n^k$ with $k = 4$. For $c = 1/(2\pi)$, it is like $1/n^k$ with $k = 3.7$. For $c = .5$ it seems to behave like $1/n^k$ with $k = 2.2$. For $c = 1$, it looks like $1/n^k$ with $k = 1.4$ and for $c = 2$, it is like $1/n^k$ with $k = 1.15$.

In figure III.4.4, we have a Log-Log plot of the L_2 norm of the error versus the number of modes n , for $\alpha = x + .11 + c \sin(2\pi x)$, for $c = .001, .01, .05, .1, .14, 1/(2\pi), .5, 1, 2$, for $H = .1$.

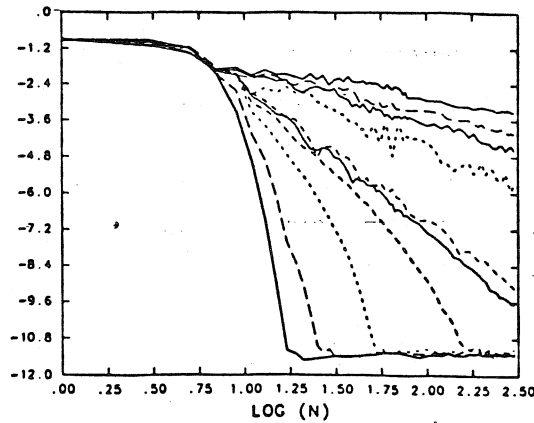


Figure III.4.4 Log-Log plot of the L_2 norm of the error vs. the number of modes n , for $\alpha = x + .11 + c \sin(2\pi x)$, for $c = .001, .01, .05, .1, .14, 1/(2\pi), .5, 1, 2$, for $H = .1$, and for $Q = 1 + .5 \sin(2\pi x) + .5 \sin(4\pi x) + .5 \sin(6\pi x) + .1 \sin(10\pi x)$.

In figure III.4.4, we notice that there are less oscillations in the L_2 norm of the error than in maximum norm. The previous remarks made on figures III.4.1,

III.4.2, and III.4.3 are still valid. For $c \leq .01$, the error curves seem to have an infinite slope, so the convergence is exponential. It is no longer true for $c > .01$. For $c = .05$, the slope of the error curve is 10. For $c = .1$, it is 7. For $c = .14$, it is 4.8. For $c = 1/(2\pi)$, it is 4.6. For $c = .5$, it is 2.8. For $c = 1$ and $c = 2$ it is a little bigger than 1, respectively 1.7 and 1.2.

From III.4.1, III.4.2, III.4.3, and III.4.4, we conclude that unless the solution of the model equation (II.0.1) is extremely smooth, the Fourier method is of little interest. That is due to two facts, the cost to implement it and the size of the error in general. We have noticed that the shift function α has two effects on the numerical solution. As the value of parameter c increases, the solution becomes less and less smooth, and more and more Fourier modes are needed to compute an accurate solution.

III.5 Comparison of the second-order finite difference, of the third-order finite difference, and of cubic spline interpolation schemes

We have seen from the previous sections that the Fourier method is of little interest because of its cost and of the loss of smoothness of the solution in most cases. From this, we deduce that the most interesting schemes to be studied are the second-order finite difference, the third-order finite difference, and the cubic spline interpolation schemes. Here we would like to compare the numerical errors for these three schemes, for the same value of the parameter c of the function α . We need to point out that for the second-order and third-order finite difference schemes, we numerically solve the equation (II.0.1) and that for the cubic spline interpolation scheme we solve the equation (II.0.2).

In figure III.5.1, we plot the logarithm of the maximum norm of the error for different values of n for the second-order finite difference, for the third-order finite difference, and for the cubic spline interpolation schemes, for $\alpha = x + .11 + .001 \sin(2\pi x)$.

From figure III.5.1, we see that for the second-order finite difference scheme the error behaves like $1/n^2$, for the third-order finite difference it behaves like $1/n^3$, and for the cubic spline interpolation scheme it behaves like $1/n^4$. From this plot, we notice that the initial error for the cubic spline interpolation scheme is much smaller than for the second-order and third-order finite difference schemes. It is difficult to figure out whether it comes from the scheme itself or from the equation we solve because as said before we numerically solve the equation (II.0.2) with the cubic spline interpolation scheme and the equation (II.0.1) with the other ones.

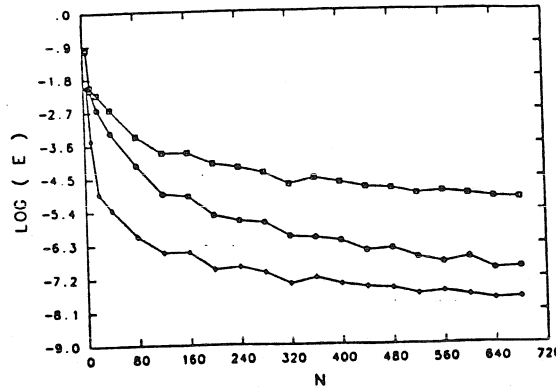


Figure III.5.1 The logarithm of the maximum norm of the error for different values of n , $n = 5, 10, 20, 40, 80, 120, 160, 200, 240, 280, 320, 360, 400, 440, 480, 520, 560, 600, 640, 680$, for a second-order finite difference, for a third-order finite difference, and for a cubic spline interpolation scheme. $\alpha = x + .11 + .001 \sin(2\pi x)$, $H = .1$ or $H = 10$, and $Q = 1 + .5 \sin(2\pi x) + .5 \sin(4\pi x) + .5 \sin(6\pi x) + .1 \sin(10\pi x)$.

In figure III.5.2, we plot the logarithm of the L_2 norm of the error for different values of n for the second-order finite difference, for the third-order finite difference, and for the cubic spline interpolation schemes, for $\alpha = x + .11 + .001 \sin(2\pi x)$.

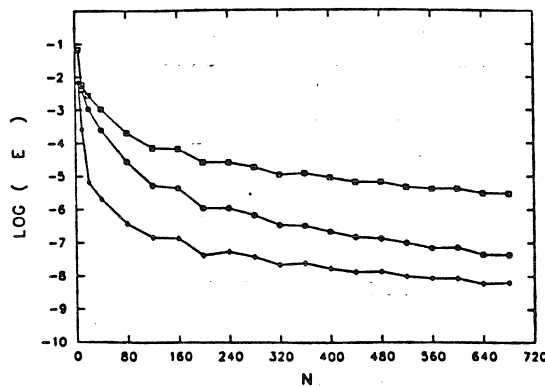


Figure III.5.2 The logarithm of the L_2 norm for different values of n , $n = 5, 10, 20, 40, 80, 120, 160, 200, 240, 280, 320, 360, 400, 440, 480, 520, 560, 600, 640, 680$, for a second-order finite difference, for a third-order finite difference, and for a cubic spline interpolation scheme. $\alpha = x + .11 + .001 \sin(2\pi x)$, $H = .1$ or $H = 10$, and $Q = 1 + .5 \sin(2\pi x) + .5 \sin(4\pi x) + .5 \sin(6\pi x) + .1 \sin(10\pi x)$.

From figure III.5.2, we see that for the second-order finite difference scheme the

error behaves like $1/n^2$, for the third-order finite difference scheme it behaves like $1/n^3$, and for the cubic spline interpolation scheme it behaves like $1/n^4$. From this plot, we notice that the initial error for the cubic spline interpolation scheme is much smaller than for the second-order and the third-order finite difference schemes.

If we have a Log-Log plot of the maximum norm of the error or of the L_2 norm of the error versus the number of meshpoints n , we have for the second-order finite difference scheme a curve of slope 2, for the third-order finite difference scheme a curve of slope 3, and for the cubic spline interpolation scheme a curve of slope 4.

In figure III.5.3, we plot the logarithm of the maximum norm of the error for different values of n for the second-order finite difference, for the third-order finite difference, and for the cubic spline interpolation schemes, for $\alpha = x + .11 + .5 \sin(2\pi x)$.

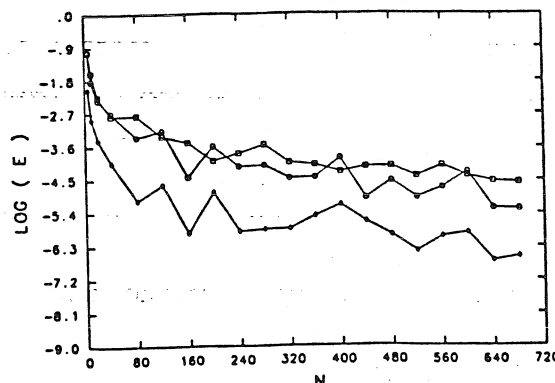


Figure III.5.3 The logarithm of the maximum norm of the error for different values of n , $n = 5, 10, 20, 40, 80, 120, 160, 200, 240, 280, 320, 360, 400, 440, 480, 520, 560, 600, 640, 680$, for a second-order finite difference, for a third-order finite difference, and for a cubic spline interpolation scheme. $\alpha = x + .11 + .5 \sin(2\pi x)$, $H = .1$ or $H = 10$, and $Q = 1 + .5 \sin(2\pi x) + .5 \sin(4\pi x) + .5 \sin(6\pi x) + 1. \sin(10\pi x)$.

From figure III.5.3, we see that for the second-order finite difference scheme the error behaves like $1/n^2$, for the third-order finite difference scheme it is a little better than second-order but not by much, and for the cubic spline interpolation scheme the envelope of the curve seems to be $1/n^2$. We notice that the error oscillates. These numerical results are better than the estimates obtained from the theoretical results, because the solution of the continuous problem is supposed to be only continuously differentiable.

In figure III.5.4, we plot the logarithm of the L_2 norm of the error for different values of n for the second-order finite difference, for the third-order finite difference,

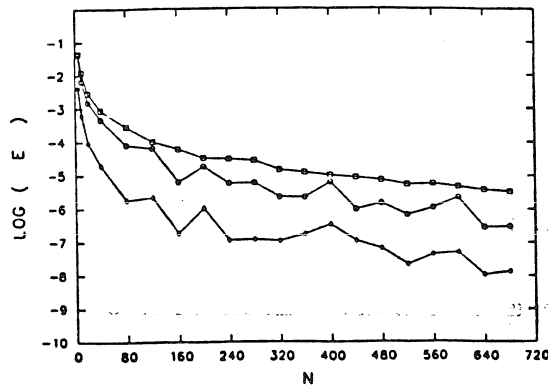


Figure III.5.4 The logarithm of the L_2 norm for different values of n , $n = 5, 10, 20, 40, 80, 120, 160, 200, 240, 280, 320, 360, 400, 440, 480, 520, 560, 600, 640, 680$, for a second-order finite difference, for a third-order finite difference, and for a cubic spline interpolation scheme. $\alpha = x + .11 + .5 \sin (2 \pi x)$, $H = .1$ or $H = 10$, and $Q = 1 + .5 \sin (2 \pi x) + .5 \sin (4 \pi x) + .5 \sin (6 \pi x) + .1 \sin (10 \pi x)$.

and for the cubic spline interpolation schemes, for $\alpha = x + .11 + .5 \sin (2 \pi x)$.

From figure III.5.4, we see that for the second-order finite difference scheme the error behaves like $1/n^2$, for the third-order finite difference scheme it is a little bit better than second-order but not by much, and for the cubic spline interpolation scheme the envelope of the error curve seems to be $1/n^2$. We see that the L_2 norm of the error for the second-order finite difference scheme does not oscillate. For the other schemes, it oscillates a little.

If we have a Log-Log plot of the maximum norm of the error versus the number of meshpoints n , we have for the second-order finite difference scheme a curve of slope 2, for the third-order finite difference scheme a curve of slope slightly larger than 2, and for the cubic spline interpolation scheme a curve of slope slightly larger than 2 also. These remarks still apply for the Log-Log plot of the L_2 norm of the error versus the number meshpoints n . We notice that the oscillations are less pronounced for the L_2 norm of the error than for the maximum norm and that the slopes for the third-order finite difference and for the cubic spline interpolation schemes are larger than for the maximum norm.

In figure III.5.5, we plot the logarithm of the maximum norm of the error for different values of n for the second-order finite difference, for the third-order finite difference, and for the cubic spline interpolation schemes, for $\alpha = x + .11 + \sin (2 \pi x)$.

From figure III.5.5, we see that for all three schemes, second-order finite difference scheme, third-order finite difference scheme, and cubic spline interpolation

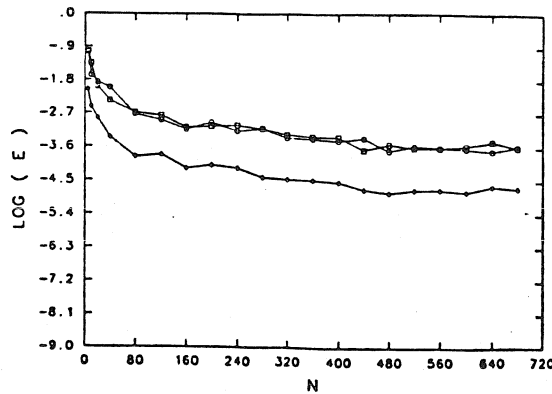


Figure III.5.5 The logarithm of the maximum norm of the error for different values of n , $n = 5, 10, 20, 40, 80, 120, 160, 200, 240, 280, 320, 360, 400, 440, 480, 520, 560, 600, 640, 680$, for a second-order finite difference, for a third-order finite difference, and for a cubic spline interpolation scheme. $\alpha = x + .11 + \sin(2\pi x)$, $H = .1$ or $H = 10$, and $Q = 1 + .5 \sin(2\pi x) + .5 \sin(4\pi x) + .5 \sin(6\pi x) + 1. \sin(10\pi x)$.

scheme, the error behaves like $1/n$. We don't gain anything by using high-order schemes assuming some smoothness of the solution of the continuous problem to numerically solve an equation whose solution is not smooth enough for the scheme.

In figure III.5.6, we plot the logarithm of the L_2 norm of the error for different values of n for the second-order finite difference, for the third-order finite difference, and for the cubic spline interpolation schemes, for $\alpha = x + .11 + \sin(2\pi x)$.

From figure III.5.6, we see that for all three schemes, second-order finite difference, third-order finite difference, and cubic spline interpolation schemes the error behaves like $1/n$. We don't gain anything by using high-order schemes assuming some smoothness of the solution of the continuous problem to numerically solve an equation whose solution is not smooth enough for the scheme.

If we have a Log-Log plot of the maximum norm of the error or of the L_2 norm of the error versus the number of meshpoints n , we have for all three schemes a curve of slope 1.

In figure III.5.7, we plot the logarithm of the maximum norm of the error for different values of n for the second-order finite difference, for the third-order finite difference, and for the cubic spline interpolation schemes, for $\alpha = x + .11 + 2 \sin(2\pi x)$.

From figure III.5.7, we see that for all three schemes, second-order finite difference scheme, third-order finite difference scheme, and cubic spline interpolation scheme, the error is independent of the number of meshpoints.

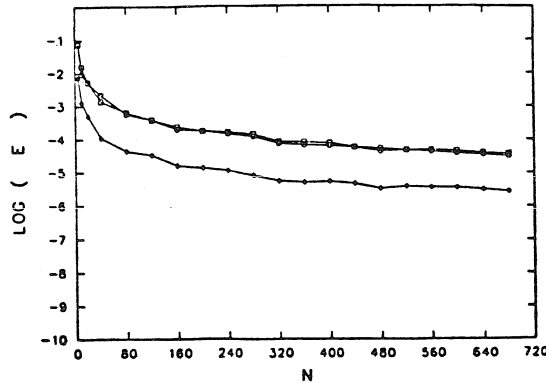


Figure III.5.6 The logarithm of the L_2 norm for different values of n , $n = 5, 10, 20, 40, 80, 120, 160, 200, 240, 280, 320, 360, 400, 440, 480, 520, 560, 600, 640, 680$, for a second-order finite difference, for a third-order finite difference, and for a cubic spline interpolation scheme. $\alpha = x + .11 + \sin(2\pi x)$, $H = .1$ or $H = 10$, and $Q = 1 + .5 \sin(2\pi x) + .5 \sin(4\pi x) + .5 \sin(6\pi x) + .1 \sin(10\pi x)$.

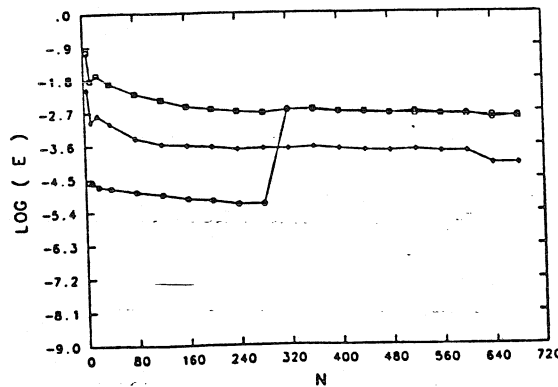


Figure III.5.7 The logarithm of the maximum norm of the error for different values of n , $n = 5, 10, 20, 40, 80, 120, 160, 200, 240, 280, 320, 360, 400, 440, 480, 520, 560, 600, 640, 680$, for a second-order finite difference, for a third-order finite difference, and for a cubic spline interpolation scheme. $\alpha = x + .11 + 2 \sin(2\pi x)$, $H = .1$ or $H = 10$, and $Q = 1 + .5 \sin(2\pi x) + .5 \sin(4\pi x) + .5 \sin(6\pi x) + 1. \sin(10\pi x)$.

In figure III.5.8, we plot the logarithm of the L_2 norm of the error for different values of n for the second-order finite difference, for the third-order finite difference, and for the cubic spline interpolation schemes, for $\alpha = x + .11 + 2 \sin(2\pi x)$.

From figure III.5.8, we see that for all three schemes, second-order finite dif-

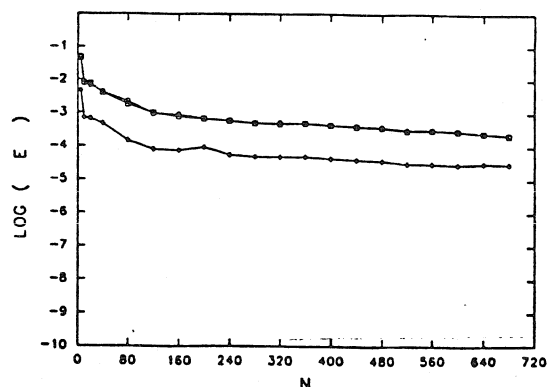


Figure III.5.8 The logarithm of the L_2 norm for different values of n , $n = 5, 10, 20, 40, 80, 120, 160, 200, 240, 280, 320, 360, 400, 440, 480, 520, 560, 600, 640, 680$, for a second-order finite difference, for a third-order finite difference, and for a cubic spline interpolation scheme. $\alpha = x + .11 + 2 \sin (2 \pi x)$, $H = .1$ or $H = 10$, and $Q = 1 + .5 \sin (2 \pi x) + .5 \sin (4 \pi x) + .5 \sin (6 \pi x) + .1 \sin (10 \pi x)$.

ference scheme, third-order finite difference scheme, and cubic spline interpolation scheme, the error is independent of the number of meshpoints.

We have in section 3 of this chapter plotted the solution of (II.0.2) discretized with a cubic spline interpolation scheme for $H = 10/7$. We also have numerically solved (II.0.1), which has been discretized with a second-order and third-order finite difference scheme for $H = .7$. We can as for $H = .1$ or $H = 10$ compare the error curves for these three different schemes. We will obtain for $H = .7$ or $H = 10/7$ results of a similar type to the ones obtained for $H = .1$ or $H = 10$.

CHAPTER IV

CONCLUSIONS AND DISCUSSION

We have shown that the solution of a functional equation under certain restrictions on the coefficient functions H , Q , and α of the equation exists and is unique. We also have proven that under even more restrictions on the functions H and α that the solution of the continuous problem is k -times continuously differentiable. We have analytically studied the behavior of the discretization error when we discretize the continuous equation with second-order and third-order finite difference schemes, with a cubic spline interpolation scheme, and when the solution of the continuous problem is approximated with a truncated Fourier series. We first have derived estimates when the functional equation is discretized with a second-order finite difference scheme. We have considered the cases of the solution of the continuous problem being at least twice continuously differentiable, being continuously differentiable, and being only continuous. We have then derived error estimates when the functional equation is discretized with a third-order finite difference scheme. We have considered the cases of the solution of the continuous problem being at least three-times continuously differentiable, being twice continuously differentiable, being continuously differentiable, and being only continuous. We have also studied the behavior of the error when the functional equation is discretized with a cubic spline interpolation scheme. We have considered the cases of the solution of the continuous problem being at least four-times continuously differentiable, being three-times continuously differentiable, being twice continuously differentiable, being continuously differentiable, and being only continuous. We have derived an estimate in L_2 norm for the continuous operator

$$L: \begin{cases} C \rightarrow C \\ R \rightarrow R \circ \alpha \end{cases},$$

where C is the set of continuous functions defined on the unit circle S^1 .

We have plotted the numerical solution of the functional equation for the parameters $H = .1$ and $\alpha = x + .11 + c \sin(2\pi x)$ with $0 \leq c \leq 2$ and for the parameters $H = .7$ and $\alpha = x + .11 + c \sin(2\pi x)$ with $0 \leq c \leq 2$. The model equation has been discretized with a second-order finite difference scheme and a cubic spline interpolation scheme. We have an analytical expression for the solution of the model equation so we can derive expressions for the error. We have

plotted the error curves derived from the discretization of the model equation with a second-order finite difference scheme, with a third-order finite difference scheme, with a cubic spline interpolation scheme, and with a truncated Fourier series when the parameter c in the function α is varied and the other functions are fixed. We have compared these different error curves for the same value of the parameters for the model equation that has been discretized with three different schemes: a second-order finite difference scheme, a third-order finite difference scheme, and a cubic spline interpolation scheme.

From the execution time spent solving the linear systems resulting from the discretization of either (II.0.1) or (II.0.2) with a second-order or third-order finite difference scheme, with a cubic spline interpolation scheme, and when the solution is approximated by a Fourier series, we realize that there is no point in using a truncated Fourier series. It is due to the fact that the Fourier expansion assumes a lot of smoothness of the solution of the continuous problem. It is also very expensive to set up and solve the system in this case. On the other hand, the finite difference schemes are much less expensive and their execution time is much shorter. Nevertheless, they are only interesting for linear problems. Because the discrete solution does not possess a continuous first derivative on its domain of definition, the only method that can be used to solve nonlinear equations is a linear iterative method. If the discrete solution possesses a continuous first derivative everywhere on the domain of definition, it is of interest for solving nonlinear problems. A good compromise between a rather low execution time and a rather low discretization cost is a cubic spline interpolation scheme. The cubic spline interpolation scheme has also the advantage of having continuous first and second derivatives on the domain of definition. From the analytical and numerical study, we deduce that there is no point in using a high-order, sophisticated scheme unless estimates have shown that the solution of the continuous problem is extremely smooth. We will try, in general, to choose a low-order scheme. The scheme should be such that the solution interpolated from the discrete solution has at least a continuous first derivative on the domain of definition so that we can use Newton's method to solve nonlinear problems.

As said before, the cubic spline interpolation scheme is of interest for nonlinear problems. We will try to justify this assertion. Consider the nonlinear system of ordinary differential equations

$$\begin{aligned} \text{(IV.1a)} \quad & \frac{d}{dt} \theta = a(\theta, t, r), \\ \text{(IV.1b)} \quad & \frac{d}{dt} r = b(\theta, t, r), \end{aligned}$$

where a and b are smooth functions from $S^1 \times S^1$ to $(-\infty, \infty)$.

We integrate system (IV.1) with respect to time. Consider the initial conditions (θ_0, r_0) . So the solution of (IV.1) at time t , with initial conditions (θ_0, r_0) is given by $(\theta(\theta_0, t, r_0), r(\theta_0, t, r_0))$. We consider the same Poincaré map as in chapter 1. As in chapter 1, we would like to find an expression for an invariant curve under the Poincaré map \mathbf{P} which has the form $\Gamma = \{(x, R(x)), x \in S^1\}$ where the function R is an unknown function from S^1 to $(-\infty, \infty)$. The curve Γ is invariant under the Poincaré map \mathbf{P} if the point $\mathbf{P}(x, R(x))$ is on the curve Γ for all $x \in S^1$. To simplify the notations, we have $\theta(\theta_0, 1, r_0) = \xi(\theta_0, r_0)$ and $r(\theta_0, 1, r_0) = \rho(\theta_0, r_0)$. We then require, for $\mathbf{P}(x, R(x)) = (\xi(x, R(x)), \rho(x, R(x)))$ to satisfy

$$(IV.2) \quad R(\xi(x, R(x))) = \rho(x, R(x)).$$

We cannot solve (IV.2) with a direct method because it is nonlinear in R . We will have to linearize it about a given solution and then iterate. If we linearize (IV.2) about a given solution $R_0(x)$, $R(x) = R_0(x) + S(x)$, we are lead to

$$(IV.3) \quad \begin{aligned} R_0(\beta(x)) + R_0'(\beta(x)) \xi_R(\beta(x)) S(x) + S(\beta(x)) = \\ \rho(x, R_0(x)) + \rho_R(x, R_0(x)) S(x), \end{aligned}$$

where $\beta(x) = \xi(x, R_0(x))$. Because of the term $R_0'(\beta(x))$ arising in (IV.3), we see that we need a continuous approximation of $R_0'(x)$. That is why we will prefer a cubic spline interpolation scheme instead of a finite difference one.

The methods we have chosen to discretize the model equation are quite similar to those used in [13] and [14]. As in there, we compute the image of the function $R(x_i)$ by the operator L , $(R \circ \alpha)(x_i)$, then we approximate $(R \circ \alpha)(x_i)$, if it is not equal to $R(x_j)$ by some interpolation scheme, by some weighted average of the solution at the discretization points x_{m-1} , x_m , and x_{m+1} $R(x_{m-1})$, $R(x_m)$, and $R(x_{m+1})$. The point x_m depends on the function α . The weights of the interpolation scheme depend on the kind of scheme chosen. For example, if we choose a second-order finite difference scheme, and if $0 \leq \alpha(x_i) - x_j < h$ modulo 1, then $(R \circ \alpha)(x_i) = \theta_i R(x_{j+1}) + (1 - \theta_i) R(x_j)$ with $\theta_i h = \alpha(x_i) - x_j$ and $0 \leq \theta_i < 1$. To get the weights for the third-order finite difference scheme, we proceed in a similar fashion. For the cubic spline interpolation scheme, it is more complex and there is no easy way to figure the value of the weights. Because the model equation is linear, we do not need to iterate as in [13] and [14]. If we want to compare our methods to his, we have to solve the same examples as he does and compare our results to his. We just have run model problems up to now.

In the near future, we want to study a nonlinear functional equation. We want to know under which assumptions the solution exists and is unique. We also would

like to know under which further restrictions the solution of the model equation possesses k continuous derivatives. We will plot the numerical solution of the model equation for different values of the parameters. We then will apply the algorithms we have analyzed to some problems like the van der Pol equation or the delayed logistic map already solved numerically with other numerical schemes.

REFERENCES

- [1] D. G. Aronson, M. A. Chory, G. R. Hall, and R. P. McGehee *Bifurcations from an Invariant Circle for Two-Parameter Families of Maps of the Plane: A Computed-Assisted Study*. Commun. Math. Phys. 83, pp 303-354 1982.
- [2] H. Brezis *Analyse Fonctionnelle Théorie et Applications*. Collection Mathématiques Appliquées pour la Maîtrise, Masson, Paris 1983.
- [3] L. Dieci, J. Lorenz, R. D. Russel *Numerical Calculation of Invariant Manifolds*. to appear.
- [4] N. Fenichel *Persistence and Smoothness of Invariant Manifolds for Flows*. Indiana University Mathematics Journal 21, pp 193-226 1971.
- [5] J. Guckenheimer, P. J. Holmes *Nonlinear Oscillations, Dynamical Systems and Bifurcations of Vector Fields*. Springer Verlag, New York 1983.
- [6] P. J. Holmes and D. A. Rand *Bifurcations of the Forced van der Pol Oscillator*. Quart. Appl. Math. 35, pp 495-509 1978.
- [7] R. Johnsonbaugh, W. E. Pfaffenberger *Foundations of Mathematical Analysis*. Marcel Decker Inc 1981.
- [8] Chr. Kaas-Petersen *Computation, Continuation, and Bifurcation of Torus Solutions for Dissipative Maps and Ordinary Differential Equations*. Physica 25D, pp 288-306 1987.
- [9] I. G. Kevrekidis, R. Aris, L. D. Schmidt, and S. Pelikan *Numerical Computation of Invariant Circles of Maps*. Physica 16D, pp 243-251 1985.
- [10] H.-O. Kreiss, J. Lorenz *Initial-Boundary Value Problems and the Navier-Stokes Equations*. Academic Press 1989.
- [11] J. Lorenz *Numerical Solution of Partial Differential and Integral Equations*. California Institute of Technology, Course Lecture Notes 1987.

- [12] J. Stoer, R. Burlisch *Introduction to Numerical Analysis*. Springer Verlag, New York Heidelberg Berlin 1980.
- [13] M. Van Veldhuizen *A New Algorithm for the Numerical Approximation of an Invariant Curve*. SIAM J. Sci. Stat. Comp. 8, pp 951-962 1987.
- [14] M. Van Veldhuizen *Convergence Results for Invariant Curves Algorithms*. Mathematics of Computation 51, pp 677-697 1988.

PART II: NUMERICAL CONVERGENCE RESULTS FOR A ONE-DIMENSIONAL STEFAN PROBLEM

CHAPTER I

NUMERICAL CONVERGENCE RESULTS FOR A ONE-DIMENSIONAL STEFAN PROBLEM

I.1 Introduction

Free boundary problems have been of interest for many years from both a mathematical and a physical viewpoint. They simulate a large class of phenomena: the propagation of interfaces, which occur in distinct fields of research, for example hydrodynamics, crystal growth, and combustion. In hydrodynamics, the Saffman-Taylor finger is an example; the goal is to determine the motion of an interface between two fluids of different viscosities in a Hele-Shaw cell. In crystal growth, it is to find the position and the shape of the interface between two different phases of a substance. In combustion, it is to locate the interface between fresh and burned gas for a premixed flame propagating in a reactive mixture. In all cases, given some control parameters, free boundary problems give the morphology of the interface and its propagation velocity.

In this chapter, we will focus on the model equations for crystal growth problems. These problems have been studied for many years and many approximate models have been built. The model considered in [14], [34], and [38] assumes that the paraboloid shape of the dendrite is conserved and only one of the boundary conditions is applied at the tip. These models determine a curve $U = f(\rho)$ which has a maximum because it has been conjectured for a long time that the dendritic growth occurs at maximum velocity. Nash and Glicksman in [28] and [29] proposed a more precise study where they derive an integral equation for the interface shape and a maximum velocity numerically. Langer and Müller-Krumbhaar in [21], [22], [27] assume that the growth velocity is dynamically selected. They introduce a marginal stability criterion enforcing either the selected radius of curvature to be proportional to the most unstable wavelength or to the ratio

$$\sigma = \frac{2 D d_0}{\rho^2 U} = \sigma_c,$$

where U is the growth velocity of the crystal, D the thermal coefficient, d_0 a capillarity length, and ρ the density, σ_c a constant. Some simpler models have also been studied, geometrical models [4], [5], [16], [17], and boundary layer models [1], [2],

to understand more generally the problem of velocity selection of a needle crystal. These models share common features with the realistic models, such as existence of continuum of needle crystals moving with arbitrary velocity when the higher derivative terms are neglected (zero surface tension). In [20], [23], these simpler models enable us to understand analytically how the continuum of solutions without surface tension can be broken when small surface tension is added.

Because most of the physical models we refer to above are given by a complex set of equations and because we want to analyze the convergence analytically as well as numerically, we will consider here a one-dimensional Stefan problem which is supposed to give a rather good model of a one-dimensional crystal growth problem. We will show existence and uniqueness of the solution with L_2 estimates. We will prove that the numerical solution converges to the analytical solution.

As mentioned earlier, this chapter will focus on model equations for the simulation of dendrite growth, that can be described to first approximation by a Stefan problem under the assumptions, [31]:

- the solid and liquid are pure substances,
- the characteristic diffusion time of transfer of molecules between solid and liquid is very fast compared with the characteristic diffusion time of heat,
- the growth is limited by the diffusion of latent heat in the medium, released at the interface.

The temperature fields in the solid and liquid and the interface position are unknown. Four equations describe the physical phenomenon, two are diffusion equations in the solid and in the liquid, the third one is a kinematic condition at the interface, and the last one is a dynamical condition derived from thermodynamic considerations.

The two diffusion equations are

$$(I.1.1a) \quad \frac{\partial}{\partial t} T_s = \nabla(D_s \nabla T_s) \quad \text{in } \Omega_s(t), \quad t \in [0, T],$$

$$(I.1.1b) \quad \frac{\partial}{\partial t} T_l = \nabla(D_l \nabla T_l) \quad \text{in } \Omega_l(t), \quad t \in [0, T],$$

where ∇ is the gradient operator in n -dimensional space

$$\nabla = \begin{bmatrix} \frac{\partial}{\partial x_1} \\ \frac{\partial}{\partial x_2} \\ \vdots \\ \frac{\partial}{\partial x_j} \\ \vdots \\ \frac{\partial}{\partial x_n} \end{bmatrix}$$

and where T_l and T_s are the temperature fields of the liquid and of the solid, $D_l = \lambda_l/c_{p_l}$ and $D_s = \lambda_s/c_{p_s}$ are the diffusion constants of the liquid and of the solid, λ_l and λ_s are the thermal conductivities of the liquid and of the solid and c_{p_l} and c_{p_s} are the specific heats per unit volume of the liquid and of the solid. D_l and D_s are strictly positive functions bounded away from 0 on the domains considered.

We have not yet prescribed the time interval $[0, T]$. The Stefan problem is nonlinear and its solution can break down in a finite time. The breakdown time imposes an upper bound on the value of T .

The third equation is a kinematic condition at the interface, derived from the conservation of energy at the interface

$$(I.1.1c) \quad Q v \cdot n = (D_s c_{p_s} \nabla T_s - D_l c_{p_l} \nabla T_l) \cdot n \quad \text{on } \Gamma(t) = (\partial\Omega_l(t) \cap \partial\Omega_s(t)), \quad t \in [0, T],$$

where $Q = (h_l - h_s)\rho_s$ is the latent heat per unit of volume of the solid, h_l and h_s are the enthalpies per unit of mass of the liquid and of the solid, $v \cdot n$ is the normal velocity of the interface, n is the unit vector normal to the interface.

The last equation is a dynamical condition, derived from a thermodynamic relation, the Gibbs-Thomson relation

$$(I.1.1d) \quad T_s - T^* = T_l - T^* = -\frac{T^*}{Q} \left[\left(\sigma + \frac{\partial^2}{\partial\phi_1^2} \sigma \right) \frac{1}{R_1} + \left(\sigma + \frac{\partial^2}{\partial\phi_2^2} \sigma \right) \frac{1}{R_2} \right] \quad \text{on } \Gamma(t) = (\partial\Omega_l(t) \cap \partial\Omega_s(t)), \quad t \in [0, T],$$

where T^* is a reference temperature, σ is the anisotropic liquid-solid surface tension, R_1 and R_2 are the principal radii of curvature of the interface, taken positive when they are directed toward the solid side, ϕ_1 and ϕ_2 are the angles of the normal to the interface with some fixed direction inside each main plane.

We also prescribe initial and boundary conditions, namely $T_s(x, 0)$, $T_l(x, 0)$, $\Gamma(0)$ and $T_s(x, t)$ is given on $\partial\Omega_s(t) \setminus \Gamma(t)$, and $T_l(x, t)$ is given on $\partial\Omega_l(t) \setminus \Gamma(t)$ for $t \in [0, T]$.

Instead of studying the general n -dimensional problem described by (I.1.1), we derive results in this chapter for a one-phase one-dimensional Stefan problem on a semi-infinite domain and in appendix III, we extend the results to the two-phase case. We do this as a first step in the analysis because the n -dimensional problem is very involved and because many of the analysis issues arise already in the one-dimensional case. In the one-dimensional case, we write (I.1.1) as

$$(I.1.2a) \quad \frac{\partial}{\partial t} T_s(x, t) = \frac{\partial}{\partial x} \left(D_s \frac{\partial}{\partial x} T_s(x, t) \right),$$

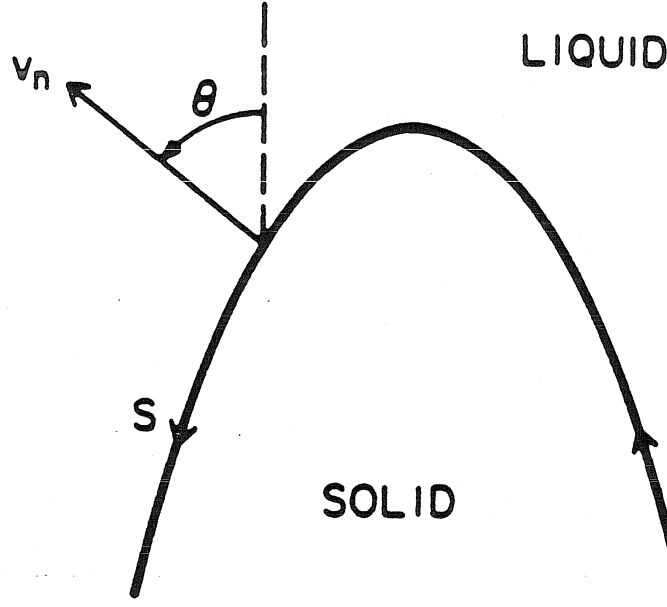


Figure I.1.1 Geometry of the interface for a two-dimensional model. (figure from reference [23])

$$(I.1.2b) \quad \frac{\partial}{\partial t} T_l(x, t) = \frac{\partial}{\partial x} \left(D_l \frac{\partial}{\partial x} T_l(x, t) \right),$$

$$(I.1.2c) \quad \frac{d}{dt} s(t) = D_s c_p \frac{\partial}{\partial x} T_s(s(t), t) - D_l c_{pl} \frac{\partial}{\partial x} T_l(s(t), t),$$

$$(I.1.2d) \quad T_s(s(t), t) = T_l(s(t), t) = T^*(t),$$

$$(I.1.2e) \quad s(0) = s_0,$$

$$(I.1.2f) \quad T_s(x, 0) = T_{s0}(x),$$

$$(I.1.2g) \quad T_l(x, 0) = T_{l0}(x),$$

$$(I.1.2h) \quad T_s(x, t) \rightarrow \Delta_s \quad \text{as } x \rightarrow -\infty,$$

$$(I.1.2i) \quad T_l(x, t) \rightarrow \Delta_l \quad \text{as } x \rightarrow \infty.$$

Here T_s , T_l , T_{s0} and T_{l0} are defined on $(-\infty, s(t)]$, $[s(t), \infty)$, for $t \in [0, T]$, $(-\infty, s_0]$ and $[s_0, \infty)$.

Because we have assumed that D_s and D_l are strictly positive functions, bounded away from 0, the equations (I.1.2a) and (I.1.2b) are uniformly parabolic.

The convenient transformation, $x' = x - s(t)$, already introduced in [25], transforms (I.1.2) to a nonlinear problem on a fixed domain. In this coordinate system, the moving boundary $s(t)$ has been fixed at the point, $x' = 0$. We introduce this mapping because for the two-dimensional case, we want to solve the equations via a mapping procedure. Dropping primes, the nonlinear system becomes

$$(I.1.3a) \quad \begin{aligned} \frac{\partial}{\partial t} \hat{T}_s(x, t) &= \frac{\partial}{\partial x} \left(\hat{D}_s \frac{\partial}{\partial x} \hat{T}_s(x, t) \right) \\ &+ \left(\hat{D}_s \hat{c}_{p_s} \frac{\partial}{\partial x} \hat{T}_s - \hat{D}_l \hat{c}_{p_l} \frac{\partial}{\partial x} \hat{T}_l \right) (0, t) \frac{\partial}{\partial x} \hat{T}_s(x, t), \end{aligned}$$

$$(I.1.3b) \quad \begin{aligned} \frac{\partial}{\partial t} \hat{T}_l(x, t) &= \frac{\partial}{\partial x} \left(\hat{D}_l \frac{\partial}{\partial x} \hat{T}_l(x, t) \right) \\ &+ \left(\hat{D}_s \hat{c}_{p_s} \frac{\partial}{\partial x} \hat{T}_s - \hat{D}_l \hat{c}_{p_l} \frac{\partial}{\partial x} \hat{T}_l \right) (0, t) \frac{\partial}{\partial x} \hat{T}_l(x, t), \end{aligned}$$

$$(I.1.3c) \quad \hat{T}_s(0, t) = \hat{T}_l(0, t) = T^*(t),$$

$$(I.1.3d) \quad \hat{T}_s(x, 0) = \hat{T}_{s0}(x),$$

$$(I.1.3e) \quad \hat{T}_l(x, 0) = \hat{T}_{l0}(x),$$

$$(I.1.3f) \quad \hat{T}_s(x, t) \rightarrow \Delta_s \quad \text{as } x \rightarrow -\infty,$$

$$(I.1.3g) \quad \hat{T}_l(x, t) \rightarrow \Delta_l \quad \text{as } x \rightarrow \infty,$$

$$(I.1.3h) \quad \frac{d}{dt} s(t) = \left(D_s c_{p_s} \frac{\partial}{\partial x} \hat{T}_s - D_l c_{p_l} \frac{\partial}{\partial x} \hat{T}_l \right) (0, t),$$

$$(I.1.3i) \quad s(0) = s_0,$$

where $\hat{u}(x, t) = u(x + s(t), t)$. \hat{T}_s , \hat{T}_l , \hat{T}_{s0} and \hat{T}_{l0} are defined on $(-\infty, 0] \times [0, T]$, $[0, \infty) \times [0, T]$, $(-\infty, 0]$ and $[0, \infty)$, respectively.

In the following sections, we take Δ_s and Δ_l to be 0 because if we write \hat{T}_l in the form $\hat{T}_l = S_l + \Delta_l (1 - e^{-x^2})$, and \hat{T}_s in the form $S_s + \Delta_s (1 - e^{-x^2})$, S_l and S_s satisfy homogeneous boundary conditions at ∞ and at $-\infty$. S_l and S_s satisfy equations (I.1.3b) and (I.1.3a) with a forcing term added, depending on derivatives of $\Delta_l (1 - e^{-x^2})$ and $\Delta_s (1 - e^{-x^2})$. Except for (I.1.3f) and (I.1.3g), the other equations are unchanged. The same transformation applies to (I.1.2).

Systems of type (I.1.2) and (I.1.3) have already been extensively studied in the past from a mathematical viewpoint. In [11], local existence of a solution has been proven. In [26], the uniqueness of the position of the interface and its continuous dependence upon the data has been shown. Some numerical simulations have been carried out both for the one-phase and two-phase one-dimensional Stefan problem in [3], [24], and [30].

The goal of this chapter is to show that the numerical solution of either (I.1.2) or (I.1.3) discretized in space with a fourth-order scheme and in time with Crank-Nicholson scheme convergences to the solution of the continuous system in the limit

of zero meshsize and timestep. To simplify the algebra in this chapter, we prove corresponding results for a one-sided Stefan problem, discretized with a centered second-order finite difference scheme in space, Crank-Nicholson scheme in time. Fourth-order methods in space are considered in Appendix 4. Also for simplicity the diffusion constant will be a constant function and, without restrictions, will be taken 1. The term Dc_p will also be 1. For simplicity, it will be assumed that $u \rightarrow 0$ for $|x| \rightarrow \infty$ and that the forcing terms introduced to make the boundary conditions homogeneous at infinity are $F_s = 0$, $F_l = 0$. The one-sided Stefan problem reads

$$(I.1.4a) \quad \frac{\partial}{\partial t} u(x, t) = \frac{\partial^2}{\partial x^2} u(x, t) + \frac{\partial}{\partial x} u(0, t) \frac{\partial}{\partial x} u(x, t),$$

$$(I.1.4b) \quad u(0, t) = T^*(t),$$

$$(I.1.4c) \quad u(x, 0) = u_0(x),$$

$$(I.1.4d) \quad u(x, t) \rightarrow 0 \quad \text{as } x \rightarrow \infty,$$

$$(I.1.4e) \quad \frac{d}{dt} s(t) = -\frac{\partial}{\partial x} u(0, t),$$

$$(I.1.4f) \quad s(0) = s_0.$$

Here u and u_0 are defined on $[0, \infty) \times [0, T]$ and on $[0, \infty)$, respectively.

An outline of this chapter and of this part follows.

In section 2, we derive the discrete equations approximating (I.1.4), the semi-discrete equation, the semi-discrete error equation, the linearized semi-discrete error equation, its continuous equivalent, the linearized discrete equation, and the nonlinear discrete error equation. For the equations discretized in space, the mesh points are located at $x_j = (j - 1/2)h$, $j = 0, 1, 2, \dots$. In section 3, we obtain L_2 estimates for (I.1.4). First, we show short term existence of the solution; we deduce uniqueness of the solution as well. Then we write down sufficient conditions for global existence. In section 4, we compute L_2 estimates for the linearized continuous error equation. In section 5, we do the same for the semi-discrete linearized error equation. In section 6, we analyze the linearized error equation. In section 7, we show that the solution of the nonlinear equation stays in the "neighborhood" of the solution of the linearized discrete error equation provided the meshsize is small enough. In section 8, we describe a numerical scheme for (I.1.3) and we provide numerical evidence of the accuracy of the scheme. In the appendices, we recall some basic results on L_2 estimates for continuous equations and semi-discrete ones, we sketch a generalization of the results proven in this chapter to a two-phase Stefan problem, and we explain the numerical method to be implemented for a centered fourth-order finite difference scheme in space. In appendix V, we show numerical

results for (I.1.2) discretized in time with the Crank-Nicholson scheme and with the Collatz Mehrstellenverfahren in space.

I.2 The Discrete Equations

As mentioned before, the goal of this work is to show that the numerical solution converges to the solution of the continuous system. This will be done in several steps. The continuous system (I.1.4) is first discretized in space with a centered second-order scheme. This leads to

$$(I.2.1a) \quad \frac{\partial}{\partial t} \tilde{u}_j(t) = D_+ D_- \tilde{u}_j(t) + D_+ \tilde{u}_0(t) D_0 \tilde{u}_j(t) \quad j = 1, 2, \dots,$$

$$(I.2.1b) \quad A_{02} \tilde{u}_0(t) = T^*(t),$$

$$(I.2.1c) \quad \tilde{u}_j(0) = u_0(x_j) \quad j = 0, 1, \dots,$$

$$(I.2.1d) \quad \tilde{u}_j(t) \rightarrow 0 \quad \text{as } j \rightarrow \infty,$$

$$(I.2.1e) \quad \frac{d}{dt} \tilde{s}(t) = -D_+ \tilde{u}_0(t),$$

$$(I.2.1f) \quad \tilde{s}(0) = s_0,$$

where \tilde{u}_j is the difference approximation of u at $(x_j, t) = ((j - 1/2)h, t)$, for $j = 0, 1, \dots$ on $[0, T]$. The equations (I.2.1e) and (I.2.1f) are needed to determine the linear transformation $x' = x - s(t)$ for all time. We will compute \tilde{u}_j outside the domain $[0, \infty)$. We will compute an initial value of \tilde{u}_0 , at $-h/2$. We will extrapolate the function u_0 outside its domain of definition with an interpolant that is at least linear. The difference operators A_{02} , D_+ , D_- , D_0 , $D_+ D_-$ are defined as follows:

$$A_{02} v_0 = \frac{1}{2} (v_0 + v_1) \sim v(0),$$

$$D_+ v_0 = \frac{1}{h} (v_1 - v_0) \sim v_x(0),$$

$$D_- v_1 = \frac{1}{h} (v_1 - v_0) \sim v_x(0),$$

$$D_0 v_j = \frac{1}{2} (D_+ + D_-) v_j = \frac{1}{2h} (v_{j+1} - v_{j-1}) \sim v_x(x_j),$$

$$D_+ D_- v_j = \frac{1}{h^2} (v_{j+1} - 2v_j + v_{j-1}) \sim v_{xx}(x_j),$$

We first derive an equation that the error satisfies. This equation will give a good measure of the deviation of the semi-discrete solution from the continuous one. We

substitute in the semi-discrete system (I.2.1) the solution of the continuous problem (u, s) . It satisfies a semi-discrete system, similar to (I.2.1) with forcing terms coming from the truncation errors of the discrete operators. The solution of the continuous problem can be written as $u(x_j, t) = \tilde{u}_j(t) + \tilde{e}_j(t)$ and $s(t) = \tilde{s}(t) + \tilde{c}(t)$. We obtain the error equation by subtracting the semi-discrete system (I.2.1) from the one the solution of the continuous problem satisfies. It reads

$$\begin{aligned}
 \frac{\partial}{\partial t} \tilde{e}_j(t) &= D_+ D_- \tilde{e}_j(t) + D_+ \tilde{e}_0(t) D_0 \tilde{u}_j(t) \\
 &\quad + D_+ \tilde{u}_0(t) D_0 \tilde{e}_j(t) + D_+ \tilde{e}_0(t) D_0 \tilde{e}_j(t) \\
 &\quad + \tilde{f}_j(t) \quad j = 1, 2, \dots, \\
 \text{(I.2.2a)} & \\
 \text{(I.2.2b)} & \quad A_{02} \tilde{e}_0(t) = g(t), \\
 \text{(I.2.2c)} & \quad \tilde{e}_j(0) = h_j \quad j = 0, 1, \dots, \\
 \text{(I.2.2d)} & \quad \tilde{e}_j(t) \rightarrow 0 \quad \text{as } j \rightarrow \infty, \\
 \text{(I.2.2e)} & \quad \frac{d}{dt} \tilde{c}(t) = k(t), \\
 \text{(I.2.2f)} & \quad \tilde{c}(0) = 0.
 \end{aligned}$$

where $\tilde{f}_j(t)$, $g(t)$, h_j and $k(t)$ are given by

$$\begin{aligned}
 \tilde{f}_j(t) &= -h^2 \left(\frac{1}{12} u_{xxxx}(x_j, t) + \frac{1}{24} u_{xxx}(0, t) u_x(x_j, t) \right. \\
 &\quad \left. + \frac{1}{6} u_x(0, t) u_{xxx}(x_j, t) \right) + o(h^2), \\
 g(t) &= -\frac{h^2}{8} u_{xx}(0, t) + o(h^2), \\
 h_j &= \begin{cases} 0 & \text{if } j = 1, 2, \dots, \\ o(h^2) & \text{if } j = 0, \end{cases} \\
 k(t) &= \frac{h^2}{24} u_{xxx}(0, t) + o(h^2),
 \end{aligned}$$

where h_0 depends on the values of u_0 at $x = h/2, \dots$ and also on the type of interpolant chosen to compute the extrapolated value of u_0 at $x = -h/2$.

The semi-discrete error equation (I.2.2a) obtained is nonlinear. First, instead of studying it, a linearized equation derived by neglecting the quadratic terms and by linearizing the equation (I.2.2a) about a given solution is analyzed. We will later justify neglecting the quadratic terms. Because the error is supposed to be small, the equation (I.2.2a) will be linearized about the solution $\tilde{e} = 0$. Even though the function \tilde{e} of (I.2.2a) does not satisfy the linearized error equation, we will still call

the error function \tilde{e} to simplify the notation. This leads to

$$(I.2.3a) \quad \frac{\partial}{\partial t} \tilde{e}_j(t) = D_+ D_- \tilde{e}_j(t) + D_+ \tilde{e}_0(t) D_0 \tilde{u}_j(t) \\ + D_+ \tilde{u}_0(t) D_0 \tilde{e}_j(t) + \tilde{f}_j(t) \quad j = 1, 2, \dots,$$

$$(I.2.3b) \quad A_{02} \tilde{e}_0(t) = g(t),$$

$$(I.2.3c) \quad \tilde{e}_j(0) = h_j \quad j = 0, 1, \dots,$$

$$(I.2.3d) \quad \tilde{e}_j(t) \rightarrow 0 \quad \text{as } j \rightarrow \infty,$$

$$(I.2.3e) \quad \frac{d}{dt} \tilde{c}(t) = k(t),$$

$$(I.2.3f) \quad \tilde{c}(0) = 0.$$

We will bound the semi-discrete function \tilde{e} , its divided differences in L_2 and maximum norm. We will show that the upper bound goes to zero like h^2 , h being the meshsize. In general, instead of estimating directly the semi-discrete function \tilde{e} , we first study the continuous error function e . The function e satisfies an equation deduced from its semi-discrete equivalent by replacing all the discrete operators and the discretized known functions by their continuous equivalents. The function e satisfies

$$(I.2.4a) \quad \frac{\partial}{\partial t} e(x, t) = \frac{\partial^2}{\partial x^2} e(x, t) + \frac{\partial}{\partial x} e(0, t) \frac{\partial}{\partial x} u(x, t) \\ + \frac{\partial}{\partial x} u(0, t) \frac{\partial}{\partial x} e(x, t) + f(x, t),$$

$$(I.2.4b) \quad e(0, t) = g(t),$$

$$(I.2.4c) \quad e(x, 0) = 0,$$

$$(I.2.4d) \quad e(x, t) \rightarrow 0 \quad \text{as } x \rightarrow \infty,$$

$$(I.2.4e) \quad \frac{d}{dt} c(t) = k(t),$$

$$(I.2.4f) \quad c(0) = 0,$$

where f is given by

$$f(x, t) = -h^2 \left(\frac{1}{12} u_{xxxxx}(x, t) + \frac{1}{24} u_{xxx}(0, t) u_x(x, t) \right. \\ \left. + \frac{1}{6} u_x(0, t) u_{xxx}(x, t) \right) + o(h^2),$$

The functions g and k are the same as before.

Once we have obtained estimates for the continuous error equation, calculations similar to the ones already done on the continuous system (I.2.4) will be carried

out on the system (I.2.3). In general, the function e_x discretized on the meshsize is different from the function $D_0 \tilde{e}_i$, where \tilde{e}_i is a discrete approximation of the function e at the meshpoint x_i . Because in system (I.2.4), we have the term $e_x(0, t) u_x(x, t)$, we will in section 5 introduce a new function $y = e_x$ and derive estimates for the system the vector $[e, y]^T$ satisfies. We will then discretize this continuous system in space with a centered second-order finite difference scheme. Then we study (I.2.3) discretized in time with Crank-Nicholson scheme

$$(I.2.5a) \quad \begin{aligned} \frac{\hat{e}_j^{n+1} - \hat{e}_j^n}{\tau} &= \frac{1}{2} D_+ D_- (\hat{e}_j^{n+1} + \hat{e}_j^n) \\ &+ \frac{1}{4} D_+ (\hat{e}_0^{n+1} + \hat{e}_0^n) D_0 (\hat{u}_j^{n+1} + \hat{u}_j^n) \\ &+ \frac{1}{4} D_+ (u_0^{n+1} + u_0^n) D_0 (\hat{e}_j^{n+1} + \hat{e}_j^n) \\ &+ \frac{1}{2} (\hat{f}_j^{n+1} + \hat{f}_j^n) \quad j = 1, \dots \quad n = 0, \dots, \end{aligned}$$

$$(I.2.5b) \quad A_{02} (\hat{e}_0^{n+1} + \hat{e}_0^n) = g((n+1)\tau) + g(n\tau) \quad n = 0, \dots,$$

$$(I.2.5c) \quad \hat{e}_j^0 = h_j \quad j = 0, \dots,$$

$$(I.2.5d) \quad \hat{e}_j^n \rightarrow 0 \quad \text{as } j \rightarrow \infty \quad n = 0, \dots,$$

$$(I.2.5e) \quad \hat{c}^{n+1} = \hat{c}^n + \frac{1}{2} \tau (k((n+1)\tau) + k(n\tau)) \quad n = 0, \dots,$$

$$(I.2.5f) \quad \hat{c}^0 = 0,$$

where \hat{f}_j^n is given by

$$\begin{aligned} \hat{f}_j^n &= -h^2 \left(\frac{1}{12} u_{xxxx}(x_j, n\tau) + \frac{1}{24} u_{xxx}(0, n\tau) u_x(x_j, n\tau) \right. \\ &+ \left. \frac{1}{6} u_x(0, n\tau) u_{xxx}(x_j, n\tau) \right) + \tau^2 \left(\frac{1}{24} u_{ttt}(x_j, n\tau) \right. \\ &+ \left. \frac{1}{8} u_{xtt}(x_j, n\tau) + \frac{1}{8} u_{xtt}(0, n\tau) u_x(x_j, n\tau) \right. \\ &+ \left. \frac{1}{8} u_x(0, n\tau) u_{xtt}(x_j, n\tau) \right) + o(h^2) + o(\tau^2). \end{aligned}$$

In section 5, we deduce estimates for the error \hat{e} satisfying (I.2.5).

Finally, we evaluate estimates for the nonlinear error equation. We will extensively use results from the previous sections, in particular, we will show that provided the meshsize is small enough, the nonlinear system behaves like the linear one. To do that, instead of defining the error \hat{e}_j^n as $u(x_j, n\tau) - \hat{u}_j^n$ and \hat{c}^n as $s(n\tau) - \hat{s}^n$, we introduce a factor h^2 . The grid functions \hat{e}_j^n and \hat{c}^n satisfy $h^2 \hat{e}_j^n = u(x_j, n\tau) - \hat{u}_j^n$ and $h^2 \hat{c}^n = s(n\tau) - \hat{s}^n$. The power of h in front of \hat{e}_j^n

depends mostly on the order of the scheme chosen and on other considerations that will be discussed in section 7. Those new functions \hat{e}_j^n and \hat{c}^n satisfy

$$\begin{aligned}
 \frac{\hat{e}_j^{n+1} - \hat{e}_j^n}{\tau} &= \frac{1}{2} D_+ D_- (\hat{e}_j^{n+1} + \hat{e}_j^n) \\
 &+ \frac{1}{4} D_+ (\hat{e}_0^{n+1} + \hat{e}_0^n) D_0 (\hat{u}_j^{n+1} + \hat{u}_j^n) \\
 &+ \frac{1}{4} D_+ (\hat{u}_0^{n+1} + \hat{u}_0^n) D_0 (\hat{e}_j^{n+1} + \hat{e}_j^n) \\
 &+ \frac{1}{4} h^2 D_+ (\hat{e}_0^{n+1} + \hat{e}_0^n) D_0 (\hat{e}_j^{n+1} + \hat{e}_j^n) \\
 (I.2.6a) \quad &+ \frac{1}{2 h^2} (\hat{f}_j^{n+1} + \hat{f}_j^n) \quad j = 1, \dots \quad n = 0, \dots, \\
 (I.2.6b) \quad A_{02} (\hat{e}_0^{n+1} + \hat{e}_0^n) &= \frac{1}{h^2} (g((n+1)\tau) + g(n\tau)) \quad n = 0, \dots, \\
 (I.2.6c) \quad \hat{e}_j^0 &= \frac{1}{h^2} h_j \quad j = 0, \dots, \\
 (I.2.6d) \quad \hat{e}_j^n &\rightarrow 0 \quad \text{as } j \rightarrow \infty \quad n = 0, \dots, \\
 (I.2.6e) \quad \hat{c}^{n+1} &= \hat{c}^n + \frac{1}{2 h^2} \tau (k((n+1)\tau) + k(n\tau)) \quad n = 0, \dots, \\
 (I.2.6f) \quad \hat{c}^0 &= 0.
 \end{aligned}$$

From the expression for \hat{f}_j^{n+1} and the assumption that the ratio $\tau/h^2 = \lambda$, where λ is a fixed constant, we see that the term \hat{f}_j^{n+1}/h^2 is well-defined and has a finite limit as $h \rightarrow 0$. A similar result is true for $g((n+1)\tau)/h^2$ and for h_j/h^2 . The term h^2 in front of the nonlinear term will help to show that some operator acting on \hat{e} is a contraction. Once this has been done, we will easily prove that the error is bounded in terms of h and τ .

I.3 Estimates for the Continuous Problem - Existence and Uniqueness of the Solution of the Continuous Problem

In section 2 we have explained why estimates for divided differences of u are needed in order to get estimates for the error. Because the continuous function u and its derivatives are a good interpolant for the corresponding discrete approximations, it is enough to estimate the continuous functions. The method that Strang chose in [37] to estimate operators does not apply in a straightforward manner to the problem considered because of the nonlinearity. We will use L_2 estimates to bound u and its derivatives. It has been shown in [6], [7], [8], [9], [10], [11], [12], and [13]

that solutions of (I.1.2), (I.1.3), and (I.1.4) and their derivatives exist on a short time interval. In [8], [9], and [10] under certain restrictions on the data and on the coefficients of the differential operator, long term existence has been proven; when long term existence could not be shown, the value of the position of the interface or bounds on the derivative of the position of the interface are given at the breakdown time. It was shown that either the interface disappears or its derivative becomes infinite. The tools chosen to prove those results were either integral equations, or maximum principles or a combination of both. For the one-sided Stefan problem, Friedman shows short term existence of the solution and its uniqueness with the parametrix method. If he assumes some *a priori* estimates on the position of the interface and on u_x , he obtains long term existence for u . Conditions for long term existence in [8], [9], and [10] are equivalent to the *a priori* estimates that Friedman assumes in [13]. Similar to what has already been done, we will show first short time existence using L_2 estimates. As done in [19] for Burgers's equation, we will derive estimates for the solution of (I.1.4) and its derivatives, we will show uniqueness and then we will show existence via an iteration procedure. We derive those bounds again because the equation does not have the same mathematical particularities as Burger's equation even though it is nonlinear and of parabolic type. Then we will see under which conditions there is long term existence for this problem.

Because of the homogeneous Dirichlet boundary conditions, it is easy to estimate u in the L_2 and maximum norms. These results summarize in

Lemma I.3.1.

Under the assumptions that $T^* = 0$, that the initial and boundary conditions are compatible, and that u is L_2 integrable in x , satisfying (I.1.4), upper bounds for u in the L_2 and maximum norm are given by

$$(I.3.1) \quad \| u(\cdot, t) \|^2 \leq \| u_0 \|^2$$

$$(I.3.2) \quad | u(\cdot, t) |_\infty \leq | u_0 |_\infty$$

In the case of inhomogeneous Dirichlet boundary condition at $x = 0$, we can transform the boundary condition to an homogeneous one by introducing an adequate forcing term in (I.1.4a).

Proof of Lemma I.3.1:

If we apply simple L_2 manipulations to (I.1.4), we get

$$\frac{d}{dt} \| u \|^2 = - 2 \| u_x \|^2,$$

from which we immediately deduce (I.3.1). (I.3.2) is a direct application of the maximum principle for parabolic equations [32].

The estimates (I.3.1) and (I.3.2) change if there is a forcing term $F(x, t)$ in (I.1.4). They become

$$(I.3.1') \quad \| u(\cdot, t) \|^2 \leq e^t \| u_0 \|^2 + \int_0^t e^{t-\tau} \| F(\cdot, \tau) \|^2 d\tau,$$

$$(I.3.2') \quad | u(\cdot, t) |_\infty \leq \max \left(\int_0^t | F(\cdot, \tau) |_\infty d\tau, | u_0 |_\infty \right).$$

In the rest of this section, it will be assumed that the Dirichlet boundary condition at $x = 0$ is homogeneous, i.e., $T^* = 0$. Getting estimates for spatial derivatives of u is a harder task, due to the nonlinear term $u_x(0, t) u_x(x, t)$ in (I.1.4a). First we estimate the functions $\alpha = u_x$, $\beta = u_{xx}$, and $\gamma = u_{xxx}$ in L_2 norm. In fact in order to get these estimates, we first estimate the function $\| \alpha \|^2 + \| \beta \|^2 + \| \gamma \|^2$, because of the nonlinearity and of the inhomogeneous Dirichlet boundary condition for the function β . We will also assume that the functions α , β , and γ satisfy homogeneous boundary conditions at ∞ . Once an upper bound for the function $| \alpha |_\infty$ is known, the equation can be treated further like a linear equation.

One useful tool for calculating the required bounds is Sobolev's inequality. It gives a bound on the maximum norm of a function v in terms of the L_2 norm of v and v_x . It will be extensively used all through the analysis and reads

$$(I.3.3) \quad | v |_\infty^2 \leq 2 \| v \|^2 \| v_x \|^2 \leq \epsilon \| v_x \|^2 + \frac{1}{\epsilon} \| v \|^2.$$

The first inequality of (I.3.3) is not true if v is constant, but this case is not considered because we have assumed that v is L_2 -integrable on $[0, \infty)$.

The functions $\alpha = u_x$, $\beta = u_{xx}$ and $\gamma = u_{xxx}$ satisfy

$$(I.3.4a) \quad \frac{\partial}{\partial t} \alpha(x, t) = \frac{\partial^2}{\partial x^2} \alpha(x, t) + \alpha(0, t) \frac{\partial}{\partial x} \alpha(x, t),$$

$$(I.3.4b) \quad \frac{\partial}{\partial x} \alpha(0, t) = -\alpha^2(0, t),$$

$$(I.3.4c) \quad \alpha(x, 0) = \frac{d}{dx} u_0(x),$$

$$(I.3.4d) \quad \alpha(x, t) \rightarrow 0 \quad \text{as } x \rightarrow \infty,$$

$$(I.3.5a) \quad \frac{\partial}{\partial t} \beta(x, t) = \frac{\partial^2}{\partial x^2} \beta(x, t) + \alpha(0, t) \frac{\partial}{\partial x} \beta(x, t),$$

$$(I.3.5b) \quad \beta(0, t) = -\alpha^2(0, t),$$

$$(I.3.5c) \quad \beta(x, 0) = \frac{d^2}{dx^2} u_0(x),$$

$$(I.3.5d) \quad \beta(x, t) \rightarrow 0 \quad \text{as } x \rightarrow \infty,$$

$$(I.3.6a) \quad \frac{\partial}{\partial t} \gamma(x, t) = \frac{\partial^2}{\partial x^2} \gamma(x, t) + \alpha(0, t) \frac{\partial}{\partial x} \gamma(x, t),$$

$$(I.3.6b) \quad \frac{\partial}{\partial x} \gamma(0, t) = -3 \alpha(0, t) \gamma(0, t) + 2 \alpha^4(0, t),$$

$$(I.3.6c) \quad \gamma(x, 0) = \frac{d^3}{dx^3} u_0(x),$$

$$(I.3.6d) \quad \gamma(x, t) \rightarrow 0 \quad \text{as } x \rightarrow \infty.$$

Here the functions α , β and γ are defined on the same domain as u , i.e., on $[0, \infty) \times [0, T]$. It is assumed that u and all its partial derivatives go to zero as $x \rightarrow \infty$. As mentioned before, T will be computed. Before starting to compute an upper bound for the function $z = \|\alpha\|^2 + \|\beta\|^2 + \|\gamma\|^2$, we note the other useful inequality, Young's inequality

$$(I.3.7) \quad a b \leq \frac{1}{p} a^p + \frac{1}{q} b^q, \quad \text{with } \frac{1}{p} + \frac{1}{q} = 1.$$

We apply the algebraic manipulations described in [19] and in Appendix I, as well as Sobolev's inequality (I.3.3) to (I.3.4)

$$(I.3.8) \quad \begin{aligned} \frac{d}{dt} z \leq & -2 \left(\|\alpha_x\|^2 + \|\beta_x\|^2 + \|\gamma_x\|^2 \right) + 2^{\frac{3}{2}} \left(\|\alpha\|^{\frac{3}{2}} \|\beta\|^{\frac{3}{2}} \right. \\ & \left. + \|\alpha\|^{\frac{1}{2}} \|\beta\|^{\frac{3}{2}} \|\gamma\| + 5 \|\alpha\|^{\frac{1}{2}} \|\beta\|^{\frac{1}{2}} \|\gamma\| \|\gamma_x\| \right) \\ & + 4 \left(\|\beta\|^{\frac{1}{2}} \|\gamma\| \|\gamma_x\|^{\frac{1}{2}} + 2^{\frac{5}{2}} \|\alpha\|^2 \|\beta\|^2 \|\gamma\|^{\frac{1}{2}} \|\gamma_x\|^{\frac{1}{2}} \right). \end{aligned}$$

Using Young's inequality with the correct value of p and $\|\alpha\|^2 \leq z$, $\|\beta\|^2 \leq z$, $\|\gamma\|^2 \leq z$, (I.3.8) transforms to

$$(I.3.9) \quad \frac{d}{dt} z \leq C z + C_1 z^{\frac{3}{2}} + C_2 z^2 + C_3 z^{\frac{7}{3}},$$

where C , C_1 , C_2 , and C_3 depend on the values of p and q , and on the value of ϵ . The constant ϵ has been chosen such that -2 balances the positive constant in front of $\|\gamma_x\|^2$. We obtain a bound for z from the generalization of the Gronwall-Bellman inequality to nonlinear problems. The Gronwall-Bellman inequality reads

Lemma I.3.2.

Let $\Phi \in C^1([0, \infty))$, and let $y(t)$ and $y_0(t)$ denote nonnegative C^1 functions defined for $0 \leq t \leq T$. If

$$\begin{aligned} y'(t) &\leq \Phi(y(t)), \\ y_0'(t) &= \Phi(y_0(t)), \end{aligned}$$

for $0 \leq t \leq T$ and

$$y(0) \leq y_0(0),$$

then

$$(I.3.10) \quad y(t) \leq y_0(t),$$

for $0 \leq t \leq T$.

As a consequence, there exists T_∞ , T_∞ a strictly positive constant, and a function Z , an upper bound for z on the interval $[0, T]$, with $T < T_\infty$. Z is the solution of the ordinary differential equation

$$(I.3.11a) \quad \frac{d}{dt} Z = C Z + C_1 Z^{\frac{3}{2}} + C_2 Z^2 + C_3 Z^{\frac{7}{3}}, \quad [0, T_\infty),$$

$$(I.3.11b) \quad Z(0) = \|u_0'\|^2 + \|u_0''\|^2 + \|u_0'''\|^3,$$

where $'$ denotes the differentiation with respect to x .

T_∞ is said to be the breakdown time of the ordinary differential equation, meaning that $Z(T_\infty)$ is infinite. T_∞ depends on the initial data of the ordinary differential equation.

We should note that the bound for z is not sharp. By a restarting process, we prove that the solution exists on the interval $[T, \tilde{T}]$. Later, we will show when we expect to have a solution on the interval $[0, \infty)$.

From the Gronwall-Bellman inequality and Sobolev's inequality, we deduce

Lemma I.3.3.

With the functions α , β and γ as earlier defined, satisfying homogeneous boundary conditions at ∞ , with compatible initial and boundary conditions, and Z the solution of the ordinary differential equation (I.3.11), on $[0, T]$, with T strictly smaller than the breakdown time of (I.3.11), T_∞ , we bound α and β both in L_2 and maximum norms and γ in L_2 norm:

$$(I.3.12a) \quad \|\alpha\|^2 \leq Z,$$

$$(I.3.12b) \quad \|\beta\|^2 \leq Z,$$

$$(I.3.12c) \quad \|\gamma\|^2 \leq Z,$$

$$(I.3.12d) \quad |\alpha|_\infty^2 \leq 2Z,$$

$$(I.3.12e) \quad |\beta|_\infty^2 \leq 2Z,$$

Proof of Lemma I.3.3:

We get a bound for $\|\alpha\|^2$, $\|\beta\|^2$, and $\|\gamma\|^2$ from (I.3.9) and the Gronwall-Bellman inequality. Sobolev's inequality gives the bounds for the functions $|\alpha|_\infty^2$ and $|\beta|_\infty^2$ because bounds for the functions $\|\alpha\|^2$, $\|\beta\|^2$ and $\|\gamma\|^2$ are already known.

Now we want estimates for higher-order derivatives of u . As for lower order derivatives of u , we assume that the boundary condition at ∞ is homogeneous. Two different types of difficulties arise: those with inhomogeneous Dirichlet boundary conditions and those with Neumann boundary conditions. These difficulties cover the cases to be considered. If δ is an even order partial spatial derivative of u , $\partial^{2k}/\partial x^{2k} u$, $k = 2, 3, \dots$, it satisfies

$$(I.3.13a) \quad \frac{\partial}{\partial t} \delta(x, t) = \frac{\partial^2}{\partial x^2} \delta(x, t) + \alpha(0, t) \frac{\partial}{\partial x} \delta(x, t),$$

$$(I.3.13b) \quad \delta(0, t) = E \alpha(0, t) \bar{\delta}(0, t) + G(t),$$

$$(I.3.13c) \quad \delta(x, 0) = g(x),$$

$$(I.3.13d) \quad \delta(x, t) \rightarrow 0 \quad \text{as } x \rightarrow \infty,$$

where $\delta(x, t) = \bar{\delta}_x(x, t)$ and where G is a known function depending on lower order derivatives of α that we have already bounded in L_2 and maximum norms. E is a constant depending on the order of the partial spatial derivative of u . $g(x) = d^{2k}/dx^{2k} u_0(x)$. δ is defined on the same domain as u , on $[0, \infty) \times [0, T]$.

If η is an odd order partial spatial derivative of u , $\partial^{2k+1}/\partial x^{2k+1} u$, $k = 2, 3, \dots$, it satisfies

$$(I.3.14a) \quad \frac{\partial}{\partial t} \eta(x, t) = \frac{\partial^2}{\partial x^2} \eta(x, t) + \alpha(0, t) \frac{\partial}{\partial x} \eta(x, t),$$

$$(I.3.14b) \quad \frac{\partial}{\partial x} \eta(0, t) = \tilde{E} \alpha(0, t) \eta(0, t) + \tilde{G}(t),$$

$$(I.3.14c) \quad \eta(x, 0) = \tilde{g}(x),$$

$$(I.3.14d) \quad \eta(x, t) \rightarrow 0 \quad \text{as } x \rightarrow \infty,$$

where $\tilde{g}(x) = d^{2k+1}/dx^{2k+1} u_0(x)$. Here η is defined on the same domain as u , $[0, \infty) \times [0, T]$ and \tilde{E} is a constant depending on the order of the partial spatial derivative of u considered. We cannot compute a bound for $\|\delta\|^2$ directly from (I.3.13) because the term $\delta(0, t) \delta_x(0, t)$ cannot be bounded in terms of $\|\delta\|^2$ and $\|\delta_x\|^2$. Furthermore, because we have not yet bounded $\bar{\delta}$ in maximum norm, we will estimate the function $\|\bar{\delta}\|^2 + \|\delta\|^2 + \|\delta_x\|^2$. Applying L_2 estimates to the

equations that $\bar{\delta}$, δ , and δ_x satisfy we are lead to

$$(I.3.15) \quad \frac{d}{dt} \left(\|\bar{\delta}\|^2 + \|\delta\|^2 + \|\delta_x\|^2 \right) \leq L \left(\|\bar{\delta}\|^2 + \|\delta\|^2 + \|\delta_x\|^2 \right) \\ + |\bar{G}(t)|^2 + |G(t)|^2 + |G_1(t)|^2 + |\bar{G}'(t)|^2,$$

where $\bar{G}(t)$ and $G_1(t)$ are known functions. $G_1(t) = \tilde{G}(t)$ if $\eta = \delta_x$ and $\bar{G}(t)$ is the forcing term in the equivalent of (I.3.13b) for $\bar{\delta}$. primes denote differentiation with respect to t . The Gronwall-Bellman inequality tells that

$$(I.3.16) \quad \|\bar{\delta}\|^2 + \|\delta\|^2 + \|\delta_x\|^2 \leq H(t),$$

where $H(t)$ is

$$H(t) = e^{L t} \left(\|\bar{g}\|^2 + \|g\|^2 + \left\| \frac{d}{dx} g \right\|^2 \right) \\ + \int_0^t e^{L(t-\tau)} \left(|\bar{G}(\tau)|^2 + |\bar{G}'(\tau)|^2 + |G(\tau)|^2 + |G_1(\tau)|^2 \right) d\tau.$$

These results are summarized in

Lemma I.3.4.

Define $\bar{\delta} = \partial^{2k-1} / \partial x^{2k-1} u$, $\delta = \partial^{2k} / \partial x^{2k} u$. Assume that the boundary conditions at ∞ are homogeneous. Assume the data are smooth, the initial and boundary conditions are compatible, then $\bar{\delta}$ and δ both in L_2 and maximum norms and δ_x in L_2 norm satisfy the inequalities

$$(I.3.17a) \quad \|\bar{\delta}\|^2 \leq H(t),$$

$$(I.3.17b) \quad \|\delta\|^2 \leq H(t),$$

$$(I.3.17c) \quad \|\delta_x\|^2 \leq H(t),$$

$$(I.3.17d) \quad |\bar{\delta}|_{\infty}^2 \leq 2 H(t),$$

$$(I.3.17e) \quad |\delta|_{\infty}^2 \leq 2 H(t),$$

on $[0, \infty) \times [0, T]$.

Proof of Lemma I.3.4:

We derive (I.3.17a), (I.3.17b), and (I.3.17c) from (I.3.16). Then we deduce (I.3.17d) and (I.3.17e) from (I.3.17a), (I.3.17b), and (I.3.17c) and Sobolev's inequality.

We do not need to estimate time derivatives or mixed derivatives because we replace time derivatives by space derivatives using the equations that u and its derivatives satisfy. So we get

Theorem I.3.5.

Under the assumptions that u_0 and T^* are smooth and bounded on $[0, \infty)$, that the initial and boundary conditions are compatible, that the boundary conditions for the solution and its derivatives are homogeneous at ∞ , that (I.1.4) has a unique solution u on the time interval $[0, T]$, with $T < T_\infty$, T_∞ the breakdown time of the ordinary differential equation (I.3.11), then u and its derivatives satisfy the following estimates in L_2 and maximum norms:

$$(I.3.18a) \quad \left\| \frac{\partial^{l+m}}{\partial x^l \partial t^m} u \right\|^2 \leq K_{1,m}$$

$$(I.3.18b) \quad \left| \frac{\partial^{l+m}}{\partial x^l \partial t^m} u \right|_\infty^2 \leq \tilde{K}_{1,m}$$

Proof of Theorem I.3.5:

We derive these estimates from lemmas I.3.1, I.3.3, I.3.4, and from the equation satisfied by u because we substitute space derivatives for time derivatives of u .

We will show uniqueness of the solution to (I.1.4):

Theorem I.3.6.

The system (I.1.4) with compatible initial and boundary conditions has at most one classical solution.

Proof of Theorem I.3.6:

Let u and v be solutions of (I.1.4). Define $w = u - v$. The function w satisfies

$$(I.3.19a) \quad \frac{\partial}{\partial t} w(x, t) = \frac{\partial^2}{\partial x^2} w(x, t) + \frac{\partial}{\partial x} u(0, t) \frac{\partial}{\partial x} w(x, t) + \frac{\partial}{\partial x} w(0, t) \frac{\partial}{\partial x} v(x, t),$$

$$(I.3.19b) \quad w(0, t) = 0,$$

$$(I.3.19c) \quad w(x, 0) = 0,$$

$$(I.3.19d) \quad w(x, t) \rightarrow 0 \quad \text{as} \quad x \rightarrow \infty.$$

Because of the term $w_x(0, t) v_x(x, t)$, we will see that we cannot derive an estimate for w immediately. We need to estimate the quantity $\|w\|^2 + \|w_x\|^2$. Define $y = w_x$. The function y satisfies

$$(I.3.20a) \quad \frac{\partial}{\partial t} y(x, t) = \frac{\partial^2}{\partial x^2} y(x, t) + \frac{\partial}{\partial x} u(0, t) \frac{\partial}{\partial x} y(x, t) + y(0, t) \frac{\partial^2}{\partial x^2} v(x, t),$$

$$(I.3.20b) \quad \frac{\partial}{\partial x} y(0, t) = -\left(\frac{\partial}{\partial x} u(0, t) + \frac{\partial}{\partial x} v(0, t)\right) y(0, t),$$

$$(I.3.20c) \quad y(x, 0) = 0,$$

$$(I.3.20d) \quad y(x, t) \rightarrow 0 \quad \text{as } x \rightarrow \infty.$$

After a few classical manipulations with L_2 estimates, we obtain

$$(I.3.21a) \quad \frac{d}{dt} \|w\|^2 \leq \|v_x\| \left(\epsilon \|y_x\|^2 + \frac{1}{\epsilon} \|y\|^2 + \|w\|^2 \right),$$

$$(I.3.21b) \quad \frac{d}{dt} \|y\|^2 \leq \left(-2 + \epsilon \left(|u_x(0, t)| + |v_x(0, t)| + \|v_{xx}\| \right) \right) \|y_x\|^2 + \left(1 + \frac{1}{\epsilon} \left(|u_x(0, t)| + |v_x(0, t)| + \|v_{xx}\| \right) \right) \|y\|^2.$$

So by combining (I.3.21a) and (I.3.21b), by choosing an adequate value for ϵ , and by using the fact that u, v , and derivatives of u, v are bounded, we get

$$(I.3.22) \quad \frac{d}{dt} \left(\|w\|^2 + \|y\|^2 \right) \leq C \left(\|w\|^2 + \|y\|^2 \right),$$

where C is a constant depending on u, v , their derivatives, and ϵ .

The initial conditions on w and y imply that those functions are zero. So there exists at most one classical solution to (I.1.4).

Now we want to show local existence of the solution to (I.1.4). We assume that the initial and boundary conditions are compatible and the function u^{n+1} and its derivatives satisfy homogeneous boundary conditions at ∞ . As in [19], we do that via iteration. We consider

$$(I.3.23a) \quad \frac{\partial}{\partial t} u^{n+1}(x, t) = \frac{\partial^2}{\partial x^2} u^{n+1}(x, t) + \frac{\partial}{\partial x} u^n(0, t) \frac{\partial}{\partial x} u^{n+1}(x, t),$$

$$(I.3.23b) \quad u^{n+1}(0, t) = 0,$$

$$(I.3.23c) \quad u^{n+1}(x, 0) = f(x),$$

$$(I.3.23d) \quad u^{n+1}(x, t) \rightarrow 0 \quad \text{as } x \rightarrow \infty.$$

Assuming that the initial and boundary conditions are compatible is equivalent to say that $u^{n+1}(0,0) = f(0)$ and that $f(x) \rightarrow 0$ as $x \rightarrow \infty$. To start the iteration, we choose $u^0(x,t) = f(x)$. We obtain

Lemma I.3.7.

For a suitable time $T_1 = T_1(\|f\|_{H^3}) > 0$, it holds that

$$(I.3.24) \quad \|u^n(\cdot, t)\|_{H^3} \leq C \|f\|_{H^3} \quad 0 \leq t \leq T_1,$$

where $C > 1$, and H^3 is the Sobolev space of functions having three L_2 integrable spatial derivatives.

Proof of Lemma I.3.7:

We use induction on n . The case $n = 0$ is trivial. Define $w = u^n$ and $v = u^{n+1}$. The function v then satisfies

$$(I.3.25a) \quad \frac{\partial}{\partial t} v(x,t) = \frac{\partial^2}{\partial x^2} v(x,t) + \frac{\partial}{\partial x} w(0,t) \frac{\partial}{\partial x} v(x,t),$$

$$(I.3.25b) \quad v(0,t) = 0,$$

$$(I.3.25c) \quad v(x,0) = f(x),$$

$$(I.3.25d) \quad v(x,t) \rightarrow 0 \quad \text{as } x \rightarrow \infty.$$

Because we will need to estimate v in the H^3 norm, we will derive systems that the functions $y = v_x$, $z = v_{xx}$, and $r = v_{xxx}$ satisfy

$$(I.3.26a) \quad \frac{\partial}{\partial t} y(x,t) = \frac{\partial^2}{\partial x^2} y(x,t) + \frac{\partial}{\partial x} w(0,t) \frac{\partial}{\partial x} y(x,t),$$

$$(I.3.26b) \quad \frac{\partial}{\partial x} y(0,t) = -\frac{\partial}{\partial x} w(0,t) y(0,t),$$

$$(I.3.26c) \quad y(x,0) = \frac{d}{dx} f(x),$$

$$(I.3.26d) \quad y(x,t) \rightarrow 0 \quad \text{as } x \rightarrow \infty,$$

$$(I.3.27a) \quad \frac{\partial}{\partial t} z(x,t) = \frac{\partial^2}{\partial x^2} z(x,t) + \frac{\partial}{\partial x} w(0,t) \frac{\partial}{\partial x} z(x,t),$$

$$(I.3.27b) \quad z(0,t) = -\frac{\partial}{\partial x} w(0,t) y(0,t),$$

$$(I.3.27c) \quad z(x,0) = \frac{d^2}{dx^2} f(x),$$

$$(I.3.27d) \quad z(x,t) \rightarrow 0 \quad \text{as } x \rightarrow \infty,$$

$$\begin{aligned}
 \text{(I.3.28a)} \quad & \frac{\partial}{\partial t} r(x, t) = \frac{\partial^2}{\partial x^2} r(x, t) + \frac{\partial}{\partial x} w(0, t) \frac{\partial}{\partial x} r(x, t), \\
 & \frac{\partial}{\partial x} r(0, t) = -\frac{\partial^2}{\partial x \partial t} w(0, t) y(0, t) - 2 \frac{\partial}{\partial x} w(0, t) r(0, t) \\
 \text{(I.3.28b)} \quad & - \left[\frac{\partial}{\partial x} w(0, t) \right]^2 z(0, t), \\
 \text{(I.3.28c)} \quad & r(x, 0) = \frac{d^3}{dx^3} f(x), \\
 \text{(I.3.28d)} \quad & r(x, t) \rightarrow 0 \quad \text{as } x \rightarrow \infty.
 \end{aligned}$$

After some classical L_2 manipulations on (I.3.25), (I.3.26), (I.3.27), and (I.3.28), we obtain

$$\text{(I.3.29)} \quad \frac{d}{dt} \|v\|_{H^3}^2 \leq \tilde{C} \|v\|_{H^3}^2,$$

where $\tilde{C} = 2(1 + C \|f\|_{H^3})^4$. So from the Gronwall-Bellman inequality, the requirement on T_1 will be

$$\text{(I.3.30)} \quad \exp(2(1 + C \|f\|_{H^3})^4 T_1) \leq C^2.$$

For T_1 sufficiently small (I.3.30) is satisfied because $C > 1$.

We can now derive bounds for higher derivatives of u^n .

Lemma I.3.8.

For each $j = 3, 4, \dots$, there exists a K_j with

$$\text{(I.3.31)} \quad \|u^n(\cdot, t)\|_{H^j} \leq K_j \quad 0 \leq t \leq T_1.$$

The constant K_j depends only on $\|f\|_{H^j}$, but is independent of n .

Proof of Lemma I.3.8:

As in the proof of lemma I.3.7, we proceed by induction. We carry out classical L_2 manipulations on the systems for v_j , and derive estimates of the type (I.3.31).

So we have estimated all the space derivatives of u^n on the time interval $[0, T_1]$. From Sobolev's inequality, we know that all space derivatives of u^n are bounded in maximum norm. Using the differential equation, we can replace the space derivatives by time derivatives, from which follows

Theorem I.3.9.

For a suitable time $T_1 = T_1(\|f\|_{H^3}) > 0$, it holds

$$(I.3.32a) \quad \left\| \frac{\partial^{p+q}}{\partial x^p \partial t^q} u^n(\cdot, t) \right\| \leq K_{p,q},$$

$$(I.3.32b) \quad \left| \frac{\partial^{p+q}}{\partial x^p \partial t^q} u^n(\cdot, t) \right|_{\infty} \leq \tilde{K}_{p,q}.$$

Now we want to prove that the solution of (I.1.4) exists and is in C^∞ on the interval $[0, T_1]$.

Theorem I.3.10.

The solution of (I.1.4) is in C^∞ on $[0, T_1]$, with T_1 determined in lemma I.3.7.

Proof of Theorem I.3.10:

Define $v = u^{n+1} - u^n$ and $w = u^n - u^{n-1}$. Then the function v satisfies

$$(I.3.33a) \quad \begin{aligned} \frac{\partial}{\partial t} v(x, t) &= \frac{\partial^2}{\partial x^2} v(x, t) + \frac{\partial}{\partial x} w(0, t) \frac{\partial}{\partial x} u^{n+1}(x, t) \\ &+ \frac{\partial}{\partial x} u^{n-1}(0, t) \frac{\partial}{\partial x} v(x, t), \end{aligned}$$

$$(I.3.33b) \quad v(0, t) = 0,$$

$$(I.3.33c) \quad v(x, 0) = 0,$$

$$(I.3.33d) \quad v(x, t) \rightarrow 0 \quad \text{as } x \rightarrow \infty.$$

Because of the term $w_x(0, t) u_x^{n+1}(x, t)$ in (I.3.33), we will have to estimate $\|v\|_{H^3}$ in terms of $\|w\|_{H^3}$. Define $y = v_x$, $z = v_{xx}$, and $r = v_{xxx}$. The functions y , z , and r satisfy

$$(I.3.34a) \quad \begin{aligned} \frac{\partial}{\partial t} y(x, t) &= \frac{\partial^2}{\partial x^2} y(x, t) + \frac{\partial}{\partial x} w(0, t) \frac{\partial^2}{\partial x^2} u^{n+1}(x, t) \\ &+ \frac{\partial}{\partial x} u^{n-1}(0, t) \frac{\partial}{\partial x} y(x, t), \end{aligned}$$

$$(I.3.34b) \quad \begin{aligned} \frac{\partial}{\partial x} y(0, t) &= -\frac{\partial}{\partial x} w(0, t) \frac{\partial}{\partial x} u^{n+1}(0, t) \\ &- \frac{\partial}{\partial x} u^{n-1}(0, t) y(0, t), \end{aligned}$$

$$(I.3.34c) \quad y(x, 0) = 0,$$

$$(I.3.34d) \quad y(x, t) \rightarrow 0 \quad \text{as } x \rightarrow \infty,$$

$$\frac{\partial}{\partial t} z(x, t) = \frac{\partial^2}{\partial x^2} z(x, t) + \frac{\partial}{\partial x} w(0, t) \frac{\partial^3}{\partial x^3} u^{n+1}(x, t)$$

$$(I.3.35a) \quad + \frac{\partial}{\partial x} u^{n-1}(0, t) \frac{\partial}{\partial x} z(x, t),$$

$$(I.3.35b) \quad z(0, t) = -\frac{\partial}{\partial x} w(0, t) \frac{\partial}{\partial x} u^{n+1}(0, t) - \frac{\partial}{\partial x} u^{n-1}(0, t) y(0, t),$$

$$(I.3.35c) \quad z(x, 0) = 0,$$

$$(I.3.35d) \quad z(x, t) \rightarrow 0 \quad \text{as} \quad x \rightarrow \infty,$$

$$(I.3.36a) \quad \begin{aligned} \frac{\partial}{\partial t} r(x, t) &= \frac{\partial^2}{\partial x^2} r(x, t) + \frac{\partial}{\partial x} w(0, t) \frac{\partial^4}{\partial x^4} u^{n+1}(x, t) \\ &+ \frac{\partial}{\partial x} u^{n-1}(0, t) \frac{\partial}{\partial x} r(x, t), \end{aligned}$$

$$(I.3.36b) \quad \begin{aligned} \frac{\partial}{\partial x} r(0, t) &= -\frac{\partial^2}{\partial x \partial t} w(0, t) \frac{\partial}{\partial x} u^{n+1}(0, t) \\ &- \frac{\partial}{\partial x} w(0, t) \frac{\partial^2}{\partial x \partial t} u^{n+1}(0, t) - \frac{\partial^2}{\partial x \partial t} u^{n-1}(0, t) y(0, t) \\ &- 2 \frac{\partial}{\partial x} u^{n-1}(0, t) r(0, t) \\ &- \frac{\partial}{\partial x} u^{n-1}(0, t) \frac{\partial}{\partial x} w(0, t) \frac{\partial^2}{\partial x^2} u^{n+1}(0, t) \\ &- \left[\frac{\partial}{\partial x} u^{n-1}(0, t) \right]^2 z(0, t) - \frac{\partial}{\partial x} w(0, t) \frac{\partial^3}{\partial x^3} u^{n+1}(0, t), \end{aligned}$$

$$(I.3.36c) \quad r(x, 0) = 0,$$

$$(I.3.36d) \quad r(x, t) \rightarrow \infty \quad \text{as} \quad x \rightarrow \infty.$$

After classical L_2 manipulations, we get

$$(I.3.37) \quad \frac{d}{dt} \|v\|_{H^3}^2 \leq \hat{C} (\|v\|_{H^3}^2 + \|w\|_{H^3}^2),$$

where \hat{C} is a constant depending on u^{n+1} , u^{n-1} , and their first four derivatives. Applying the Gronwall-Bellman inequality to (I.3.37), we are lead to

$$(I.3.38) \quad \|v(\cdot, t)\|_{H^3} \leq K \int_0^t \|w(\cdot, \tau)\|_{H^3} d\tau,$$

where $K = e^{\hat{C} T_1/2}$. K is independent of n .

So the sequence u^n converges to a function $u(\cdot, t)$ in H^3 . From the estimates previously obtained, we know that $u \in C^\infty$ and by the Arzela-Ascoli theorem, the convergence $u^n \rightarrow u$ holds pointwise and for all derivatives. So the function u solves (I.1.4).

Now we state under which conditions one can prove long term existence for u . One way to do this is to get a sufficiently strong *a priori* estimate for u on $[0, T]$, which depends only on the initial data and not on T itself. Because of the term $u_x(0, t) u_x(x, t)$ in (I.1.4a), we have difficulties bounding $|u_x|_\infty$ in terms of the initial data. Without this *a priori* estimate, we may choose to use a restarting process as many times as wanted, but we have no indications that the length of the interval on which the restarted solution exists does not shrink to 0.

Instead, we will take into account results from [8], [9], and [10] to show long term existence of u under certain restrictions on the data and on the coefficients of the differential operator. First, recall the main results of interest from [8], [9], and [10]. Consider the system

$$\begin{aligned} \text{(I.3.39a)} \quad & \frac{\partial^2}{\partial x^2} u(x, t) - \frac{\partial}{\partial t} u(x, t) = q(x, t) \\ \text{(I.3.39b)} \quad & u(x, 0) = h(x) \\ \text{(I.3.39c)} \quad & u(0, t) = \phi(t) \\ \text{(I.3.39d)} \quad & u(s(t), t) = f(s(t), t) \\ \text{(I.3.39e)} \quad & \frac{\partial}{\partial x} u(s(t), t) = \lambda(s(t), t) \frac{d}{dt} s(t) + \mu(s(t), t) \end{aligned}$$

with

$$\text{(I.3.40a)} \quad \lambda(x, t) \leq -\lambda_0, \quad \lambda_0 > 0,$$

and

$$\text{(I.3.40b)} \quad h(x) \leq 0, \quad \phi(t) \leq 0, \quad f(x, t) = 0, \quad q(x, t) \leq 0.$$

Furthermore assume that q is locally Hölder continuous in $\bar{\Omega}$, $\Omega = \{(x, t) \mid 0 < x < \infty, 0 < t < \infty\}$ and that in $\bar{\Omega}$

$$\text{(I.3.40c)} \quad |q(x, t)| \leq Q,$$

that f, f_x are continuous and bounded in $\bar{\Omega}$, that $f_{xx} - f_t$ is bounded and locally Hölder continuous in $\bar{\Omega}$, that ϕ is continuous for positive t and satisfies on $[0, \infty)$

$$\text{(I.3.40d)} \quad |\phi(t)| \leq \Phi,$$

that $\lambda(x, t)$ and its first derivatives are continuous in $\bar{\Omega}$ and that in $\bar{\Omega}$

$$\text{(I.3.40e)} \quad |\lambda(x, t)| \geq \lambda_0 > 0,$$

that $\mu(x, t)$ is continuous in $\overline{\Omega}$, Lipschitz continuous with respect to x uniformly in bounded sets and that in $\overline{\Omega}$,

$$(I.3.40f) \quad |\mu(x, t)| \leq M.$$

Assume also that $h(x)$ is continuous in $[0, b]$ and that there exists a positive constant H such that on $[0, b]$

$$(I.3.40g) \quad |h(x) - f(b, 0)| \leq H(b - x),$$

with

$$(I.3.40h) \quad Hb \geq \Phi + |f(b, 0)|.$$

From theorem 7 of [8], we know that if $s(t)$ is non decreasing in $(0, T^*)$, then $T^* = \infty$, T^* the maximum of the upper bound of the time intervals on which the solution exists. From collary 6 of [8], we know that if the conditions cited above are satisfied on $(0, \theta)$ with $b > 0$, then the solution exists on an interval $(0, T^*)$ with $T^* > \theta$ and $\dot{s}(t)$ satisfies

$$0 \leq \frac{d}{dt} s(t) \leq \overline{A},$$

\overline{A} a constant to be determined in terms of the data.

Theorem 8 of [8] gives a condition on $\dot{s}(t)$ in the case of a finite breakdown time.

Those results are perfectly extendable to our case, because we know that the systems (I.1.3) and (I.1.2) are equivalent. The only difference between [8] and our case is the spatial domain, which is $[s(t), \infty)$ instead of $[0, s(t)]$. From [8], if the spatial domain is $[s(t), 1]$, if λ satisfies

$$(I.3.41a) \quad \lambda(x, t) \leq \lambda_0 > 0,$$

and if the following conditions are fulfilled

$$(I.3.41b) \quad h(x) \leq 0, \quad \phi(t) \leq 0, \quad f(x, t) = 0, \quad q(x, t) \geq 0.$$

We get similar results to the ones we have already stated for a function defined on $[0, s(t)]$.

Theorem I.3.11.

The solution for (I.1.4) exists for all time if the conditions (I.3.40c), (I.3.40d), (I.3.40e), (I.3.40f), (I.3.40g), (I.3.40h), (I.3.41a) and (I.3.41b) are fulfilled.

I.4 Estimates for the Linearized Continuous Error Equations

Because we have proved that on $[0, T]$, the function u and its derivatives are bounded, we will estimate the error e and its partial derivatives in terms of the initial and boundary conditions and their derivatives. We compute also bounds for the error in the position of the interface because

$$(I.4.1) \quad c(t) = \int_0^t k(\tau) d\tau,$$

where the functions c and k are the one defined in section 2 of this chapter. Because k depends only on the derivatives of u , we obtain

Theorem I.4.1.

On the interval $[0, T]$, with $T < T_\infty$, T_∞ the breakdown time of (I.3.11),

$$(I.4.2) \quad |c(t)| \leq h^2 C T$$

Proof of Theorem I.4.1:

We immediately deduce this bound from (I.3.17b) and the expression for k .

In fact, as said before, the only term giving difficulties in this analysis is the term $e_x(0, t) u_x(x, t)$. So instead of analyzing (I.2.4), we consider

$$(I.4.3a) \quad \frac{\partial}{\partial t} e(x, t) = \frac{\partial^2}{\partial x^2} e(x, t) + \frac{\partial}{\partial x} e(0, t) \frac{\partial}{\partial x} u(x, t) + f(x, t),$$

$$(I.4.3b) \quad e(0, t) = 0,$$

$$(I.4.3c) \quad e(x, 0) = 0,$$

$$(I.4.3d) \quad e(x, t) \rightarrow 0 \quad \text{as } x \rightarrow \infty.$$

We will get results for (I.2.4) from appendix I and from the bounds computed for the solution of (I.4.3). As shown in appendix I, lower order terms just change a few constants in the estimates. Without any restriction, we can choose homogeneous Dirichlet boundary conditions. If originally $e(0, t) = g(t)$, define $e(x, t)$ as $e_1(x, t) + g(t) e^{-x^2}$. Then the function e_1 satisfies an equation of the type (I.4.3a) with a new forcing term $f(x, t) + 2g(t)(2x^2 - 1)e^{-x^2} - g'(t)e^{-x^2}$. So without loss of generality, we can choose the initial condition to be homogeneous. We assume

that the function e and its spatial partial derivatives have homogeneous boundary conditions at ∞ .

In this section, we derive estimates for e , e_x in the L_2 , and maximum norms. Once we have estimated e_x in maximum norm, the classical L_2 manipulations apply immediately because the term $e_x(0, t) u_{x \dots x}(x, t)$ is now forcing.

We cannot bound e immediately because of the term $e_x(0, t) u_x(x, t)$. Nevertheless we can compute an estimate for $\|e\|^2 + \|e_x\|^2$. The function $y = e_x$ satisfies

$$(I.4.4a) \quad \frac{\partial}{\partial t} y(x, t) = \frac{\partial^2}{\partial x^2} y(x, t) + y(0, t) \frac{\partial^2}{\partial x^2} u(x, t) + \frac{\partial}{\partial x} f(x, t),$$

$$(I.4.4b) \quad \frac{\partial}{\partial x} y(0, t) = -y(0, t) \frac{\partial}{\partial x} u(0, t) - f(0, t),$$

$$(I.4.4c) \quad y(x, 0) = 0,$$

$$(I.4.4d) \quad y(x, t) \rightarrow 0 \quad \text{as } x \rightarrow \infty.$$

So $\|e\|$, $\|e_x\|$, and $|e|_\infty$ satisfy

Lemma I.4.2.

Under the assumptions that u and f and their derivatives are smooth, and bounded on $[0, \infty) \times [0, T]$, we have the estimates

$$(I.4.5a) \quad \|e\|^2 \leq M_1(t),$$

$$(I.4.5b) \quad \|y\|^2 \leq M_1(t),$$

$$(I.4.5c) \quad |e|_\infty^2 \leq 2 M_1(t),$$

with

$$M_1(t) = \int_0^t e^{C(t-\tau)} \left(\|f(\cdot, \tau)\|^2 + \|f_x(\cdot, \tau)\|^2 + |f(0, \tau)|^2 \right) d\tau.$$

If the initial condition h is inhomogeneous, smooth, and L_2 integrable on $[0, \infty)$, $M_1(t)$ becomes

$$M_1(t) = \int_0^t e^{C(t-\tau)} \left(\|f(\cdot, \tau)\|^2 + \|f_x(\cdot, \tau)\|^2 + |f(0, \tau)|^2 \right) d\tau + e^{Ct} \left(\|h\|^2 + \left\| \frac{d}{dx} h \right\|^2 \right).$$

Proof of Lemma I.4.2:

If we apply L_2 estimates to (I.4.3), (I.4.4), it leads to

$$\begin{aligned} \frac{d}{dt} \| e \|^2 &\leq -2 \| e_x \|^2 + \| u_x \| \left(\| y \|_\infty^2 + \| e \|^2 \right) + \| e \|^2 + \| f \|^2, \\ \frac{d}{dt} \| y \|^2 &\leq -2 \| y_x \|^2 + 2 \| u_x \|_\infty \| y \|_\infty^2 + 2 \| y \|_\infty \| y \| \| u_{xx} \| \\ &\quad + 2 \| f(0, t) \| \| y \|_\infty + \| y \|^2 + \| f_x \|^2. \end{aligned}$$

Combining those two inequalities and using Sobolev's inequality (I.3.3) gives

$$\begin{aligned} \frac{d}{dt} \left(\| e \|^2 + \| y \|^2 \right) &\leq -2 \left(\| e_x \|^2 + \| y_x \|^2 \right) \\ &\quad + \epsilon \left(2 \| u_x \|_\infty + \| u_x \| + \| u_{xx} \| + 1 \right) \| y_x \|^2 \\ &\quad + \left(1 + \| u_{xx} \| + \frac{2}{\epsilon} \| u_x \|_\infty + \frac{1}{\epsilon} \| u_x \| + \frac{1}{\epsilon} \| u_{xx} \| + \frac{1}{\epsilon} \right) \| y \|^2 \\ &\quad + \left(\| u_x \| + 1 \right) \| e \|^2 + \| f \|^2 + \| f_x \|^2 + | f(0, t) |^2. \end{aligned}$$

So an inequality of the type

$$\frac{d}{dt} v(t) \leq C(t) v(t) + F(t),$$

is obtained if ϵ is chosen to be

$$2 / (D_1 + D_2 + D_3 + 1),$$

and where

$$C(t) = \max \left(\| u_x \| + 1, 1 + \| u_{xx} \| + 1/\epsilon (2 \| u_x \|_\infty + \| u_x \| + \| u_{xx} \| + 1) \right),$$

and

$$F(t) = \| f(\cdot, t) \|^2 + \| f_x(\cdot, t) \|^2 + | f(0, t) |^2.$$

D_1, D_2 and D_3 are given by

$$D_1 = \max_{0 \leq t \leq T} \| u_x \|_\infty,$$

$$D_2 = \max_{0 \leq t \leq T} \| u_x \|,$$

$$D_3 = \max_{0 \leq t \leq T} \| u_{xx} \|.$$

If C is the maximum of $C(t)$ over the interval $[0, T]$, then the Gronwall-Bellman inequality leads to (I.4.5a), (I.4.5b). Sobolev's inequality gives (I.4.5d).

Now we will estimate the functions y and y_x in maximum norm and the functions y_x and y_{xx} in L_2 norm.

Lemma I.4.3.

Under the assumptions that u, f and their derivatives are smooth and bounded on $[0, \infty) \times [0, T]$

$$(I.4.6a) \quad \|y_x\|^2 \leq M(t),$$

$$(I.4.6b) \quad \|y_{xx}\|^2 \leq M(t),$$

$$(I.4.6c) \quad |y|_{\infty}^2 \leq 2 [M(t)]^{\frac{1}{2}} [M_1(t)]^{\frac{1}{2}},$$

$$(I.4.6d) \quad |y_x|_{\infty}^2 \leq 2 M(t),$$

where $M(t)$ is given by

$$\begin{aligned} M(t) = \int_0^t e^{C_1(t-\tau)} & \left(\|f_x(\cdot, \tau)\|^2 + \|f_{xx}(\cdot, \tau)\|^2 + \|f_{xxx}(\cdot, \tau)\|^2 \right. \\ & + |f(0, \tau)|^2 + |f_t(0, \tau)|^2 \\ & \left. + |f_x(0, \tau)|^2 |u_x(0, \tau)|^2 + |f_{xx}(0, \tau)|^2 \right) d\tau. \end{aligned}$$

If the initial condition h is inhomogeneous, smooth, and L_2 integrable on $[0, \infty)$, the expression $M(t)$ becomes

$$\begin{aligned} M(t) = \int_0^t e^{C_1(t-\tau)} & \left(\|f_x(\cdot, \tau)\|^2 + \|f_{xx}(\cdot, \tau)\|^2 + \|f_{xxx}(\cdot, \tau)\|^2 \right. \\ & + |f(0, \tau)|^2 + |f_t(0, \tau)|^2 \\ & \left. + |f_x(0, \tau)|^2 |u_x(0, \tau)|^2 + |f_{xx}(0, \tau)|^2 \right) d\tau \\ & + e^{C_1 t} \left(\left\| \frac{d}{dx} h \right\|^2 + \left\| \frac{d^2}{dx^2} h \right\|^2 + \left\| \frac{d^3}{dx^3} h \right\|^2 \right). \end{aligned}$$

Proof of Lemma I.4.3:

First, we write down the equations that the functions $y_1 = y_x$ and $y_2 = y_{xx}$ satisfy

$$(I.4.7a) \quad \frac{\partial}{\partial t} y_1(x, t) = \frac{\partial^2}{\partial x^2} y_1(x, t) + y(0, t) \frac{\partial^3}{\partial x^3} u(x, t) + \frac{\partial^2}{\partial x^2} f(x, t),$$

$$(I.4.7b) \quad y_1(0, t) = -y(0, t) \frac{\partial}{\partial x} u(0, t) - f(0, t),$$

$$(I.4.7c) \quad y_1(x, 0) = 0,$$

$$(I.4.7d) \quad y_1(x, t) \rightarrow 0 \quad \text{as } x \rightarrow \infty,$$

$$(I.4.8a) \quad \frac{\partial}{\partial t} y_2(x, t) = \frac{\partial^2}{\partial x^2} y_2(x, t) + y(0, t) \frac{\partial^4}{\partial x^4} u(x, t) + \frac{\partial^3}{\partial x^3} f(x, t),$$

$$\begin{aligned} \frac{\partial}{\partial x} y_2(0, t) = & -\frac{\partial}{\partial x} u(0, t) y_2(0, t) - y(0, t) \left(\frac{\partial^2}{\partial x \partial t} u(0, t) \right. \\ & \left. + \frac{\partial^2}{\partial x^2} u(0, t) \frac{\partial}{\partial x} u(0, t) + \frac{\partial^3}{\partial x^3} u(0, t) \right) \end{aligned}$$

$$(I.4.8b) \quad -\frac{\partial}{\partial t} f(0, t) - \frac{\partial^2}{\partial x^2} f(0, t) - \frac{\partial}{\partial x} f(0, t) \frac{\partial}{\partial x} u(0, t),$$

$$(I.4.8c) \quad y_2(x, 0) = 0,$$

$$(I.4.8d) \quad y_2(x, t) \rightarrow 0 \quad \text{as } x \rightarrow \infty.$$

We will estimate the function $\|y\|^2 + \|y_x\|^2 + \|y_{xx}\|^2$ because the boundary condition of (I.4.7) is an inhomogeneous Dirichlet one and because $\|y\|_\infty$ has not yet been estimated. After we have applied L_2 manipulations to (I.4.4), (I.4.7), and (I.4.8), we get

$$\begin{aligned} \frac{d}{dt} \left(\|y\|^2 + \|y_x\|^2 + \|y_{xx}\|^2 \right) \leq & C_1 \left(\|y\|^2 + \|y_x\|^2 + \|y_{xx}\|^2 \right) \\ & + \|f_x\|^2 + \|f_{xx}\|^2 + \|f_{xxx}\|^2 + |f(0, t)|^2 \\ & + |f_t(0, t)|^2 + |f_x(0, t)|^2 + |u_x(0, t)|^2 + |f_{xx}(0, t)|^2. \end{aligned}$$

The Gronwall-Bellman inequality gives a bound for $\|y\|^2 + \|y_x\|^2 + \|y_{xx}\|^2$. Then we deduce (I.4.6a) and (I.4.6b) immediately. We derive (I.4.6c) from (I.4.6a), (I.4.5b), and Sobolev's inequality (I.3.3); (I.4.6d) from (I.4.6a), (I.4.6b), and (I.3.3).

Because we have estimated the function e_x in maximum norm, the partial differential equation that higher space derivatives of e satisfy behaves like a linear parabolic equation. Nevertheless, boundary conditions may introduce some terms that have not already been estimated in maximum norm, as noticed in (I.4.8). Using the partial differential equation, we can substitute space derivatives for time derivatives. The results are summarized in the following theorem:

Theorem I.4.4.

Under the assumptions that u and f and their derivatives are smooth and bounded on $[0, \infty) \times [0, T]$, the error e satisfies the bounds

$$(I.4.9a) \quad \left\| \frac{\partial^{m+l}}{\partial x^m \partial t^l} e \right\|^2 \leq N_{m,l}$$

$$(I.4.9b) \quad \left| \frac{\partial^{m+l}}{\partial x^m \partial t^l} e \right|_\infty \leq \tilde{N}_{m,l}$$

Proof of Theorem I.4.4

We derive (I.4.9a) and (I.4.9b) from lemmas I.4.2 and I.4.3 and the results from appendix I. Because we have only estimated spatial derivatives of the error, we will take into consideration the equation for the function e to substitute space derivatives for time derivatives.

I.5 Estimates for the Linearized Semi-Discrete Error Equations

As mentioned in the introduction, the goal of this work is to show that the discrete solution converges to the solution of the continuous problem. The continuous error equation does not provide the bounds needed and so as an intermediate step in the calculations, we will study the semi-discrete error equation. The analysis of the continuous error equation indicated a method to obtain estimates for the solution of the semi-discrete equation. Because the lower order term in (I.2.4a) $u_x(0, t) e_x(x, t)$ does not fundamentally change the behavior of the equation, we will discretize (I.4.2a) instead of (I.2.4a). For the continuous error equation, we have seen that we easily deduce boundary conditions for higher-order space derivatives by evaluating the equation at $x = 0$. In the semi-discrete case, deriving boundary conditions is a much harder task and the term $D_+ e_0 D_0 u_j$, the equivalent of $e_x(0, t) u_x(x, t)$, introduces difficulties. In order to get around them, instead of dealing with a modified form of (I.2.4), we treat a slightly different problem. The equations that the functions e and $y = e_x$ satisfy are embedded in a system for $[e, y]^T$. With this notation, we write (I.4.2) and (I.4.3) as

$$(I.5.1a) \quad \frac{\partial}{\partial t} e(x, t) = \frac{\partial^2}{\partial x^2} e(x, t) + y(0, t) v(x, t) + f(x, t),$$

$$(I.5.1b) \quad e(0, t) = 0,$$

$$(I.5.1c) \quad e(x, 0) = g(x),$$

$$(I.5.1d) \quad e(x, t) \rightarrow 0 \quad \text{as } x \rightarrow \infty,$$

$$(I.5.2a) \quad \frac{\partial}{\partial t} y(x, t) = \frac{\partial^2}{\partial x^2} y(x, t) + y(0, t) \frac{\partial}{\partial x} v(x, t) + \frac{\partial}{\partial x} f(x, t),$$

$$(I.5.2b) \quad \frac{\partial}{\partial x} y(0, t) = -y(0, t) v(0, t) - f(0, t),$$

$$(I.5.2c) \quad y(x, 0) = \frac{d}{dx} g(x),$$

$$(I.5.2d) \quad y(x, t) \rightarrow 0 \quad \text{as } x \rightarrow \infty,$$

where $v = u_x$. In the continuous case, the functions v and u_x are identical; in the semi-discrete case, v_j and $D_0 u_j$ almost give the same value, but the term $D_0 u_j$ introduces some truncation error. Define the vectors \underline{p} and \underline{g} as

$$\underline{p}(x, t) = \begin{bmatrix} e(x, t) \\ y(x, t) \end{bmatrix},$$

$$\underline{g}(x, t) = \begin{bmatrix} g(x) \\ \frac{d}{dx} g(x) \end{bmatrix}.$$

With this notation, we can write (I.5.1) and (I.5.2) as a system for \underline{p}

$$(I.5.3a) \quad \frac{\partial}{\partial t} \underline{p}(x, t) = \frac{\partial^2}{\partial x^2} \underline{p}(x, t) + \begin{bmatrix} 0 & v(x, t) \\ 0 & v_x(x, t) \end{bmatrix} \underline{p}(0, t) + \begin{bmatrix} f(x, t) \\ f_x(x, t) \end{bmatrix},$$

$$(I.5.3b) \quad \begin{bmatrix} 0 & 0 \\ 0 & 1 \end{bmatrix} \frac{\partial}{\partial x} \underline{p}(0, t) + \begin{bmatrix} 1 & 0 \\ 0 & v(0, t) \end{bmatrix} \underline{p}(0, t) = \begin{bmatrix} 0 \\ f(0, t) \end{bmatrix},$$

$$(I.5.3c) \quad \underline{p}(x, 0) = \underline{g}(x),$$

$$(I.5.3d) \quad \underline{p}(x, t) \rightarrow 0 \quad \text{as } x \rightarrow \infty.$$

Then we discretize the system (I.5.3) in space with a centered second-order finite difference scheme, on the grid with meshpoints at $((j - 1/2)h, t)$, $j = 0, 1, \dots$. The function \tilde{p} satisfies

$$(I.5.4a) \quad \frac{\partial}{\partial t} \tilde{p}_j(t) = D_+ D_- \tilde{p}_j(t) + \begin{bmatrix} 0 & \tilde{v}_j(t) \\ 0 & D_0 \tilde{v}_j(t) \end{bmatrix} A_{02} \tilde{p}_0(t) + \begin{bmatrix} \tilde{f}_j(t) \\ D_0 \tilde{f}_j(t) \end{bmatrix},$$

$$(I.5.4b) \quad \begin{bmatrix} 0 & 0 \\ 0 & 1 \end{bmatrix} D_+ \tilde{p}_0(t) + \begin{bmatrix} 1 & 0 \\ 0 & A_{02} \tilde{v}_0(t) \end{bmatrix} A_{02} \tilde{p}_0(t) = \begin{bmatrix} 0 \\ A_{02} \tilde{f}_0(t) \end{bmatrix},$$

$$(I.5.4c) \quad \tilde{p}_j(0) = \tilde{g}_j,$$

$$(I.5.4d) \quad \tilde{p}_j(t) \rightarrow 0 \quad \text{as } j \rightarrow \infty.$$

We estimate first $\|\tilde{p}\|$ and $|\tilde{p}|_\infty$. Then using the results from appendix II, we deduce bounds for higher divided differences of \tilde{p} . Once we have bounded $|\tilde{p}|_\infty$, the functions we need to evaluate satisfy linear systems. As detailed later, a fast way to estimate $|\tilde{p}|_\infty$, with \tilde{p} a discrete function in space but not in time, is to bound successively $\|\tilde{p}\|$, $\|\tilde{p}_t\|$, and $\|D_+ \tilde{p}\|$. Sobolev's inequality gives the bound for $|\tilde{p}|_\infty$. We proceed this way due to the difficulties in deriving boundary conditions for $D_+ \tilde{p}$. We deduce bounds for $\|D_- \tilde{p}\|$, $\|D_0 \tilde{p}\|$ from those that $\|D_+ \tilde{p}\|$ and

$|D_+ \underline{\tilde{p}}|_\infty$ satisfy. Then we estimate higher-order time derivatives or spatial finite difference approximations. The function $\underline{\tilde{p}}$ satisfies the bound in L_2 norm given by

Lemma I.5.1.

Under the assumptions that u, f , and their derivatives on $[0, \infty) \times [0, T]$, and that g and its derivatives on $[0, \infty)$ are smooth and bounded, we have

$$(I.5.5) \quad \|\underline{\tilde{p}}\|^2 \leq R(t),$$

where $R(t)$ is given by

$$R(t) = \int_0^t e^{L(t-\tau)} \left(\|\tilde{f}(\tau)\|^2 + \|D_0 \tilde{f}(\tau)\|^2 + C_4 |\tilde{f}_0(\tau)|^2 + C_4 |\tilde{f}_1(\tau)|^2 \right) d\tau + e^{L t} \left(\|\tilde{g}\|^2 + \|D_0 \tilde{g}\|^2 + |\tilde{g}_0|^2 \right).$$

Proof of Lemma I.5.1:

We evaluate the scalar product $(\underline{\tilde{p}}, \underline{\tilde{p}}_t)$ and summing $(\underline{\tilde{p}}, D_+ D_- \underline{\tilde{p}})$ by parts, we deduce for $(\underline{\tilde{p}}, \underline{\tilde{p}}_t)$ the estimate

$$(I.5.6a) \quad \begin{aligned} \frac{d}{dt} \|\underline{\tilde{p}}\|^2 &= -2 \|D_+ \underline{\tilde{p}}\|^2 - \frac{2}{h} \underline{\tilde{p}}_1^T (\underline{\tilde{p}}_1 - \underline{\tilde{p}}_0) \\ &\quad + 2 \left(\underline{\tilde{p}}, \begin{bmatrix} 0 & \tilde{v} \\ 0 & D_0 \tilde{v} \end{bmatrix} A_{02} \underline{\tilde{p}}_0 \right) + 2 \left(\underline{\tilde{p}}, \begin{bmatrix} \tilde{f} \\ D_0 \tilde{f} \end{bmatrix} \right), \end{aligned}$$

$$(I.5.6b) \quad \begin{aligned} &\leq -2 \|D_+ \underline{\tilde{p}}\|^2 - \frac{2}{h} \underline{\tilde{p}}_1^T (\underline{\tilde{p}}_1 - \underline{\tilde{p}}_0) + \|\underline{\tilde{p}}\|^2 \\ &\quad + \|\tilde{f}\|^2 + \|D_0 \tilde{f}\|^2 + 2 \left(\underline{\tilde{p}}, \begin{bmatrix} 0 & \tilde{v} \\ 0 & D_0 \tilde{v} \end{bmatrix} A_{02} \underline{\tilde{p}}_0 \right). \end{aligned}$$

From appendix II and the boundary conditions that $\underline{\tilde{p}}$ satisfies, we bound $-2 \underline{\tilde{p}}_1^T (\underline{\tilde{p}}_1 - \underline{\tilde{p}}_0) / h$

$$(I.5.7a) \quad -\frac{2}{h} \underline{\tilde{p}}_1^T (\underline{\tilde{p}}_1 - \underline{\tilde{p}}_0) \leq \underline{\tilde{p}}_1^2 (\underline{\tilde{p}}_1^2 - \underline{\tilde{p}}_0^2),$$

$$(I.5.7b) \quad \leq C_1 |\underline{\tilde{p}}|_\infty^2 + C_2 (|\tilde{f}_0|^2 + |\tilde{f}_1|^2).$$

The superscript i of $\underline{\tilde{p}}_j^i$ indicates which component of the vector we consider.

Details discussed in appendix II and some algebraic manipulations provide a bound for the last scalar product in (I.5.6b). This leads to

$$\begin{aligned}
 (I.5.8a) \quad \left(\begin{array}{c} \tilde{\underline{p}}, \left[\begin{array}{cc} 0 & \tilde{v} \\ 0 & D_0 \tilde{v} \end{array} \right] A_{02} \tilde{\underline{p}}_0 \end{array} \right) &= h (\tilde{\underline{p}}_0^2 + \tilde{\underline{p}}_1^2) \sum_{j=1}^{\infty} \tilde{\underline{p}}_j^1 \tilde{v}_j \\
 &+ h (\tilde{\underline{p}}_0^2 + \tilde{\underline{p}}_1^2) \sum_{j=1}^{\infty} \tilde{\underline{p}}_j^2 D_0 \tilde{v}_j, \\
 (I.5.8b) \quad &\leq \| \tilde{\underline{p}} \| \left(\| \tilde{v} \| + \| D_0 \tilde{v} \| \right) \\
 &\left(C | \tilde{\underline{p}} |_{\infty} + \tilde{C} (| \tilde{f}_0 | + | \tilde{f}_1 |) \right),
 \end{aligned}$$

because

$$| \tilde{\underline{p}}_0 | \leq C | \tilde{\underline{p}}_1 | + \tilde{C} (| \tilde{f}_0 | + | \tilde{f}_1 |).$$

Here C is a constant greater than 1 so that the inequality is valid for both homogeneous Dirichlet and Neumann boundary conditions.

After we have substituted (I.5.7b) and (I.5.8b) in (I.5.6b), $(\tilde{\underline{p}}, \tilde{\underline{p}}_t)$ satisfies

$$\begin{aligned}
 (I.5.9a) \quad \frac{d}{dt} \| \tilde{\underline{p}} \|^2 &\leq -2 \| D_+ \tilde{\underline{p}} \|^2 + \| \tilde{\underline{p}} \|^2 + C_1 | \tilde{\underline{p}} |_{\infty}^2 \\
 &+ C \left(\| \tilde{v} \| + \| D_0 \tilde{v} \| \right) | \tilde{\underline{p}} |_{\infty} \| \tilde{\underline{p}} \| \\
 &+ \tilde{C} \left(\| \tilde{v} \| + \| D_0 \tilde{v} \| \right) \| \tilde{\underline{p}} \| \left(| \tilde{f}_0 | + | \tilde{f}_1 | \right) \\
 &+ \| \tilde{f} \|^2 + \| D_0 \tilde{f} \|^2,
 \end{aligned}$$

$$\begin{aligned}
 (I.5.9b) \quad &\leq -\| D_+ \tilde{\underline{p}} \|^2 + L \| \tilde{\underline{p}} \|^2 + C_4 \left(| \tilde{f}_0 |^2 + | \tilde{f}_1 |^2 \right) \\
 &+ \| \tilde{f} \|^2 + \| D_0 \tilde{f} \|^2.
 \end{aligned}$$

We derive (I.5.9b) from (I.5.9a) using the discrete Sobolev's inequality

$$(I.5.10) \quad | v |_{\infty}^2 \leq 2 \| D_+ v \| \| v \| \leq \epsilon \| D_+ v \|^2 + \frac{1}{\epsilon} \| v \|^2,$$

and the boundedness of u and its derivatives, and substituting

$$\left(\frac{C_5}{\epsilon} + \frac{1}{2} \right) \| \tilde{\underline{p}} \|^2 + C_5 \epsilon \| D_+ \tilde{\underline{p}} \|^2,$$

for $\| \tilde{\underline{p}} \| | \tilde{\underline{p}} |_{\infty} (\| \tilde{v} \| + \| D_0 \tilde{v} \|)$, where C_5 is a constant depending on the upper bounds for $\| \tilde{v} \|$ and $\| D_0 \tilde{v} \|$. We bound the other term in (I.5.9a) in a similar

way. The requirement that the coefficient in front of $\| D_+ \tilde{p} \|^2$ be smaller than or equal to -1, fixes ϵ and L .

The Gronwall-Bellman inequality applied to (I.5.9b) gives the final estimate (I.5.5).

As mentioned earlier, a quick way to estimate $|\tilde{p}|_\infty$ is to bound $\|\tilde{p}_t\|$. Differentiating (I.5.4) with respect to time leads to the system for $\tilde{q} = \tilde{p}_t$

$$(I.5.11a) \quad \frac{\partial}{\partial t} \tilde{q}_j(t) = D_+ D_- \tilde{q}_j(t) + \begin{bmatrix} 0 & \tilde{v}_j(t) \\ 0 & D_0 \tilde{v}_j(t) \end{bmatrix} A_{02} \tilde{q}_0(t) \\ + \begin{bmatrix} 0 & \frac{d}{dt} \tilde{v}_j(t) \\ 0 & \frac{d}{dt} D_0 \tilde{v}_j(t) \end{bmatrix} A_{02} \tilde{p}_0(t) + \begin{bmatrix} \frac{d}{dt} \tilde{f}_j(t) \\ \frac{d}{dt} D_0 \tilde{f}_j(t) \end{bmatrix},$$

$$(I.5.11b) \quad \begin{bmatrix} 0 & 0 \\ 0 & 1 \end{bmatrix} D_+ \tilde{q}_0(t) + \begin{bmatrix} 1 & 0 \\ 0 & A_{02} \tilde{v}_0(t) \end{bmatrix} A_{02} \tilde{q}_0(t) \\ + \begin{bmatrix} 0 & 0 \\ 0 & \frac{d}{dt} A_{02} \tilde{v}_0(t) \end{bmatrix} A_{02} \tilde{p}_0(t) = \begin{bmatrix} 0 \\ \frac{d}{dt} A_{02} \tilde{f}_0(t) \end{bmatrix},$$

$$(I.5.11c) \quad \tilde{q}_j(0) = \tilde{h}_j,$$

$$(I.5.11d) \quad \tilde{q}_j(t) \rightarrow 0 \quad \text{as } j \rightarrow \infty,$$

where \tilde{h} is

$$\tilde{h}_j = D_+ D_- \tilde{g}_j + \begin{bmatrix} 0 & \tilde{v}_j(0) \\ 0 & D_0 \tilde{v}_j(0) \end{bmatrix} A_{02} \tilde{g}_0 + \begin{bmatrix} \tilde{f}_j(0) \\ D_0 \tilde{f}_j(0) \end{bmatrix}.$$

So \tilde{q} satisfies the bound, in L_2 norm given in

Lemma I.5.2.

Under the assumptions that u , f , and their derivatives on $[0, \infty) \times [0, T]$, and that g and its derivatives on $[0, \infty)$ are smooth and bounded, we have

$$(I.5.12) \quad \|\tilde{q}\|^2 \leq S(t),$$

where $S(t)$ is given by

$$S(t) = \int_0^t e^{Q(t-\tau)} \left(\|\tilde{f}(\tau)\|^2 + \|D_0 \tilde{f}(\tau)\|^2 + \left\| \frac{d}{dt} f(\tau) \right\|^2 \right. \\ + \left. \left\| \frac{d}{dt} D_0 \tilde{f}(\tau) \right\|^2 \right) d\tau + C \int_0^t e^{Q(t-\tau)} \left(|\tilde{f}_0(\tau)|^2 + |\tilde{f}_1(\tau)|^2 \right. \\ + \left. \left| \frac{d}{dt} f_0(\tau) \right|^2 + \left| \frac{d}{dt} f_1(\tau) \right|^2 \right) d\tau + e^{Qt} \left(\|\tilde{g}\|^2 + \|D_0 \tilde{g}\|^2 \right. \\ + \left. |\tilde{g}_0|^2 + \|\tilde{h}\|^2 + \|D_0 \tilde{h}\|^2 + |\tilde{h}_0|^2 \right),$$

and where \tilde{h} is the first component of the vector \underline{h} and $D_0 \tilde{h}$ the second one.

Proof of Lemma I.5.2:

We evaluate $\|\underline{\tilde{p}}\|^2 + \|\underline{\tilde{q}}\|^2$ because one term in (I.5.11a) depends explicitly on $\underline{\tilde{p}}_0$ and $\underline{\tilde{p}}_1$, and because we have not yet bounded $|\underline{\tilde{p}}|_\infty$. From the classical L_2 manipulations on semi-discrete equations described in appendix II, similar to the ones already carried out in the proof of lemma I.5.1, we deduce that

$$\begin{aligned}
 \frac{d}{dt} \|\underline{\tilde{q}}\|^2 &\leq -2 \|\underline{D}_+ \underline{\tilde{q}}\|^2 - \frac{2}{h} \underline{\tilde{q}}_1^T (\underline{\tilde{q}}_1 - \underline{\tilde{q}}_0) + \|\underline{\tilde{q}}\|^2 \\
 &\quad + \|\underline{\tilde{q}}\| \left(\|\tilde{v}\| + \|\underline{D}_0 \tilde{v}\| \right) \left(C_1 |\underline{\tilde{q}}|_\infty + C_2 |\underline{\tilde{p}}|_\infty \right. \\
 &\quad \left. + C_3 \left[|\tilde{f}_0| + |\tilde{f}_1| \right] + C_4 \left[\left| \frac{d}{dt} \tilde{f}_0 \right| + \left| \frac{d}{dt} \tilde{f}_1 \right| \right] \right) \\
 &\quad + \|\underline{\tilde{q}}\| \left(\left\| \frac{d}{dt} \tilde{v} \right\| + \left\| \frac{d}{dt} \underline{D}_0 \tilde{v} \right\| \right) \\
 &\quad - \left(C |\underline{\tilde{p}}|_\infty + \tilde{C} \left(|\tilde{f}_0| + |\tilde{f}_1| \right) \right) \\
 &\quad + \left\| \frac{d}{dt} \tilde{f} \right\|^2 + \left\| \frac{d}{dt} \underline{D}_0 \tilde{f} \right\|^2.
 \end{aligned}
 \tag{I.5.13}$$

To express the right-hand side of (I.5.13) in terms of $\|\underline{\tilde{p}}\|^2$, $\|\underline{\tilde{q}}\|^2$, $|\underline{\tilde{p}}|_\infty^2$, $|\underline{\tilde{q}}|_\infty^2$, $\|\underline{D}_+ \underline{\tilde{p}}\|^2$, and $\|\underline{D}_+ \underline{\tilde{q}}\|^2$, as in the proof of lemma I.5.1, we use Cauchy-Scharzwz's inequality, the boundedness of u and its derivatives. Then because

$$|\underline{\tilde{q}}_0| \leq C \left(|\underline{\tilde{p}}_1| + |\underline{\tilde{q}}_1| \right) + C_1 \left(|\tilde{f}_0| + |\tilde{f}_1| \right) + \left(\left| \frac{d}{dt} \tilde{f}_0 \right| + \left| \frac{d}{dt} \tilde{f}_1 \right| \right),$$

and if we put together (I.5.9a) and (I.5.13), we get for $\|\underline{\tilde{p}}\|^2 + \|\underline{\tilde{q}}\|^2$ the inequality

$$\begin{aligned}
 \frac{d}{dt} \left(\|\underline{\tilde{q}}\|^2 + \|\underline{\tilde{p}}\|^2 \right) &\leq -2 \|\underline{D}_+ \underline{\tilde{q}}\|^2 - 2 \|\underline{D}_+ \underline{\tilde{p}}\|^2 + D_1 \|\underline{\tilde{p}}\|^2 \\
 &\quad + D_2 \|\underline{\tilde{q}}\|^2 + D_3 |\underline{\tilde{p}}|_\infty^2 + D_4 |\underline{\tilde{q}}|_\infty^2 + \|\tilde{f}\|^2 \\
 &\quad + \left\| \frac{d}{dt} \tilde{f} \right\|^2 + \left\| \frac{d}{dt} \underline{D}_0 \tilde{f} \right\|^2 + D_5 \left(|\tilde{f}_0|^2 + |\tilde{f}_1|^2 \right) \\
 &\quad + D_6 \left(\left| \frac{d}{dt} \tilde{f}_0 \right|^2 + \left| \frac{d}{dt} \tilde{f}_1 \right|^2 \right) + \|\underline{D}_0 \tilde{f}\|^2.
 \end{aligned}
 \tag{I.5.14}$$

$D_1, D_2, D_3, D_4, D_5,$ and D_6 are constants depending on \tilde{u} and on the initial data. We apply Sobolev's inequality to (5.14) to bound $|\underline{\tilde{p}}|_\infty$ and $|\underline{\tilde{q}}|_\infty$ in terms of $\|\underline{\tilde{p}}\|$, $\|\underline{\tilde{q}}\|$, $\|\underline{D}_+ \underline{\tilde{p}}\|$ and $\|\underline{D}_+ \underline{\tilde{q}}\|$. The requirement that the coefficient in front

of $\| D_+ \underline{\tilde{p}} \|^2$ be negative or nul and that the coefficient in front of $\| D_+ \underline{\tilde{q}} \|^2$ be smaller than or equal to -1, fixes ϵ and the constant Q in front of $\| \underline{\tilde{p}} \|^2 + \| \underline{\tilde{q}} \|^2$. So

$$\begin{aligned}
 \frac{d}{dt} (\| \underline{\tilde{p}} \|^2 + \| \underline{\tilde{q}} \|^2) &\leq -\| D_+ \underline{\tilde{q}} \|^2 + Q (\| \underline{\tilde{p}} \|^2 + \| \underline{\tilde{q}} \|^2) + \| \tilde{f} \|^2 \\
 &+ \| D_0 \tilde{f} \|^2 + \left\| \frac{d}{dt} \tilde{f} \right\|^2 + \left\| \frac{d}{dt} D_0 \tilde{f} \right\|^2 \\
 &+ D_5 (| \tilde{f}_0 |^2 + | \tilde{f}_1 |^2) \\
 \text{(I.5.15)} \quad &+ D_6 \left(\left| \frac{d}{dt} \tilde{f}_0 \right|^2 + \left| \frac{d}{dt} \tilde{f}_1 \right|^2 \right).
 \end{aligned}$$

The Gronwall-Bellman inequality gives (I.5.12).

Because we have estimated $\underline{\tilde{q}}$ in L_2 norm, from (I.5.9b), we deduce an upper bound for $D_+ \underline{\tilde{p}}$ in L_2 norm.

Lemma I.5.3.

Under the assumptions that u , f , and their derivatives on $[0, \infty) \times [0, T]$, and that g and its derivatives on $[0, \infty)$ are smooth and bounded, we have

$$\text{(I.5.16)} \quad \| D_+ \underline{\tilde{p}} \|^2 \leq X(t),$$

where $X(t)$ is given by

$$X(t) = (L + 1) R(t) + S(t) + \| \tilde{f} \|^2 + \| D_0 \tilde{f} \|^2 + C_4 (| \tilde{f}_0 |^2 + | \tilde{f}_1 |^2),$$

and where $R(t)$ and $S(t)$ are the bounds calculated above for $\| \underline{\tilde{p}} \|^2$ and $\| \underline{\tilde{q}} \|^2$.

Proof of Lemma I.5.3:

From (I.5.9b), we deduce

$$\begin{aligned}
 \| D_+ \underline{\tilde{p}} \|^2 &\leq 2 \| \underline{\tilde{p}} \| \| \underline{\tilde{q}} \| + L \| \underline{\tilde{p}} \|^2 \\
 \text{(I.5.17a)} \quad &+ \| \tilde{f} \|^2 + \| D_0 \tilde{f} \|^2 + C_4 (| \tilde{f}_0 |^2 + | \tilde{f}_1 |^2),
 \end{aligned}$$

$$\begin{aligned}
 &\leq (L + 1) \| \underline{\tilde{p}} \|^2 + \| \underline{\tilde{q}} \|^2 \\
 \text{(I.5.17b)} \quad &+ \| \tilde{f} \|^2 + \| D_0 \tilde{f} \|^2 + C_4 (| \tilde{f}_0 |^2 + | \tilde{f}_1 |^2),
 \end{aligned}$$

We obtain an expression for $X(t)$ immediately from (I.5.17b) once we have substituted in (I.5.17b) upper bounds for $\| \underline{\tilde{p}} \|^2$ and $\| \underline{\tilde{q}} \|^2$.

So because we have bounded $\underline{\tilde{p}}$ and $D_+ \underline{\tilde{p}}$ in L_2 norm, we can then estimate $\underline{\tilde{p}}$ in maximum norm.

Lemma I.5.4.

Under the assumptions that u , f , and their derivatives on $[0, \infty) \times [0, T]$, and that g and its derivatives on $[0, \infty)$ are smooth and bounded, we have that

$$(I.5.18a) \quad |\underline{\tilde{p}}|_{\infty}^2 \leq 2 R^{\frac{1}{2}}(t) X^{\frac{1}{2}}(t),$$

$$(I.5.18b) \quad |\underline{\tilde{q}}|_{\infty}^2 \leq 2 S^{\frac{1}{2}}(t) Z^{\frac{1}{2}}(t),$$

where $Z(t)$ is an upper bound for $\|D_+ \underline{\tilde{q}}\|^2$.

Proof of Lemma I.5.4:

We derive (I.5.18a) from Sobolev's inequality (I.5.10), (I.5.5), and (I.5.16). Similarly, we obtain (I.5.18b) from (I.5.10), (I.5.12), and the equivalent of (I.5.16) for $\underline{\tilde{q}}$.

We will then bound $D_- \underline{\tilde{p}}$ in L_2 norm.

Lemma I.5.5.

Under the assumptions that u , f , and their derivatives on $[0, \infty) \times [0, T]$, and that g and its derivatives on $[0, \infty)$ are smooth and bounded, we have

$$(I.5.19) \quad \|D_- \underline{\tilde{p}}\|^2 \leq Y(t),$$

where $Y(t)$ is given by

$$Y(t) = N X(t) + \tilde{N} R(t) + N_0 S(t) + \tilde{N}_0 Z(t) \\ + N_1 W(t) + N_2 \left(|\tilde{f}_0|^2 + |\tilde{f}_1|^2 \right),$$

where $X(t)$, $R(t)$, $S(t)$, $Z(t)$, and $W(t)$ are the upper bounds computed above for $\|D_+ \underline{\tilde{p}}\|^2$, $\|\underline{\tilde{p}}\|^2$, $\|\underline{\tilde{q}}\|^2$, $\|D_+ \underline{\tilde{q}}\|^2$, and $\|D_+^2 \underline{\tilde{p}}\|$. N , \tilde{N} , N_0 , \tilde{N}_0 , N_1 , and N_2 are constants depending on the initial condition and on the coefficients of the differential operator.

We will prove an intermediate result necessary to bound $\|D_- \underline{\tilde{p}}\|$. While bounding $\|D_- \underline{\tilde{p}}\|$, the term $|D_+ \underline{\tilde{p}}|_{\infty}$ arises, if the boundary conditions are

of homogeneous Dirichlet type or of mixed type. We will compute a bound for $\|D_+^2 \underline{\tilde{p}}\|$. Define $\underline{\tilde{r}} = D_+ \underline{\tilde{p}}$. The function $\underline{\tilde{r}}$ satisfies

$$(I.5.20a) \quad \begin{aligned} \frac{\partial}{\partial t} \underline{\tilde{r}}_j(t) &= D_+ D_- \underline{\tilde{r}}_j(t) + \begin{bmatrix} 0 & D_+ \tilde{v}_j(t) \\ 0 & D_+ D_0 \tilde{v}_j(t) \end{bmatrix} A_{02} \underline{\tilde{p}}_0(t) \\ &+ \begin{bmatrix} D_+ \tilde{f}_j(t) \\ D_+ D_0 \tilde{f}_j(t) \end{bmatrix}, \end{aligned}$$

$$(I.5.20b) \quad \begin{aligned} \begin{bmatrix} 1 & 0 \\ 0 & 0 \end{bmatrix} D_+ \underline{\tilde{r}}_0(t) + \begin{bmatrix} 0 & 0 \\ 0 & 1 \end{bmatrix} A_{02} \underline{\tilde{r}}_0(t) \\ = -A_{02} \tilde{v}_0(t) A_{02} \underline{\tilde{p}}_0(t) - A_{02} \tilde{f}_0(t) \begin{bmatrix} 1 \\ 1 \end{bmatrix}, \end{aligned}$$

$$(I.5.20c) \quad \underline{\tilde{r}}_j(0) = D_+ \underline{\tilde{g}}_j,$$

$$(I.5.20d) \quad \underline{\tilde{r}}_j(t) \rightarrow 0 \quad \text{as } j \rightarrow \infty.$$

We obtain (I.5.20a) and (I.5.20c) from (I.5.4a) and (I.5.4c), by applying the difference operator D_+ to them. We deduce (I.5.20b) from the boundary condition for the continuous problem (I.5.3b), by differentiating it with respect to time, then by discretizing it with a centered second-order scheme.

Because one component of $\underline{\tilde{r}}$ satisfies inhomogeneous Dirichlet boundary conditions, a new function $\underline{\tilde{s}}$, satisfying homogeneous Dirichlet boundary conditions is introduced,

$$\underline{\tilde{s}} = \underline{\tilde{r}} + \left(A_{02} \tilde{v}_0(t) \begin{bmatrix} 0 & 0 \\ 0 & 1 \end{bmatrix} A_{02} \underline{\tilde{p}}_0(t) + \begin{bmatrix} 0 \\ A_{02} \tilde{f}_0(t) \end{bmatrix} \right) \Lambda,$$

where Λ is the discrete function given by

$$\Lambda_j = e^{-(j-1/2)^2 h^2}.$$

The function $\underline{\tilde{s}}$ satisfies

$$(I.5.21a) \quad \begin{aligned} \frac{\partial}{\partial t} \underline{\tilde{s}}_j(t) &= D_+ D_- \underline{\tilde{s}}_j(t) + \begin{bmatrix} 0 & D_+ \tilde{v}_j(t) \\ 0 & D_+ D_0 \tilde{v}_j(t) \end{bmatrix} A_{02} \underline{\tilde{p}}_0(t) \\ &+ A_{02} \tilde{v}_0(t) \begin{bmatrix} 0 & 0 \\ 0 & D_+ D_- \Lambda_j \end{bmatrix} A_{02} \underline{\tilde{p}}_0(t) \\ &+ \begin{bmatrix} D_+ \tilde{f}_j(t) \\ D_+ D_0 \tilde{f}_j(t) + A_{02} \tilde{f}_0(t) D_+ D_- \Lambda_j \end{bmatrix}, \\ \begin{bmatrix} 1 & 0 \\ 0 & 0 \end{bmatrix} D_+ \underline{\tilde{s}}_0(t) + \begin{bmatrix} 0 & 0 \\ 0 & 1 \end{bmatrix} A_{02} \underline{\tilde{s}}_0(t) \end{aligned}$$

$$(I.5.21b) \quad = - \begin{bmatrix} A_{02} \tilde{v}_0(t) & 0 \\ 0 & 0 \end{bmatrix} A_{02} \tilde{p}_0(t) - \begin{bmatrix} A_{02} \tilde{f}_0(t) \\ 0 \end{bmatrix},$$

$$\tilde{s}_j(0) = D_+ \tilde{g}_j$$

$$(I.5.21c) \quad + \left(A_{02} \tilde{v}_0(0) \begin{bmatrix} 0 & 0 \\ 0 & 1 \end{bmatrix} A_{02} \tilde{g}_0 + \begin{bmatrix} 0 \\ A_{02} \tilde{f}_0(0) \end{bmatrix} \right) \Lambda_j,$$

$$(I.5.21d) \quad \tilde{s}_j(t) \rightarrow 0 \quad \text{as } j \rightarrow \infty.$$

So $D_+^2 \tilde{p}$ satisfies the bound in L_2 norm given in

Lemma I.5.6.

Under the assumptions that u , f , and their derivatives on $[0, \infty) \times [0, T]$ and g and its derivatives on $[0, \infty)$ are smooth and bounded, we have

$$(I.5.22) \quad \| D_+^2 \tilde{p} \|^2 \leq W(t),$$

where

$$W(t) = 2 W_1(t) + 2(A+1) W_0(t) + 2 \| D_+ \tilde{f} \|^2 + 2 \| D_+ D_0 \tilde{f} \|^2 + \tilde{B} (|\tilde{f}_0|^2 + |\tilde{f}_1|^2) + \tilde{C} X^{\frac{1}{2}}(t) R^{\frac{1}{2}}(t),$$

and where A , \tilde{B} and \tilde{C} are constants depending on the coefficients of the differential operator, on the initial data, and on Λ and its divided differences.

Proof of Lemma I.5.6:

From classical L_2 manipulations, we deduce that $\| \tilde{s} \|$ satisfies the differential inequality

$$(I.5.23) \quad \frac{d}{dt} \| \tilde{s} \|^2 \leq - \| D_+ \tilde{s} \|^2 + A \| \tilde{s} \|^2 + \| D_+ \tilde{f} \|^2 + \| D_+ D_0 \tilde{f} \|^2 + B (|\tilde{f}_0|^2 + |\tilde{f}_1|^2) + C \| \tilde{p} \|_\infty^2,$$

and the inequality

$$(I.5.24) \quad \| \tilde{s} \|^2 \leq W_0(t),$$

where

$$W_0(t) = 2 X(t) + 2 \| \Lambda \|^2 \left(2 D X^{\frac{1}{2}}(t) R^{\frac{1}{2}}(t) + E |\tilde{f}_0|^2 + E |\tilde{f}_1|^2 \right),$$

because we have already bounded \tilde{x} in L_2 norm.

Because we want an estimate for $\|D_+ \tilde{p}_t\|$, because \tilde{x} satisfies homogeneous Dirichlet boundary conditions, and because we easily deduce a bound for $\|D_+ \tilde{p}_t\|$ from the bound for $\|D_+ \tilde{x}_t\|$, we estimate $\tilde{t} = \tilde{x}_t$. After a few algebraic manipulations, \tilde{t} satisfies the differential inequality

$$(I.5.25) \quad \begin{aligned} \frac{d}{dt} \|\tilde{t}\|^2 &\leq A_1 \|\tilde{t}\|^2 + \left\| \frac{d}{dt} D_+ \tilde{f} \right\|^2 + \left\| \frac{d}{dt} D_+ D_0 \tilde{f} \right\|^2 \\ &\quad + B_1 \left(\left| \frac{d}{dt} \tilde{f}_0 \right|^2 + \left| \frac{d}{dt} \tilde{f}_1 \right|^2 \right) + C_1 (|\tilde{f}_0|^2 + |\tilde{f}_1|^2) \\ &\quad + D_1 |\tilde{p}|_\infty^2 + E_1 |\tilde{q}|_\infty^2. \end{aligned}$$

The Gronwall-Bellman inequality gives

$$(I.5.26) \quad \|\tilde{t}\|^2 \leq W_1(t),$$

where

$$\begin{aligned} W_1(t) &= \int_0^t e^{A_1(t-\tau)} \left(\left\| \frac{d}{dt} D_+ \tilde{f}(\tau) \right\|^2 + \left\| \frac{d}{dt} D_+ D_0 \tilde{f}(\tau) \right\|^2 \right. \\ &\quad + B_1 \left| \frac{d}{dt} \tilde{f}_0(\tau) \right|^2 + B_1 \left| \frac{d}{dt} \tilde{f}_1(\tau) \right|^2 + C_1 |\tilde{f}_0(\tau)|^2 \\ &\quad \left. + C_1 |\tilde{f}_1(\tau)|^2 + D_1 X^{\frac{1}{2}}(\tau) R^{\frac{1}{2}}(\tau) + E_1 S^{\frac{1}{2}}(\tau) Z^{\frac{1}{2}}(\tau) \right) d\tau \\ &\quad + e^{A_1 t} \left(\|D_+ \tilde{h}\|^2 + \|D_+ D_0 \tilde{h}\|^2 \right). \end{aligned}$$

From (I.5.26) and (I.5.23), we calculate an upper bound for $\|D_+ \tilde{x}\|$,

$$(I.5.27) \quad \begin{aligned} \|D_+ \tilde{x}\|^2 &\leq \|\tilde{t}\|^2 + (A+1) \|\tilde{x}\|^2 + \|D_+ \tilde{f}\|^2 + \|D_+ D_0 \tilde{f}\|^2 \\ &\quad + B \left(|\tilde{f}_0|^2 + |\tilde{f}_1|^2 \right) + C X^{\frac{1}{2}}(t) R^{\frac{1}{2}}(t). \end{aligned}$$

From this, we obtain the upper bound for $\|D_+ \tilde{x}\|$, because

$$\begin{aligned} \|D_+ \tilde{x}\|^2 &\leq 2 \|D_+ \tilde{x}\|^2 \\ &\quad + 2 \|D_+ \Lambda\|^2 \left(C R^{\frac{1}{2}}(t) X^{\frac{1}{2}}(t) + |\tilde{f}_0(t)|^2 + |\tilde{f}_1(t)|^2 \right). \end{aligned}$$

Proof of Lemma I.5.5:

The operators D_+ and D_- are related by

$$D_+ v_j = D_- v_{j+1}.$$

So we deduce that an estimate for $D_- \underline{\tilde{p}}$ in L_2 norm can be computed from the bounds already obtained for $D_+ \underline{\tilde{p}}$, $D_+^2 \underline{\tilde{p}}$ in L_2 norm and the boundary conditions imposed on $\underline{\tilde{p}}$ at the origin. The following relation between the L_2 norm of the two expressions holds

$$(I.5.28) \quad \| D_- \underline{\tilde{p}} \|^2 = \| D_+ \underline{\tilde{p}} \|^2 + \frac{1}{h} (\underline{\tilde{p}}_1 - \underline{\tilde{p}}_0)^T (\underline{\tilde{p}}_1 - \underline{\tilde{p}}_0).$$

If the boundary conditions are of Neumann type, then

$$(I.5.29) \quad | D_+ \underline{\tilde{p}}_0 |^2 \leq C | \underline{\tilde{p}} |_\infty^2 + \tilde{C} (| \tilde{f}_0 |^2 + | \tilde{f}_1 |^2).$$

If we replace $| D_+ \underline{\tilde{p}}_0 |^2$ and $\| D_+ \underline{\tilde{p}} \|^2$ by their upper bounds in (I.5.28), if we use Sobolev's inequality to estimate $| \underline{\tilde{p}} |^2$, we obtain (I.5.19) immediately.

If the boundary conditions are of homogeneous Dirichlet type, then from (I.5.4a), we find that

$$(I.5.30a) \quad \frac{1}{h} (\underline{\tilde{p}}_1 - \underline{\tilde{p}}_0)^T (\underline{\tilde{p}}_1 - \underline{\tilde{p}}_0) = 2 h \underline{\tilde{p}}_1^T [-\tilde{q}_1 + \tilde{f}_1] + \frac{2}{h} \underline{\tilde{p}}_1^T (\underline{\tilde{p}}_2 - \underline{\tilde{p}}_1),$$

$$\leq F \| \underline{\tilde{p}} \|^2 + F_1 \| \underline{\tilde{q}} \|^2 + F_2 \| D_+ \underline{\tilde{p}} \|^2$$

$$+ F_1 \| D_+ \underline{\tilde{q}} \|^2$$

$$(I.5.30b) \quad + F_3 | \tilde{f}_1 |^2 + F_4 \| D_+^2 \underline{\tilde{p}} \|^2.$$

We get (I.5.19) immediately once we have substituted (I.5.30b) into (I.5.28).

If the boundary conditions are for one component of homogeneous Dirichlet type and for the other one of Neumann type, the scalar product composed of the sum of two terms will have each of its terms satisfying inequalities either of type (I.5.29) or of type (I.5.30b). From (I.5.28), we deduce that (I.5.19) is satisfied.

Because we have estimated $D_+ \underline{\tilde{p}}$, $D_- \underline{\tilde{p}}$ in L_2 norm, then we have also estimated $D_0 \underline{\tilde{p}}$ in L_2 norm.

Lemma I.5.7.

Under the assumptions that u , f , and their derivatives on $[0, \infty) \times [0, T]$, and that g and its derivatives on $[0, \infty)$ are smooth and bounded, we have

$$(I.5.31) \quad \| D_0 \underline{\tilde{p}} \|^2 \leq \frac{1}{2} X(t) + \frac{1}{2} Y(t).$$

Proof of Lemma I.5.7:

We deduce (I.5.31) immediately from lemmas I.5.3 and I.5.5, because

$$\| D_0 \underline{\tilde{p}} \| \leq \frac{1}{2} \| D_+ \underline{\tilde{p}} \| + \frac{1}{2} \| D_- \underline{\tilde{p}} \|.$$

For higher derivatives, we get the bounds directly from the results of appendix II and the previous calculations. We summarize these estimates in

Theorem I.5.8.

Under the assumptions that u , f , and their derivatives on $[0, \infty) \times [0, T]$, and that g and its derivatives on $[0, \infty)$ are smooth and bounded, we have

$$(I.5.32a) \quad \left\| \frac{d^k}{dt^k} D_+^l D_-^m D_0^n \underline{\tilde{p}} \right\|^2 \leq Q_{k,l,m,n},$$

$$(I.5.32b) \quad \left| \frac{d^k}{dt^k} D_+^l D_-^m D_0^n \underline{\tilde{p}} \right|_\infty^2 \leq \tilde{Q}_{k,l,m,n}.$$

Proof of Theorem I.5.8:

We derive (I.5.32a) and (I.5.32b) from lemmas I.5.3, I.5.4, I.5.5, and I.5.7 as well as from the equation the function $\underline{\tilde{p}}$ satisfies. Because it is easier to estimate time derivatives of $\underline{\tilde{p}}$ than spatial divided differences of $\underline{\tilde{p}}$, each time it is possible, we replace spatial divided differences by time derivatives, by using the equation. So using these arguments and repeating the procedure as many times as needed, we deduce (I.5.32a) and (I.5.32b).

What we were interested in, was to bound $\tilde{\epsilon}$ in both L_2 and maximum norms.

Theorem I.5.9.

Under the assumptions that u , f , and their derivatives on $[0, \infty) \times [0, T]$, and g and its derivatives on $[0, \infty)$ are smooth and bounded, we have

$$(I.5.33a) \quad \left\| \frac{d^k}{dt^k} D_+^l D_-^m D_0^n \tilde{\epsilon} \right\|^2 \leq Q_{k,l,m,n},$$

$$(I.5.33b) \quad \left| \frac{d^k}{dt^k} D_+^l D_-^m D_0^n \tilde{\epsilon} \right|_\infty^2 \leq \tilde{Q}_{k,l,m,n}.$$

Proof of Theorem I.5.9:

We derive (I.5.33a) and (I.5.33b) from (I.5.32a) and (I.5.32b) because the function $\tilde{\epsilon}$ is the first component of the vector $\underline{\tilde{p}}$.

I.6 Estimates for the Linearized Discrete Error Equations

The estimates obtained up to now are for functions continuous with respect to time. So, now, we would like to derive bounds for the functions satisfying the linear error equation, discretized both in time and in space. As in sections 4 and 5, instead of considering the system with lower order terms, equivalent to (I.2.4) or (I.2.5), (I.5.4) will be discretized in time with Crank-Nicholson scheme. We can drop lower order terms because they do not fundamentally change the behavior of the equation. As explained at the end of appendix II, we only need to modify a few constants in the final estimates if these terms are present. If we discretize in time (I.5.4), it reads

$$(I.6.1a) \quad \frac{\hat{p}_j^{n+1} - \hat{p}_j^n}{\tau} = \frac{1}{2} D_+^x D_-^x (\hat{p}_j^{n+1} + \hat{p}_j^n) + \frac{1}{4} \begin{bmatrix} 0 & \hat{v}_j^{n+1} + \hat{v}_j^n \\ 0 & D_0^x \hat{v}_j^{n+1} + D_0^x \hat{v}_j^n \end{bmatrix} A_{02} (\hat{p}_0^{n+1} + \hat{p}_0^n) + \frac{1}{2} \begin{bmatrix} \hat{f}_j^{n+1} + \hat{f}_j^n \\ D_0^x \hat{f}_j^{n+1} + D_0^x \hat{f}_j^n \end{bmatrix},$$

$$(I.6.1b) \quad \begin{bmatrix} 0 & 0 \\ 0 & 1 \end{bmatrix} (D_+^x \hat{p}_0^{n+1} + D_+^x \hat{p}_0^n) + \frac{1}{2} \begin{bmatrix} 2 & 0 \\ 0 & A_{02} (\hat{v}_0^{n+1} + \hat{v}_0^n) \end{bmatrix} A_{02} (\hat{p}_0^{n+1} + \hat{p}_0^n) = \begin{bmatrix} 0 \\ A_{02} (\hat{f}_0^{n+1} + \hat{f}_0^n) \end{bmatrix},$$

$$(I.6.1c) \quad \hat{p}_j^0 = \tilde{g}_j,$$

$$(I.6.1d) \quad \hat{p}_j^n \rightarrow 0 \quad \text{as } j \rightarrow \infty.$$

\hat{v}^n means that we have discretized the function v in time and have evaluated it at the time level n , or at the time $n \tau$, τ being the time step. The vector \hat{p}_j^n is an approximation of $\underline{p}((j - 1/2) h, n \tau)$ $j = 0, 1, \dots, n = 0, 1, \dots$. D^x means that the finite differences operator operates on the space variable, similarly, D^t means that it operates on the time variable. As explained in [25], once we have estimated the continuous solution in time, we derive bounds for the solution of the equation discretized in time with Crank-Nicholson scheme in a straightforward manner.

To simplify the notation, we will refer to (I.5.4) as

$$(I.6.2) \quad \frac{d}{dt} \tilde{p}_j = \mathcal{L}(t) \tilde{p}_j.$$

With this notation, we can write (I.6.1) as

$$(I.6.3) \quad \frac{\hat{p}_j^{n+1} - \hat{p}_j^n}{\tau} = \frac{1}{4} (\mathcal{L}^{n+1} + \mathcal{L}^n) (\hat{p}_j^{n+1} + \hat{p}_j^n).$$

In this section, we will derive results similar to the ones obtained in section 5, with the sole exception that time is a discrete variable and that there is a restriction on the size of the time step. So as in section 5, first we estimate $\|\hat{p}_-\|^n$ and $|\hat{p}_-^n|_\infty$. Then we will estimate higher-order divided differences of \hat{p}_- . The systems we will consider are linear once we have bounded $|\hat{p}_-^n|_\infty$. As in section 5, we compute a bound for $|\hat{p}_-^n|_\infty$, by estimating $\|\hat{p}_-\|^n$, $\|D_+^t \hat{p}_-\|^n$, $\|D_+^x \hat{p}_-\|^n$, and then using the discrete Sobolev's inequality. We proceed in this way due to the difficulties we have in deriving boundary conditions for $D_+^x \hat{p}_-$ in the semi-discrete case. We deduce bounds for $\|D_-^x \hat{p}_-\|^n$, $\|D_0^x \hat{p}_-\|^n$ from the bounds $\|D_+^x \hat{p}_-\|^n$, $\|D_+^t \hat{p}_-\|^n$, and $|D_+ \hat{p}_-|_\infty$ satisfy. Then we estimate higher-order finite difference approximations in a similar fashion.

Lemma I.6.1.

Under the assumptions that u, f , and their derivatives on $[0, \infty) \times [0, T]$, and g and its derivatives on $[0, \infty)$ are smooth and bounded, we have

$$(I.6.4) \quad \|\hat{p}_-\|^n \leq \hat{R}^n,$$

where \hat{R}^n

$$\begin{aligned} \hat{R}^n = & e^{L n \tau} \left(\|\tilde{g}\|^2 + \|D_0^x \tilde{g}\|^2 + |\tilde{g}_0|^2 \right) + \frac{1}{4} C_4 \tau \sum_{k=0}^{n-1} e^{L (k+1/2) \tau} \left(|\hat{f}_0^{n-k}|^2 \right. \\ & \left. + |\hat{f}_0^{n-k-1}|^2 + |\hat{f}_1^{n-k}|^2 + |\hat{f}_1^{n-k-1}|^2 \right) + \frac{\tau}{4} \sum_{k=0}^{n-1} e^{L (k+1/2) \tau} \\ & \left(\|\hat{f}^{n-k}\|^2 + \|\hat{f}^{n-k-1}\|^2 + \|D_0^x \hat{f}^{n-k}\|^2 + \|D_0^x \hat{f}^{n-k-1}\|^2 \right) \end{aligned}$$

Proof of Lemma I.6.1:

From (I.5.9a) of section 5, we know that

$$(I.6.5) \quad \begin{aligned} (\mathcal{L} p, p) + (p, \mathcal{L} p) \leq & - \|D_+ p\|^2 + L \|p\|^2 \\ & + C_4 (|\tilde{f}_0|^2 + |\tilde{f}_1|^2) + \|\tilde{f}\|^2 + \|D_0 \tilde{f}\|^2, \end{aligned}$$

for all time $t \in [0, T]$ and any solution p of (I.5.4).

The inequality (I.6.5) is true at the time levels $n \tau$ and $(n + 1) \tau$. So if we evaluate the discrete scalar product of (6.3) with the vector $\hat{\underline{p}}^n + \hat{\underline{p}}^{n+1}$ and take into account (I.6.5) at time levels n and $n + 1$, it leads to

$$\begin{aligned} \frac{1}{\tau} (\|\hat{\underline{p}}^{n+1}\|^2 - \|\hat{\underline{p}}^n\|^2) &\leq -\frac{1}{4} \|\mathbb{D}_+^x \hat{\underline{p}}^{n+1} + \mathbb{D}_+^x \hat{\underline{p}}^n\|^2 \\ &\quad + \frac{1}{4} L \|\hat{\underline{p}}^{n+1} + \hat{\underline{p}}^n\|^2 + \frac{1}{4} C_4 \left(|\hat{f}_0^n|^2 + |\hat{f}_0^{n+1}|^2 + |\hat{f}_1^n|^2 \right. \\ &\quad \left. + |\hat{f}_1^{n+1}|^2 \right) + \frac{1}{4} \left(\|\hat{f}^n\|^2 + \|\hat{f}^{n+1}\|^2 \right. \\ (I.6.6a) \quad &\quad \left. + \|\mathbb{D}_0^x \hat{f}^n\|^2 + \|\mathbb{D}_0^x \hat{f}^{n+1}\|^2 \right), \end{aligned}$$

$$\begin{aligned} &\leq -\frac{1}{4} \|\mathbb{D}_+^x \hat{\underline{p}}^{n+1} + \mathbb{D}_+^x \hat{\underline{p}}^n\|^2 \\ &\quad + \frac{1}{2} L \left(\|\hat{\underline{p}}^{n+1}\|^2 + \|\hat{\underline{p}}^n\|^2 \right) + \frac{1}{4} C_4 \left(|\hat{f}_0^n|^2 + |\hat{f}_0^{n+1}|^2 \right. \\ &\quad \left. + |\hat{f}_1^n|^2 + |\hat{f}_1^{n+1}|^2 \right) + \frac{1}{4} \left(\|\hat{f}^n\|^2 + \|\hat{f}^{n+1}\|^2 \right. \\ (I.6.6b) \quad &\quad \left. + \|\mathbb{D}_0^x \hat{f}^n\|^2 + \|\mathbb{D}_0^x \hat{f}^{n+1}\|^2 \right). \end{aligned}$$

From (I.6.6b), we notice that we can express $\|\hat{\underline{p}}^{n+1}\|^2$ in terms of $\|\hat{\underline{p}}^n\|^2$ and of the forcing term. We will introduce a restriction on the time step to ensure that $1 - L/2 \tau$ is always positive, to obtain an upper bound for $\|\hat{\underline{p}}^{n+1}\|^2$ and not a lower one. So provided $\tau < 2/L$,

$$\begin{aligned} \|\hat{\underline{p}}^{n+1}\|^2 &\leq \frac{1 + L/2 \tau}{1 - L/2 \tau} \|\hat{\underline{p}}^n\|^2 + \frac{1}{4} \frac{C_4 \tau}{1 - L/2 \tau} \left(|\hat{f}_0^n|^2 \right. \\ &\quad \left. + |\hat{f}_0^{n+1}|^2 + |\hat{f}_1^n|^2 + |\hat{f}_1^{n+1}|^2 \right) + \frac{1}{4} \frac{\tau}{1 - L/2 \tau} \left(\|\hat{f}^n\|^2 \right. \\ (I.6.7) \quad &\quad \left. + \|\hat{f}^{n+1}\|^2 + \|\mathbb{D}_0^x \hat{f}^n\|^2 + \|\mathbb{D}_0^x \hat{f}^{n+1}\|^2 \right). \end{aligned}$$

From (I.6.7), we deduce a recurrence relation for $\|\hat{\underline{p}}^n\|^2$ in terms of the initial condition, forcing term, and boundary condition,

$$\begin{aligned} \|\hat{\underline{p}}^n\|^2 &\leq \left(\frac{1 + L/2 \tau}{1 - L/2 \tau} \right)^n \left(\|\tilde{g}\|^2 + \|\mathbb{D}_0^x \tilde{g}\|^2 \right) \\ &\quad + \frac{1}{4} \frac{C_4 \tau}{1 - L/2 \tau} \sum_{k=0}^{n-1} \left(\frac{1 + L/2 \tau}{1 - L/2 \tau} \right)^k \left(|\hat{f}_0^{n-k}|^2 + |\hat{f}_0^{n-k-1}|^2 \right. \end{aligned}$$

$$(I.6.8) \quad \begin{aligned} & + | \hat{f}_1^{n-k} |^2 + | \hat{f}_1^{n-k-1} |^2) + \frac{1}{4} \frac{\tau}{1 - L/2 \tau} \sum_{k=0}^{n-1} \left(\frac{1 + L/2 \tau}{1 - L/2 \tau} \right)^k \\ & (\| \hat{f}^{n-k} \|^2 + \| \hat{f}^{n-k-1} \|^2 + \| D_0^x \hat{f}^{n-k} \|^2 + \| D_0^x \hat{f}^{n-k-1} \|^2). \end{aligned}$$

From (I.6.8), we obtain (I.6.4) immediately because for $L > 0$,

$$(I.6.9a) \quad \frac{1 + L/2 \tau}{1 - L/2 \tau} \leq e^{L \tau},$$

$$(I.6.9b) \quad \frac{1}{1 - L/2 \tau} \leq e^{L \tau/2}.$$

As in section 5, we will compute an estimate for $\| D_+^t \hat{p}^n \|$ first, to bound $| \hat{p}^n |_\infty$. Define $D_+^t \hat{p}^n = \hat{q}^n$. The function \hat{q}^n satisfies

$$(I.6.10a) \quad \begin{aligned} \frac{\hat{q}_j^{n+1} - \hat{q}_j^n}{\tau} &= \frac{1}{2} D_+^x D_-^x (\hat{q}_j^{n+1} + \hat{q}_j^n) \\ &+ \frac{1}{4} \begin{bmatrix} 0 & D_+^t (\hat{v}_j^{n+1} + \hat{v}_j^n) \\ 0 & D_+^t D_0^x (\hat{v}_j^{n+1} + \hat{v}_j^n) \end{bmatrix} A_{02} (\hat{p}_0^{n+1} + \hat{p}_0^n) \\ &+ \frac{1}{4} \begin{bmatrix} 0 & \hat{v}_j^{n+1} + \hat{v}_j^n \\ 0 & D_0^x (\hat{v}_j^{n+1} + \hat{v}_j^n) \end{bmatrix} A_{02} (\hat{q}_0^{n+1} + \hat{q}_0^n) \\ &+ \frac{1}{2} \begin{bmatrix} D_+^t (\hat{f}_j^{n+1} + \hat{f}_j^n) \\ D_+^t D_0^x (\hat{f}_j^{n+1} + \hat{f}_j^n) \end{bmatrix}, \end{aligned}$$

$$(I.6.10b) \quad \begin{aligned} & \begin{bmatrix} 0 & 0 \\ 0 & 1 \end{bmatrix} D_+^x (\hat{q}_0^{n+1} + \hat{q}_0^n) \\ & + \frac{1}{2} \begin{bmatrix} 0 & 0 \\ 0 & D_+^t A_{02} (\hat{v}_0^{n+1} + \hat{v}_0^n) \end{bmatrix} A_{02} (\hat{p}_0^{n+1} + \hat{p}_0^n) \\ & + \frac{1}{2} \begin{bmatrix} 2 & 0 \\ 0 & A_{02} (\hat{v}_0^{n+1} + \hat{v}_0^n) \end{bmatrix} A_{02} (\hat{q}_0^{n+1} + \hat{q}_0^n) \\ & = \begin{bmatrix} 0 \\ D_+^t A_{02} (\hat{f}_0^{n+1} + \hat{f}_0^n) \end{bmatrix}, \end{aligned}$$

$$(I.6.10c) \quad \hat{q}_j^0 = \hat{h}_j + \tau \hat{l}_j,$$

$$(I.6.10d) \quad \hat{q}_j^n \rightarrow 0 \quad \text{as } j \rightarrow \infty,$$

where \hat{h} is

$$\hat{h}_j = D_+^x D_-^x \tilde{g}_j + \begin{bmatrix} 0 & \hat{v}_j^0 \\ 0 & \hat{D}_0^x \hat{v}_j^0 \end{bmatrix} A_{02} \tilde{g}_0 + \begin{bmatrix} \hat{f}_j^0 \\ D_0^x \hat{f}_j^0 \end{bmatrix},$$

and $\hat{\underline{1}}$

$$\hat{\underline{1}}_j = D_+^x D_-^x \hat{\underline{h}}_j + \begin{bmatrix} 0 & \hat{v}_j^0 \\ 0 & D_0^x \hat{v}_j^0 \end{bmatrix} A_{02} \hat{\underline{h}}_0 + \begin{bmatrix} 0 & \hat{w}_j^0 \\ 0 & D_0^x \hat{w}_j^0 \end{bmatrix} A_{02} \hat{\underline{g}}_0 + \begin{bmatrix} \hat{i}_j^0 \\ D_0^x \hat{i}_j^0 \end{bmatrix},$$

where \hat{w}_j^0 and \hat{i}_j^0 are discrete approximations for $d \tilde{v}_j(0)/dt$ and $d \tilde{f}_j(0)/dt$.

We deduce the equations (I.6.10a) and (I.6.10b) by applying the difference operator D_+^t to (I.6.1a) and (I.6.1b). We derive (I.6.10c) noting that

$$\hat{\underline{p}}^1 = \hat{\underline{p}}^0 + \tau \frac{d}{dt} \tilde{\underline{p}}(0) + \frac{1}{2} \tau^2 \frac{d^2}{dt^2} \tilde{\underline{p}}(0) + O(\tau^3).$$

The function $\hat{\underline{1}} = d^2 \tilde{\underline{p}}(0)/dt^2$.

The function $\hat{\underline{q}}^n$, similarly to $\hat{\underline{q}}$ in section 5, satisfies the estimate in L_2 norm.

Lemma I.6.2.

Under the assumptions that u and f and their derivatives on $[0, \infty) \times [0, T]$, and g and its derivatives on $[0, \infty)$ are smooth and bounded, we have

$$(I.6.11) \quad \|\hat{\underline{q}}^n\|^2 \leq \hat{S}^n,$$

where

$$\begin{aligned} \hat{S}^n &= e^{Q n \tau} \|\hat{\underline{q}}^0\|^2 + \frac{\tau}{4} \sum_{k=0}^{n-1} e^{Q(k+1/2)\tau} \left(\|\hat{f}^{n-k}\|^2 + \|\hat{f}^{n-k-1}\|^2 \right. \\ &\quad + \|\hat{D}_0^x \hat{f}^{n-k}\|^2 + \|D_0 \hat{f}^{n-k-1}\|^2 + \|D_+^t \hat{f}^{n-k}\|^2 \\ &\quad \left. + \|D_+^t \hat{f}^{n-k-1}\|^2 + \|D_+^t D_0^x \hat{f}^{n-k}\|^2 + \|D_+^t D_0^x \hat{f}^{n-k-1}\|^2 \right) \\ &\quad + \frac{D_5 \tau}{4} \sum_{k=0}^{n-1} e^{Q(k+1/2)\tau} \left(|\hat{f}_0^{n-k}|^2 + |\hat{f}_0^{n-k-1}|^2 + |\hat{f}_1^{n-k}|^2 \right. \\ &\quad \left. + |\hat{f}_1^{n-k-1}|^2 \right) + \frac{D_6 \tau}{4} \sum_{k=0}^{n-1} e^{Q(k+1/2)\tau} \left(|D_+^t \hat{f}_0^{n-k}|^2 + |D_+^t \hat{f}_0^{n-k-1}|^2 \right. \\ &\quad \left. + |D_+^t \hat{f}_1^{n-k}|^2 + |D_+^t \hat{f}_1^{n-k-1}|^2 \right) + Q \tau \sum_{k=0}^{n+1} e^{Q(k+1/2)\tau} \hat{R}^{n+1-k} \\ &\quad + \sum_{k=0}^n e^{Q k \tau} \hat{R}^{n-k}. \end{aligned}$$

Proof of Lemma I.6.2:

From the inequality (I.5.15) of section 5, we know that

$$\begin{aligned}
 (\mathcal{L} p, p) + (p, \mathcal{L} p) + (\tilde{\mathcal{L}} q, q) + (q, \tilde{\mathcal{L}} q) &\leq -\|D_+ q\|^2 \\
 &+ Q (\|p\|^2 + \|q\|^2) + \|\tilde{f}\|^2 + \|D_0 \tilde{f}\|^2 + \left\| \frac{d}{dt} \tilde{f} \right\|^2 \\
 &+ \left\| \frac{d}{dt} D_0 \tilde{f} \right\|^2 + D_5 (|\tilde{f}_0|^2 + |\tilde{f}_1|^2) \\
 \text{(I.6.12)} \quad &+ D_6 \left(\left| \frac{d}{dt} \tilde{f}_0 \right|^2 + \left| \frac{d}{dt} \tilde{f}_1 \right|^2 \right),
 \end{aligned}$$

where $\tilde{q}_t(t) = \tilde{\mathcal{L}} \tilde{q}$ corresponds to the system (I.5.11). The inequality (I.6.12) is satisfied for all time $t \in [0, T]$ and for any solutions p of (I.5.4) and q of (I.5.11).

If we evaluate the discrete scalar product of (I.6.1) with the vector $\hat{p}^n + \hat{p}^{n+1}$ and the discrete scalar product of (I.6.10) with the vector $\hat{q}^n + \hat{q}^{n+1}$, use (I.6.12) at the time levels n and $n+1$, it leads to an inequality similar to (I.6.6b):

$$\begin{aligned}
 \frac{1}{\tau} (\|\hat{p}^{n+1}\|^2 + \|\hat{q}^{n+1}\|^2 - \|\hat{p}^n\|^2 - \|\hat{q}^n\|^2) &\leq -\frac{1}{4} \|D_+^x \hat{q}^{n+1} + D_+^x \hat{q}^n\|^2 \\
 &+ \frac{Q}{2} (\|\hat{p}^{n+1}\|^2 + \|\hat{p}^n\|^2 + \|\hat{q}^{n+1}\|^2 + \|\hat{q}^n\|^2) \\
 &+ \frac{1}{4} (\|\hat{f}^n\|^2 + \|\hat{f}^{n+1}\|^2 + \|D_0^x \hat{f}^n\|^2 + \|D_0^x \hat{f}^{n+1}\|^2 \\
 &+ \|D_+^t \hat{f}^n\|^2 + \|D_+^t \hat{f}^{n+1}\|^2 + \|D_+^t D_0^x \hat{f}^n\|^2 \\
 &+ \|D_+^t D_0^x \hat{f}^{n+1}\|^2) + \frac{D_5}{4} (|\hat{f}_0^n|^2 + |\hat{f}_0^{n+1}|^2 + |\hat{f}_1^n|^2 \\
 &+ |\hat{f}_1^{n+1}|^2) + \frac{D_6}{4} (|D_+^t \hat{f}_0^n|^2 + |D_+^t \hat{f}_0^{n+1}|^2 \\
 \text{(I.6.13)} \quad &+ |D_+^t \hat{f}_1^n|^2 + |D_+^t \hat{f}_1^{n+1}|^2).
 \end{aligned}$$

So from the inequality (I.6.13), as in the proof of lemma I.6.1, we can express $\|\hat{q}^{n+1}\|^2$ in terms of $\|\hat{q}^n\|^2$, $\|\hat{p}^n\|^2$, $\|\hat{p}^{n+1}\|^2$, and the forcing terms. Because we substitute the bound for $\|\hat{p}^n\|^2$ from lemma I.6.1 in the inequality (I.6.13), and because we want to ensure that $1 - Q/2 \tau$ is strictly positive, we require $\tau < 2/L$ and $\tau < 2/Q$. Then the function $\|\hat{q}^n\|^2$ satisfies the relation

$$\|\hat{q}^{n+1}\|^2 \leq \frac{1 + Q/2 \tau}{1 - Q/2 \tau} (\|\hat{q}^n\|^2 + \|\hat{p}^n\|^2) + \frac{1}{2} \frac{Q \tau}{1 - Q/2 \tau} \|\hat{p}^{n+1}\|^2$$

$$\begin{aligned}
& + \frac{1}{4} \frac{\tau}{1-Q/2} \left(\| \hat{f}^n \|^2 + \| \hat{f}^{n+1} \|^2 + \| D_0^x \hat{f}^n \|^2 + \| D_0^x \hat{f}^{n+1} \|^2 \right. \\
& + \| D_+^t \hat{f}^n \|^2 + \| D_+^t \hat{f}^{n+1} \|^2 + \| D_+^t D_0^x \hat{f}^n \|^2 \\
& + \left. \| D_+^t D_0^x \hat{f}^{n+1} \|^2 \right) + \frac{1}{4} \frac{D_5 \tau}{1-Q/2} \left(| \hat{f}_0^n |^2 + | \hat{f}_0^{n+1} |^2 \right. \\
& + | \hat{f}_1^n |^2 + | \hat{f}_1^{n+1} |^2 \left. \right) + \frac{1}{4} \frac{D_6 \tau}{1-Q/2} \left(| D_+^t \hat{f}_0^n |^2 \right. \\
\text{(I.6.14)} \quad & \left. + | D_+^t \hat{f}_0^{n+1} |^2 + | D_+^t \hat{f}_1^n |^2 + | D_+^t \hat{f}_1^{n+1} |^2 \right).
\end{aligned}$$

We deduce a recurrence relation for $\| \hat{q}^n \|^2$, in terms of the initial condition, the forcing term, and boundary condition. Then we use relations similar to (I.6.9a) and (I.6.9b) to get (I.6.11).

We can then estimate $D_+^x \hat{p}^n$ in L_2 norm.

Lemma I.6.3.

Under the assumptions that u , f and their derivatives are smooth and bounded on $[0, \infty) \times [0, T]$, that g and its derivatives are smooth and bounded on $[0, \infty)$, we have

$$\text{(I.6.15)} \quad \| D_+^x \hat{p}^n \|^2 \leq \hat{X}^n,$$

where

$$\begin{aligned}
\hat{X}^n = & 2 \| D_+ \tilde{g} \|^2 + 8(L+1) \sum_{k=0}^{n-1} \hat{R}^k + 4(L+1) \hat{R}^n + 4 \sum_{k=0}^{n-1} \hat{S}^k \\
& + 2 C_4 \sum_{k=0}^{n-1} \left(| \hat{f}_0^k |^2 + | \hat{f}_0^{k+1} |^2 + | \hat{f}_1^k |^2 + | \hat{f}_1^{k+1} |^2 \right) \\
& + 2 \sum_{k=0}^{n-1} \left(\| \hat{f}^k \|^2 + \| \hat{f}^{k+1} \|^2 + \| D_0^x \hat{f}^k \|^2 + \| \hat{f}^{k+1} \|^2 \right),
\end{aligned}$$

and where \hat{R}^n and \hat{S}^n are the bounds calculated above for $\| \hat{p}^n \|^2$ and $\| \hat{q}^n \|^2$

Proof of Lemma I.6.3:

From the inequality (I.6.6b), we deduce

$$\begin{aligned}
 & \| D_+^x \underline{\hat{p}}^{n+1} + D_+^x \underline{\hat{p}}^n \|^2 \leq 4 \| \underline{\hat{p}}^{n+1} + \underline{\hat{p}}^n \|^2 \| \underline{\hat{q}}^n \|^2 \\
 & \quad + 2 L \left(\| \underline{\hat{p}}^{n+1} \|^2 + \| \underline{\hat{p}}^n \|^2 \right) + \| \hat{f}^n \|^2 + \| \hat{f}^{n+1} \|^2 \\
 & \quad + \| D_0 \hat{f}^n \|^2 + \| D_0 \hat{f}^{n+1} \|^2 + C_4 \left(| \hat{f}_0^n |^2 + | \hat{f}_0^{n+1} |^2 \right. \\
 (I.6.16a) \quad & \left. + | \hat{f}_1^n |^2 + | \hat{f}_1^{n+1} |^2 \right),
 \end{aligned}$$

$$\begin{aligned}
 & \leq 2 (L + 1) \left(\| \underline{\hat{p}}^{n+1} \|^2 + \| \underline{\hat{p}}^n \|^2 \right) \\
 & \quad + 2 \| \underline{\hat{q}} \|^2 + \| \hat{f}^n \|^2 + \| \hat{f}^{n+1} \|^2 + \| D_0 \hat{f}^n \|^2 \\
 & \quad + \| D_0 \hat{f}^{n+1} \|^2 + C_4 \left(| \hat{f}_0^n |^2 + | \hat{f}_0^{n+1} |^2 \right. \\
 (I.6.16b) \quad & \left. + | \hat{f}_1^n |^2 + | \hat{f}_1^{n+1} |^2 \right).
 \end{aligned}$$

From (I.6.16b), we compute an upper bound for $D_+^x \underline{\hat{p}}^{n+1} + D_+^x \underline{\hat{p}}^n$ in L_2 norm. We know from the triangular inequality that $\| D_+^x \underline{\hat{p}}^{n+1} \| - \| D_+^x \underline{\hat{p}}^n \|$ is a lower bound for $\| D_+^x \underline{\hat{p}}^{n+1} + D_+^x \underline{\hat{p}}^n \|$. So $\| D_+^x \underline{\hat{p}}^n \|$ satisfies the recurrence relation

$$\begin{aligned}
 & \| D_+^x \underline{\hat{p}}^{n+1} \|^2 \leq 2 \| D_+^x \underline{\hat{p}}^n \|^2 + 4 (L + 1) \left(\| \underline{\hat{p}}^{n+1} \|^2 + \| \underline{\hat{p}}^n \|^2 \right) \\
 & \quad + 4 \| \underline{\hat{q}}^n \|^2 + 2 \| \hat{f}^n \|^2 + 2 \| \hat{f}^{n+1} \|^2 + 2 \| D_0^x \hat{f}^n \|^2 \\
 & \quad + 2 \| D_0^x \hat{f}^{n+1} \|^2 + 2 C_4 \left(| \hat{f}_0^n |^2 + | \hat{f}_0^{n+1} |^2 \right. \\
 (I.6.17) \quad & \left. + | \hat{f}_1^n |^2 + | \hat{f}_1^{n+1} |^2 \right).
 \end{aligned}$$

We then obtain \hat{X}^n recursively from (I.6.17).

Because we have bounded $\underline{\hat{p}}^n$ and $D_+ \underline{\hat{p}}^n$ in L_2 norm, then we deduce a bound for $\underline{\hat{p}}^n$ in maximum norm.

Lemma I.6.4.

Under the assumptions that u, f , and their derivatives on $[0, \infty) \times [0, T]$, and that g and its derivatives on $[0, \infty)$ are smooth and bounded, we have

$$(I.6.18a) \quad | \underline{\hat{p}}^n |_\infty^2 \leq 2 \left[\hat{R}^n \right]^{\frac{1}{2}} \left[\hat{X}^n \right]^{\frac{1}{2}},$$

$$(I.6.18b) \quad | \underline{\hat{q}}^n |_\infty^2 \leq 2 \left[\hat{S}^n \right]^{\frac{1}{2}} \left[\hat{Z}^n \right]^{\frac{1}{2}},$$

where \hat{Z}^n is an upper bound for $\| D_+^x \hat{q}^n \|^2$.

Proof of Lemma I.6.4:

We deduce (I.6.18a) from Sobolev's inequality (I.5.10), (I.6.4), and (I.6.15). Similarly, we obtain (I.6.18b) from (I.5.10), (I.6.11), and the equivalent of (I.6.15) for \hat{q}^n .

We then compute an estimate for $D_-^x \hat{p}^n$ in L_2 norm.

Lemma I.6.5.

Under the assumptions that u , f and their derivatives on $[0, \infty) \times [0, T]$, and that g and its derivatives on $[0, \infty)$ are smooth and bounded, we have

$$(I.6.19) \quad \| D_-^x \hat{p}^n \|^2 \leq \hat{Y}^n,$$

where \hat{Y}^n is given by

$$\begin{aligned} \hat{Y}^n = & M \hat{X}^n + \tilde{M} \hat{R}^n + M_0 \hat{S}^n + \tilde{M}_0 \hat{Z}^n \\ & + M_1 \hat{W}^n + M_2 \left(|\hat{f}_0^n|^2 + |\hat{f}_1^n|^2 \right), \end{aligned}$$

where \hat{X}^n , \hat{R}^n , \hat{S}^n , \hat{Z}^n , and \hat{W}^n are the upper bounds computed above for $\| D_+^x \hat{p}^n \|^2$, $\| \hat{p}^n \|^2$, $\| \hat{q}^n \|^2$, $\| D_+^x \hat{q}^n \|^2$ and $\| (D_+^x)^2 \hat{p}^n \|^2$. M , \tilde{M} , M_0 , \tilde{M}_0 , M_1 and M_2 are constants depending on the initial condition and on the coefficients of the differential operator.

We will first prove an intermediate result. While bounding $\| D_- \hat{p}^n \|^2$, the term $\| D_+ \hat{p}^n \|_\infty$ arises, if the boundary conditions are of homogeneous Dirichlet type or of mixed type. We will then compute a bound for $\| (D_+^x)^2 \hat{p}^n \|^2$. As in section 5, \hat{p}^n , the equivalent of $\tilde{p}(n \tau)$, satisfies a system directly derived from (I.5.20) by discretizing (I.5.20) with Crank-Nicholson scheme. We derive in a similar way the equation that the function \hat{s}^n , the discrete equivalent of $\tilde{s}(n \tau)$, satisfies.

So $(D_+^x)^2 \hat{p}^n$ satisfies the bound, in L_2 norm given in

Lemma I.6.6.

Under the assumptions that u , f , and their derivatives on $[0, \infty) \times [0, T]$, and that g and its derivatives on $[0, \infty)$ are smooth and bounded, we have

$$(I.6.20) \quad \| (D_+^x)^2 \hat{p}^n \|^2 \leq \hat{W}^n,$$

where

$$\hat{W}^n = 2 \hat{W}_2^n + 2 \|\Lambda\|^2 \left(2 \hat{D} \left[\hat{R}^n \hat{X}^n \right]^{\frac{1}{2}} + \hat{E} | \hat{f}_0^n |^2 + \hat{E} | \hat{f}_1^n |^2 \right)$$

Proof of Lemma I.6.6:

From classical L_2 manipulations, we conclude that $\|\hat{s}\|$ satisfies the inequality

$$\begin{aligned} \frac{1}{\tau} (\|\hat{s}^{n+1}\|^2 - \|\hat{s}^n\|^2) &\leq -\frac{1}{4} \|D_+^x \hat{s}^{n+1} + D_+^x \hat{s}^n\|^2 + \frac{1}{2} A \left(\|\hat{s}^{n+1}\|^2 \right. \\ &\quad \left. + \|\hat{s}^n\|^2 \right) + \frac{1}{4} \left(\|D_+^x \hat{f}^{n+1}\|^2 + \|D_+^x \hat{f}^n\|^2 \right. \\ &\quad \left. + \|D_+^x D_0^x \hat{f}^{n+1}\|^2 + \|D_+^x D_0^x \hat{f}^n\|^2 \right) \\ &\quad + \frac{1}{4} B \left(| \hat{f}_0^n |^2 + | \hat{f}_0^{n+1} |^2 + | \hat{f}_1^n |^2 + | \hat{f}_1^{n+1} |^2 \right) \\ \text{(I.6.21)} \quad &+ \frac{1}{2} C \left(| \hat{p}^{n+1} |^2 + | \hat{p}^n |^2 \right), \end{aligned}$$

and the estimate

$$\text{(I.6.22)} \quad \|\hat{s}^n\|^2 \leq \hat{W}_0^n,$$

where

$$\hat{W}_0^n = 2 \hat{X}^n + 2 \|\Lambda\|^2 \left(2 \hat{D} \left[\hat{R}^n \hat{X}^n \right]^{\frac{1}{2}} + \hat{E} | \hat{f}_0^n |^2 + \hat{E} | \hat{f}_1^n |^2 \right),$$

because we have already bounded \hat{f}^n in L_2 norm.

As seen before, we will compute an estimate for $\hat{t}^n = (\hat{s}^{n+1} - \hat{s}^n)/\tau$. Here, the function \hat{t} satisfies the system

$$\begin{aligned} \frac{\hat{t}_j^{n+1} - \hat{t}_j^n}{\tau} &= \frac{1}{2} D_+^x D_-^x (\hat{t}_j^{n+1} + \hat{t}_j^n) \\ &\quad + \frac{1}{4} \begin{bmatrix} 0 & D_+^t (\hat{v}_j^{n+1} + \hat{v}_j^n) \\ 0 & D_+^t D_0^x (\hat{v}_j^{n+1} + \hat{v}_j^n) \end{bmatrix} A_{02} (\hat{p}_0^{n+1} + \hat{p}_0^n) \\ &\quad + \frac{1}{4} \begin{bmatrix} 0 & \hat{v}_j^{n+1} + \hat{v}_j^n \\ 0 & D_0^x (\hat{v}_j^{n+1} + \hat{v}_j^n) \end{bmatrix} A_{02} (\hat{q}_0^{n+1} + \hat{q}_0^n) \\ &\quad + \frac{1}{4} D_+^t A_{02} (\hat{v}_0^{n+1} + \hat{v}_0^n) \begin{bmatrix} 0 & 0 \\ 0 & D_+^x D_-^x \Lambda_j \end{bmatrix} A_{02} (\hat{p}_0^{n+1} + \hat{p}_0^n) \\ &\quad + \frac{1}{4} A_{02} (\hat{v}_0^{n+1} + \hat{v}_0^n) \begin{bmatrix} 0 & 0 \\ 0 & D_+^x D_-^x \Lambda_j \end{bmatrix} A_{02} (\hat{q}_0^{n+1} + \hat{q}_0^n) \end{aligned}$$

$$(I.6.23a) \quad \begin{aligned} & + \frac{1}{2} \left[\begin{array}{c} D_+^t (\hat{f}_j^{n+1} + \hat{f}_j^n) \\ D_+^t D_0^x (\hat{f}_j^{n+1} + \hat{f}_j^n) \end{array} \right] \\ & + \frac{1}{2} \left[\begin{array}{c} 0 \\ D_+^t A_{02} (\hat{f}_0^{n+1} + \hat{f}_0^n) D_+^x D_-^x \Lambda_j \end{array} \right], \end{aligned}$$

$$\begin{aligned} & \begin{bmatrix} 0 & 0 \\ 0 & 1 \end{bmatrix} D_+^x (\hat{t}_0^{n+1} + \hat{t}_0^n) + \begin{bmatrix} 0 & 0 \\ 0 & 1 \end{bmatrix} A_{02} (\hat{t}_0^{n+1} + \hat{t}_0^n) \\ & = -\frac{1}{2} \left[\begin{array}{cc} D_+^t A_{02} (\hat{v}_0^{n+1} + \hat{v}_0^n) & 0 \\ 0 & 0 \end{array} \right] A_{02} (\hat{p}_0^{n+1} + \hat{p}_0^n) \\ & - \frac{1}{2} \left[\begin{array}{cc} A_{02} (\hat{v}_0^{n+1} + \hat{v}_0^n) & 0 \\ 0 & 0 \end{array} \right] A_{02} (\hat{q}_0^{n+1} + \hat{q}_0^n) \end{aligned}$$

$$(I.6.23b) \quad - \left[\begin{array}{c} D_+^t A_{02} (\hat{f}_0^{n+1} + \hat{f}_0^n) \\ 0 \end{array} \right],$$

$$(I.6.23c) \quad \hat{t}_j^0 = D_+^x \hat{h}_j + \tau D_+^x \hat{l}_j,$$

$$(I.6.23d) \quad \hat{t}_j^n \rightarrow 0 \quad \text{as } j \rightarrow \infty.$$

After a few algebraic manipulations, the function \hat{t}^n satisfies the inequality

$$(I.6.24) \quad \begin{aligned} \frac{1}{\tau} (\|\hat{t}^{n+1}\|^2 - \|\hat{t}^n\|^2) & \leq \frac{1}{2} (\|\hat{t}^{n+1}\|^2 + \|\hat{t}^n\|^2) + \frac{1}{4} (\|D_+^t D_+^x \hat{f}^{n+1}\|^2 \\ & + \|D_+^t D_+^x \hat{f}^n\|^2 + \|D_+^t D_+^x D_0^x \hat{f}^{n+1}\|^2 \\ & + \|D_+^t D_+^x D_0^x \hat{f}^n\|^2) + \frac{1}{4} B_1 (|D_+^t \hat{f}_0^{n+1}|^2 + |D_+^t \hat{f}_0^n|^2 \\ & + |D_+^t \hat{f}_1^{n+1}|^2 + |D_+^t \hat{f}_1^n|^2) + \frac{1}{4} C_1 (|\hat{f}_0^{n+1}|^2 + |\hat{f}_0^n|^2 \\ & + |\hat{f}_1^{n+1}|^2 + |\hat{f}_1^n|^2) + \frac{1}{2} D_1 (|\hat{p}^{n+1}|_\infty^2 + |\hat{p}^n|_\infty^2) \\ & + \frac{1}{2} E_1 (|\hat{q}^{n+1}|_\infty^2 + |\hat{q}^n|_\infty^2). \end{aligned}$$

This leads to, if $\tau < 2/A_1$,

$$(I.6.25) \quad \|\hat{t}^n\|^2 \leq \hat{W}_1^n,$$

where

$$\begin{aligned} \hat{W}_1^n & = e^{A_1 n \tau} \|\hat{t}^0\|^2 \\ & + \frac{1}{4} \tau \sum_{k=0}^{n-1} e^{A_1 (k+1/2) \tau} \left(\|D_+^t D_+^x \hat{f}^{n-k}\|^2 + \|D_+^t D_+^x \hat{f}^{n-k-1}\|^2 \right. \\ & \left. + \|D_+^t D_+^x D_0^x \hat{f}^{n-k}\|^2 + \|D_+^t D_+^x D_0^x \hat{f}^{n-k-1}\|^2 \right) \end{aligned}$$

$$\begin{aligned}
& + \frac{1}{4} B_1 \tau \sum_{k=0}^{n-1} e^{A_1 (k+1/2) \tau} \left(|D_+^t \hat{f}_0^{n-k}|^2 + |D_+^t \hat{f}_0^{n-k-1}|^2 \right. \\
& + |D_+^t \hat{f}_1^{n-k}|^2 + |D_+^t \hat{f}_1^{n-k-1}|^2 \left. \right) \\
& + \frac{1}{4} C_1 \tau \sum_{k=0}^{n-1} e^{A_1 (k+1/2) \tau} \left(|\hat{f}_0^{n-k}|^2 + |\hat{f}_0^{n-k-1}|^2 \right. \\
& + |\hat{f}_1^{n-k}|^2 + |\hat{f}_1^{n-k-1}|^2 \left. \right) \\
& + D_1 \tau \sum_{k=0}^{n-1} e^{A_1 (k+1/2) \tau} \left(\left[\hat{R}^{n-k} \hat{X}^{n-k} \right]^{\frac{1}{2}} + \left[\hat{R}^{n-k-1} \hat{X}^{n-k-1} \right]^{\frac{1}{2}} \right) \\
& + E_1 \tau \sum_{k=0}^{n-1} e^{A_1 (k+1/2) \tau} \left(\left[\hat{S}^{n-k} \hat{Z}^{n-k} \right]^{\frac{1}{2}} + \left[\hat{S}^{n-k-1} \hat{Z}^{n-k-1} \right]^{\frac{1}{2}} \right).
\end{aligned}$$

From the inequalities (I.6.22) and (I.6.25), we calculate an upper bound for $\|D_+^x \hat{\underline{s}}^n\|$,

$$\begin{aligned}
\|D_+^x \hat{\underline{s}}^{n+1}\|^2 & \leq 2 \|D_+^x \hat{\underline{s}}^n\|^2 + 4 \|\hat{\underline{t}}^n\|^2 + 4(A+1) \left(\|\hat{\underline{s}}^{n+1}\|^2 \right. \\
& + \|\hat{\underline{s}}^n\|^2 \left. \right) + 2 \|D_+^x \hat{f}^{n+1}\|^2 + 2 \|D_+^x \hat{f}^n\|^2 \\
& + 2 \|D_+^x D_0^x \hat{f}^{n+1}\|^2 + 2 \|D_+^x D_0^x \hat{f}^n\|^2 \\
& + 2 B \left(|\hat{f}_0^{n+1}|^2 + |\hat{f}_0^n|^2 + |\hat{f}_1^{n+1}|^2 + |\hat{f}_1^n|^2 \right) \\
& + 4 C \left(\left[\hat{X}^{n+1} \hat{R}^{n+1} \right]^{\frac{1}{2}} + \left[\hat{X}^n \hat{R}^n \right]^{\frac{1}{2}} \right).
\end{aligned} \tag{I.6.26}$$

So $\|D_+^x \hat{\underline{s}}^n\|$ satisfies

$$\|D_+^x \hat{\underline{s}}^n\|^2 \leq \hat{W}_2^n, \tag{I.6.27}$$

where

$$\begin{aligned}
\hat{W}_2^n & = 2 \left\| (D_+^x)^2 \hat{\underline{s}}^0 \right\|^2 + 8(A+1) \sum_{k=0}^{n-1} \hat{W}_0^k \\
& + 4(A+1) \hat{W}_0^n + 4 \sum_{k=0}^{n-1} \hat{W}_1^k + 2 \sum_{k=0}^{n-1} \left(\|D_+^x \hat{f}^k\|^2 \right. \\
& + \|D_+^x \hat{f}^{k+1}\|^2 + \|D_+^x D_0^x \hat{f}^k\|^2 + \|D_+^x D_0^x \hat{f}^{k+1}\|^2 \left. \right) \\
& + 2 B \sum_{k=0}^{n-1} \left(|\hat{f}_0^k|^2 + |\hat{f}_0^{k+1}|^2 + |\hat{f}_1^k|^2 + |\hat{f}_1^{k+1}|^2 \right)
\end{aligned}$$

$$+ 4 C \sum_{k=0}^{n-1} \left(\left[\hat{R}^k \hat{X}^k \right]^{\frac{1}{2}} + \left[\hat{R}^{k+1} \hat{X}^{k+1} \right]^{\frac{1}{2}} \right).$$

From this, we get an estimate for $D_+^x \hat{r}^n$ in L_2 norm.

Proof of Lemma I.6.5:

The proof is identical to the proof of lemma I.5.6, given in section 5.

As in section 5, we estimate $D_0^x \hat{p}^n$ in L_2 norm.

Lemma I.6.7.

Under the assumptions that u , f , and their derivatives on $[0, \infty) \times [0, T]$, and that g and its derivatives on $[0, \infty)$ are smooth and bounded, we have

$$(I.6.28) \quad \| D_0^x \hat{p}^n \|^2 \leq \frac{1}{2} \hat{X}^n + \frac{1}{2} \hat{Y}^n.$$

Proof of Lemma I.6.7:

It is identical to the proof of lemma I.5.7.

We then bound all derivatives of the function \hat{p}^n both in L_2 and in maximum norms. These estimates summarize in

Theorem I.6.8.

Under the assumptions that u , f , and their derivatives on $[0, \infty) \times [0, T]$, and that g and its derivatives on $[0, \infty)$ are smooth and bounded, we have

$$(I.6.29a) \quad \left\| \left(D_+^t \right)^k \left(D_+^x \right)^l \left(D_-^x \right)^m \left(D_0^x \right)^i \hat{p}^n \right\|^2 \leq I_{k,l,m,i},$$

$$(I.6.29b) \quad \left| \left(D_+^t \right)^k \left(D_+^x \right)^l \left(D_-^x \right)^m \left(D_0^x \right)^i \hat{p}^n \right|_{\infty}^2 \leq \tilde{I}_{k,l,m,i}.$$

Proof of Theorem I.6.8:

We derive (I.6.29a) and (I.6.29b) immediately from lemmas I.6.3, I.6.4, I.6.5, I.6.7 and from the equation the function \hat{p} satisfies. If we apply the techniques considered for the proof of theorem I.5.8 of section 5, to the discretized equations in time, as many times as needed, we deduce (I.6.29a) and (I.6.29b).

What we were interested in, was to bound \hat{e}^n in both L_2 and maximum norms.

Theorem I.6.9.

Under the assumptions that u , f , and their derivatives on $[0, \infty) \times [0, T]$, and g and its derivatives on $[0, \infty)$ are smooth and bounded, we have

$$(I.6.30a) \quad \left\| \left(D_+^t \right)^k \left(D_+^x \right)^l \left(D_-^x \right)^m \left(D_0^x \right)^i \hat{e}^n \right\|^2 \leq I_{k,l,m,i},$$

$$(I.6.30b) \quad \left| \left(D_+^t \right)^k \left(D_+^x \right)^l \left(D_-^x \right)^m \left(D_0^x \right)^i \hat{e}^n \right|_{\infty}^2 \leq \tilde{I}_{k,l,m,i}.$$

Proof of Theorem I.6.9:

We get (I.6.30a) and (I.6.30b) from (I.6.29a) and (I.6.29b) because the function \hat{e} is the first component of the vector \hat{p} .

I.7 Estimates for the Discrete Equation

In the previous section, we have shown that the linearized discrete error equation, resulting from the linearization of (I.2.2) about the solution $\hat{e} = 0$, then discretized in time with Crank-Nicholson scheme, has a solution, which is bounded in terms of the initial and boundary conditions, of its coefficients, and of the forcing terms. We have already proven that the discrete operator \mathcal{L} has a bounded inverse; the bound the inverse satisfies depends on the initial data and on the coefficients of the differential operator.

As mentioned in section 2, we define in this section the error as $h^2 \hat{e}_j^n = u(x_j, n \tau) - \hat{u}_j^n$ instead of $\hat{e}_j^n = u(x_j, n \tau) - \hat{u}_j^n$. We introduce the factor h^2 , because we would like to write the nonlinear system as $A x + \epsilon F(x) = b$, where A will represent the linear part of the operator, F the nonlinear one. With this new definition of the error, we put a factor h^2 in front of the nonlinear term and this factor will play the role of ϵ , because h is small. We obtain from the following theorem found in [25] the final result

Theorem I.7.1.

Consider

$$(I.7.1) \quad A x + \epsilon F(x) = b.$$

Let x_0^* be the solution of $A x = b$. Suppose that A^{-1} exists and that F is locally Lipschitz continuous of Lipschitz constant L in the neighborhood of x_0^*

$$(I.7.2) \quad |F(y) - F(x)| \leq L |x - y|, \quad |x - x_0^*| \leq 1, \quad |y - x_0^*| \leq 1.$$

Suppose that the constants κ and ζ satisfy the inequalities

$$\begin{aligned} \kappa &= \epsilon |A^{-1}| L < 1, \\ \zeta &= \frac{1}{1 - \kappa} \epsilon |A^{-1} F(x_0^*)| \leq 1, \end{aligned}$$

then

$$(I.7.3) \quad |x_\epsilon^* - x_0^*| \leq \zeta,$$

where x_ϵ is the solution of the equation (I.7.1).

Strang in [37] chooses another approach to a problem of a similar nature. He tries to compute the solution of a nonlinear hyperbolic system discretized with an explicit finite difference scheme of order $q+1$. If he assumes some bounds on the L_2 norm of the product of the first variation $M(t, \Delta x)$ of the operator, of the type

$$\|M(t - \Delta t, \Delta x) M(t - 2\Delta t, \Delta x) \dots M(t - n\Delta t, \Delta x)\| \leq K, \quad n\Delta t \leq t \leq t_0,$$

he shows that the analytical solution and the numerical solution are close.

As mentioned many times in the previous sections, the lower order terms of the linear operator do not fundamentally change the behavior of the equation and the bound of the inverse operator. Because the system is of parabolic type, we will assume that the ratio $\tau/h^2 = \lambda$ is fixed so that we can express all the truncation errors in power of h . The equation that \tilde{e} , $h^2 \tilde{e}^T = [u, u_x]^T - \tilde{p}^T$ satisfies reads, after division by h^2

$$(I.7.4a) \quad \begin{aligned} \frac{\partial}{\partial t} \tilde{e}_j(t) &= D_+ D_- \tilde{e}_j(t) + \begin{bmatrix} 0 & \tilde{v}_j(t) \\ 0 & D_0 \tilde{v}_j(t) \end{bmatrix} A_{02} \tilde{e}_0(t) \\ &+ h^2 A_{02} \tilde{e}_0^T(t) \begin{bmatrix} 0 \\ 1 \end{bmatrix} D_0 \tilde{e}_j(t) + \begin{bmatrix} \tilde{f}_j(t) \\ D_0 \tilde{f}_j(t) \end{bmatrix}, \end{aligned}$$

$$(I.7.4b) \quad \begin{aligned} \begin{bmatrix} 0 & 0 \\ 0 & 1 \end{bmatrix} D_+ \tilde{e}_0(t) + \begin{bmatrix} 1 & 0 \\ 0 & A_{02} \tilde{v}_0(t) \end{bmatrix} A_{02} \tilde{e}_0(t) \\ = \begin{bmatrix} 0 \\ A_{02} \tilde{f}_0(t) \end{bmatrix}, \end{aligned}$$

$$(I.7.4c) \quad \tilde{e}_j(0) = \tilde{g}_j,$$

$$(I.7.4d) \quad \tilde{e}_j(t) \rightarrow 0 \quad \text{as } j \rightarrow \infty,$$

where \tilde{f} and \tilde{g} are not the functions \tilde{f} and \tilde{g} of section 5, but these functions divided by h^2 .

From section 5, we know that the linear part of the operator representing (I.7.4) has a bounded inverse, that there exists a bounded solution to the linearized system (I.5.4) obtained from the linearization of (I.7.4) about the solution $\tilde{e} = \underline{0}$, $\tilde{p}^0(t)$. So before applying theorem I.7.1 to (I.7.4), we will prove that the nonlinear term in (I.7.4a) is locally Lipschitz continuous, that the nonlinear term evaluated at $\tilde{p}^0(t)$ is bounded. To show that the nonlinear term is locally Lipschitz, we will express

$$\left\| A_{02} \tilde{p}_0^T \begin{bmatrix} 0 \\ 1 \end{bmatrix} D_0 \tilde{p} - A_{02} \tilde{q}_0^T \begin{bmatrix} 0 \\ 1 \end{bmatrix} D_0 \tilde{q} \right\|$$

in terms of $\|\tilde{p} - \tilde{q}\|$, if we choose the L_2 norm, or

$$\left| A_{02} \tilde{p}_0^T \begin{bmatrix} 0 \\ 1 \end{bmatrix} D_0 \tilde{p} - A_{02} \tilde{q}_0^T \begin{bmatrix} 0 \\ 1 \end{bmatrix} D_0 \tilde{q} \right|_\infty$$

in terms of $|\tilde{p} - \tilde{q}|_\infty$, if we consider the maximum norm. We express the difference of those two terms as

$$(I.7.5) \quad \begin{aligned} & A_{02} \tilde{p}_0^T \begin{bmatrix} 0 \\ 1 \end{bmatrix} D_0 \tilde{p} - A_{02} \tilde{q}_0^T \begin{bmatrix} 0 \\ 1 \end{bmatrix} D_0 \tilde{q} = \\ & A_{02} (\tilde{p}_0 - \tilde{q}_0)^T \begin{bmatrix} 0 \\ 1 \end{bmatrix} D_0 \tilde{p} + A_{02} \tilde{q}_0^T \begin{bmatrix} 0 \\ 1 \end{bmatrix} D_0 (\tilde{p} - \tilde{q}). \end{aligned}$$

If we choose the L_2 norm, the first term of (I.7.5) satisfies

$$(I.7.6a) \quad \begin{aligned} \left\| A_{02} (\tilde{p}_0 - \tilde{q}_0)^T \begin{bmatrix} 0 \\ 1 \end{bmatrix} D_0 \tilde{p} \right\| &\leq (C+1) |\tilde{p} - \tilde{q}|_\infty \|D_0 \tilde{p}\|, \\ &\leq h^{-\frac{1}{2}} (C+1) \|D_0 \tilde{p}\| \|\tilde{p} - \tilde{q}\|, \\ &\leq h^{-2} \tilde{C} \|\tilde{p}\| \|\tilde{p} - \tilde{q}\| \\ &\quad + h^{-1} \tilde{D} \|\tilde{p}_t\| \|\tilde{p} - \tilde{q}\|, \\ &\leq h^{-3} E \left(\|\tilde{p}\| + |\tilde{f}_0| + |\tilde{f}_1| \right. \\ &\quad \left. + \left| \frac{d}{dt} \tilde{f}_0 \right| + \left| \frac{d}{dt} \tilde{f}_1 \right| \right) \|\tilde{p} - \tilde{q}\|, \end{aligned}$$

while the second term satisfies,

$$\left\| A_{02} \tilde{q}_0^T \begin{bmatrix} 0 \\ 1 \end{bmatrix} D_0 (\tilde{p} - \tilde{q}) \right\| \leq ((C+1) |\tilde{q}|_\infty$$

$$\begin{aligned}
 & + \tilde{C} (|\tilde{f}_0| + |\tilde{f}_1|) \|\mathbf{D}_0(\underline{\tilde{p}} - \underline{\tilde{q}})\|, \\
 & \leq h^{-1} \mathbf{B} \left((C+1) |\underline{\tilde{q}}|_\infty \right. \\
 & \quad \left. + \tilde{C} (|\tilde{f}_0| + |\tilde{f}_1|) \right) \|\underline{\tilde{p}} - \underline{\tilde{q}}\|, \\
 & \leq h^{-\frac{3}{2}} \tilde{\mathbf{B}} \left(\|\underline{\tilde{q}}\| + |\tilde{f}_0| + |\tilde{f}_1| \right. \\
 & \quad \left. + \left| \frac{d}{dt} \tilde{f}_0 \right| + \left| \frac{d}{dt} \tilde{f}_1 \right| \right) \|\underline{\tilde{p}} - \underline{\tilde{q}}\|.
 \end{aligned}
 \tag{I.7.6b}$$

So we bound the term (I.7.5) in the L_2 norm by

$$\begin{aligned}
 & h^{-3} \left[\mathbf{E} \left(\|\underline{\tilde{p}}\| + |\tilde{f}_0| + |\tilde{f}_1| + \left| \frac{d}{dt} \tilde{f}_0 \right| + \left| \frac{d}{dt} \tilde{f}_1 \right| \right) \right. \\
 & \quad \left. + h^{\frac{3}{2}} \tilde{\mathbf{B}} \left(\|\underline{\tilde{q}}\| + |\tilde{f}_0| + |\tilde{f}_1| + \left| \frac{d}{dt} \tilde{f}_0 \right| + \left| \frac{d}{dt} \tilde{f}_1 \right| \right) \right] \|\underline{\tilde{p}} - \underline{\tilde{q}}\|.
 \end{aligned}$$

Because $\underline{\tilde{p}}$ and $\underline{\tilde{q}}$ are in the neighborhood of $\underline{\tilde{p}}^0(t)$, the solution of the linearized system, we can bound the term

$$\begin{aligned}
 & \mathbf{E} \left(\|\underline{\tilde{p}}\| + |\tilde{f}_0| + |\tilde{f}_1| + \left| \frac{d}{dt} \tilde{f}_0 \right| + \left| \frac{d}{dt} \tilde{f}_1 \right| \right) \\
 & \quad + h^{\frac{3}{2}} \tilde{\mathbf{B}} \left(\|\underline{\tilde{q}}\| + |\tilde{f}_0| + |\tilde{f}_1| + \left| \frac{d}{dt} \tilde{f}_0 \right| + \left| \frac{d}{dt} \tilde{f}_1 \right| \right),
 \end{aligned}$$

by a constant independent of h because $h \leq h_0$.

If we choose the maximum norm for the computation, we can show in a similar way that we can bound (I.7.5) by

$$h^{-2} \mathbf{C} |\underline{\tilde{p}} - \underline{\tilde{q}}|_\infty,$$

because $\underline{\tilde{p}}$ and $\underline{\tilde{q}}$ are in the neighborhood of $\underline{\tilde{p}}^0(t)$ the solution of the linearized system.

We now will check the last hypothesis of theorem I.7.1, the boundedness of the nonlinear term evaluated at the solution of the linearized system, (I.5.4). In section 5, we have estimated $\mathbf{D}_0 \underline{\tilde{p}}$ both in L_2 and maximum norms; we also have bounded the solution of the linearized system $\underline{\tilde{p}}_0$ in terms of $|\underline{\tilde{p}}|_\infty$ and the forcing term. Therefore we can bound the nonlinear term at the solution of the linearized system (I.5.4). We have verified all of the hypothesis of theorem I.7.1.

Because the Lipschitz constant L we find is proportional to h^{-3} , if we have chosen the L_2 norm, the results of theorem I.7.1 do not apply immediately to the system considered. We only get a factor h^2 in front of the nonlinear term of (I.7.4a) while we would need at least a factor h^4 . The function \tilde{e} possesses an asymptotic expansion in h because the forcing term and the initial condition have one. So we can write \tilde{e} as

$$\tilde{e}_j(t) = \tilde{e}_j^0(t) + h \tilde{e}_j^1(t) + h^2 \tilde{e}_j^2(t) + h^3 \tilde{e}_j^3(t) + \dots$$

We will define \tilde{e}^0 , \tilde{e}^1 , and \tilde{e}^2 so that the exponent of h is large enough to get ζ smaller than 1 for $h \in [0, h_1]$. Similarly we have for \tilde{f} ,

$$\tilde{f}_j(t) = \tilde{f}_j^0(t) + h \tilde{f}_j^1(t) + h^2 \tilde{f}_j^2(t) + h^3 \tilde{f}_j^3(t) + \dots,$$

and for \tilde{g} ,

$$\tilde{g}_j = \tilde{g}_j^0 + h \tilde{g}_j^1 + h^2 \tilde{g}_j^2 + h^3 \tilde{g}_j^3 + \dots$$

If we substitute in (I.7.4) these asymptotic expansions up to the third-order term, this leads to

$$\begin{aligned} & \frac{\partial}{\partial t} \tilde{e}_j^0 - D_+ D_- \tilde{e}_j^0 - \begin{bmatrix} 0 & \tilde{v}_j \\ 0 & D_0 \tilde{v}_j \end{bmatrix} A_{02} \tilde{e}_0^0 - \begin{bmatrix} \tilde{f}_j^0 \\ D_0 \tilde{f}_j^0 \end{bmatrix} \\ & + h \left(\frac{\partial}{\partial t} \tilde{e}_j^1 - D_+ D_- \tilde{e}_j^1 - \begin{bmatrix} 0 & \tilde{v}_j \\ 0 & D_0 \tilde{v}_j \end{bmatrix} A_{02} \tilde{e}_0^1 - \begin{bmatrix} \tilde{f}_j^1 \\ D_0 \tilde{f}_j^1 \end{bmatrix} \right) \\ & + h^2 \left(\frac{\partial}{\partial t} \tilde{e}_j^2 - D_+ D_- \tilde{e}_j^2 - \begin{bmatrix} 0 & \tilde{v}_j \\ 0 & D_0 \tilde{v}_j \end{bmatrix} A_{02} \tilde{e}_0^2 \right. \\ & \left. - \begin{bmatrix} \tilde{f}_j^2 \\ D_0 \tilde{f}_j^2 \end{bmatrix} - A_{02} (\tilde{e}_0^0)^T \begin{bmatrix} 0 \\ 1 \end{bmatrix} D_0 \tilde{e}_j^0 \right) \\ & + h^3 \left(\frac{\partial}{\partial t} \tilde{e}_j^3 - D_+ D_- \tilde{e}_j^3 - \begin{bmatrix} 0 & \tilde{v}_j \\ 0 & D_0 \tilde{v}_j \end{bmatrix} A_{02} \tilde{e}_0^3 \right. \\ & \left. - \begin{bmatrix} \tilde{f}_j^3 \\ D_0 \tilde{f}_j^3 \end{bmatrix} - A_{02} (\tilde{e}_0^1)^T \begin{bmatrix} 0 \\ 1 \end{bmatrix} D_0 \tilde{e}_j^0 - A_{02} (\tilde{e}_0^0)^T \begin{bmatrix} 0 \\ 1 \end{bmatrix} D_0 \tilde{e}_j^1 \right) \\ & + h^4 \left(A_{02} (\tilde{e}_0^0)^T \begin{bmatrix} 0 \\ 1 \end{bmatrix} D_0 \tilde{e}_j^2 + A_{02} (\tilde{e}_0^1)^T \begin{bmatrix} 0 \\ 1 \end{bmatrix} D_0 \tilde{e}_j^1 \right. \\ & \left. + A_{02} (\tilde{e}_0^2)^T \begin{bmatrix} 0 \\ 1 \end{bmatrix} D_0 \tilde{e}_j^0 \right) \end{aligned}$$

$$\begin{aligned}
 & + h^5 \left(A_{02} (\tilde{\epsilon}_0^0)^T \begin{bmatrix} 0 \\ 1 \end{bmatrix} D_0 \tilde{\epsilon}_j^3 + A_{02} (\tilde{\epsilon}_0^1)^T \begin{bmatrix} 0 \\ 1 \end{bmatrix} D_0 \tilde{\epsilon}_j^2 \right. \\
 & \left. + A_{02} (\tilde{\epsilon}_0^2)^T \begin{bmatrix} 0 \\ 1 \end{bmatrix} D_0 \tilde{\epsilon}_j^1 + A_{02} (\tilde{\epsilon}_0^3)^T \begin{bmatrix} 0 \\ 1 \end{bmatrix} D_0 \tilde{\epsilon}_j^0 \right) \\
 & + h^6 \left(A_{02} (\tilde{\epsilon}_0^1)^T \begin{bmatrix} 0 \\ 1 \end{bmatrix} D_0 \tilde{\epsilon}_j^3 + A_{02} (\tilde{\epsilon}_0^2)^T \begin{bmatrix} 0 \\ 1 \end{bmatrix} D_0 \tilde{\epsilon}_j^2 \right. \\
 & \left. + A_{02} (\tilde{\epsilon}_0^3)^T \begin{bmatrix} 0 \\ 1 \end{bmatrix} D_0 \tilde{\epsilon}_j^1 \right) \\
 & + h^7 \left(A_{02} (\tilde{\epsilon}_0^2)^T \begin{bmatrix} 0 \\ 1 \end{bmatrix} D_0 \tilde{\epsilon}_j^3 + A_{02} (\tilde{\epsilon}_0^3)^T \begin{bmatrix} 0 \\ 1 \end{bmatrix} D_0 \tilde{\epsilon}_j^2 \right) \\
 (I.7.7a) \quad & + h^8 A_{02} (\tilde{\epsilon}_0^3)^T \begin{bmatrix} 0 \\ 1 \end{bmatrix} D_0 \tilde{\epsilon}_j^3 = 0.
 \end{aligned}$$

$$\begin{aligned}
 & \begin{bmatrix} 0 & 0 \\ 0 & 1 \end{bmatrix} D_+ \left(\tilde{\epsilon}_0^0 + h \tilde{\epsilon}_0^1 + h^2 \tilde{\epsilon}_0^2 + h^3 \tilde{\epsilon}_0^3 \right) \\
 & + \begin{bmatrix} 1 & 0 \\ 0 & A_{02} \tilde{v}_0 \end{bmatrix} A_{02} \left(\tilde{\epsilon}_0^0 + h \tilde{\epsilon}_0^1 + h^2 \tilde{\epsilon}_0^2 + h^3 \tilde{\epsilon}_0^3 \right) \\
 (I.7.7b) \quad & = \begin{bmatrix} 0 \\ A_{02} (\tilde{f}_0^0 + h \tilde{f}_0^1 + h^2 \tilde{f}_0^2 + h^3 \tilde{f}_0^3) \end{bmatrix},
 \end{aligned}$$

$$\begin{aligned}
 & \tilde{\epsilon}_j^0(0) + h \tilde{\epsilon}_j^1(0) + h^2 \tilde{\epsilon}_j^2(0) + h^3 \tilde{\epsilon}_j^3(0) = \\
 (I.7.7c) \quad & \tilde{g}_j^0 + h \tilde{g}_j^1 + h^2 \tilde{g}_j^2 + h^3 \tilde{g}_j^3,
 \end{aligned}$$

$$(I.7.7d) \quad \tilde{\epsilon}_j^0 + h \tilde{\epsilon}_j^1 + h^2 \tilde{\epsilon}_j^2 + h^3 \tilde{\epsilon}_j^3 \rightarrow 0 \quad \text{as } j \rightarrow \infty.$$

Because we want the coefficients in front of the nonlinear term to be at least h^4 , we choose $\tilde{\epsilon}^0$, $\tilde{\epsilon}^1$, and $\tilde{\epsilon}^2$ as the solutions of a linear system, derived from the system (I.7.7). From the previous sections, we know that the functions $\tilde{\epsilon}^0$, $\tilde{\epsilon}^1$, and $\tilde{\epsilon}^2$ are bounded. Then we will apply theorem I.7.1 to the system $\tilde{\epsilon}^3$ satisfies.

We choose $\tilde{\epsilon}^0$ as the solution of

$$\begin{aligned}
 & \frac{\partial}{\partial t} \tilde{\epsilon}_j^0(t) = D_+ D_- \tilde{\epsilon}_j^0(t) + \begin{bmatrix} 0 & \tilde{v}_j(t) \\ 0 & D_0 \tilde{v}_j(t) \end{bmatrix} A_{02} \tilde{\epsilon}_0^0(t) \\
 (I.7.8a) \quad & + \begin{bmatrix} \tilde{f}_j^0(t) \\ D_0 \tilde{f}_j^0(t) \end{bmatrix}, \\
 & \begin{bmatrix} 0 & 0 \\ 0 & 1 \end{bmatrix} D_+ \tilde{\epsilon}_0^0(t) + \begin{bmatrix} 1 & 0 \\ 0 & A_{02} \tilde{v}_0(t) \end{bmatrix} A_{02} \tilde{\epsilon}_0^0(t)
 \end{aligned}$$

$$(I.7.8b) \quad = \begin{bmatrix} 0 \\ A_{02} \tilde{f}_0^0(t) \end{bmatrix},$$

$$(I.7.8c) \quad \tilde{\underline{e}}_j^0(0) = \tilde{g}_j^0,$$

$$(I.7.8d) \quad \tilde{\underline{e}}_j^0(t) \rightarrow 0 \quad \text{as } j \rightarrow \infty.$$

From section 5, we know that $\tilde{\underline{e}}^0$, its derivatives, and its divided differences are bounded.

Similarly, we take $\tilde{\underline{e}}^1$ to be the solution of

$$(I.7.9a) \quad \begin{aligned} \frac{\partial}{\partial t} \tilde{\underline{e}}_j^1(t) &= D_+ D_- \tilde{\underline{e}}_j^1(t) + \begin{bmatrix} 0 & \tilde{v}_j(t) \\ 0 & D_0 \tilde{v}_j(t) \end{bmatrix} A_{02} \tilde{\underline{e}}_0^1(t) \\ &+ \begin{bmatrix} \tilde{f}_j^1(t) \\ D_0 \tilde{f}_j^1(t) \end{bmatrix}, \end{aligned}$$

$$(I.7.9b) \quad \begin{aligned} \begin{bmatrix} 0 & 0 \\ 0 & 1 \end{bmatrix} D_+ \tilde{\underline{e}}_0^1(t) + \begin{bmatrix} 1 & 0 \\ 0 & A_{02} \tilde{v}_0(t) \end{bmatrix} A_{02} \tilde{\underline{e}}_0^1(t) \\ = \begin{bmatrix} 0 \\ -A_{02} \tilde{f}_0^1(t) \end{bmatrix}, \end{aligned}$$

$$(I.7.9c) \quad \tilde{\underline{e}}_j^1(0) = \tilde{g}_j^1,$$

$$(I.7.9d) \quad \tilde{\underline{e}}_j^1(t) \rightarrow 0 \quad \text{as } j \rightarrow \infty.$$

As the function $\tilde{\underline{e}}^0$, the vector $\tilde{\underline{e}}^1$ and its divided differences and time derivatives are bounded.

We choose $\tilde{\underline{e}}^2$ to be the solution of

$$(I.7.10a) \quad \begin{aligned} \frac{\partial}{\partial t} \tilde{\underline{e}}_j^2(t) &= D_+ D_- \tilde{\underline{e}}_j^2(t) + \begin{bmatrix} 0 & \tilde{v}_j(t) \\ 0 & D_0 \tilde{v}_j(t) \end{bmatrix} A_{02} \tilde{\underline{e}}_0^2(t) \\ &+ \begin{bmatrix} \tilde{f}_j^2(t) \\ D_0 \tilde{f}_j^2(t) \end{bmatrix} + A_{02} \tilde{\underline{e}}_0^0(t)^T \begin{bmatrix} 0 \\ 1 \end{bmatrix} D_0 \tilde{\underline{e}}_j^0(t), \end{aligned}$$

$$(I.7.10b) \quad \begin{aligned} \begin{bmatrix} 0 & 0 \\ 0 & 1 \end{bmatrix} D_+ \tilde{\underline{e}}_0^2(t) + \begin{bmatrix} 1 & 0 \\ 0 & A_{02} \tilde{v}_0(t) \end{bmatrix} A_{02} \tilde{\underline{e}}_0^2(t) \\ = \begin{bmatrix} 0 \\ A_{02} \tilde{f}_0^2(t) \end{bmatrix}, \end{aligned}$$

$$(I.7.10c) \quad \tilde{\underline{e}}_j^2(0) = \tilde{g}_j^2,$$

$$(I.7.10d) \quad \tilde{\underline{e}}_j^2(t) \rightarrow 0 \quad \text{as } j \rightarrow \infty.$$

As the two previous functions, the vector $\tilde{\underline{e}}^2$ is bounded.

We take the function $\tilde{\underline{e}}^3$ to be the solution of

$$\frac{\partial}{\partial t} \tilde{\underline{e}}_j^3(t) = D_+ D_- \tilde{\underline{e}}_j^3(t) + \begin{bmatrix} 0 & \tilde{v}_j(t) \\ 0 & D_0 \tilde{v}_j(t) \end{bmatrix} A_{02} \tilde{\underline{e}}_0^3(t)$$

$$(I.7.11a) \quad \begin{aligned} & + A_{02} \tilde{\epsilon}_0^3(t)^T \begin{bmatrix} 0 \\ 1 \end{bmatrix} A_j^3(t) + B^T(t) \begin{bmatrix} 0 \\ 1 \end{bmatrix} D_0 \tilde{\epsilon}_j^3(t) \\ & + h^5 A_{02} \tilde{\epsilon}_0^3(t)^T \begin{bmatrix} 0 \\ 1 \end{bmatrix} D_0 \tilde{\epsilon}_0^3(t) + \begin{bmatrix} \tilde{F}_j^3(t) \\ D_0 \tilde{F}_j^3(t) \end{bmatrix}, \end{aligned}$$

$$(I.7.11b) \quad \begin{aligned} & \begin{bmatrix} 0 & 0 \\ 0 & 1 \end{bmatrix} D_+ \tilde{\epsilon}_0^3(t) + \begin{bmatrix} 1 & 0 \\ 0 & A_{02} \tilde{v}_0(t) \end{bmatrix} A_{02} \tilde{\epsilon}_0^3(t) \\ & = \begin{bmatrix} 0 \\ A_{02} \tilde{f}_0^3(t) \end{bmatrix}, \end{aligned}$$

$$(I.7.11c) \quad \tilde{\epsilon}_j^3(0) = \tilde{g}_j^3,$$

$$(I.7.11d) \quad \tilde{\epsilon}_j^3(t) \rightarrow 0 \quad \text{as } j \rightarrow \infty,$$

where $A_j^3(t)$ is given by

$$A_j^3(t) = h^2 D_0 \tilde{\epsilon}_j^0(t) + h^3 D_0 \tilde{\epsilon}_j^1(t) + h^4 D_0 \tilde{\epsilon}_j^2(t),$$

where

$$B(t) = h^2 A_{02} \tilde{\epsilon}_0^0(t) + h^3 A_{02} \tilde{\epsilon}_0^1(t) + h^4 A_{02} \tilde{\epsilon}_0^2(t),$$

and where F_j^3 is given by

$$\begin{aligned} F_j^3 &= \begin{bmatrix} \tilde{f}_j^3 \\ D_0 \tilde{f}_j^3 \end{bmatrix} + A_{02} (\tilde{\epsilon}_0^1)^T \begin{bmatrix} 0 \\ 1 \end{bmatrix} D_0 \tilde{\epsilon}_j^0 + A_{02} (\tilde{\epsilon}_0^0)^T \begin{bmatrix} 0 \\ 1 \end{bmatrix} D_0 \tilde{\epsilon}_j^1 \\ &+ h \left(A_{02} (\tilde{\epsilon}_0^0)^T \begin{bmatrix} 0 \\ 1 \end{bmatrix} D_0 \tilde{\epsilon}_j^2 + A_{02} (\tilde{\epsilon}_0^1)^T \begin{bmatrix} 0 \\ 1 \end{bmatrix} D_0 \tilde{\epsilon}_j^1 \right. \\ &\left. + A_{02} (\tilde{\epsilon}_0^2)^T \begin{bmatrix} 0 \\ 1 \end{bmatrix} D_0 \tilde{\epsilon}_j^0 \right) \\ &+ h^2 \left(A_{02} (\tilde{\epsilon}_0^1)^T \begin{bmatrix} 0 \\ 1 \end{bmatrix} D_0 \tilde{\epsilon}_j^2 + A_{02} (\tilde{\epsilon}_0^2)^T \begin{bmatrix} 0 \\ 1 \end{bmatrix} D_0 \tilde{\epsilon}_j^1 \right) \\ &+ h^3 A_{02} (\tilde{\epsilon}_0^2)^T \begin{bmatrix} 0 \\ 1 \end{bmatrix} D_0 \tilde{\epsilon}_j^2. \end{aligned}$$

The equation that $\tilde{\epsilon}^3(t)$ satisfies is nonlinear and theorem I.7.1 applies, because all of the hypothesis of theorem I.7.1 is satisfied. We then deduce that for h sufficiently small,

$$(I.7.12a) \quad \left\| \tilde{\epsilon}^3 - \bar{\epsilon}^3 \right\| \leq C h^{\frac{3}{2}},$$

$$(I.7.12b) \quad \left| \tilde{\epsilon}^1 - \bar{\epsilon}^1 \right|_{\infty} \leq \tilde{C} h,$$

where $\bar{\tilde{e}}^3$ is the solution of the linearized system (I.7.11) about the solution 0

$$\begin{aligned} \frac{\partial}{\partial t} \bar{\tilde{e}}_j^3(t) &= D_+ D_- \bar{\tilde{e}}_j^3(t) + \begin{bmatrix} 0 & \tilde{v}_j(t) \\ 0 & D_0 \tilde{v}_j(t) \end{bmatrix} A_{02} \bar{\tilde{e}}_0^3(t) \\ &\quad + A_{02} \bar{\tilde{e}}_0^3(t)^T \begin{bmatrix} 0 \\ 1 \end{bmatrix} A_j^3(t) + B^T(t) \begin{bmatrix} 0 \\ 1 \end{bmatrix} D_0 \bar{\tilde{e}}_j^3(t) \\ &\quad + \begin{bmatrix} \tilde{F}_j^3(t) \\ D_0 \tilde{F}_j^3(t) \end{bmatrix}, \end{aligned} \tag{I.7.13a}$$

$$\begin{aligned} \begin{bmatrix} 0 & 0 \\ 0 & 1 \end{bmatrix} D_+ \bar{\tilde{e}}_0^3(t) + \begin{bmatrix} 1 & 0 \\ 0 & A_{02} \tilde{v}_0(t) \end{bmatrix} A_{02} \bar{\tilde{e}}_0^3(t) \\ = \begin{bmatrix} 0 \\ A_{02} \tilde{f}_0^3(t) \end{bmatrix}, \end{aligned} \tag{I.7.13b}$$

$$\bar{\tilde{e}}_j^3(0) = \tilde{g}_j^3, \tag{I.7.13c}$$

$$\bar{\tilde{e}}_j^3(t) \rightarrow 0 \quad \text{as } j \rightarrow \infty. \tag{I.7.13d}$$

We obtain the second inequality with a method similar to the one adopted to get the first one. The function $\bar{\tilde{e}}^1$ satisfies the system

$$\begin{aligned} \frac{\partial}{\partial t} \bar{\tilde{e}}_j^1(t) &= D_+ D_- \bar{\tilde{e}}_j^1(t) + \begin{bmatrix} 0 & \tilde{v}_j(t) \\ 0 & D_0 \tilde{v}_j(t) \end{bmatrix} A_{02} \bar{\tilde{e}}_0^1(t) \\ &\quad + h^2 A_{02} \bar{\tilde{e}}_0^1(t)^T \begin{bmatrix} 0 \\ 1 \end{bmatrix} D_0 \tilde{\tilde{e}}_j^0(t) + h^2 A_{02} \tilde{\tilde{e}}_0^0(t)^T \begin{bmatrix} 0 \\ 1 \end{bmatrix} \bar{\tilde{e}}_j^1(t) \\ &\quad + \begin{bmatrix} \tilde{f}_j^1(t) \\ D_0 \tilde{f}_j^1(t) \end{bmatrix} + A_{02} \tilde{\tilde{e}}_0^0(t)^T \begin{bmatrix} 0 \\ 1 \end{bmatrix} D_0 \tilde{\tilde{e}}_j^0(t), \end{aligned} \tag{I.7.14a}$$

$$\begin{aligned} \begin{bmatrix} 0 & 0 \\ 0 & 1 \end{bmatrix} D_+ \bar{\tilde{e}}_0^1(t) + \begin{bmatrix} 1 & 0 \\ 0 & A_{02} \tilde{v}_0(t) \end{bmatrix} A_{02} \bar{\tilde{e}}_0^1(t) \\ = \begin{bmatrix} 0 \\ A_{02} \tilde{f}_0^1(t) \end{bmatrix}, \end{aligned} \tag{I.7.14b}$$

$$\bar{\tilde{e}}_j^1(0) = \tilde{g}_j^1, \tag{I.7.14c}$$

$$\bar{\tilde{e}}_j^1(t) \rightarrow 0 \quad \text{as } j \rightarrow \infty., \tag{I.7.14d}$$

Because the Lipschitz constant is proportional to h^{-2} , only the first two terms in the asymptotic expansion of \tilde{e} in h are required to apply theorem I.7.1.

From (I.7.12a) and (I.7.12b), we deduce

$$\| \tilde{\tilde{e}}^3 \| \leq L, \tag{I.7.15a}$$

$$| \tilde{\tilde{e}}^1 |_\infty \leq \tilde{L}, \tag{I.7.15b}$$

because we easily show with the results from section 5 and the remarks from appendix II, that $\bar{e}^3(t)$ and $\bar{e}^1(t)$, the solutions of linear systems, are bounded.

From the boundedness of the functions $\underline{\hat{e}}^3(t)$ and $\underline{\hat{e}}^1(t)$, we deduce

$$(I.7.16a) \quad \| u - \tilde{u} - h^2 \tilde{e}^0 - h^3 \tilde{e}^1 - h^4 \tilde{e}^2 \| \leq L h^5,$$

$$(I.7.16b) \quad | u - \tilde{u} - h^2 \tilde{e}^0 |_\infty \leq \tilde{L} h^3,$$

because the first component of $\underline{\hat{e}}^3$ satisfies (I.7.15a) and the first one of $\underline{\hat{e}}^1$ (I.7.15b). In (I.7.16), \tilde{e}^i is the first component of $\underline{\hat{e}}^i$.

Similarly, we show that inequalities of type (I.7.16a) and (I.7.16b) still hold for the discrete solution \hat{u} . The proof is identical up to minor changes, because the time discretization does not change the properties of the nonlinear term.

Theorem I.7.2.

Under the assumptions that f and its derivatives on $[0, \infty) \times [0, T]$, and that g and its derivatives on $[0, \infty)$ are smooth and bounded, and that (I.1.4) is discretized in space with a second-order centered finite difference scheme and in time with Crank-Nicholson scheme, then u the solution of (I.1.4) is smooth and its derivatives are bounded on $[0, \infty) \times [0, T]$, and

$$(I.7.17a) \quad \| u - \hat{u} - h^2 \hat{e}^0 - h^3 \hat{e}^1 - h^4 \hat{e}^2 \| \leq N h^5,$$

$$(I.7.17b) \quad | u - \hat{u} - h^2 \hat{e}^0 |_\infty \leq \tilde{N} h^3,$$

where \hat{u} is the solution of the discrete equation, \hat{e}^0 , \hat{e}^1 , and \hat{e}^2 are the solutions of (I.7.8), (I.7.9), and (I.7.10) discretized in time with Crank-Nicholson scheme. The function \hat{e}^i is the first component of the vector $\underline{\hat{e}}^i$. It is understood that the function $u - \hat{u}$ is only defined at the discretization points and its value at the point (j, n) is $u((j - 1/2)h, n\tau) - \hat{u}_j^n$.

I.8 Numerical Example

In this section, we will present some numerical results for the system (I.1.3) in the special case of diffusion constants and the specific heat per unit volume being 1. We have discretized these equations with a fourth-order scheme in space and Crank-Nicholson scheme in time. The grid points are located at $((j - 1/2)h, n\tau)$, $j = 0, \dots, n = 0, 1, \dots$. Because the equations are nonlinear, we will choose a modified Newton's method to solve them in order to solve banded systems and to couple the

solid and liquid solutions through the right-hand-side and not through the right-hand-side and the jacobian. The fourth-order scheme is a five point scheme so the direct discretization of (I.1.3c) does not provide all the boundary conditions. We get the two extra equations, near $x = 0$, needed by discretizing the partial differential equation the solid satisfies at $x = -hsol/2$ with a non-centered fourth-order scheme in space and Crank-Nicholson in time and the partial differential equation the liquid satisfies at $x = hliq/2$ with a non-centered fourth-order scheme in space and Crank-Nicholson scheme in time. We get the extra equations at $x = -1 + hsol$ and at $x = 1 - hliq$ by discretizing the equation with a non-centered fourth-order scheme in space and Crank-Nicholson in time. We will solve the system

$$\begin{aligned}
 & \frac{\eta_j}{\tau} - \frac{1}{2} D_{24} \eta_j - \frac{1}{4} \left(D_{14}^* (\hat{v}_M^{n+1} + \hat{v}_M^n) - D_{14}^* (\hat{u}_0^{n+1} + \hat{u}_0^n) \right) D_{14} \eta_j \\
 & = - \frac{\hat{u}_j^{n+1} - \hat{u}_j^n}{\tau} + \frac{1}{2} D_{24} (\hat{u}_j^{n+1} + \hat{u}_j^n) \quad j = 2, \dots, N-1 \\
 \text{(I.8.1a)} \quad & + \frac{1}{4} \left(D_{14}^* (\hat{v}_M^{n+1} + \hat{v}_M^n) - D_{14}^* (\hat{u}_0^{n+1} + \hat{u}_0^n) \right) D_{14} (\hat{u}_j^{n+1} + \hat{u}_j^n), \\
 & \frac{\epsilon_j}{\tau} - \frac{1}{2} D_{24} \epsilon_j - \frac{1}{4} \left(D_{14}^* (\hat{v}_M^{n+1} + \hat{v}_M^n) - D_{14}^* (\hat{u}_0^{n+1} + \hat{u}_0^n) \right) D_{14} \epsilon_j \\
 & + \frac{1}{2} D_{24} (\hat{v}_j^{n+1} + \hat{v}_j^n) \quad j = 1, \dots, M-1 \\
 \text{(I.8.1b)} \quad & + \frac{1}{4} \left(D_{14}^* (\hat{v}_M^{n+1} + \hat{v}_M^n) - D_{14}^* (\hat{u}_0^{n+1} + \hat{u}_0^n) \right) D_{14} (\hat{v}_j^{n+1} + \hat{v}_j^n), \\
 & A_{02}^* \eta_0 = 2 \Delta - A_{02} (\hat{u}_0^{n+1} + \hat{u}_0^n) \\
 \text{(I.8.1c)} \quad & - \frac{h^2}{16} \left(D_- (\hat{v}_M^{n+1} + \hat{v}_M^n) - D_+ (\hat{u}_0^{n+1} + \hat{u}_0^n) \right) D_+ (\hat{u}_0^{n+1} + \hat{u}_0^n), \\
 & A_{02}^* \epsilon_M = 2 \Delta - A_{02} (\hat{v}_M^{n+1} + \hat{v}_M^n) \\
 \text{(I.8.1d)} \quad & - \frac{h^2}{16} \left(D_- (\hat{v}_M^{n+1} + \hat{v}_M^n) - D_+ (\hat{u}_0^{n+1} + \hat{u}_0^n) \right) D_- (\hat{v}_M^{n+1} + \hat{v}_M^n), \\
 \text{(I.8.1e)} \quad & \eta_{N+1} = 0, \\
 \text{(I.8.1f)} \quad & \epsilon_0 = 0, \\
 & \frac{\eta_N}{\tau} - \frac{1}{2} D_{24}^\circ \eta_N - \frac{1}{4} \left(D_{14}^* (\hat{v}_M^{n+1} + \hat{v}_M^n) - D_{14}^* (\hat{u}_0^{n+1} + \hat{u}_0^n) \right) D_{14}^\circ \eta_N \\
 & = - \frac{\hat{u}_N^{n+1} - \hat{u}_N^n}{\tau} + \frac{1}{2} D_{24}^\circ (\hat{u}_N^{n+1} + \hat{u}_N^n) \\
 \text{(I.8.1g)} \quad & + \frac{1}{4} \left(D_{14}^* (\hat{v}_M^{n+1} + \hat{v}_M^n) - D_{14}^* (\hat{u}_0^{n+1} + \hat{u}_0^n) \right) D_{14}^\circ (\hat{u}_N^{n+1} + \hat{u}_N^n), \\
 & \frac{\epsilon_1}{\tau} - \frac{1}{2} D_{24}^\circ \epsilon_1 - \frac{1}{4} \left(D_{14}^* (\hat{v}_M^{n+1} + \hat{v}_M^n) - D_{14}^* (\hat{u}_0^{n+1} + \hat{u}_0^n) \right) D_{14}^\circ \epsilon_1
 \end{aligned}$$

$$\begin{aligned}
 &= -\frac{\hat{v}_1^{n+1} - \hat{v}_1^n}{\tau} + \frac{1}{2} D_{24}^\circ (\hat{v}_1^{n+1} + \hat{v}_1^n) \\
 \text{(I.8.1h)} \quad &+ \frac{1}{4} \left(D_{14}^* (\hat{v}_M^{n+1} + \hat{v}_M^n) - D_{14}^* (\hat{u}_0^{n+1} + \hat{u}_0^n) \right) D_{14}^\circ (\hat{v}_1^{n+1} + \hat{v}_1^n), \\
 &\frac{\eta_1}{\tau} - \frac{1}{2} D_{24}^\circ \eta_1 - \frac{1}{4} \left(D_{14}^* (\hat{v}_M^{n+1} + \hat{v}_M^n) - D_{14}^* (\hat{u}_0^{n+1} + \hat{u}_0^n) \right) D_{14}^\circ \eta_1 \\
 &= -\frac{\hat{u}_1^{n+1} - \hat{u}_1^n}{\tau} + \frac{1}{2} D_{24}^\circ (\hat{u}_1^{n+1} + \hat{u}_1^n) \\
 \text{(I.8.1i)} \quad &+ \frac{1}{4} \left(D_{14}^* (\hat{v}_M^{n+1} + \hat{v}_M^n) - D_{14}^* (\hat{u}_0^{n+1} + \hat{u}_0^n) \right) D_{14}^\circ (\hat{u}_1^{n+1} + \hat{u}_1^n), \\
 &\frac{\epsilon_M}{\tau} - \frac{1}{2} D_{24}^\circ \epsilon_M - \frac{1}{4} \left(D_{14}^* (\hat{v}_M^{n+1} + \hat{v}_M^n) - D_{14}^* (\hat{u}_0^{n+1} + \hat{u}_0^n) \right) D_{14}^\circ \epsilon_M \\
 &= -\frac{v_M^{n+1} - v_M^n}{\tau} + \frac{1}{2} D_{24}^\circ (\hat{v}_M^{n+1} + \hat{v}_M^n) \\
 \text{(I.8.1j)} \quad &+ \frac{1}{4} \left(D_{14}^* (\hat{v}_M^{n+1} + \hat{v}_M^n) - D_{14}^* (\hat{u}_0^{n+1} + \hat{u}_0^n) \right) D_{14}^\circ (\hat{v}_M^{n+1} + \hat{v}_M^n), \\
 \text{(I.8.1k)} \quad &\hat{u}_j^0 = \tilde{u}_j, \\
 \text{(I.8.1l)} \quad &\hat{v}_j^0 = \tilde{v}_j,
 \end{aligned}$$

where the finite difference operators D_{24} , D_{14} , D_{14}^* , D_{14}° , A_{02}^* , A_{02}° , D_{24}° , D_{24}° , D_{14}° , and D_{14}° are

$$\begin{aligned}
 D_{24} v_j &= \left(I - \frac{h^2}{12} D_+ D_- \right) D_+ D_- v_j \sim v_{xx} (x_j), \\
 D_{14} v_j &= \left(I - \frac{h^2}{6} D_+ D_- \right) D_0 v_j \sim v_x (x_j), \\
 D_{14}^* v_0 &= \frac{1}{24 h} (-22 v_0 + 17 v_1 + 9 v_2 - 5 v_3 - v_4) \sim v_x (0), \\
 D_{14}^* v_M^* &= \frac{1}{24 h} (22 v_{M+1} - 17 v_M - 9 v_{M-1} + 5 v_{M-2} - v_{M-3}) \sim v_x(0), \\
 A_{02}^* v_0 &= A_{02} v_0 - \frac{h}{16} \left(D_- (\hat{v}_M^{n+1} + \hat{v}_M^n) - D_+ (\hat{u}_0^{n+1} + \hat{u}_0^n) \right) D_+ v_0 \sim v (0), \\
 A_{02}^* v_M &= A_{02} v_M - \frac{h}{16} \left(D_- (\hat{v}_M^{n+1} + \hat{v}_M^n) - D_+ (\hat{u}_0^{n+1} + \hat{u}_0^n) \right) D_- v_M \sim v (0), \\
 D_{24}^\circ v_j &= \frac{1}{12 h^2} (v_{j-4} - 6 v_{j-3} + 14 v_{j-2} - 4 v_{j-1} \\
 &\quad - 15 v_j + 10 v_{j+1}) \sim v_{xx} (x_j), \\
 D_{24}^\circ v_j &= \frac{1}{12 h^2} (v_{j+4} - 6 v_{j+3} + 14 v_{j+2} - 4 v_{j+1} \\
 &\quad - 15 v_j + 10 v_{j-1}) \sim v_{xx} (x_j), \\
 D_{14}^\circ v_j &= \frac{1}{12 h} (-v_{j-3} + 6 v_{j-2} - 18 v_{j-1}
 \end{aligned}$$

$$\begin{aligned}
 &+ 10 v_j + 3 v_{j+1}) \sim v_x(x_j), \\
 D_{14}^{\circ} v_0 = \frac{1}{12 h} &(-3 v_{j-1} - 10 v_j + 18 v_{j+1} \\
 &- 6 v_{j+2} + v_{j+3}) \sim v_x(x_j),
 \end{aligned}$$

and where \hat{u}^n and \hat{v}^n are the solutions at time level n , \hat{u}^{n+1} and \hat{v}^{n+1} are the solutions at time level $n+1$, after the k th iteration. The solution at the $(k+1)$ th iteration is given by $\hat{u}^{n+1} + \eta$ and $\hat{v}^{n+1} + \epsilon$. The convergence criterion, for the iterations, when we solve the system with different meshsizes and a fixed timestep, is that $|f_{sol}|_{\infty} < 1.e-14$, $|f_{liq}|_{\infty} < 1.e-14$, $|\eta|_{\infty} < 1.e-14$, and $|\epsilon|_{\infty} < 1.e-14$, where f_{sol} and f_{liq} are respectively the right-hand-side of the systems to be solved for the solid and the liquid and where η and ϵ the solutions of the systems. The convergence criterion, for the iterations, when we solve the system with different timesteps and a fixed meshsize, is $|f_{sol}|_{\infty} < 1.e-12$, $|f_{liq}|_{\infty} < 1.e-12$, $|\eta|_{\infty} < 1.e-12$, and $|\epsilon|_{\infty} < 1.e-12$.

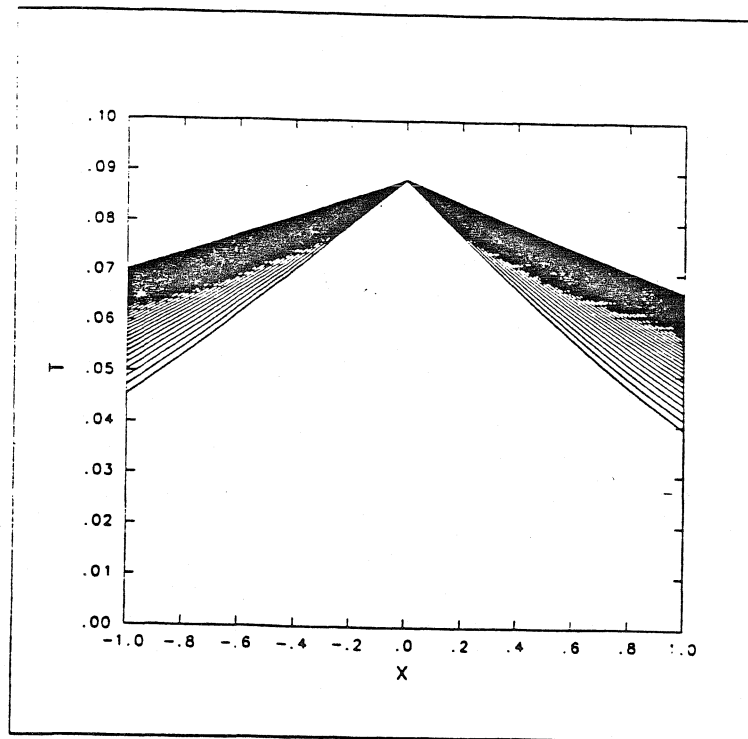


Figure I.8.1 Solution of the equation for the solid and the liquid at the times $t = 1 + .1 n$, $n = 0, 1, \dots, 50$. The lowest curve corresponds to the initial condition.

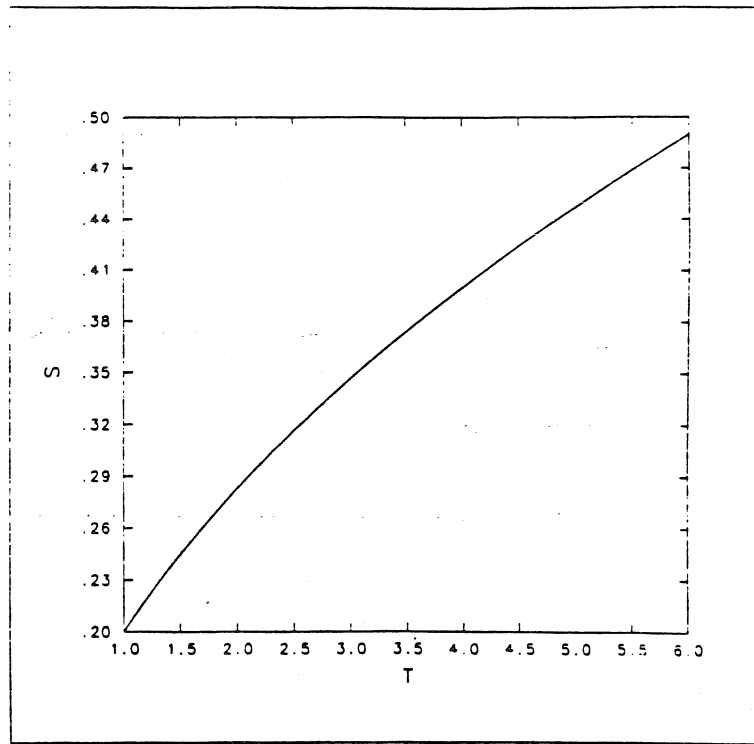


Figure I.8.2 Position of the interface between the times $t = 1$ and $t = 6$.

In fact, to get a better condition number for the matrices we need to solve the system (I.8.1), we have multiplied the equations (I.8.1a), (I.8.1b), (I.8.1g), (I.8.1h), (I.8.1i), and (I.8.1j) by τ .

Because we can compute an analytical solution for the two-sided Stefan problem on an infinite domain, we have decided to compare the numerical solution to the analytical one. We derive the initial and boundary conditions from this analytical solution. We need to get a few starting values of the jump of the solution at $x = 0$ to compute the interface position using Adams's formula. Because we know the exact position of the interface, we will take these values to start the numerical implementation. Otherwise, one would compute those with a special start-up scheme. The analytical solution is

$$(I.8.2a) \quad s(t) = 2 \lambda \sqrt{t},$$

$$(I.8.2b) \quad u(x, t) = \frac{\sqrt{\pi}}{2} \lambda e^{\lambda^2} (1 + \operatorname{erf}(\lambda)) \operatorname{erfc}\left(\lambda + \frac{x}{2\sqrt{t}}\right),$$

$$(I.8.2c) \quad v(x, t) = \frac{\sqrt{\pi}}{2} \lambda e^{\lambda^2} \operatorname{erfc}(\lambda) \left(1 + \operatorname{erf}\left(\lambda + \frac{x}{2\sqrt{t}}\right)\right),$$

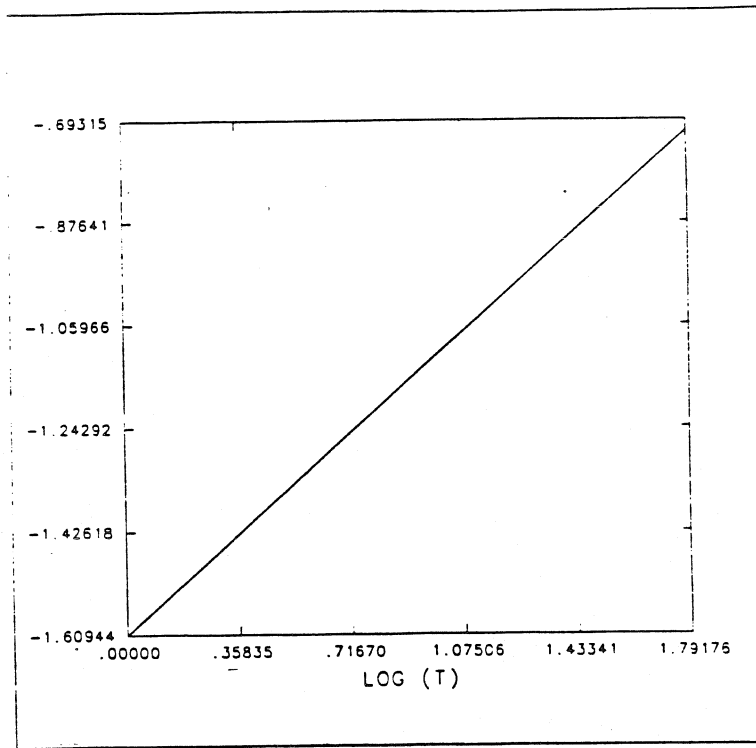


Figure I.8.3 Log-Log plot of the position of the interface vs. time.

n	8	15	30	45
interface error	4.194 d-7	3.469 d-8	2.047 d-9	3.449 d-10
liquid L_2 error	1.780 d-8	1.046 d-9	6.343 d-11	2.953 d-11
solid L_2 error	1.415 d-8	7.677 d-10	4.456 d-11	2.771 d-11
liquid max error	4.015 d-9	2.971 d-10	1.775 d-11	4.124 d-12
solid max error	3.270 d-9	2.352 d-10	1.410 d-11	2.957 d-12

Table I.8.1 Table of errors at the time $t = 3.5$ for a fixed timestep $\tau = .00001$ and different meshsizes.

with v defined on $(-\infty, 0] \times [0, \infty)$, u on $[0, \infty) \times [0, \infty)$, where λ is the solution of the algebraic relation

$$(I.8.2d) \quad \Delta = \frac{\sqrt{\pi}}{2} \lambda e^{\lambda^2} \operatorname{erfc}(\lambda) (1 + \operatorname{erf}(\lambda)),$$

and erf and erfc are the error function and the complementary error function defined

n_1 / n_2	8/15	15/30	30/45
interface error	3.781	3.985	4.332
liquid L_2 error	4.299	3.946	1.86
solid L_2 error	4.42	4.008	1.156
liquid max error	3.95	3.966	3.552
solid max error	3.993	3.955	3.812

Table I.8.2 Table of the exponents at the time $t = 3.5$ for a fixed timestep $\tau = .00001$ and different meshsizes.

n	8	15	30	45
interface error	4.648 d-7	3.815 d-8	2.280 d-9	4.154 d-10
liquid L_2 error	1.799 d-8	9.823 d-10	5.188 d-11	2.640 d-11
solid L_2 error	1.401 d-8	7.634 d-10	4.4104 d-11	2.642 d-11
liquid max error	4.229 d-9	3.051 d-10	1.917 d-11	5.791 d-12
solid max error	3.365 d-9	2.431 d-10	1.327 d-11	2.875 d-12

Table I.8.3 Table of errors at the time $t = 6$ for a fixed timestep $\tau = .00001$ and different meshsizes.

n_1 / n_2	8/15	15/30	30/45
interface error	3.792	3.967	4.142
liquid L_2 error	4.411	4.141	1.643
solid L_2 error	4.097	4.116	1.071
liquid max error	3.988	3.896	2.912
solid max error	3.986	4.096	3.72

Table I.8.4 Table of the exponents at the time $t = 6$ for a fixed timestep $\tau = .00001$ and different meshsizes.

as

$$\operatorname{erfc}(z) = \frac{2}{\sqrt{\pi}} \int_z^{\infty} e^{-x^2} dx,$$

$$\operatorname{erf}(z) = 1 - \operatorname{erfc}(z) = \frac{2}{\sqrt{\pi}} \int_0^z e^{-x^2} dx.$$

We run the numerical test on the interval $[-1, 1]$, with initial and boundary conditions

$$(I.8.3a) \quad y_j^0 = \frac{\sqrt{\pi}}{2} \lambda e^{\lambda^2} (1 + \operatorname{erf}(\lambda)) \operatorname{erfc}\left(\lambda + \frac{j h_1}{2}\right),$$

τ	5. d-3	2.5d-3	1.25 d-3	6.125 d-4
interface error	2.206 d-8	5.514 d-9	1.377 d-9	3.441 d-10
liquid L_2 error	1.923 d-9	4.827 d-10	1.244 d-10	3.218 d-11
solid L_2 error	1.178 d-9	2.965 d-10	8.441 d-11	2.116 d-11
liquid max error	2.001 d-10	5.022 d-11	1.405 d-11	3.341 d-12
solid max error	1.279 d-10	3.218 d-11	9.135 d-12	2.285 d-12

Table I.8.5 Table of the errors at the time $t = 3.5$ for a fixed meshsize $h_1 = .008368$ and $h_2 = .008368$ and different timesteps.

τ_1/τ_2	5. d-3/2.5 d-3	2.5 d-3/1.25 d-3	1.25 d-3/6.125 d-4
interface error	2.000	2.002	2.001
liquid L_2 error	1.995	1.979	1.927
solid L_2 error	1.99	1.963	1.845
liquid max error	1.994	1.980	1.930
solid max error	1.991	1.964	1.852

Table I.8.6 Table of the exponents at the time $t = 3.5$ for a fixed meshsize $h_1 = .008368$ and $h_2 = .008368$ and different timesteps.

τ	5. d-3	2.5 d-3	1.25 d-3	6.125 d-4
interface error	2.298 d-8	5.747 d-9	1.440 d-9	3.637 d-10
liquid L_2 error	2.898 d-10	7.430 d-11	2.030 d-11	6.785 d-12
solid L_2 error	1.615 d-10	4.214 d-11	1.250 d-11	5.094 d-12
liquid max error	3.137 d-11	8.030 d-12	2.186 d-12	7.274 d-13
solid max error	1.817 d-11	4.736 d-12	1.393 d-12	5.618 d-13

Table I.8.7 Table of the errors at the time $t = 6$ for a fixed meshsize $h_1 = .008368$ and $h_2 = .008368$ and different timesteps.

$$(I.8.3b) \quad z_k^0 = \frac{\sqrt{\pi}}{2} \lambda e^{\lambda^2} \operatorname{erfc}(\lambda) \left(1 + \operatorname{erf} \left(\lambda + \frac{-1 + k h_2}{2} \right) \right),$$

$$(I.8.3c) \quad s_0 = 2 \lambda,$$

$$(I.8.3d) \quad f_1(n \tau) = \frac{\sqrt{\pi}}{2} \lambda e^{\lambda^2} (1 + \operatorname{erf}(\lambda)) \operatorname{erfc} \left(\lambda + \frac{1}{2 \sqrt{1 + n \tau}} \right),$$

$$(I.8.3e) \quad f_2(n \tau) = \frac{\sqrt{\pi}}{2} \lambda e^{\lambda^2} \operatorname{erfc}(\lambda) \left(1 + \operatorname{erf} \left(\lambda - \frac{1}{2 \sqrt{1 + n \tau}} \right) \right),$$

τ_1/τ_2	5. d-3/2.5 d-3	2.5 d-3/1.25 d-3	1.25 d-3/6.125 d-4
interface error	1.999	1.997	1.985
liquid L_2 error	1.964	1.872	1.581
solid L_2 error	1.938	1.753	1.295
liquid max error	1.966	1.877	1.587
solid max error	1.94	1.765	1.310

Table I.8.8 Table of the exponents at the time $t = 6$ for a fixed meshsize $h_1 = .008368$ and $h_2 = .008368$ and different timesteps.

with j taken between 0 and $J + 1$, $h_1 = 1/(J - .5)$ and k taken between 0 and $K + 1$, $h_2 = 1/(K - .5)$.

Because we use an iterative procedure to compute the solution, we get as a guess for the solution at the time $n + 1$ the converged solution at the time n except for the boundary points at $x = -1$ and $x = 1$ where we impose the known values.

We have run the code for different values of τ , h_1 , and h_2 between the times $t = 1$ and $t = 6$, for a value of $\lambda = .1$. For the values of the parameters $\tau = .00001$, $h_1 = .02247$, and $h_2 = .02247$, we have plotted in figure I.8.1 the solution of the equation for both solid and liquid and in figure I.8.2 the interface position for the time between $t = 1$ and $t = 6$.

We have also plotted in figure AV.3 the logarithm of the position of the interface versus the logarithm of the time. It will show that the interface location is proportional to $t^{\frac{1}{2}}$.

First we fix τ and vary the value of h_1 and h_2 . We get the information about the convergence rate of the spatial scheme, because for τ sufficiently small, the total error is dominated by the spatial error.

At the time $t = 3.5$, with $\tau = 1.e - 5$ and $\lambda = .1$, for different values of n , we have in table I.8.1 the table of errors.

In table I.8.2, we calculate from table I.8.1 the order of the spatial scheme. If the scheme is of order k , we should find that the error behaves like $C h^k$, C a constant depending on the data, h the meshsize. Because we are unable to evaluate C , we find the value of k by computing the ratio of two consecutive errors corresponding to the number of discretization points $n_1 + 1$ and $n_2 + 1$, taking its logarithm, then dividing it by the logarithm of $(n_1 - .5)/(n_2 - .5)$. This is a good approximation for k .

For the same values of λ , τ , h_1 , and h_2 , we have in table I.8.3 the table of errors at $t = 6$.

At $t = 6$, we have in table I.8.4 the spatial convergence rate.

The tables show that the spatial convergence rate is 4. The theory and the numerical experiment agree, even though probably because of the round-off errors in the computation of the L_2 norm, the convergence rate is much smaller than predicted for the L_2 norm of the error for a fixed timestep, $\tau = 1.e - 5$ and 45 meshpoints on both sides of the interface, at the time $t = 6$.

Then we fix h_1 and h_2 and vary τ . We get the information about the convergence of the temporal scheme, because for h_1 and h_2 to be sufficiently small, the error due to the space discretization is negligible compared to the temporal error. We choose again $\lambda = .1$ and fix $h_1 = h_2 = .008368$. We have in table I.8.5 the table of errors at the time $t = 3.5$ and in table I.8.6 the temporal convergence rate.

For the same values of λ , τ , h_1 , and h_2 , we have in table I.8.7 the table of errors at $t = 6$ and in table I.8.8 the temporal convergence rate.

The remark made about the round-off error at $t = 6$ is still valid. The numerical and theoretical results agree.

I.9 Conclusions and Discussion

We have proven for a one-dimensional Stefan problem that the numerical solution converges to the solution of the continuous equations in the limit of zero meshsize and timestep. We have applied the transformation $x' = x - s(t)$, $s(t)$ the interface position at time t , to the set of equations describing a one-dimensional problem. We have discretized the equations with a second-order finite difference scheme in space and Crank-Nicholson scheme in time.

We first have shown with L_2 estimates that if the solution to the partial differential equations exists, the solution is C^∞ on a short time interval. Then, via iteration, we have shown there exists a unique classical solution, with the Arzela-Ascoli theorem. We also have proven that the solution exists on a long time interval under certain assumptions.

After having derived the nonlinear discrete error equations, we have linearized them about the solution $e \equiv 0$, substituted for the discrete finite difference operators their continuous equivalents, because we are unable to derive bounds for the solution of the nonlinear discrete error equations directly. Using L_2 estimates, and the techniques described in appendix I, we have bounded the solution of the linear continuous error equations in terms of the truncation errors of the scheme. We then derive bounds for the solution of the linear semi-discrete equations, using L_2 estimates for semi-discrete equations, explained in appendix II. The next step was to bound the solution of the linear discrete error equations. Because we solved a

one-dimensional two-phase Stefan problem numerically, we have derived estimates for the solution of a one-dimensional two-phase Stefan problem, in appendix III. We proceeded as in this chapter, following the same steps, deriving bounds for the solution of the linear continuous error equations, of the linear semi-discrete error ones, of the linear discrete error ones, then of the nonlinear discrete error ones.

Because we have shown that the linear discrete operator has a bounded inverse, we then prove bounds for the solution of the nonlinear discrete equations. We use the fact that the nonlinear term is locally Lipschitz continuous and that for meshsize h and timestep τ to be sufficiently small and such that $\tau/h^2 = \lambda$, we have a bound on the difference between the solution of the nonlinear discrete equations and the solution of the linear discrete ones. We have shown that we can bound the solution of the nonlinear discrete error equation in terms of the truncation errors.

We have run some numerical examples to confirm the analytical results. We have discretized the equations with a fourth-order finite difference scheme in space and Crank-Nicholson in time. Because we have derived estimates for a second-order finite difference scheme in space in this chapter, in appendix IV, we have derived estimates for the heat equation discretized with a centered fourth-order finite difference scheme in space. We have considered both Dirichlet and Neumann boundary conditions.

In section 8 of this chapter, we have given tables of errors for the numerical solution of the partial differential equations we have analyzed. The equations we have studied are nonlinear and we need to use an iterative method to solve them. In appendix V, we have described another way of coding the one-dimensional two-phase Stefan problem. Instead of mapping the interface at a given point at each timestep, we solve the equations on variable domains. This method is less costly than the method described in section 8 of this chapter because it is a direct method only requiring the interpolation of the solution computed at the previous timestep on the grid at the new timestep.

The equations describing the one-dimensional two-phase Stefan problem are of mathematical interest but are not sufficient if we want to accurately simulate dendrite growth, because for simplifications we have assumed that the diffusion constants, are constant in each domain and do not depend on the domain, on the solution itself, or on parameters describing the physical problem. This does not represent a major difficulty because without major changes, the estimates and the analysis carried out in this chapter can be extended to the variable coefficients case.

To simplify the analysis and derive the equations, we have assumed that the solid and the liquid are pure substances. If the substances are not pure, we will introduce some extra diffusion equations for the concentration of the species. De-

pending on the nature of these diffusion equations, we may or may not be able to extend the analysis to the unpure substance case. If the diffusion equations for the concentration of the species are linear, estimates can be derived for the solutions of these equations. Nonlinear problems must be considered on a case to case basis.

It should be pointed out that when the physical assumptions, that is the characteristic diffusion time of transfer of molecules between solid and liquid is fast compared with the characteristic diffusion time of heat, and the growth is limited by the diffusion of latent heat in the medium, released at the interface, are no longer satisfied, the Stefan problem may not be an accurate model for dendrite growth. It is not clear how much of the analysis is valid.

As a next step, we should try to analyze a two-dimensional two-phase Stefan problem. As for the one-dimensional Stefan problem, it is not too restricting, as a first step, to assume that the diffusion coefficients are constant and that the substances are pure. One of the major difficulties in the two-dimensional case is the fact that the interface is no longer a point but a curve. The mapping, if we are able to define it, is more complex than in the one-dimensional case, even if the curve is smooth. In [15] and [35], they have implemented a conformal mapping technique. They have assumed that the domain was simply connected and the conformal mapping maps the exterior of the domain onto the exterior of the unit disk in the z plane. This mapping provides a parameterization of the contour of the domain and the evolution of the contour may be specified by the evolution of the mapping. This has been implemented analytically. We expect that we will be able to implement a similar technique to the two-dimensional Stefan problem we want to solve.

APPENDIX I

BASIC RESULTS ON L₂ ESTIMATES FOR CONTINUOUS EQUATIONS

As seen in chapter I, to obtain upper bounds for functions using L₂ estimates, the same manipulations are carried again and again. Most of the equations considered belong to one of two categories: linear equations with Dirichlet boundary conditions and linear equations with Neumann boundary conditions. Even though L₂ estimates for linear parabolic equations have been thoroughly studied in [18], we recall here the principal results for the heat equation. We drop the lower order terms because as we show later they do not fundamentally change the final estimate. In this section, we first study the heat equation with Dirichlet boundary conditions then the heat equation with Neumann boundary conditions.

The heat equation with Dirichlet boundary conditions is given by

$$\begin{aligned} \text{(AI.1a)} \quad & \frac{\partial}{\partial t} u(x, t) = \frac{\partial^2}{\partial x^2} u(x, t), \\ \text{(AI.1b)} \quad & u(0, t) = f(t), \\ \text{(AI.1c)} \quad & u(x, 0) = g(x), \\ \text{(AI.1d)} \quad & u(x, t) \rightarrow 0 \quad \text{as } x \rightarrow \infty. \end{aligned}$$

The solution of (AI.1) satisfies the bound given in

Lemma AI.1.

Under the assumptions that f and its derivatives on $[0, T]$ and that g and its derivatives on $[0, \infty)$ are smooth and in L₂, we have

$$\text{(AI.2)} \quad \|u\|^2 \leq 2 \left[\int_0^t e^{t-\tau} \|f_0(\cdot, \tau)\|^2 d\tau + e^t \|g_0\|^2 \right] + \frac{1}{2} f^2(t) \pi,$$

where

$$\begin{aligned} f_0(x, t) &= e^{-x^2} \left(2f(t)(2x^2 - 1) - f'(t) \right), \\ g_0(x) &= g(x) - f(0)e^{-x^2}, \end{aligned}$$

and where / denotes differentiation with respect to t.

The norm $\| \cdot \|$ is derived from the scalar product

$$(y, z) = \int_0^{\infty} y(\xi) z(\xi) d\xi,$$

with the assumption that the functions y and z are real valued.

Proof of Lemma AI.1:

Because the Dirichlet boundary conditions for (AI.1) are inhomogeneous, we cannot derive an estimate immediately. One way to get around the difficulty is to introduce a new function, v , defined by $v = u - f(t) e^{-x^2}$, that satisfies homogeneous Dirichlet boundary conditions and the evolution equation

$$(AI.3a) \quad \frac{\partial}{\partial t} v(x, t) = \frac{\partial^2}{\partial x^2} v(x, t) + f_0(x, t),$$

$$(AI.3b) \quad v(0, t) = 0,$$

$$(AI.3c) \quad v(x, 0) = g_0(x),$$

$$(AI.3d) \quad v(x, t) \rightarrow 0 \quad \text{as } x \rightarrow \infty.$$

We first take the scalar product of v with (AI.3a). Then by integrating the term (v, v_{xx}) by parts and using the Cauchy-Schwarz inequality, we get

$$(AI.4a) \quad \frac{d}{dt} \|v\|^2 \leq -2 \|v_x\|^2 + \|v\|^2 + \|f_0\|^2,$$

$$(AI.4b) \quad \leq \|v\|^2 + \|f_0\|^2.$$

Then the Gronwall-Bellman inequality applied to (AI.4b) gives

$$(AI.5) \quad \|v\|^2 \leq \int_0^t e^{(t-\tau)} \|f_0(\cdot, \tau)\|^2 d\tau + e^t \|g_0\|^2.$$

The triangle inequality and the relation

$$(a + b)^2 \leq 2(a^2 + b^2),$$

lead to (AI.2).

Another way to get an estimate for u if we do not want to introduce a new function, is to compute an upper bound for the quantity $\|u\|^2 + \|u_x\|^2$. If the Dirichlet boundary condition is inhomogeneous, the term (u, u_{xx}) when integrated

by parts gives the integrated term $u(0, t) u_x(0, t)$, which cannot be estimated in terms of $\|u\|^2, \|u_x\|^2$. From Sobolev's inequality, we know

$$\begin{aligned} 2 |u(0, t) u_x(0, t)| &\leq |u(0, t)|^2 + |u_x(0, t)|^2 \\ &\leq 2 \|u\| \|u_x\| + 2 \|u_x\| \|u_{xx}\|. \end{aligned}$$

This is why we will estimate the term $\|u_x\|^2$ along with $\|u\|^2$.

The other class of equations to be considered is

$$\begin{aligned} \text{(AI.6a)} \quad & \frac{\partial}{\partial t} w(x, t) = \frac{\partial^2}{\partial x^2} w(x, t), \\ \text{(AI.6b)} \quad & \frac{\partial}{\partial x} w(0, t) = c(t) w(0, t) + f(t), \\ \text{(AI.6c)} \quad & w(x, 0) = g(x), \\ \text{(AI.6d)} \quad & w(x, t) \rightarrow 0 \quad \text{as } x \rightarrow \infty. \end{aligned}$$

This leads to

Lemma AI.2.

Under the assumptions that c, f , and their derivatives on $[0, T]$, and that g and its derivatives on $[0, \infty)$ are smooth, in the L_2 norm we have

$$\text{(AI.7)} \quad \|w\|^2 \leq \int_0^t e^{M(t-\tau)} |f(\tau)|^2 d\tau + e^{Mt} \|g\|^2.$$

Here, M is a constant depending only on c .

Proof of Lemma AI.2:

As in the proof of lemma AI.1, we compute the scalar product of w with (AI.6a). After some integration by parts and algebraic manipulations, it leads to

$$\begin{aligned} \text{(AI.8a)} \quad \frac{d}{dt} \|w\|^2 &\leq -2 \|w_x\|^2 - 2c(t) w^2(0, t) - 2f(t) w(0, t), \\ &\leq -2 \|w_x\|^2 + \epsilon (2c(t) + 1) \|w_x\|^2 \\ \text{(AI.8b)} \quad &+ \frac{1}{\epsilon} (2c(t) + 1) \|w\|^2 + |f(t)|^2. \end{aligned}$$

Because $c(t)$ is bounded, there exists a constant m such that

$$m = \max_{0 \leq t \leq T} |c(t)|.$$

We then choose ϵ such that -2 balances the term $\epsilon (2 c (t) + 1)$, for all times,

$$\epsilon = \frac{2}{2 m + 1}.$$

Once we have fixed ϵ , we deduce the value of M in (AI.7) immediately,

$$M = 2 (2 m + 1)^2,$$

and (AI.8b) becomes

$$(AI.9) \quad \frac{d}{dt} \| u \|^2 \leq M \| u \|^2 + | f (t) |^2.$$

The Gronwall-Bellman inequality gives (AI.7).

Those two lemmas cover all linear cases that need to be considered. If there are lower order terms in (AI.1a) or in (AI.6a), we will add either the terms $(u, b u_x)$ and $(u, c u)$ to (u, u_{xx}) in the scalar product (u, u_{xx}) or the terms $(w, b w_x)$ and $(w, c w)$ to (w, w_{xx}) in the scalar product (w, w_t) . If we assume some smoothness and boundedness on the coefficients b and c , brute force estimates and Sobolev's inequality provide the bounds

$$\begin{aligned} |(u, b u_x)| &\leq |b|_{\infty} \| u \| \| u_x \| \leq |b|_{\infty} \left(\epsilon \| u_x \| + \frac{1}{\epsilon} \| u \|^2 \right), \\ |(u, c u)| &\leq |c|_{\infty} \| u \|^2. \end{aligned}$$

APPENDIX II

BASIC RESULTS ON L₂ ESTIMATES FOR SEMI DISCRETE EQUATIONS

As seen in chapter I, section 5, to obtain upper bounds for discrete functions using L₂ estimates, manipulations similar to the ones of appendix I need to be carried out. They do not basically differ from these obtained for continuous functions, but taking boundary conditions into consideration can be even more difficult in the discrete case. As in appendix I, we will derive results for linear parabolic equations with both Dirichlet boundary conditions and Neumann boundary conditions. Because the lower order terms do not fundamentally change the final upper bound, we will drop them. We will recall the main results for the discrete heat equation. We discretize the heat equation with a centered-second order finite difference scheme with mesh points located at $(j - 1/2) h$, $j = 0, 1, 2, \dots$. We first study the discrete heat equation with Dirichlet boundary conditions, then the discrete heat equation with Neumann boundary conditions.

The discrete heat equation with Dirichlet boundary conditions is given by

$$(AII.1a) \quad \frac{\partial}{\partial t} y_j(t) = D_+ D_- y_j(t), \quad j = 1, 2, \dots$$

$$(AII.1b) \quad A_{02} y_0(t) = f(t),$$

$$(AII.1c) \quad y_j(0) = g_j, \quad j = 0, 1, \dots$$

$$(AII.1d) \quad y_j(t) \rightarrow 0 \quad \text{as } j \rightarrow \infty,$$

where the discrete operators are defined in chapter I.

The function y satisfies the bound given in

Lemma AII.1.

Under the assumptions that f and its derivatives are smooth and bounded on $[0, T]$, and that g and its divided differences are bounded in L₂, we have

$$(AII.2) \quad \begin{aligned} \|y\|^2 \leq & 2 \int_0^t e^{(t-\tau)} \|F(\tau)\|^2 d\tau \\ & + 2 e^t (\|k\|^2 + |k_0|^2) + 2 |f(t)|^2 \|\Lambda\|^2, \end{aligned}$$

where

$$\begin{aligned} F_j(t) &= f(t) D_+ D_- \Lambda_j - f'(t) \Lambda_j, \\ \Lambda_j &= e^{-(j-1/2)^2 h^2}, \\ k_j &= g_j - f(0) \Lambda_j. \end{aligned}$$

The norm $\| \cdot \|$ is derived from the discrete scalar product

$$(u, v) = h \sum_{j=1}^{\infty} u_j v_j,$$

with the assumption that the functions u and v are real valued.

Proof of Lemma AII.1:

Because the Dirichlet boundary conditions for (AII.1) are inhomogeneous, we cannot obtain an estimate immediately. In order to get around this difficulty we introduce a new function, $z_j = y_j - f(t) \Lambda_j$, which satisfies homogeneous Dirichlet boundary conditions and the evolution equation

$$\begin{aligned} \text{(AII.3a)} \quad & \frac{\partial}{\partial t} z_j(t) = D_+ D_- z_j(t) + F_j(t), \quad j = 1, 2, \dots \\ \text{(AII.3b)} \quad & A_{02} z_0(t) = 0, \\ \text{(AII.3c)} \quad & z_j(0) = k_j, \quad j = 0, 1, \dots \\ \text{(AII.3d)} \quad & z_j(t) \rightarrow 0 \quad \text{as } j \rightarrow \infty. \end{aligned}$$

We first take the scalar product of z with (AII.3a). Then by summing the term $(z, D_+ D_- z)$ by parts and using the Cauchy-Schwarz inequality, we get

$$\begin{aligned} \text{(AII.4a)} \quad & \frac{d}{dt} \|z\|^2 \leq -2 \|D_+ z\|^2 - \frac{2}{h} z_1 (z_1 - z_0) + \|z\|^2 + \|F\|^2, \\ \text{(AII.4b)} \quad & \leq \|z\|^2 + \|F\|^2. \end{aligned}$$

The Gronwall-Bellman inequality applied to (AII.4b) gives

$$\text{(AII.5)} \quad \|z\|^2 \leq \int_0^t e^{(t-\tau)} \|F(\tau)\|^2 d\tau + e^t (\|j\|^2 + |j_0|^2).$$

The triangle inequality and the relation

$$(a + b)^2 \leq 2(a^2 + b^2),$$

leads to (AII.2).

The other class of equations to be considered is

$$(AII.6a) \quad \frac{\partial}{\partial t} r_j(t) = D_+ D_- r_j(t), \quad j = 1, 2, \dots$$

$$(AII.6b) \quad D_+ r_0(t) = \frac{1}{2} c(t) (r_0(t) + r_1(t)) + f(t),$$

$$(AII.6c) \quad r_j(0) = g_j, \quad j = 0, 1, \dots$$

$$(AII.6d) \quad r_j(t) \rightarrow 0 \quad \text{as } j \rightarrow \infty.$$

This leads to

Lemma AII.2.

Under the assumptions that f and c and their derivatives are smooth and bounded on $[0, T]$, that g and its divided differences are bounded, in L_2 norm we have the estimate

$$(AII.7) \quad \|r\|^2 \leq \tilde{C} \int_0^t e^{M(t-\tau)} |f(\tau)|^2 d\tau + e^{Mt} (\|g\|^2 + |g_0|^2).$$

Here M is a constant depending only on c .

Proof of Lemma AII.2:

Summing the term $(r, D_+ D_- r)$ by parts, the computation of (r, r_t) gives

$$(AII.8) \quad \frac{d}{dt} \|r\|^2 \leq -2 \|D_+ r\|^2 - \frac{2}{h} r_1 (r_1 - r_0).$$

The boundary condition (AII.6b) provides a bound for the term $r_1 (r_1 - r_0)/h$ because we can express $(r_1 - r_0)/h$ in terms of r_1 and r_0 . First we calculate a bound for $|r_0|$ in terms of r_1 , $f(t)$, and $c(t)$. Then we deduce an estimate for $r_1 (r_1 - r_0)/h$. From (AII.6b), r_0 is given by

$$r_0 = \frac{2 - hc(t)}{2 + hc(t)} r_1 + \frac{2h}{2 + hc(t)} f(t).$$

Because we have assumed that $c(t)$ is bounded, the term $2 + hc(t)$ is bounded away from 0 for $h \leq h_0$. So

$$(AII.9) \quad |r_0| \leq C_1 |r_1| + C_2 |f(t)|.$$

Then (AII.8) becomes

$$(AII.10a) \quad \frac{d}{dt} \| r \|^2 \leq -2 \| D_+ r \|^2 + C | r_1 |^2 + \tilde{C} | f(t) |^2,$$

$$(AII.10b) \quad \leq M \| r \|^2 + \tilde{C} | f(t) |^2,$$

where M is $2C^2$. We deduce this value of M after having used the discrete Sobolev's inequality to bound $| r_1 |^2$ and after having chosen ϵ such that -2 balances the term ϵC .

The Gronwall-Bellman inequality applied to (AII.10b) gives (AII.7).

As in Appendix I, those two lemmas cover all linear cases that we need to consider. If there are lower order terms in (AII.1a) or (AII.6a), we add either the terms $(y, b D_0 y)$ and $(y, c y)$ to $(y, D_+ D_- y)$ in the scalar product (y, y_t) or the terms $(r, b D - 0 r)$ and $(r, c r)$ to $(r, D_+ D_- r)$ in the scalar product (r, r_t) . If we have assumed that c is bounded, brute force estimation provides the bound

$$| (y, c y) | \leq | c |_\infty \| y \|^2.$$

The term $(y, b D_0 y)$ is more difficult to bound and we will take into consideration the boundary conditions. We again assume that b and its divided differences are bounded.

$$\begin{aligned} (y, b D_0 y) &= h \sum_{j=1}^{\infty} b_j y_j \frac{y_{j+1} - y_{j-1}}{2h}, \\ &= h \sum_{j=1}^{\infty} \frac{b_j - b_{j+1}}{2h} y_j y_{j+1} + \frac{b_1}{2} y_1 y_0, \\ &= h \sum_{j=1}^{\infty} \frac{b_j - b_{j+1}}{2h} y_j^2 + h \sum_{j=1}^{\infty} \frac{b_j - b_{j+1}}{2} y_j \frac{y_{j+1} - y_j}{h} + \frac{b_1}{2} y_1 y_0, \\ &\leq \frac{1}{2} | D_+ b |_\infty \| y \|^2 + | b |_\infty \| y \| \| D_+ y \| + \frac{b_1}{2} y_1 y_0. \end{aligned}$$

If the boundary conditions are of homogeneous Dirichlet type,

$$b_1 y_1 y_0 \leq | b |_\infty | y |_\infty^2.$$

If the boundary conditions are of Neumann type,

$$b_1 y_1 y_0 \leq | b |_\infty \left(C_3 | y |_\infty^2 + \frac{1}{2} C_2 | f(t) |^2 \right),$$

where $C_3 = C_1 + C_2/2$.

So an upper bound for $| (y, b D_0 y) |$ is of the form

$$\epsilon D \| D_+ y \|^2 + E \| y \|^2 + \tilde{D} | f(t) |^2,$$

where E depends on ϵ , $| b |_\infty$, $| D_+ b |_\infty$, and on some other previously defined constants.

APPENDIX III

GENERALIZATION TO THE TWO-PHASE ONE-DIMENSIONAL STEFAN PROBLEM

In this appendix, we would like to extend the results that have been obtained in chapter I to the two-phase case described by (I.1.3) if we deal with the system of continuous equations. We will assume that the diffusion constants and the specific heat per unit volume are identical and equal to 1. The procedure to prove those results is identical to the one adopted in chapter I except for minor changes that will be clearly pointed out. For simplification, we will assume that the boundary conditions at $-\infty$ and ∞ are homogeneous as well as the one at $x = 0$. We introduce a forcing term to compensate for the restrictive boundary conditions, because as explained in chapter I, inhomogeneous boundary conditions are equivalent to a forcing term if we have chosen the adequate transformations. The system to analyze is

$$(AIII.1a) \quad \begin{aligned} \frac{\partial}{\partial t} T_s(x, t) &= \frac{\partial^2}{\partial x^2} T_s(x, t) \\ &+ \left(\frac{\partial}{\partial x} T_s(0, t) - \frac{\partial}{\partial x} T_l(0, t) \right) \frac{\partial}{\partial x} T_s(x, t) + F_s(x, t), \end{aligned}$$

$$(AIII.1b) \quad \begin{aligned} \frac{\partial}{\partial t} T_l(x, t) &= \frac{\partial^2}{\partial x^2} T_l(x, t) \\ &+ \left(\frac{\partial}{\partial x} T_s(0, t) - \frac{\partial}{\partial x} T_l(0, t) \right) \frac{\partial}{\partial x} T_l(x, t) + F_l(x, t), \end{aligned}$$

$$(AIII.1c) \quad T_s(0, t) = T_l(0, t) = 0,$$

$$(AIII.1d) \quad T_s(x, 0) = T_{s0}(x),$$

$$(AIII.1e) \quad T_l(x, 0) = T_{l0}(x),$$

$$(AIII.1f) \quad T_s(x, t) \rightarrow 0 \quad \text{as } x \rightarrow -\infty,$$

$$(AIII.1g) \quad T_l(x, t) \rightarrow 0 \quad \text{as } x \rightarrow \infty,$$

$$(AIII.1h) \quad \frac{d}{dt} s(t) = \frac{\partial}{\partial x} T_s(0, t) - \frac{\partial}{\partial x} T_l(0, t),$$

$$(AIII.1i) \quad s(0) = s_0,$$

where T_s , T_l , T_{s0} , and T_{l0} are respectively defined on $(-\infty, 0] \times [0, T]$, $[0, \infty) \times [0, T]$, $(-\infty, 0]$ and $[0, \infty)$.

We will then show how the results we have proved for the one-sided Stefan problem can be applied to the two-phase one. As in chapter I, we will first estimate the functions T_s and T_l in both L_2 and maximum norms. Then we will bound the error, by studying first the continuous linear error system, then the semi-discrete and discrete linear cases and finally the discrete nonlinear system.

The functions T_s and T_l satisfy the bounds in L_2 and maximum norms.

Lemma AIII.1.

Under the assumptions that the boundary condition at $x = 0$ is homogeneous, that the initial and boundary conditions are compatible, that T_s and T_l satisfy (I.1.3), upper bounds for T_s and T_l both in L_2 and maximum norms are given by

$$(AIII.2a) \quad \| T_s \|^2 \leq e^t \| T_{s0} \|^2 + \int_0^t e^{(t-\tau)} \| F_s(\cdot, \tau) \|^2 d\tau,$$

$$(AIII.2b) \quad | T_s |_\infty \leq \max \left(| T_{s0} |_\infty, \int_0^t | F_s(\cdot, \tau) |_\infty d\tau \right),$$

$$(AIII.2c) \quad \| T_l \|^2 \leq e^t \| T_{l0} \|^2 + \int_0^t e^{(t-\tau)} \| F_l(\cdot, \tau) \|^2 d\tau,$$

$$(AIII.2d) \quad | T_l |_\infty \leq \max \left(| T_{l0} |_\infty, \int_0^t | F_l(\cdot, \tau) |_\infty d\tau \right).$$

Proof of Lemma AIII.1:

We derive those bounds just by applying maximum principle and L_2 estimates to the system (I.1.3).

We want to bound higher order spatial derivatives of T_s and T_l . We assume that all these derivatives satisfy homogeneous boundary conditions at $-\infty$ and ∞ .

Lemma AIII.2.

Consider $W(t)$ the solution of the ordinary differential equation

$$(AIII.3.a) \quad \frac{d}{dt} W = C W + C_1 W^{\frac{3}{2}} + C_2 W^2 + C_3 W^{\frac{7}{3}},$$

$$W(0) = \| T'_{s0} \|^2 + \| T''_{s0} \|^2 + \| T'''_{s0} \|^2$$

$$(AIII.3b) \quad + \| T'_{l0} \|^2 + \| T''_{l0} \|^2 + \| T'''_{l0} \|^2,$$

with

$$W(t) = \|T_{sx}\|^2 + \|T_{sxx}\|^2 + \|T_{sxxx}\|^2 \\ + \|T_{lx}\|^2 + \|T_{lxx}\|^2 + \|T_{lxxx}\|^2,$$

where l denotes differentiation with respect to x , and $C, C_1, C_2,$ and C_3 are some constants depending on the differential operators.

We then know that if there exists a bounded solution (T_s, T_l) to (AIII.1) on $[0, T]$, with T strictly smaller than the breakdown time of (AIII.3) and with compatible initial and boundary conditions, with homogeneous boundary conditions at $-\infty$ and ∞ , then the functions $\|T_{sx}\|, \|T_{sxx}\|, \|T_{sxxx}\|, |T_{sx}|_\infty, |T_{sxx}|_\infty, \|T_{lx}\|, \|T_{lxx}\|, \|T_{lxxx}\|, |T_{lx}|_\infty,$ and $|T_{lxx}|_\infty$ satisfy

$$\begin{aligned} \text{(AIII.4a)} \quad & \|T_{sx}\|^2 \leq W(t), \\ \text{(AIII.4b)} \quad & \|T_{sxx}\|^2 \leq W(t), \\ \text{(AIII.4c)} \quad & \|T_{sxxx}\|^2 \leq W(t), \\ \text{(AIII.4d)} \quad & |T_{sx}|_\infty^2 \leq 2W(t), \\ \text{(AIII.4e)} \quad & |T_{sxx}|_\infty^2 \leq 2W(t), \\ \text{(AIII.4f)} \quad & \|T_{lx}\|^2 \leq W(t), \\ \text{(AIII.4g)} \quad & \|T_{lxx}\|^2 \leq W(t), \\ \text{(AIII.4h)} \quad & \|T_{lxxx}\|^2 \leq W(t), \\ \text{(AIII.4i)} \quad & |T_{lx}|_\infty^2 \leq 2W(t), \\ \text{(AIII.4j)} \quad & |T_{lxx}|_\infty^2 \leq 2W(t). \end{aligned}$$

Proof of Lemma AIII.2:

Because the terms $T_{lx}(0, t) T_{sx}(x, t)$ in (I.3a) and $T_{sx}(0, t) T_{lx}(x, t)$ appear in (I.3b), we will estimate the functions T_{sx} and T_{lx} simultaneously. We will carry out the same manipulations as the ones used in the proof of lemma I.3.2, then we obtain (AIII.4).

Because we have estimated T_{sx} and T_{lx} in maximum norm, the equations that higher spacial derivatives satisfy are linear. We then deduce that those functions satisfy the bounds in L_2 and maximum norms.

Lemma AIII.3.

Define $\bar{\delta}$ as the $2k$ th spatial derivative of T_s , δ as the $2k+1$ th and $\bar{\eta}$ as the $2k$ th spacial derivative of T_l , η as the $2k+1$ th, $k \geq 2$. Assume the data are smooth and the initial and boundary conditions are compatible, that the boundary conditions at $-\infty$ and ∞ are homogeneous, then $\bar{\delta}, \delta,$ and δ_x satisfy on $(-\infty, 0] \times [0, T]$

$$\begin{aligned}
 \text{(AIII.5a)} \quad & \| \bar{\delta} \|^2 \leq H(t), \\
 \text{(AIII.5b)} \quad & \| \delta \|^2 \leq H(t), \\
 \text{(AIII.5c)} \quad & \| \delta_x \|^2 \leq H(t), \\
 \text{(AIII.5d)} \quad & | \bar{\delta} |_\infty^2 \leq 2 H(t), \\
 \text{(AIII.5e)} \quad & | \delta |_\infty^2 \leq 2 H(t),
 \end{aligned}$$

and $\bar{\eta}$, η , and η_x satisfy on $[0, \infty) \times [0, T]$

$$\begin{aligned}
 \text{(AIII.5f)} \quad & \| \bar{\eta} \|^2 \leq H(t), \\
 \text{(AIII.5g)} \quad & \| \eta \|^2 \leq H(t), \\
 \text{(AIII.5h)} \quad & \| \eta_x \|^2 \leq H(t), \\
 \text{(AIII.5i)} \quad & | \bar{\eta} |_\infty^2 \leq 2 H(t), \\
 \text{(AIII.5j)} \quad & | \eta |_\infty^2 \leq 2 H(t),
 \end{aligned}$$

where $H(t)$ is

$$\begin{aligned}
 H(t) = e^{L t} & \left(\| \bar{g}_s \|^2 + \| g_s \|^2 + \| g_{sx} \|^2 \right. \\
 & \left. + \| \bar{g}_l \|^2 + \| g_l \|^2 + \| g_{lx} \|^2 \right) \\
 & + \int_0^t e^{L(t-\tau)} \left(| \bar{G}_s(\tau) |^2 + | \bar{G}'_s(\tau) |^2 + | G_s(\tau) |^2 + | G_{s1}(\tau) |^2 \right. \\
 & \left. + | \bar{G}_l(\tau) |^2 + | \bar{G}'_l(\tau) |^2 + | G_l(\tau) |^2 + | G_{l1}(\tau) |^2 \right) d\tau,
 \end{aligned}$$

and $\bar{g}_s = d^{2k}/dx^{2k} T_{s0}$, $g_s = d^{2k+1}/dx^{2k+1} T_{s0}$, G_s , \bar{G}_s , and G_{s1} known functions depending on lower order spacial derivatives of T_s . We define \bar{g}_l , g_l , G_l , \bar{G}_l , and G_{l1} similarly.

Proof of Lemma AIII.3:

We follow the same steps as in the proof of lemma I.3.3 and estimate the derivatives of the functions T_s and T_l at the same time again, because of the appearance of the terms $T_{lx}(0, t) T_{sx}(x, t)$ and $T_{sx}(0, t) T_{lx}(x, t)$ in (I.1.3a) and (I.1.3b).

We derive bounds for all order derivatives of T_s and T_l .

Theorem AIII.4.

Under the assumptions that T_{s0} and T_{l0} and their derivatives on $(-\infty, 0]$ and $[0, \infty)$, that F_s and F_l on $(-\infty, 0] \times [0, T]$ and $[0, \infty) \times [0, T]$ are smooth and bounded, that the initial and boundary conditions are compatible, that the boundary conditions at $-\infty$ and ∞ are homogeneous, and that (AIII.1) has a unique solution (T_s, T_l) on the interval $[0, T]$, with $T < T_\infty$, T_∞ the breakdown time of the ordinary differential equation (AIII.3), then the functions T_s and T_l and their derivatives satisfy the estimates

$$(AIII.6a) \quad \left\| \frac{\partial^{m+n}}{\partial x^n \partial t^m} T_s \right\|^2 \leq K_{n,m},$$

$$(AIII.6b) \quad \left| \frac{\partial^{m+n}}{\partial x^n \partial t^m} T_s \right|_\infty^2 \leq \tilde{K}_{n,m},$$

$$(AIII.6c) \quad \left\| \frac{\partial^{m+n}}{\partial x^n \partial t^m} T_l \right\|^2 \leq K_{n,m},$$

$$(AIII.6d) \quad \left| \frac{\partial^{m+n}}{\partial x^n \partial t^m} T_l \right|_\infty^2 \leq \tilde{K}_{n,m},$$

Proof of Theorem AIII.4:

We derive these estimates from lemmas AIII.1, AIII.2, AIII.3, and from the equations T_s and T_l satisfy because we have only estimated spatial derivatives of T_s and T_l and we want estimates for both temporal and spatial derivatives.

We now want to show local existence of the solution of (AIII.1).

Theorem AIII.5.

The system (AIII.1) has, with compatible initial and boundary conditions, at most one classical solution.

Proof of Theorem AIII.5:

Let (u_s, u_l) and (v_s, v_l) be the solution of (AIII.1). Define $w_s = u_s - v_s$ and $w_l = u_l - v_l$. The functions w_s and w_l satisfy

$$\frac{\partial}{\partial t} w_s(x, t) = \frac{\partial^2}{\partial x^2} w_s(x, t)$$

$$(AIII.7a) \quad \begin{aligned} & + \left(\frac{\partial}{\partial x} w_s(0, t) - \frac{\partial}{\partial x} w_l(0, t) \right) \frac{\partial}{\partial x} v_s(x, t) \\ & + \left(\frac{\partial}{\partial x} u_s(0, t) - \frac{\partial}{\partial x} u_l(0, t) \right) \frac{\partial}{\partial x} w_s(x, t), \end{aligned}$$

$$(AIII.7b) \quad \begin{aligned} \frac{\partial}{\partial t} w_l(x, t) &= \frac{\partial^2}{\partial x^2} w_l(x, t) \\ & + \left(\frac{\partial}{\partial x} w_s(0, t) - \frac{\partial}{\partial x} w_l(0, t) \right) \frac{\partial}{\partial x} v_l(x, t) \\ & + \left(\frac{\partial}{\partial x} u_s(0, t) - \frac{\partial}{\partial x} u_l(0, t) \right) \frac{\partial}{\partial x} w_l(x, t), \end{aligned}$$

$$(AIII.7c) \quad w_s(0, t) = 0,$$

$$(AIII.7d) \quad w_l(0, t) = 0,$$

$$(AIII.7e) \quad w_s(x, 0) = 0,$$

$$(AIII.7f) \quad w_l(x, 0) = 0,$$

$$(AIII.7g) \quad w_s(x, t) \rightarrow 0 \quad \text{as} \quad x \rightarrow -\infty,$$

$$(AIII.7h) \quad w_l(x, t) \rightarrow 0 \quad \text{as} \quad x \rightarrow \infty.$$

Because of the terms $(w_s(0, t) - w_l(0, t)) w_s(x, t)$ and $(w_s(0, t) - w_l(0, t)) w_l(x, t)$, we cannot derive an estimate for the functions w_s and w_l immediately. The quantity $\|w_s\|^2 + \|w_l\|^2 + \|w_{sx}\|^2 + \|w_{lx}\|^2$ must first be estimated. Define $y_s = w_{sx}$ and $y_l = w_{lx}$. The functions y_s and y_l satisfy

$$(AIII.8a) \quad \begin{aligned} \frac{\partial}{\partial t} y_s(x, t) &= \frac{\partial^2}{\partial x^2} y_s(x, t) + (y_s(0, t) - y_l(0, t)) \frac{\partial^2}{\partial x^2} v_s(x, t) \\ & + \left(\frac{\partial}{\partial x} u_s(0, t) - \frac{\partial}{\partial x} u_l(0, t) \right) \frac{\partial}{\partial x} y_s(x, t), \end{aligned}$$

$$(AIII.8b) \quad \begin{aligned} \frac{\partial}{\partial t} y_l(x, t) &= \frac{\partial^2}{\partial x^2} y_l(x, t) + (y_s(0, t) - y_l(0, t)) \frac{\partial^2}{\partial x^2} v_l(x, t) \\ & + \left(\frac{\partial}{\partial x} u_s(0, t) - \frac{\partial}{\partial x} u_l(0, t) \right) \frac{\partial}{\partial x} y_l(x, t), \end{aligned}$$

$$(AIII.8c) \quad \begin{aligned} \frac{\partial}{\partial x} y_s(0, t) &= - \left(\frac{\partial}{\partial x} u_s(0, t) - \frac{\partial}{\partial x} u_l(0, t) \right) y_s(0, t) \\ & - (y_s(0, t) - y_l(0, t)) \frac{\partial}{\partial x} v_s(0, t), \end{aligned}$$

$$(AIII.8d) \quad \begin{aligned} \frac{\partial}{\partial x} y_l(0, t) &= - \left(\frac{\partial}{\partial x} u_s(0, t) - \frac{\partial}{\partial x} u_l(0, t) \right) y_l(0, t) \\ & - (y_s(0, t) - y_l(0, t)) \frac{\partial}{\partial x} v_l(0, t), \end{aligned}$$

$$(AIII.8e) \quad y_s(x, 0) = 0,$$

$$(AIII.8f) \quad y_l(x, 0) = 0,$$

$$(AIII.8g) \quad y_s(x, t) \rightarrow 0 \quad \text{as} \quad x \rightarrow -\infty,$$

$$(AIII.8h) \quad y_l(x, t) \rightarrow 0 \quad \text{as} \quad x \rightarrow \infty.$$

After a few classical L_2 manipulations, using the fact that u_s, u_l, v_s, v_l , and their derivatives are bounded, we get

$$(AIII.9) \quad \frac{d}{dt} \left(\|w_s\|^2 + \|w_l\|^2 + \|y_s\|^2 + \|y_l\|^2 \right) \leq C \left(\|w_s\|^2 + \|w_l\|^2 + \|y_s\|^2 + \|y_l\|^2 \right),$$

where C is a constant depending on u_s, u_l, v_s, v_l , and their derivatives.

The initial conditions on w_s, w_l, y_s , and y_l imply that those functions are zero. So there exists at most one classical solution to (AIII.1).

Now we want to show local existence of the solution to (AIII.1). We assume that the initial and boundary conditions are compatible and that the functions u_s^{n+1} and u_l^{n+1} and their derivatives satisfy homogeneous boundary conditions at $-\infty$ and ∞ . As in [19], we do that via iteration. We consider

$$(AIII.10a) \quad \begin{aligned} \frac{\partial}{\partial t} u_s^{n+1}(x, t) &= \frac{\partial^2}{\partial x^2} u_s^{n+1}(x, t) \\ &+ \left(\frac{\partial}{\partial x} u_s^n(0, t) - \frac{\partial}{\partial x} u_l^n(0, t) \right) \frac{\partial}{\partial x} u_s^{n+1}(x, t), \end{aligned}$$

$$(AIII.10b) \quad \begin{aligned} \frac{\partial}{\partial t} u_l^{n+1}(x, t) &= \frac{\partial^2}{\partial x^2} u_l^{n+1}(x, t) \\ &+ \left(\frac{\partial}{\partial x} u_s^n(0, t) - \frac{\partial}{\partial x} u_l^n(0, t) \right) \frac{\partial}{\partial x} u_l^{n+1}(x, t), \end{aligned}$$

$$(AIII.10c) \quad u_s^{n+1}(0, t) = 0, \quad \text{---}$$

$$(AIII.10d) \quad u_l^{n+1}(0, t) = 0,$$

$$(AIII.10e) \quad u_s^{n+1}(x, 0) = f_s(x),$$

$$(AIII.10f) \quad u_l^{n+1}(x, 0) = f_l(x),$$

$$(AIII.10g) \quad u_s^{n+1}(x, t) \rightarrow 0 \quad \text{as} \quad x \rightarrow -\infty,$$

$$(AIII.10h) \quad u_l^{n+1}(x, t) \rightarrow 0 \quad \text{as} \quad x \rightarrow \infty.$$

Assuming that the initial and boundary conditions are compatible is equivalent to say that $u_s^{n+1}(0, 0) = f_s(0)$ and $u_l^{n+1}(0, 0) = f_l(0)$ and that $f_s(x) \rightarrow 0$ as $x \rightarrow -\infty$ and $f_l(x) \rightarrow 0$ as $x \rightarrow \infty$. To start the iteration, we choose $u_s^0(x, t) = f_s(x)$ and $u_l^0(x, t) = f_l(x)$.

Lemma AIII.6.

For a suitable time $T_1 = T_1(\|f_s\|_{H^3}, \|f_l\|_{H^3}) > 0$, the estimate

$$(AIII.11) \quad \| u_s^n \|_{H^3} + \| u_l^n \|_{H^3} \leq C \left(\| f_s \|_{H^3} + \| f_l \|_{H^3} \right) \quad 0 \leq t \leq T_1,$$

holds where $C > 1$.

Proof of Lemma AIII.6:

We use induction on n . The case $n = 0$ is trivial. Define $w_s = u_s^n$, $w_l = u_l^n$, $v_s = u_s^{n+1}$, and $v_l = u_l^{n+1}$. The functions v_s and v_l satisfy

$$(AIII.12a) \quad \begin{aligned} \frac{\partial}{\partial t} v_s(x, t) &= \frac{\partial^2}{\partial x^2} v_s(x, t) \\ &+ \left(\frac{\partial}{\partial x} w_s(0, t) - \frac{\partial}{\partial x} w_l(0, t) \right) \frac{\partial}{\partial x} v_s(x, t), \end{aligned}$$

$$(AIII.12b) \quad \begin{aligned} \frac{\partial}{\partial t} v_l(x, t) &= \frac{\partial^2}{\partial x^2} v_l(x, t) \\ &+ \left(\frac{\partial}{\partial x} w_s(0, t) - \frac{\partial}{\partial x} w_l(0, t) \right) \frac{\partial}{\partial x} v_l(x, t), \end{aligned}$$

$$(AIII.12c) \quad v_s(0, t) = 0,$$

$$(AIII.12d) \quad v_l(0, t) = 0,$$

$$(AIII.12e) \quad v_s(x, 0) = f_s(x),$$

$$(AIII.12f) \quad v_l(x, 0) = f_l(x),$$

$$(AIII.12g) \quad v_s(x, t) \rightarrow 0 \quad \text{as } x \rightarrow -\infty,$$

$$(AIII.12h) \quad v_l(x, t) \rightarrow 0 \quad \text{as } x \rightarrow \infty.$$

Because we will need to estimate v_s and v_l in H^3 norm, we derive the systems that the functions $y_s = v_{sx}$, $y_l = v_{lx}$, $z_s = v_{xx}$, $z_l = v_{lxx}$, $r_s = v_{sxxx}$, and $r_l = v_{lxxx}$ satisfy:

$$(AIII.13a) \quad \begin{aligned} \frac{\partial}{\partial t} y_s(x, t) &= \frac{\partial^2}{\partial x^2} y_s(x, t) \\ &+ \left(\frac{\partial}{\partial x} w_s(0, t) - \frac{\partial}{\partial x} w_l(0, t) \right) \frac{\partial}{\partial x} y_s(x, t), \end{aligned}$$

$$(AIII.13b) \quad \begin{aligned} \frac{\partial}{\partial t} y_l(x, t) &= \frac{\partial^2}{\partial x^2} y_l(x, t) \\ &+ \left(\frac{\partial}{\partial x} w_s(0, t) - \frac{\partial}{\partial x} w_l(0, t) \right) \frac{\partial}{\partial x} y_l(x, t), \end{aligned}$$

$$(AIII.13c) \quad \frac{\partial}{\partial x} y_s(0, t) = - \left(\frac{\partial}{\partial x} w_s(0, t) - \frac{\partial}{\partial x} w_l(0, t) \right) y_s(0, t),$$

$$(AIII.13d) \quad \frac{\partial}{\partial x} y_l(0, t) = - \left(\frac{\partial}{\partial x} w_s(0, t) - \frac{\partial}{\partial x} w_l(0, t) \right) y_l(0, t),$$

$$\begin{aligned}
 \text{(AIII.13e)} \quad y_s(x, 0) &= \frac{d}{dx} f_s(x), \\
 \text{(AIII.13f)} \quad y_l(x, 0) &= \frac{d}{dx} f_l(x), \\
 \text{(AIII.13g)} \quad y_s(x, t) &\rightarrow 0 \quad \text{as } x \rightarrow -\infty, \\
 \text{(AIII.13h)} \quad y_l(x, t) &\rightarrow 0 \quad \text{as } x \rightarrow \infty,
 \end{aligned}$$

$$\begin{aligned}
 \text{(AIII.14a)} \quad \frac{\partial}{\partial t} z_s(x, t) &= \frac{\partial^2}{\partial x^2} z_s(x, t) \\
 &+ \left(\frac{\partial}{\partial x} w_s(0, t) - \frac{\partial}{\partial x} w_l(0, t) \right) \frac{\partial}{\partial x} z_s(x, t), \\
 \text{(AIII.14b)} \quad \frac{\partial}{\partial t} z_l(x, t) &= \frac{\partial^2}{\partial x^2} z_l(x, t) \\
 &+ \left(\frac{\partial}{\partial x} w_s(0, t) - \frac{\partial}{\partial x} w_l(0, t) \right) \frac{\partial}{\partial x} z_l(x, t), \\
 \text{(AIII.14c)} \quad z_s(0, t) &= - \left(\frac{\partial}{\partial x} w_s(0, t) - \frac{\partial}{\partial x} w_l(0, t) \right) y_s(0, t), \\
 \text{(AIII.14d)} \quad z_l(0, t) &= - \left(\frac{\partial}{\partial x} w_s(0, t) - \frac{\partial}{\partial x} w_l(0, t) \right) y_l(0, t), \\
 \text{(AIII.14e)} \quad z_s(x, 0) &= \frac{d^2}{dx^2} f_s(x), \\
 \text{(AIII.14f)} \quad z_l(x, 0) &= \frac{d^2}{dx^2} f_l(x), \\
 \text{(AIII.14g)} \quad z_s(x, t) &\rightarrow 0 \quad \text{as } x \rightarrow -\infty, \\
 \text{(AIII.14h)} \quad z_l(x, t) &\rightarrow 0 \quad \text{as } x \rightarrow \infty,
 \end{aligned}$$

$$\begin{aligned}
 \text{(AIII.15a)} \quad \frac{\partial}{\partial t} r_s(x, t) &= \frac{\partial^2}{\partial x^2} r_s(x, t) \\
 &+ \left(\frac{\partial}{\partial x} w_s(0, t) - \frac{\partial}{\partial x} w_l(0, t) \right) \frac{\partial}{\partial x} r_s(x, t), \\
 \text{(AIII.15b)} \quad \frac{\partial}{\partial t} r_l(x, t) &= \frac{\partial^2}{\partial x^2} r_l(x, t) \\
 &+ \left(\frac{\partial}{\partial x} w_s(0, t) - \frac{\partial}{\partial x} w_l(0, t) \right) \frac{\partial}{\partial x} r_l(x, t), \\
 \text{(AIII.15c)} \quad \frac{\partial}{\partial x} r_s(0, t) &= - \left(\frac{\partial^2}{\partial x \partial t} w_s(0, t) - \frac{\partial^2}{\partial x \partial t} w_l(0, t) \right) y_s(0, t) \\
 &- 2 \left(\frac{\partial}{\partial x} w_s(0, t) - \frac{\partial}{\partial x} w_l(0, t) \right) r_s(0, t) \\
 &- \left(\frac{\partial}{\partial x} w_s(0, t) - \frac{\partial}{\partial x} w_l(0, t) \right)^2 z_s(0, t),
 \end{aligned}$$

$$\begin{aligned} \frac{\partial}{\partial x} r_l(0, t) = & - \left(\frac{\partial^2}{\partial x \partial t} w_s(0, t) - \frac{\partial^2}{\partial x \partial t} w_l(0, t) \right) y_l(0, t) \\ & - 2 \left(\frac{\partial}{\partial x} w_s(0, t) - \frac{\partial}{\partial x} w_l(0, t) \right) r_l(0, t) \\ & - \left(\frac{\partial}{\partial x} w_s(0, t) - \frac{\partial}{\partial x} w_l(0, t) \right)^2 z_l(0, t), \end{aligned} \quad (\text{AIII.15d})$$

$$r_s(x, 0) = \frac{d^3}{dx^3} f_s(x), \quad (\text{AIII.15e})$$

$$r_l(x, 0) = \frac{d^3}{dx^3} f_l(x), \quad (\text{AIII.15f})$$

$$r_s(x, t) \rightarrow 0 \quad \text{as } x \rightarrow -\infty, \quad (\text{AIII.15g})$$

$$r_l(x, t) \rightarrow 0 \quad \text{as } x \rightarrow \infty. \quad (\text{AIII.15h})$$

After some classical L_2 manipulations on (AIII.12), (AIII.13), (AIII.14), and (AIII.15), we obtain

$$\frac{d}{dt} \left(\|v_s\|_{H^3}^2 + \|v_l\|_{H^3}^2 \right) \leq \tilde{C} \left(\|v_s\|_{H^3}^2 + \|v_l\|_{H^3}^2 \right), \quad (\text{AIII.16})$$

where $\tilde{C} = 2(1 + C(\|f_s\|_{H^3} + \|f_l\|_{H^3}))^4$. So from the Gronwall-Bellman inequality, the requirement on T_1 will be

$$\exp \left(2 \left(1 + C \left(\|f_s\|_{H^3} + \|f_l\|_{H^3} \right) \right)^4 T_1 \right) \leq C^2. \quad (\text{AIII.17})$$

For T_1 to be sufficiently small, (AIII.17) is satisfied because $C > 1$.

We can now derive bounds for higher derivatives of u_s^n and u_l^n .

Lemma AIII.7.

For each $j = 3, 4, \dots$, there exists a K_j with

$$\|u_s(\cdot, t)\|_{H^j} \leq K_j \quad 0 \leq t \leq T_1, \quad (\text{AIII.18a})$$

$$\|u_l(\cdot, t)\|_{H^j} \leq K_j \quad 0 \leq t \leq T_1. \quad (\text{AIII.18b})$$

The constant K_j depends only on $\|f_s\|_{H^j}$ and on $\|f_l\|_{H^j}$, but is independent of n .

Proof of Lemma AIII.7:

As in the proof of lemma AIII.6, we proceed by induction. We carry out the classical L_2 manipulations on the systems for the functions v_{sj} and v_{lj} and derive estimates of the type (AIII.18a), (AIII.18b).

So we have estimated all the space derivatives of u_s^n and u_l^n on the time interval $[0, T_1]$. From the Sobolev inequality, we know that all space derivatives of u_s^n and u_l^n are bounded in maximum norm. Using the differential equations, we can replace space derivatives by time derivatives from which follows

Theorem AIII.8.

For a suitable time $T_1 = T_1 (\|f_s\|_{H^3}, \|f_l\|_{H^3}) > 0$, the following estimates

$$(AIII.19a) \quad \left\| \frac{\partial^{p+q}}{\partial x^p \partial t^q} u_s^n(\cdot, t) \right\| \leq K_{p,q},$$

$$(AIII.19b) \quad \left\| \frac{\partial^{p+q}}{\partial x^p \partial t^q} u_l^n(\cdot, t) \right\| \leq K_{p,q},$$

$$(AIII.19c) \quad \left| \frac{\partial^{p+q}}{\partial x^p \partial t^q} u_s^n(\cdot, t) \right|_{\infty} \leq \tilde{K}_{p,q},$$

$$(AIII.19d) \quad \left| \frac{\partial^{p+q}}{\partial x^p \partial t^q} u_l^n(\cdot, t) \right|_{\infty} \leq \tilde{K}_{p,q},$$

hold.

Now we want to prove that the solution of (AIII.1) exists and is in C^∞ on the interval $[0, T_1]$.

Theorem AIII.9.

The solution of (AIII.1) is in C^∞ on $[0, T_1]$, with T_1 determined in lemma AIII.6.

Proof of Theorem AIII.9:

Define $v_s = u_s^{n+1} - u_s^n$, $v_l = u_l^{n+1} - u_l^n$, $w_s = u_s^n - u_s^{n-1}$, and $w_l = u_l^n - u_l^{n-1}$. Then the functions v_s and v_l satisfy

$$(AIII.20a) \quad \begin{aligned} \frac{\partial}{\partial t} v_s(x, t) &= \frac{\partial^2}{\partial x^2} v_s(x, t) \\ &+ \left(\frac{\partial}{\partial x} w_s(0, t) - \frac{\partial}{\partial x} w_l(0, t) \right) \frac{\partial}{\partial x} u_s^{n+1}(x, t) \\ &+ \left(\frac{\partial}{\partial x} u_s^{n-1}(0, t) - \frac{\partial}{\partial x} u_l^{n-1}(0, t) \right) \frac{\partial}{\partial x} v_s(x, t), \\ \frac{\partial}{\partial t} v_l(x, t) &= \frac{\partial^2}{\partial x^2} v_l(x, t) \\ &+ \left(\frac{\partial}{\partial x} w_s(0, t) - \frac{\partial}{\partial x} w_l(0, t) \right) \frac{\partial}{\partial x} u_l^{n+1}(x, t) \end{aligned}$$

$$(AIII.20b) \quad + \left(\frac{\partial}{\partial x} u_s^{n-1}(0, t) - \frac{\partial}{\partial x} u_l^{n-1}(0, t) \right) \frac{\partial}{\partial x} v_l(x, t),$$

$$(AIII.20c) \quad v_s(0, t) = 0,$$

$$(AIII.20d) \quad v_l(0, t) = 0,$$

$$(AIII.20e) \quad v_s(x, 0) = 0,$$

$$(AIII.20f) \quad v_l(x, 0) = 0,$$

$$(AIII.20g) \quad v_s(x, t) \rightarrow 0 \quad \text{as } x \rightarrow -\infty,$$

$$(AIII.20h) \quad v_l(x, t) \rightarrow 0 \quad \text{as } x \rightarrow \infty.$$

Because of the terms $(w_{sx}(0, t) - w_{lx}(0, t)) u_{sx}^{n+1}(x, t)$ and $(w_{sx}(0, t) - w_{lx}(0, t)) u_{lx}^{n+1}(x, t)$ in (AIII.20), we will have to estimate $\|v_s\|_{H^3}^2 + \|v_l\|_{H^3}^2$ in terms of $\|w_s\|_{H^3}$ and $\|w_l\|_{H^3}$. Define $y_s = v_{sx}$, $y_l = v_{lx}$, $z_s = v_{sxx}$, $z_l = v_{lxx}$, $r_s = v_{sxxx}$, and $r_l = v_{lxxx}$. The functions y_s , y_l , z_s , z_l , r_s , and r_l satisfy

$$(AIII.21a) \quad \begin{aligned} \frac{\partial}{\partial t} y_s(x, t) &= \frac{\partial^2}{\partial x^2} y_s(x, t) \\ &+ \left(\frac{\partial}{\partial x} w_s(0, t) - \frac{\partial}{\partial x} w_l(0, t) \right) \frac{\partial^2}{\partial x^2} u_s^{n+1}(x, t) \\ &+ \left(\frac{\partial}{\partial x} u_s^{n-1}(0, t) - \frac{\partial}{\partial x} u_l^{n-1}(0, t) \right) \frac{\partial}{\partial x} y_s(x, t), \end{aligned}$$

$$(AIII.21b) \quad \begin{aligned} \frac{\partial}{\partial t} y_l(x, t) &= \frac{\partial^2}{\partial x^2} y_l(x, t) \\ &+ \left(\frac{\partial}{\partial x} w_s(0, t) - \frac{\partial}{\partial x} w_l(0, t) \right) \frac{\partial^2}{\partial x^2} u_l^{n+1}(x, t) \\ &+ \left(\frac{\partial}{\partial x} u_s^{n-1}(0, t) - \frac{\partial}{\partial x} u_l^{n-1}(0, t) \right) \frac{\partial}{\partial x} y_l(x, t), \end{aligned}$$

$$(AIII.21c) \quad \begin{aligned} \frac{\partial}{\partial x} y_s(0, t) &= - \left(\frac{\partial}{\partial x} w_s(0, t) - \frac{\partial}{\partial x} w_l(0, t) \right) \frac{\partial}{\partial x} u_s^{n+1}(0, t) \\ &- \left(\frac{\partial}{\partial x} u_s^{n-1}(0, t) - \frac{\partial}{\partial x} u_l^{n-1}(0, t) \right) y_s(0, t), \end{aligned}$$

$$(AIII.21d) \quad \begin{aligned} \frac{\partial}{\partial x} y_l(0, t) &= - \left(\frac{\partial}{\partial x} w_s(0, t) - \frac{\partial}{\partial x} w_l(0, t) \right) \frac{\partial}{\partial x} u_l^{n+1}(0, t) \\ &+ \left(\frac{\partial}{\partial x} u_s^{n-1}(0, t) - \frac{\partial}{\partial x} u_l^{n-1}(0, t) \right) y_l(0, t), \end{aligned}$$

$$(AIII.21e) \quad y_s(x, 0) = 0,$$

$$(AIII.21f) \quad y_l(x, 0) = 0,$$

$$(AIII.21g) \quad y_s(x, t) \rightarrow 0 \quad \text{as } x \rightarrow -\infty,$$

$$(AIII.21h) \quad y_l(x, t) \rightarrow 0 \quad \text{as } x \rightarrow \infty,$$

$$\frac{\partial}{\partial t} z_s(x, t) = \frac{\partial^2}{\partial x^2} z_s(x, t)$$

$$\begin{aligned}
 & + \left(\frac{\partial}{\partial x} w_s(0,t) - \frac{\partial}{\partial x} w_l(0,t) \right) \frac{\partial^3}{\partial x^3} u_s^{n+1}(x,t) \\
 \text{(AIII.22a)} \quad & + \left(\frac{\partial}{\partial x} u_s^{n-1}(0,t) - \frac{\partial}{\partial x} u_l^{n-1}(0,t) \right) \frac{\partial}{\partial x} z_s(x,t), \\
 \frac{\partial}{\partial t} z_l(x,t) & = \frac{\partial^2}{\partial x^2} z_l(x,t)
 \end{aligned}$$

$$\begin{aligned}
 & + \left(\frac{\partial}{\partial x} w_s(0,t) - \frac{\partial}{\partial x} w_l(0,t) \right) \frac{\partial^3}{\partial x^3} u_l^{n+1}(x,t) \\
 \text{(AIII.22b)} \quad & + \left(\frac{\partial}{\partial x} u_s^{n-1}(0,t) - \frac{\partial}{\partial x} u_l^{n-1}(0,t) \right) \frac{\partial}{\partial x} z_l(x,t),
 \end{aligned}$$

$$\begin{aligned}
 z_s(0,t) & = - \left(\frac{\partial}{\partial x} w_s(0,t) - \frac{\partial}{\partial x} w_l(0,t) \right) \frac{\partial}{\partial x} u_s^{n+1}(0,t) \\
 \text{(AIII.22c)} \quad & + \left(\frac{\partial}{\partial x} u_s^{n-1}(0,t) - \frac{\partial}{\partial x} u_l^{n-1}(0,t) \right) y_s(0,t),
 \end{aligned}$$

$$\begin{aligned}
 z_l(0,t) & = - \left(\frac{\partial}{\partial x} w_s(0,t) - \frac{\partial}{\partial x} w_l(0,t) \right) \frac{\partial}{\partial x} u_l^{n+1}(0,t) \\
 \text{(AIII.22d)} \quad & + \left(\frac{\partial}{\partial x} u_s^{n-1}(0,t) - \frac{\partial}{\partial x} u_l^{n-1}(0,t) \right) y_l(0,t),
 \end{aligned}$$

$$\text{(AIII.22e)} \quad z_s(x,0) = 0,$$

$$\text{(AIII.22f)} \quad z_l(x,0) = 0,$$

$$\text{(AIII.22g)} \quad z_s(x,t) \rightarrow 0 \quad \text{as } x \rightarrow -\infty,$$

$$\text{(AIII.22h)} \quad z_l(x,t) \rightarrow 0 \quad \text{as } x \rightarrow \infty,$$

$$\begin{aligned}
 \frac{\partial}{\partial t} r_s(x,t) & = \frac{\partial^2}{\partial x^2} r_s(x,t) \\
 & + \left(\frac{\partial}{\partial x} w_s(0,t) - \frac{\partial}{\partial x} w_l(0,t) \right) \frac{\partial^4}{\partial x^4} u_s^{n+1}(x,t) \\
 \text{(AIII.23a)} \quad & + \left(\frac{\partial}{\partial x} u_s^{n-1}(0,t) - \frac{\partial}{\partial x} u_l(0,t) \right) \frac{\partial}{\partial x} r_s(x,t),
 \end{aligned}$$

$$\begin{aligned}
 \frac{\partial}{\partial t} r_l(x,t) & = \frac{\partial^2}{\partial x^2} r_l(x,t) \\
 & + \left(\frac{\partial}{\partial x} w_s(0,t) - \frac{\partial}{\partial x} w_l(0,t) \right) \frac{\partial^4}{\partial x^4} u_l^{n+1}(x,t) \\
 \text{(AIII.23b)} \quad & + \left(\frac{\partial}{\partial x} u_s^{n-1}(0,t) - \frac{\partial}{\partial x} u_l(0,t) \right) \frac{\partial}{\partial x} r_l(x,t),
 \end{aligned}$$

$$\begin{aligned}
 \frac{\partial}{\partial x} r_s(0,t) & = - \left(\frac{\partial^2}{\partial x \partial t} w_s(0,t) - \frac{\partial^2}{\partial x \partial t} w_l(0,t) \right) \frac{\partial}{\partial x} u_s^{n+1}(0,t) \\
 & - \left(\frac{\partial}{\partial x} w_s(0,t) - \frac{\partial}{\partial x} w_l(0,t) \right) \frac{\partial^2}{\partial x \partial t} u_s^{n+1}(0,t)
 \end{aligned}$$

$$\begin{aligned}
 & - \left(\frac{\partial^2}{\partial x \partial t} u_s^{n-1}(0, t) - \frac{\partial^2}{\partial x \partial t} u_l^{n-1}(0, t) \right) y_s(0, t) \\
 & - 2 \left(\frac{\partial}{\partial x} u_s^{n-1}(0, t) - \frac{\partial}{\partial x} u_l^{n-1}(0, t) \right) r_s(0, t) \\
 & - \left(\frac{\partial}{\partial x} u_s^{n-1}(0, t) - \frac{\partial}{\partial x} u_l^{n-1}(0, t) \right) \\
 & \quad \left(\frac{\partial}{\partial x} w_s(0, t) - \frac{\partial}{\partial x} w_l(0, t) \right) \frac{\partial^2}{\partial x^2} u_s(0, t) \\
 & - \left(\frac{\partial}{\partial x} u_s(0, t) - \frac{\partial}{\partial x} w_l(0, t) \right)^2 z_s(0, t) \\
 \text{(AIII.23c)} \quad & - \left(\frac{\partial}{\partial x} w_s(0, t) - \frac{\partial}{\partial x} w_l(0, t) \right) \frac{\partial^3}{\partial x^3} u_s^{n+1}(0, t), \\
 \frac{\partial}{\partial x} r_l(0, t) = & - \left(\frac{\partial^2}{\partial x \partial t} w_s(0, t) - \frac{\partial^2}{\partial x \partial t} w_l(0, t) \right) \frac{\partial}{\partial x} u_l^{n+1}(0, t) \\
 & - \left(\frac{\partial}{\partial x} w_s(0, t) - \frac{\partial}{\partial x} w_l(0, t) \right) \frac{\partial^2}{\partial x \partial t} u_l^{n+1}(0, t) \\
 & - \left(\frac{\partial^2}{\partial x \partial t} u_s^{n-1}(0, t) - \frac{\partial^2}{\partial x \partial t} u_l^{n-1}(0, t) \right) y_l(0, t) \\
 & - 2 \left(\frac{\partial}{\partial x} u_s^{n-1}(0, t) - \frac{\partial}{\partial x} u_l^{n-1}(0, t) \right) r_l(0, t) \\
 & - \left(\frac{\partial}{\partial x} u_s(0, t) - \frac{\partial}{\partial x} u_l(0, t) \right) \\
 & \quad \left(\frac{\partial}{\partial x} w_s(0, t) - \frac{\partial}{\partial x} w_l(0, t) \right) \frac{\partial^2}{\partial x^2} u_l^{n+1}(0, t) \\
 & - \left(\frac{\partial}{\partial x} u_s(0, t) - \frac{\partial}{\partial x} u_l(0, t) \right)^2 z_l(0, t) \\
 \text{(AIII.23d)} \quad & - \left(\frac{\partial}{\partial x} w_s(0, t) - \frac{\partial}{\partial x} w_l(0, t) \right) \frac{\partial^3}{\partial x^3} u_l^{n+1}(0, t),
 \end{aligned}$$

$$\text{(AIII.23e)} \quad r_s(x, 0) = 0,$$

$$\text{(AIII.23f)} \quad r_l(x, 0) = 0,$$

$$\text{(AIII.23g)} \quad r_s(x, t) \rightarrow 0 \quad \text{as} \quad x \rightarrow -\infty,$$

$$\text{(AIII.23h)} \quad r_l(x, t) \rightarrow 0 \quad \text{as} \quad x \rightarrow \infty.$$

After classical L_2 estimates, we get

$$\begin{aligned}
 \frac{d}{dt} \left(\|v_s\|_{\mathbb{H}^3}^2 + \|v_l\|_{\mathbb{H}^3}^2 \right) & \leq \hat{C} \left(\|v_s\|_{\mathbb{H}^3}^2 \right. \\
 \text{(AIII.24)} \quad & \left. + \|v_l\|_{\mathbb{H}^3}^2 + \|w_s\|_{\mathbb{H}^3}^2 + \|w_l\|_{\mathbb{H}^3}^2 \right),
 \end{aligned}$$

where \hat{C} is a constant depending on u_s^{n+1} , u_l^{n+1} , u_s^{n-1} , u_l^{n-1} , and their first three

spatial derivatives. Applying the Gronwall-Bellman inequality to (AIII.24) leads to

$$(AIII.25) \quad \begin{aligned} & \| v_s \|_{H^3} + \| v_l \|_{H^3} \leq \\ & K \int_0^t \left(\| w_s(\cdot, \tau) \|_{H^3} + \| w_l(\cdot, \tau) \|_{H^3} \right) d\tau, \end{aligned}$$

where $K = 2 e^{\hat{C} T_1 / 2}$ is independent of n . So the sequences u_s^n and u_l^n converge respectively to the functions $u_s(\cdot, t)$ and $u_l(\cdot, t)$ in H^3 . From the estimates previously obtained, we know that $u_s \in C^\infty$ as well as $u_l \in C^\infty$ and so by the Arzela-Ascoli theorem the convergence $u_s^n \rightarrow u_s$, $u_l^n \rightarrow u_l$ holds pointwise and for all derivatives. So the functions u_s and u_l solve (AIII.1)

We prove long term existence as in section 3 of chapter I, extending the results given there to the two-phase case, provided the initial conditions, coefficients of the differential operator and forcing terms satisfy the hypothesis given in [10].

Because we have estimated all derivatives of T_s and T_l , we will bound the solution of the linearized continuous error system, (e_s, e_l) , and its derivatives. As mentioned in chapter I, because the lower order terms do not fundamentally change the behavior of the equation, we will drop them. We will only keep the terms $(e_{sx} - e_{lx})(0, t)$, $e_{sx}(x, t)$ and $(e_{sx} - e_{lx})(0, t)$, $e_{lx}(x, t)$ because they give difficulties in the analysis. The functions (e_s, e_l) and $c(t)$ satisfy

$$(AIII.26a) \quad \begin{aligned} \frac{\partial}{\partial t} e_s(x, t) &= \frac{\partial^2}{\partial x^2} e_s(x, t) \\ &+ \left(\frac{\partial}{\partial x} e_s(0, t) - \frac{\partial}{\partial x} e_l(0, t) \right) \frac{\partial}{\partial x} e_s(x, t) + f_s(x, t), \end{aligned}$$

$$(AIII.26b) \quad \begin{aligned} \frac{\partial}{\partial t} e_l(x, t) &= \frac{\partial^2}{\partial x^2} e_l(x, t) \\ &+ \left(\frac{\partial}{\partial x} e_s(0, t) - \frac{\partial}{\partial x} e_l(0, t) \right) \frac{\partial}{\partial x} e_l(x, t) + f_l(x, t), \end{aligned}$$

$$(AIII.26c) \quad e_s(0, t) = 0,$$

$$(AIII.26d) \quad e_l(0, t) = 0,$$

$$(AIII.26e) \quad e_s(x, 0) = 0,$$

$$(AIII.26f) \quad e_l(x, 0) = 0,$$

$$(AIII.26g) \quad e_s(x, t) \rightarrow 0 \quad \text{as } x \rightarrow -\infty,$$

$$(AIII.26h) \quad e_l(x, t) \rightarrow 0 \quad \text{as } x \rightarrow \infty,$$

$$(AIII.26i) \quad \frac{d}{dt} c(t) = k(t),$$

$$(AIII.26j) \quad c(0) = 0.$$

where

$$k(t) = \frac{h^2}{24} \left(T_{sxxx}(0, t) - T_{lxxx}(0, t) \right) + o(h^2).$$

and where f_s and f_l are given by

$$\begin{aligned} f_s(x, t) &= -h^2 \left(\frac{1}{12} T_{sxxxx}(x, t) + \frac{1}{24} \left(T_{sxxx}(0, t) - T_{lxxx}(0, t) \right) T_{sx}(x, t) \right. \\ &\quad \left. + \frac{1}{6} \left(T_{sx}(0, t) - T_{lx}(0, t) \right) T_{sxxx}(x, t) \right) + o(h^2) \\ f_l(x, t) &= -h^2 \left(\frac{1}{12} T_{lxxxx}(x, t) + \frac{1}{24} \left(T_{sxxx}(0, t) - T_{lxxx}(0, t) \right) T_{lx}(x, t) \right. \\ &\quad \left. + \frac{1}{6} \left(T_{sx}(0, t) - T_{lx}(0, t) \right) T_{lxxx}(x, t) \right) + o(h^2) \end{aligned}$$

Because the function $k(t)$ depends only on derivatives of T_s and T_l , we can bound $c(t)$ immediately.

Theorem AIII.10.

On the interval $[0, T]$, with $T < T_\infty$, T_∞ the breakdown time of (AIII.3), we have

$$(AIII.27) \quad |c(t)| \leq h^2 C T.$$

Proof of Theorem AIII.10:

We immediately deduce this bound from (AIII.6b) and (AIII.6d) and the expression of k .

We then estimate e_s and e_l in both L_2 and maximum norms and e_{sx} and e_{lx} in L_2 norm.

Lemma AIII.11.

Under the assumptions that T_s, f_s , and their derivatives on $(-\infty, 0] \times [0, T]$, and that T_l, f_l , and their derivatives on $[0, \infty) \times [0, T]$ are smooth and bounded, we have

$$\begin{aligned} (AIII.28a) \quad & \| e_s \|^2 \leq M_1(t), \\ (AIII.28b) \quad & \| y_s \|^2 \leq M_1(t), \\ (AIII.28c) \quad & | e_s |_\infty^2 \leq 2 M_1(t), \\ (AIII.28d) \quad & \| e_l \|^2 \leq M_1(t), \\ (AIII.28e) \quad & \| y_l \|^2 \leq M_1(t), \\ (AIII.28f) \quad & | e_l |_\infty^2 \leq 2 M_1(t), \end{aligned}$$

where $y_s = e_{sx}$, $y_l = e_{lx}$, and $M_1(t)$ is given by

$$M_1(t) = \int_0^t e^{C_1(t-\tau)} \left(\|f_s(\cdot, \tau)\|^2 + \left\| \frac{\partial}{\partial x} f_s(\cdot, \tau) \right\|^2 + \|f_l(\cdot, \tau)\|^2 + \left\| \frac{\partial}{\partial x} f_l(\cdot, \tau) \right\|^2 + |f_s(0, \tau)|^2 + |f_l(0, \tau)|^2 \right) d\tau.$$

If the initial conditions h_s and h_l are inhomogeneous, smooth, and L_2 integrable on $(-\infty, 0]$ and $[0, \infty)$, we add to $M_1(t)$ the term

$$e^{C_1 t} \left(\|h_s\|^2 + \left\| \frac{d}{dx} h_s \right\|^2 + \|h_l\|^2 + \left\| \frac{d}{dx} h_l \right\|^2 \right).$$

Proof of Lemma AIII.11:

We will carry out the same manipulations as in the proof of lemma I.4.2 on the functions e_s and e_l simultaneously because of the terms $(e_{sx}(0, t) - e_{lx}(0, t)) T_{sx}(x, t)$ and $(e_{sx}(0, t) - e_{lx}(0, t)) T_{lx}(x, t)$.

As in chapter I, we bound the functions y_{sx} , y_{sxx} , y_{lx} , and y_{lxx} in L_2 norm and the functions y_s , y_{sx} , y_l , and y_{lx} in maximum norm.

Lemma AIII.12.

Under the assumptions that T_s , f_s , and their derivatives on $(-\infty, 0] \times [0, T]$, and that T_l , f_l , and their derivatives on $[0, \infty) \times [0, T]$ are smooth and bounded, we have

- (AIII.29a) $\|y_{sx}\|^2 \leq M(t),$
- (AIII.29b) $\|y_{sxx}\|^2 \leq M(t),$
- (AIII.29c) $|y_s|_\infty^2 \leq 2 [M_1(t)]^{\frac{1}{2}} [M(t)]^{\frac{1}{2}},$
- (AIII.29d) $|y_{sx}|_\infty^2 \leq 2 M(t),$
- (AIII.29e) $\|y_{lx}\|^2 \leq M(t),$
- (AIII.29f) $\|y_{lxx}\|^2 \leq M(t),$
- (AIII.29g) $|y_l|_\infty^2 \leq 2 [M_1(t)]^{\frac{1}{2}} [M(t)]^{\frac{1}{2}},$
- (AIII.29h) $|y_{lx}|_\infty^2 \leq 2 M(t),$

where

$$\begin{aligned}
 M(t) = & \int_0^t e^{C(t-\tau)} \left(\left\| \frac{\partial}{\partial x} f_s(\cdot, \tau) \right\|^2 + \left\| \frac{\partial^2}{\partial x^2} f_s(\cdot, \tau) \right\|^2 + \left\| \frac{\partial^3}{\partial x^3} f_s(\cdot, \tau) \right\|^2 \right. \\
 & + |f_s(0, \tau)|^2 + \left| \frac{\partial}{\partial t} f_s(0, \tau) \right|^2 + \left| \frac{\partial}{\partial x} f_s(0, \tau) \right|^2 \left| \frac{\partial}{\partial x} T_s(0, \tau) \right|^2 \\
 & + \left| \frac{\partial}{\partial x} f_s(0, \tau) \right|^2 \left| \frac{\partial}{\partial x} T_l(0, \tau) \right|^2 + \left\| \frac{\partial}{\partial x} f_l(\cdot, \tau) \right\|^2 \\
 & + \left\| \frac{\partial^2}{\partial x^2} f_l(\cdot, \tau) \right\|^2 + \left\| \frac{\partial^3}{\partial x^3} f_l(\cdot, \tau) \right\|^2 + |f_l(0, \tau)|^2 \\
 & + \left| \frac{\partial}{\partial t} f_l(0, \tau) \right|^2 + \left| \frac{\partial}{\partial x} f_l(0, \tau) \right|^2 \left| \frac{\partial}{\partial x} T_s(0, \tau) \right|^2 \\
 & \left. + \left| \frac{\partial}{\partial x} f_l(0, \tau) \right|^2 \left| \frac{\partial}{\partial x} T_l(0, \tau) \right|^2 \right).
 \end{aligned}$$

If the initial conditions h_s and h_l are inhomogeneous, we add to the previous term

$$\begin{aligned}
 e^{Ct} \left(\left\| \frac{d}{dx} h_s \right\|^2 + \left\| \frac{d^2}{dx^2} h_s \right\|^2 + \left\| \frac{d^3}{dx^3} h_s \right\|^2 \right. \\
 \left. + \left\| \frac{d}{dx} h_l \right\|^2 + \left\| \frac{d^2}{dx^2} h_l \right\|^2 + \left\| \frac{d^3}{dx^3} h_l \right\|^2 \right).
 \end{aligned}$$

Proof of Lemma AIII.12:

We follow the same steps as in the proof of lemma I.4.3 and we estimate the functions y_{sx} , y_{sxx} , y_{lx} , and y_{lxx} simultaneously because of the terms $(y_s(0, t) - y_l(0, t)) T_{sx}(x, t)$ and $(y_s(0, t) - y_l(0, t)) T_{lx}(x, t)$ in (AIII.26a) and (AIII.26b).

We then can derive bounds for all derivatives of e_s and e_l .

Theorem AIII.13.

Under the assumptions that T_s , f_s , and their derivatives on $(-\infty, 0] \times [0, T]$, and that T_l , f_l , and their derivatives on $[0, \infty) \times [0, T]$ are smooth and bounded, then the error functions e_s and e_l satisfy

$$\text{(AIII.30a)} \quad \left\| \frac{\partial^{m+n}}{\partial x^m \partial t^n} e_s \right\|^2 \leq N_{m,n},$$

$$(AIII.30b) \quad \left\| \frac{\partial^{m+n}}{\partial x^m \partial t^n} e_s \right\|_{\infty}^2 \leq \tilde{N}_{m,n},$$

$$(AIII.30c) \quad \left\| \frac{\partial^{m+n}}{\partial x^m \partial t^n} e_l \right\|_{\infty}^2 \leq N_{m,n},$$

$$(AIII.30d) \quad \left\| \frac{\partial^{m+n}}{\partial x^m \partial t^n} e_l \right\|_{\infty}^2 \leq \tilde{N}_{m,n}.$$

Proof of Theorem AIII.13:

We derive (AIII.30a), (AIII.30b), (AIII.30c), and (AIII.30d) from lemmas AIII.11, AIII.12 and the results from appendix I. Because we have estimated spacial derivatives of the errors, we will use the equations the functions e_s and e_l satisfy to substitute space derivatives for time derivatives.

Now we want to study the semi-discrete equivalent of (AIII.26). We will first apply the transformation $x \rightarrow -x$ to the system (AIII.26) to work on functions defined on $[0, \infty)$. For reasons mentioned in section 5, chapter I, we will study the system that \tilde{p}_s and \tilde{p}_l satisfy, where $\underline{p}_s = [e_s, e_{sx}]^T$ and $\underline{p}_l = [e_l, e_{lx}]^T$. We discretize the system with a centered second-order spatial difference scheme. This reads

$$(AIII.31a) \quad \begin{aligned} \frac{\partial}{\partial t} \tilde{p}_{sj}(t) &= D_+ D_- \tilde{p}_{sj}(t) \\ &+ \begin{bmatrix} 0 & \tilde{v}_{sj}(t) \\ 0 & -D_0 \tilde{v}_{sj}(t) \end{bmatrix} A_{02} (\tilde{p}_{s0}(t) - \tilde{p}_{l0}(t)) \\ &+ \begin{bmatrix} \tilde{f}_{sj}(t) \\ -D_0 \tilde{f}_{sj}(t) \end{bmatrix}, \end{aligned}$$

$$(AIII.31b) \quad \begin{aligned} \frac{\partial}{\partial t} \tilde{p}_{lj}(t) &= D_+ D_- \tilde{p}_{lj}(t) \\ &+ \begin{bmatrix} 0 & \tilde{v}_{lj}(t) \\ 0 & D_0 \tilde{v}_{lj}(t) \end{bmatrix} A_{02} (\tilde{p}_{s0}(t) - \tilde{p}_{l0}(t)) \\ &+ \begin{bmatrix} \tilde{f}_{lj}(t) \\ D_0 \tilde{f}_{lj}(t) \end{bmatrix}, \end{aligned}$$

$$(AIII.31c) \quad \begin{aligned} \begin{bmatrix} 0 & 0 \\ 0 & -1 \end{bmatrix} D_+ \tilde{p}_{s0}(t) + \begin{bmatrix} 1 & 0 \\ 0 & A_{02} \tilde{v}_{s0}(t) \end{bmatrix} A_{02} (\tilde{p}_{s0}(t) - \tilde{p}_{l0}(t)) \\ = \begin{bmatrix} 0 \\ A_{02} \tilde{f}_{s0}(t) \end{bmatrix}, \end{aligned}$$

$$(AIII.31d) \quad \begin{aligned} \begin{bmatrix} 0 & 0 \\ 0 & 1 \end{bmatrix} D_+ \tilde{p}_{l0}(t) + \begin{bmatrix} 1 & 0 \\ 0 & A_{02} \tilde{v}_{l0}(t) \end{bmatrix} A_{02} (\tilde{p}_{s0}(t) - \tilde{p}_{l0}(t)) \\ = \begin{bmatrix} 0 \\ A_{02} \tilde{f}_{l0}(t) \end{bmatrix}, \end{aligned}$$

$$\begin{aligned}
 \text{(AIII.31e)} \quad & \tilde{p}_{sj}(0) = \tilde{g}_{sj}, \\
 \text{(AIII.31f)} \quad & \tilde{p}_{lj}(0) = \tilde{g}_{lj}, \\
 \text{(AIII.31g)} \quad & \tilde{p}_{sj}(t) \rightarrow 0 \quad \text{as } j \rightarrow \infty, \\
 \text{(AIII.31h)} \quad & \tilde{p}_{lj}(t) \rightarrow \quad \text{as } j \rightarrow \infty.
 \end{aligned}$$

The results obtained in chapter I for the function \tilde{p} carry over to the solution $(\tilde{p}_s, \tilde{p}_l)$ of (AIII.30). We deduce

Lemma AIII.14.

Under the assumptions that T_s, f_s , and their derivatives on $(-\infty, 0] \times [0, T]$, and that g_s and its derivatives on $(-\infty, 0]$, that T_l, f_l , and their derivatives on $[0, \infty) \times [0, T]$, and g_l and its derivatives on $[0, \infty)$ are smooth and bounded, we have

$$\begin{aligned}
 \text{(AIII.32a)} \quad & \|\tilde{p}_s\|^2 \leq R(t), \\
 \text{(AIII.32b)} \quad & \|\tilde{p}_l\|^2 \leq R(t),
 \end{aligned}$$

where $R(t)$ is given by

$$\begin{aligned}
 R(t) = & \int_0^t e^{L(t-\tau)} \left(\|\tilde{f}_s(\tau)\|^2 + \|D_0 \tilde{f}_s(\tau)\|^2 + \|\tilde{f}_l(\tau)\|^2 \right. \\
 & + \|D_0 \tilde{f}_l(\tau)\|^2 + C_4 (|\tilde{f}_{s0}(\tau)|^2 + |\tilde{f}_{s1}(\tau)|^2 + |\tilde{f}_{l0}(\tau)|^2 \\
 & \left. + |\tilde{f}_{l1}(\tau)|^2) \right) d\tau + e^{L t} \left(\|\tilde{g}_s\|^2 + \|D_0 \tilde{g}_s\|^2 + \|\tilde{g}_l\|^2 + \|D_0 \tilde{g}_l\|^2 \right).
 \end{aligned}$$

Proof of Lemma AIII.14:

We evaluate the scalar product $(\tilde{p}_s, \tilde{p}_{st}) + (\tilde{p}_l, \tilde{p}_{lt})$ and carry out the same algebra as the one that has been carried out in the proof of lemma I.5.1.

As in chapter I, we then bound the functions \tilde{q}_s and \tilde{q}_l , the time partial derivatives of the functions \tilde{p}_s and \tilde{p}_l .

Lemma AIII.15.

Under the assumptions that T_s, f_s , and their derivatives on $(-\infty, 0] \times [0, T]$, and that g_s and its derivatives on $(-\infty, 0]$, that T_l, f_l , and their derivatives on $[0, \infty) \times [0, T]$, and g_l and its derivatives on $[0, \infty)$ are smooth and bounded, we have

$$\begin{aligned}
 \text{(AIII.33a)} \quad & \|\tilde{q}_s\|^2 \leq S(t), \\
 \text{(AIII.33b)} \quad & \|\tilde{q}_l\|^2 \leq S(t),
 \end{aligned}$$

where $\tilde{q}_s = \tilde{p}_{st}$, $\tilde{q}_l = \tilde{p}_{lt}$, and

$$\begin{aligned} S(t) = & \int_0^t e^{Q(t-\tau)} \left[\|\tilde{f}_s(\tau)\|^2 + \|D_0 \tilde{f}_s(\tau)\|^2 + \left\| \frac{d}{dt} \tilde{f}_s(\tau) \right\|^2 \right. \\ & + \left\| \frac{d}{dt} D_0 \tilde{f}_s(\tau) \right\|^2 + \|\tilde{f}_l(\tau)\|^2 + \|D_0 \tilde{f}_l(\tau)\|^2 + \left\| \frac{d}{dt} \tilde{f}_l(\tau) \right\|^2 \\ & + \left\| \frac{d}{dt} D_0 \tilde{f}_l(\tau) \right\|^2 + C \left(|\tilde{f}_{s0}(\tau)|^2 + |\tilde{f}_{s1}(\tau)|^2 + \left| \frac{d}{dt} \tilde{f}_{s0}(\tau) \right|^2 \right. \\ & + \left| \frac{d}{dt} \tilde{f}_{s1}(\tau) \right|^2 + |\tilde{f}_{l0}(\tau)|^2 + |\tilde{f}_{l1}(\tau)|^2 + \left| \frac{d}{dt} \tilde{f}_{l0}(\tau) \right|^2 \\ & \left. + \left| \frac{d}{dt} \tilde{f}_{l1}(\tau) \right|^2 \right) d\tau + e^{Q t} \left(\|\tilde{g}_s\|^2 + \|D_0 \tilde{g}_s\|^2 + \|\tilde{h}_s\|^2 \right. \\ & \left. + \|D_0 \tilde{h}_s\|^2 + \|\tilde{g}_l\|^2 + \|D_0 \tilde{g}_l\|^2 + \|\tilde{h}_l\|^2 + \|D_0 \tilde{h}_l\|^2 \right) \end{aligned}$$

Proof of Lemma AIII.15:

We evaluate the scalar product $(\tilde{p}_s, \tilde{p}_{st}) + (\tilde{q}_s, \tilde{q}_{st}) + (\tilde{p}_l, \tilde{p}_{lt}) + (\tilde{q}_l, \tilde{q}_{lt})$ and carry out the same algebra as the one that has been carried out in the proof of lemma I.5.2.

From the equivalent of (I.5.15) for \tilde{p}_s and \tilde{p}_l obtained in the proof of lemma AIII.14, we bound $D_+ \tilde{p}_s$ and $D_+ \tilde{p}_l$ in L_2 norm.

Lemma AIII.16.

Under the assumptions that T_s, f_s , and their derivatives on $(-\infty, 0] \times [0, T]$, and that g_s and its derivatives on $(-\infty, 0]$, that T_l, f_l , and their derivatives on $[0, \infty) \times [0, T]$, and g_l and its derivatives on $[0, \infty)$ are smooth and bounded, we have

$$(AIII.34a) \quad \|D_+ \tilde{p}_s\|^2 \leq X(t),$$

$$(AIII.34b) \quad \|D_+ \tilde{p}_l\|^2 \leq X(t),$$

where $X(t)$ is given by

$$\begin{aligned} X(t) = & (L+1) R(t) + S(t) + \|\tilde{f}_s\|^2 + \|D_0 \tilde{f}_s\|^2 + \|\tilde{f}_l\|^2 \\ & + \|D_0 \tilde{f}_l\|^2 + C_4 (|\tilde{f}_{s0}|^2 + |\tilde{f}_{s1}|^2 + |\tilde{f}_{l0}|^2 + |\tilde{f}_{l1}|^2), \end{aligned}$$

with $R(t)$ and $S(t)$ are upper bounds for $\|\underline{\tilde{p}}_s\|^2$ and $\|\underline{\tilde{p}}_l\|^2$ and for $\|\underline{\tilde{q}}_s\|^2$ and $\|\underline{\tilde{q}}_l\|^2$ respectively.

Proof of Lemma AIII.16:

We have derived an inequality of the type (I.5.15) for $\|\underline{\tilde{p}}_s\|^2 + \|\underline{\tilde{p}}_l\|^2 + \|\underline{\tilde{q}}_s\|^2 + \|\underline{\tilde{q}}_l\|^2$. If we proceed as in the proof of lemma I.5.3, we get (AIII.34a) and (AIII.34b).

Because we have estimated $\underline{\tilde{p}}_s, \underline{\tilde{p}}_l, \underline{\tilde{q}}_s, \underline{\tilde{q}}_l, D_+ \underline{\tilde{p}}_s, D_+ \underline{\tilde{p}}_l, D_+ \underline{\tilde{q}}_s,$ and $D_+ \underline{\tilde{q}}_l,$ from Sobolev's inequality, we get estimates for $\underline{\tilde{p}}_s, \underline{\tilde{p}}_l, \underline{\tilde{q}}_s,$ and $\underline{\tilde{q}}_l$ in maximum norm.

Lemma AIII.17.

Under the assumptions that $T_s, f_s,$ and their derivatives on $(-\infty, 0] \times [0, T],$ and that g_s and its derivatives on $(-\infty, 0],$ that $T_l, f_l,$ and their derivatives on $[0, \infty) \times [0, T],$ and g_l and its derivatives on $[0, \infty)$ are smooth and bounded, we have

$$\begin{aligned} \text{(AIII.35a)} \quad & |\underline{\tilde{p}}_s|_\infty^2 \leq 2 R^{\frac{1}{2}}(t) X^{\frac{1}{2}}(t), \\ \text{(AIII.35b)} \quad & |\underline{\tilde{q}}_s|_\infty^2 \leq 2 S^{\frac{1}{2}}(t) Z^{\frac{1}{2}}(t), \\ \text{(AIII.35c)} \quad & |\underline{\tilde{p}}_l|_\infty^2 \leq 2 R^{\frac{1}{2}}(t) X^{\frac{1}{2}}(t), \\ \text{(AIII.35d)} \quad & |\underline{\tilde{q}}_l|_\infty^2 \leq 2 S^{\frac{1}{2}}(t) Z^{\frac{1}{2}}(t), \end{aligned}$$

where $Z(t)$ is an upper bound for $\|D_+ \underline{\tilde{q}}_s\|^2$ and $\|D_+ \underline{\tilde{q}}_l\|^2$.

Proof of Lemma AIII.17:

We derive (AIII.35a) from the discrete Sobolev inequality (I.5.10), (AIII.32a), and (AIII.34a), (AIII.35b) from (I.5.10), (AIII.33a), and the equivalent of (AIII.34a) for $\|D_+ \underline{\tilde{q}}_s\|^2,$ (AIII.35c) from (I.5.10), (AIII.32b), and (AIII.34b), and (AIII.35d) from (I.5.10), (AIII.33b), and the equivalent of (AIII.34b) for $\|D_+ \underline{\tilde{q}}_l\|^2$.

We will now bound $D_- \underline{\tilde{p}}_s$ and $D_- \underline{\tilde{p}}_l$ in L_2 norm. The result summarizes as

Lemma AIII.18.

Under the assumptions that $T_s, f_s,$ and their derivatives on $(-\infty, 0] \times [0, T],$ and that g_s and its derivatives on $(-\infty, 0],$ that $T_l, f_l,$ and their derivatives on $[0, \infty) \times [0, T],$ and g_l and its derivatives on $[0, \infty)$ are smooth and bounded, we have

$$(AIII.36a) \quad \| D_- \tilde{p}_s \|^2 \leq Y(t),$$

$$(AIII.36b) \quad \| D_- \tilde{p}_l \|^2 \leq Y(t),$$

where $Y(t)$ is given by

$$\begin{aligned} Y(t) = & N X(t) + \tilde{N} R(t) + N_0 S(t) + \tilde{N}_0 Z(t) \\ & + N_1 W(t) + N_2 (|\tilde{f}_{s0}|^2 + |\tilde{f}_{s1}|^2 + |\tilde{f}_{l0}|^2 + |\tilde{f}_{l1}|^2), \end{aligned}$$

where $X(t)$, $R(t)$, $S(t)$, $Z(t)$, and $W(t)$ are the upper bounds computed above for $\| D_+ \tilde{p}_s \|^2$ and $\| D_+ \tilde{p}_l \|^2$, $\| \tilde{p}_s \|^2$ and $\| \tilde{p}_l \|^2$, $\| \tilde{q}_s \|^2$ and $\| \tilde{q}_l \|^2$, $\| \tilde{q}_s \|^2$ and $\| \tilde{q}_l \|^2$, and $\| (D_+)^2 \tilde{p}_s \|^2$ and $\| (D_+)^2 \tilde{p}_l \|^2$. N , \tilde{N} , N_0 , \tilde{N}_0 , N_1 , and N_2 are constants depending on the initial conditions and on the coefficients of the differential operator.

Proof of Lemma AIII.18:

We first derive estimates for the functions $\| (D_+)^2 \tilde{p}_s \|^2$ and $\| (D_+)^2 \tilde{p}_l \|^2$. Then we proceed as in the proof of lemma I.5.5, to derive these bounds.

Because we have estimated $D_+ \tilde{p}_s$, $D_+ \tilde{p}_l$, $D_- \tilde{p}_s$, and $D_- \tilde{p}_l$, we derive bounds for $D_0 \tilde{p}_s$ and $D_0 \tilde{p}_l$ in L_2 norm.

Lemma AIII.19.

Under the assumptions that T_s , f_s , and their derivatives on $(-\infty, 0] \times [0, T]$, and that g_s and its derivatives on $(-\infty, 0]$, that T_l , f_l , and their derivatives on $[0, \infty) \times [0, T]$, and g_l and its derivatives on $[0, \infty)$ are smooth and bounded, we have

$$(AIII.37a) \quad \| D_0 \tilde{p}_s \|^2 \leq \frac{1}{2} X(t) + \frac{1}{2} Y(t),$$

$$(AIII.37b) \quad \| D_0 \tilde{p}_l \|^2 \leq \frac{1}{2} X(t) + \frac{1}{2} Y(t),$$

Proof of Lemma AIII.19:

It is identical to the proof of lemma I.5.7.

We will then get estimates for all order derivatives of \tilde{p}_s and \tilde{p}_l both in L_2 and maximum norms.

Theorem AIII.20.

Under the assumptions that T_s , f_s , and their derivatives on $(-\infty, 0] \times [0, T]$, and that g_s and its derivatives on $(-\infty, 0]$, that T_l , f_l , and their derivatives on $[0, \infty) \times [0, T]$, and g_l and its derivatives on $[0, \infty)$ are smooth and bounded, we have

$$(AIII.38a) \quad \left\| \frac{d^k}{dt^k} D_+^i D_-^m D_0^n \underline{\tilde{p}}_s \right\|^2 \leq Q_{k,i,m,n},$$

$$(AIII.38b) \quad \left| \frac{d^k}{dt^k} D_+^i D_-^m D_0^n \underline{\tilde{p}}_s \right|_\infty^2 \leq \tilde{Q}_{k,i,m,n},$$

$$(AIII.38c) \quad \left\| \frac{d^k}{dt^k} D_+^i D_-^m D_0^n \underline{\tilde{p}}_l \right\|^2 \leq Q_{k,i,m,n},$$

$$(AIII.38d) \quad \left| \frac{d^k}{dt^k} D_+^i D_-^m D_0^n \underline{\tilde{p}}_l \right|_\infty^2 \leq \tilde{Q}_{k,i,m,n}.$$

Proof of Theorem AIII.20:

We derive (AIII.38a), (AIII.38b), (AIII.38c), and (AIII.38d) from lemmas AIII.14, AIII.15, AIII.16, AIII.17, AIII.18, AIII.19, and the equations $\underline{\tilde{p}}_s$ and $\underline{\tilde{p}}_l$ satisfy.

What we were initially interested in was to bound all derivatives of \tilde{e}_s and \tilde{e}_l both in L_2 and maximum norms.

Theorem AIII.21.

Under the assumptions that T_s, f_s , and their derivatives on $(-\infty, 0] \times [0, T]$, and that g_s and its derivatives on $(-\infty, 0]$, that T_l, f_l , and their derivatives on $[0, \infty) \times [0, T]$, and g_l and its derivatives on $[0, \infty)$ are smooth and bounded, we have

$$(AIII.39a) \quad \left\| \frac{d^k}{dt^k} D_+^i D_-^m D_0^n \tilde{e}_s \right\|^2 \leq Q_{k,i,m,n},$$

$$(AIII.39b) \quad \left| \frac{d^k}{dt^k} D_+^i D_-^m D_0^n \tilde{e}_s \right|_\infty^2 \leq \tilde{Q}_{k,i,m,n},$$

$$(AIII.39c) \quad \left\| \frac{d^k}{dt^k} D_+^i D_-^m D_0^n \tilde{e}_l \right\|^2 \leq Q_{k,i,m,n},$$

$$(AIII.39d) \quad \left| \frac{d^k}{dt^k} D_+^i D_-^m D_0^n \tilde{e}_l \right|_\infty^2 \leq \tilde{Q}_{k,i,m,n},$$

Proof of Theorem AIII.21:

We derive these bounds from the bounds $\underline{\tilde{p}}_s$ and $\underline{\tilde{p}}_l$ satisfy because \tilde{e}_s and \tilde{e}_l are the first components of these vectors.

We then want to study the system (AIII.31), discretized in time with the Crank-Nicholson scheme, which reads

$$\frac{\hat{\underline{p}}_{sj}^{n+1} - \hat{\underline{p}}_{sj}^n}{\tau} = \frac{1}{2} D_+^x D_-^x (\hat{\underline{p}}_{sj}^{n+1} + \hat{\underline{p}}_{sj}^n)$$

$$(AIII.40a) \quad + \frac{1}{4} \begin{bmatrix} 0 & \hat{v}_{sj}^{n+1} + \hat{v}_{sj}^n \\ 0 & -D_0^x (\hat{v}_{sj}^{n+1} + \hat{v}_{sj}^n) \end{bmatrix} A_{02} (\hat{p}_{s0}^{n+1} + \hat{p}_{s0}^n - \hat{p}_{l0}^{n+1} - \hat{p}_{l0}^n) \\ + \frac{1}{2} \begin{bmatrix} \hat{f}_{sj}^{n+1} + \hat{f}_{sj}^n \\ -D_0^x (\hat{f}_{sj}^{n+1} + \hat{f}_{sj}^n) \end{bmatrix},$$

$$(AIII.40b) \quad \frac{\hat{p}_{lj}^{n+1} - \hat{p}_{lj}^n}{\tau} = \frac{1}{2} D_+^x D_-^x (\hat{p}_{lj}^{n+1} + \hat{p}_{lj}^n) \\ + \frac{1}{4} \begin{bmatrix} 0 & \hat{v}_{lj}^{n+1} + \hat{v}_{lj}^n \\ 0 & D_0^x (\hat{v}_{lj}^{n+1} + \hat{v}_{lj}^n) \end{bmatrix} A_{02} (\hat{p}_{s0}^{n+1} + \hat{p}_{s0}^n - \hat{p}_{l0}^{n+1} - \hat{p}_{l0}^n) \\ + \frac{1}{2} \begin{bmatrix} \hat{f}_{lj}^{n+1} + \hat{f}_{lj}^n \\ D_0^x (\hat{f}_{lj}^{n+1} + \hat{f}_{lj}^n) \end{bmatrix},$$

$$(AIII.40c) \quad \begin{bmatrix} 0 & 0 \\ 0 & -1 \end{bmatrix} D_+^x (\hat{p}_{s0}^{n+1} + \hat{p}_{s0}^n) \\ + \frac{1}{2} \begin{bmatrix} 2 & 0 \\ 0 & A_{02} (\hat{v}_{s0}^{n+1} + \hat{v}_{s0}^n) \end{bmatrix} A_{02} (\hat{p}_{s0}^{n+1} + \hat{p}_{s0}^n - \hat{p}_{l0}^{n+1} - \hat{p}_{l0}^n) \\ = \begin{bmatrix} 0 \\ A_{02} (\hat{f}_{s0}^{n+1} + \hat{f}_{s0}^n) \end{bmatrix},$$

$$(AIII.40d) \quad \begin{bmatrix} 0 & 0 \\ 0 & 1 \end{bmatrix} D_+^x (\hat{p}_{l0}^{n+1} + \hat{p}_{l0}^n) \\ + \frac{1}{2} \begin{bmatrix} 2 & 0 \\ 0 & A_{02} (\hat{v}_{l0}^{n+1} + \hat{v}_{l0}^n) \end{bmatrix} A_{02} (\hat{p}_{s0}^{n+1} + \hat{p}_{s0}^n - \hat{p}_{l0}^{n+1} - \hat{p}_{l0}^n) \\ = \begin{bmatrix} 0 \\ A_{02} (\hat{f}_{l0}^{n+1} + \hat{f}_{l0}^n) \end{bmatrix},$$

$$(AIII.40e) \quad \hat{p}_{sj}^0 = \tilde{g}_{sj},$$

$$(AIII.40f) \quad \hat{p}_{lj}^0 = \tilde{g}_{lj},$$

$$(AIII.40g) \quad \hat{p}_{sj}^n \rightarrow 0 \quad \text{as } j \rightarrow \infty,$$

$$(AIII.40h) \quad \hat{p}_{lj}^n \rightarrow 0 \quad \text{as } j \rightarrow \infty.$$

We derive results for the vectors \hat{p}_s and \hat{p}_l similar to those of section 6 of chapter I.

Lemma AIII.22.

Under the assumptions that T_s , f_s , and their derivatives on $(-\infty, 0] \times [0, T]$, and that g_s and its derivatives on $(-\infty, 0]$, that T_l , f_l , and their derivatives on $[0, \infty) \times [0, T]$, and g_l and its derivatives on $[0, \infty)$ are smooth and bounded, we have

$$(AIII.41a) \quad \|\hat{p}_s^n\|^2 \leq \hat{R}^n,$$

$$(AIII.41b) \quad \|\hat{p}_l^n\|^2 \leq \hat{R}^n,$$

where

$$\begin{aligned}
 \hat{R}^n &= e^{L \ n \ \tau} \left(\|\tilde{g}_s\|^2 + \|\mathcal{D}_0^x \tilde{g}_s\|^2 + \|\tilde{g}_l\|^2 + \|\mathcal{D}_0^x \tilde{g}_l\|^2 \right) \\
 &+ \frac{1}{4} C_4 \tau \sum_{k=0}^{n-1} e^{L \ (k+1/2) \ \tau} \left(|\hat{f}_{s0}^{n-k}|^2 + |\hat{f}_{s0}^{n-k-1}|^2 + |\hat{f}_{s1}^{n-k}|^2 \right. \\
 &+ |\hat{f}_{s1}^{n-k-1}|^2 + |\hat{f}_{l0}^{n-k}|^2 + |\hat{f}_{l0}^{n-k-1}|^2 + |\hat{f}_{l1}^{n-k}|^2 + |\hat{f}_{l1}^{n-k-1}|^2 \left. \right) \\
 &+ \frac{\tau}{4} \sum_{k=0}^{n-1} e^{L \ (k+1/2) \ \tau} \left(\|\hat{f}_s^{n-k}\|^2 + \|\hat{f}_s^{n-k-1}\|^2 + \|\mathcal{D}_0^x \hat{f}_s^{n-k}\|^2 \right. \\
 &+ \|\mathcal{D}_0^x \hat{f}_s^{n-k-1}\|^2 + \|\hat{f}_l^{n-k}\|^2 + \|\hat{f}_l^{n-k-1}\|^2 \\
 &+ \left. \|\mathcal{D}_0^x \hat{f}_l^{n-k}\|^2 + \|\mathcal{D}_0^x \hat{f}_l^{n-k-1}\|^2 \right).
 \end{aligned}$$

Proof of Lemma AIII.17:

We take the discrete scalar product of (AIII.40a) with the vector $\hat{p}_s^{n+1} + \hat{p}_s^n$ and add to it the scalar product of (AIII.40b) with the vector $\hat{p}_l^{n+1} + \hat{p}_l^n$. Then we proceed as in the proof of lemma I.6.1.

As in chapter I, we first derive bounds for $\hat{q}_s^n = \mathcal{D}_+^t \hat{p}_s^n$ and $\hat{q}_l^n = \mathcal{D}_+^t \hat{p}_l^n$ in L_2 norm before estimating $\mathcal{D}_+^x \hat{p}_s^n$ and $\mathcal{D}_+^x \hat{p}_l^n$.

Lemma AIII.23.

Under the assumptions that T_s, f_s , and their derivatives on $(-\infty, 0] \times [0, T]$, and that g_s and its derivatives on $(-\infty, 0]$, that T_l, f_l , and their derivatives on $[0, \infty) \times [0, T]$, and g_l and its derivatives on $[0, \infty)$ are smooth and bounded, we have

$$(AIII.42a) \quad \|\hat{q}_s\|^2 \leq \hat{S}^n,$$

$$(AIII.42b) \quad \|\hat{q}_l\|^2 \leq \hat{S}^n,$$

where \hat{S}^n is given by

$$\begin{aligned}
 \hat{S}^n &= e^{Q \ n \ \tau} \left(\|\hat{q}_s^0\|^2 + \|\hat{q}_l^0\|^2 \right) + \frac{\tau}{4} \sum_{k=0}^{n-1} e^{Q \ (k+1/2) \ \tau} \left(\|\hat{f}_s^{n-k}\|^2 \right. \\
 &+ \|\hat{f}_s^{n-k-1}\|^2 + \|\mathcal{D}_0^x \hat{f}_s^{n-k}\|^2 + \|\mathcal{D}_0^x \hat{f}_s^{n-k-1}\|^2 + \|\mathcal{D}_+^t \hat{f}_s^{n-k}\|^2 \\
 &+ \left. \|\mathcal{D}_+^t \hat{f}_s^{n-k-1}\|^2 + \|\mathcal{D}_+^t \mathcal{D}_0^x \hat{f}_s^{n-k}\|^2 + \|\mathcal{D}_+^t \mathcal{D}_0^x \hat{f}_s^{n-k-1}\|^2 + \|\hat{f}_l^{n-k}\|^2 \right. \\
 &+ \left. \|\hat{f}_l^{n-k-1}\|^2 + \|\mathcal{D}_0^x \hat{f}_l^{n-k}\|^2 + \|\mathcal{D}_0^x \hat{f}_l^{n-k-1}\|^2 + \|\mathcal{D}_+^t \hat{f}_l^{n-k}\|^2 \right. \\
 &+ \left. \|\mathcal{D}_+^t \hat{f}_l^{n-k-1}\|^2 + \|\mathcal{D}_+^t \mathcal{D}_0^x \hat{f}_l^{n-k}\|^2 + \|\mathcal{D}_+^t \mathcal{D}_0^x \hat{f}_l^{n-k-1}\|^2 + \|\hat{f}_l^{n-k}\|^2 \right)
 \end{aligned}$$

$$\begin{aligned}
& + \| \hat{f}_l^{n-k-1} \|^2 + \| D_0^x \hat{f}_l^{n-k} \|^2 + \| D_0^x \hat{f}_l^{n-k-1} \|^2 + \| D_+^t \hat{f}_l^{n-k} \|^2 \\
& + \| D_+^t \hat{f}_l^{n-k-1} \|^2 + \| D_+^t D_0^x \hat{f}_l^{n-k} \|^2 + \| D_+^t D_0^x \hat{f}_l^{n-k-1} \|^2 \\
& + \frac{D_5 \tau}{4} \sum_{k=0}^{n-1} e^{Q(k+1/2)\tau} \left(| \hat{f}_{s0}^{n-k} |^2 + | \hat{f}_{s0}^{n-k-1} |^2 + | \hat{f}_{s1}^{n-k} |^2 + | \hat{f}_{s1}^{n-k-1} |^2 \right. \\
& \left. + | \hat{f}_{l0}^{n-k} |^2 + | \hat{f}_{l0}^{n-k-1} |^2 + | \hat{f}_{l1}^{n-k} |^2 + | \hat{f}_{l1}^{n-k-1} |^2 \right) \\
& + \frac{D_6 \tau}{4} \sum_{k=0}^{n-1} e^{Q(k+1/2)\tau} \left(| D_+^t \hat{f}_{s0}^{n-k} |^2 + | D_+^t \hat{f}_{s0}^{n-k-1} |^2 + | D_+^t \hat{f}_{s1}^{n-k} |^2 \right. \\
& \left. + | D_+^t \hat{f}_{s1}^{n-k-1} |^2 + | D_+^t \hat{f}_{l0}^{n-k} |^2 + | D_+^t \hat{f}_{l0}^{n-k-1} |^2 + | D_+^t \hat{f}_{l1}^{n-k} |^2 \right. \\
& \left. + | D_+^t \hat{f}_{l1}^{n-k-1} |^2 \right) + Q \tau \sum_{k=0}^{n+1} e^{Q(k+1/2)\tau} \hat{R}^{n+1-k} + \sum_{k=0}^n e^{Q\tau} \hat{R}^{n-k}.
\end{aligned}$$

Proof of Lemma AIII.23:

We evaluate the discrete scalar product of (AIII.40a) with $\hat{\underline{p}}_s^{n+1} + \hat{\underline{p}}_s^n$, we add to it the scalar product of (AIII.40b) with $\hat{\underline{p}}_l^{n+1} + \hat{\underline{p}}_l^n$, the discrete scalar product of the equivalent of (AIII.40a) for $\hat{\underline{q}}_s^n$ with $\hat{\underline{q}}_s^{n+1} + \hat{\underline{q}}_s^n$, and the discrete scalar product of the equivalent of (AIII.40b) for $\hat{\underline{q}}_l^n$ and $\hat{\underline{q}}_l^{n+1} + \hat{\underline{q}}_l^n$. We then proceed as in the proof of lemma I.6.2.

Because we have estimated the functions $\hat{\underline{p}}_s^n$, $\hat{\underline{p}}_l^n$, $\hat{\underline{q}}_s^n$, and $\hat{\underline{q}}_l^n$, we then bound $D_+^x \hat{\underline{p}}_s^n$ and $D_+^x \hat{\underline{p}}_l^n$ in L_2 norm.

Lemma AIII.24.

Under the assumptions that T_s, f_s , and their derivatives on $(-\infty, 0] \times [0, T]$, and that g_s and its derivatives on $(-\infty, 0]$, that T_l, f_l , and their derivatives on $[0, \infty) \times [0, T]$, and g_l and its derivatives on $[0, \infty)$ are smooth and bounded, we have

$$(AIII.43a) \quad \| D_+^x \hat{\underline{p}}_s \|^2 \leq \hat{X}^n,$$

$$(AIII.43b) \quad \| D_+^x \hat{\underline{p}}_l \|^2 \leq \hat{X}^n,$$

where

$$\hat{X}^n = 2 \left(\| D_+^x \tilde{g}_s \|^2 + \| D_+^x \tilde{g}_l \|^2 \right) + 8(L+1) \sum_{k=0}^{n-1} \hat{R}^k + 4(L+1) \hat{R}^n$$

$$\begin{aligned}
& + 4 \sum_{k=0}^{n-1} \hat{S}^k + 2 C_4 \sum_{k=0}^{n-1} \left(| \hat{f}_{s0}^k |^2 + | \hat{f}_{s0}^{k+1} |^2 + | \hat{f}_{s1}^k |^2 \right. \\
& \left. + | \hat{f}_{s1}^{k+1} |^2 + | \hat{f}_{l0}^k |^2 + | \hat{f}_{l0}^{k+1} |^2 + | \hat{f}_{l1}^k |^2 + | \hat{f}_{l1}^{k+1} |^2 \right) \\
& + 2 \sum_{k=0}^{n-1} \left(\| \hat{f}_s^k \|^2 + \| \hat{f}_s^{k+1} \|^2 + \| D_0^x \hat{f}_s^k \|^2 + \| D_0^x \hat{f}_s^{k+1} \|^2 \right. \\
& \left. + \| \hat{f}_l^k \|^2 + \| \hat{f}_l^{k+1} \|^2 + \| D_0^x \hat{f}_l^k \|^2 + \| D_0^x \hat{f}_l^{k+1} \|^2 \right).
\end{aligned}$$

Proof of Lemma AIII.24:

It is identical to the proof of lemma I.6.3.

As in chapter I, we derive bounds for the functions \hat{p}_s^n , \hat{p}_l^n , \hat{q}_s^n , and \hat{q}_l^n in maximum norm because we have bounded the functions \hat{p}_s^n , \hat{p}_l^n , \hat{q}_s^n , \hat{q}_l^n , $D_+^x \hat{p}_s^n$, $D_+^x \hat{p}_l^n$, $D_+^x \hat{q}_s^n$, and $D_+^x \hat{q}_l^n$ in L_2 norm.

Lemma AIII.25.

Under the assumptions that T_s , f_s , and their derivatives on $(-\infty, 0] \times [0, T]$, and that g_s and its derivatives on $(-\infty, 0]$, that T_l , f_l , and their derivatives on $[0, \infty) \times [0, T]$, and g_l and its derivatives on $[0, \infty)$ are smooth and bounded, we have

$$(AIII.44a) \quad | \hat{p}_s^n |_\infty^2 \leq 2 \left[\hat{R}^n \right]^{\frac{1}{2}} \left[\hat{X}^n \right]^{\frac{1}{2}},$$

$$(AIII.44b) \quad | \hat{q}_s^n |_\infty^2 \leq 2 \left[\hat{S}^n \right]^{\frac{1}{2}} \left[\hat{Z}^n \right]^{\frac{1}{2}},$$

$$(AIII.44c) \quad | \hat{p}_l^n |_\infty^2 \leq 2 \left[\hat{R}^n \right]^{\frac{1}{2}} \left[\hat{X}^n \right]^{\frac{1}{2}},$$

$$(AIII.44d) \quad | \hat{q}_l^n |_\infty^2 \leq 2 \left[\hat{S}^n \right]^{\frac{1}{2}} \left[\hat{Z}^n \right]^{\frac{1}{2}},$$

where \hat{Z}^n is an upper bound for $\| D_+^x \hat{q}_s^n \|^2$ and $\| D_+^x \hat{q}_l^n \|^2$.

Proof of Lemma AIII.25:

We derive (AIII.44a) from (I.5.10), (AIII.41a), and (AIII.43a), (AIII.44b) from (I.5.10), (AIII.42a), and the equivalent of (AIII.43a) for \hat{q}_s^n , (AIII.44c) from (I.5.10), (AIII.41b), and (AIII.43b), and (AIII.44d) from (I.5.10), (AIII.42b), and the equivalent of (AIII.43b) for \hat{q}_l^n .

We also need to bound the functions $D_-^x \hat{p}_s^n$ and $D_-^x \hat{p}_l^n$ in L_2 norm.

Lemma AIII.26.

Under the assumptions that T_s, f_s , and their derivatives on $(-\infty, 0] \times [0, T]$, and that g_s and its derivatives on $(-\infty, 0]$, that T_l, f_l , and their derivatives on $[0, \infty) \times [0, T]$, and g_l and its derivatives on $[0, \infty)$ are smooth and bounded, we have

$$(AIII.45a) \quad \| D_-^x \hat{p}_s^n \|^2 \leq \hat{Y}^n,$$

$$(AIII.45b) \quad \| D_-^x \hat{p}_l^n \|^2 \leq \hat{Y}^n,$$

where

$$\begin{aligned} \hat{Y}^n = & M \hat{X}^n + \tilde{M} \hat{R}^n + M_0 \hat{S}^n + \tilde{M}_0 \hat{Z}^n \\ & + M_1 W^n + M_2 \left(| \hat{f}_{s0}^n |^2 + | \hat{f}_{s1}^n |^2 + | \hat{f}_{l0}^n |^2 + | \hat{f}_{l1}^n |^2 \right), \end{aligned}$$

and where $\hat{X}^n, \hat{R}^n, \hat{S}^n, \hat{Z}^n$, and \hat{W}^n are the estimates for $\| D_+^x \hat{p}_s^n \|^2$ and $\| D_+^x \hat{p}_l^n \|^2$, $\| \hat{p}_s^n \|^2$ and $\| \hat{p}_l^n \|^2$, $\| \hat{q}_s^n \|^2$ and $\| \hat{q}_l^n \|^2$, $\| D_+^x \hat{q}_s^n \|^2$ and $\| D_+^x \hat{q}_l^n \|^2$, and $\| (D_+^x)^2 \hat{p}_s^n \|^2$ and $\| (D_+^x)^2 \hat{p}_l^n \|^2$. $M, \tilde{M}, M_0, \tilde{M}_0, M_1$, and M_2 are constants depending on the initial conditions and the coefficients of the difference operator.

Proof of Lemma AIII.26:

The proof is identical to the proof of lemma AIII.18.

Because we have estimated the functions $D_+^x \hat{p}_s^n, D_+^x \hat{p}_l^n, D_-^x \hat{p}_s^n$, and $D_-^x \hat{p}_l^n$, we get bounds for the functions $D_0^x \hat{p}_s^n$ and $D_0^x \hat{p}_l^n$ in L_2 norm.

Lemma AIII.27.

Under the assumptions that T_s, f_s , and their derivatives on $(-\infty, 0] \times [0, T]$, and that g_s and its derivatives on $(-\infty, 0]$, that T_l, f_l , and their derivatives on $[0, \infty) \times [0, T]$, and g_l and its derivatives on $[0, \infty)$ are smooth and bounded, we have

$$(AIII.46a) \quad \| D_0^x \hat{p}_s^n \|^2 \leq \frac{1}{2} \hat{X}^n + \frac{1}{2} \hat{Y}^n,$$

$$(AIII.46b) \quad \| D_0^x \hat{p}_l^n \|^2 \leq \frac{1}{2} \hat{X}^n + \frac{1}{2} \hat{Y}^n.$$

Proof of Lemma AIII.27:

The proof is identical to the proof of lemma AIII.19.

We will get estimates for all order divided differences of the functions \hat{p}_s^n and \hat{p}_l^n , both in L_2 and maximum norms.

Theorem AIII.28.

Under the assumptions that T_s, f_s , and their derivatives on $(-\infty, 0] \times [0, T]$, and that g_s and its derivatives on $(-\infty, 0]$, that T_l, f_l , and their derivatives on $[0, \infty) \times [0, T]$, and g_l and its derivatives on $[0, \infty)$ are smooth and bounded, we have

$$(AIII.47a) \quad \left\| (D_+^t)^k (D_+^x)^j (D_-^x)^m (D_0^x)^i \hat{p}_s^n \right\|^2 \leq I_{k,j,m,i},$$

$$(AIII.47b) \quad \left| (D_+^t)^k (D_+^x)^j (D_-^x)^m (D_0^x)^i \hat{p}_s^n \right|_\infty^2 \leq \tilde{I}_{k,j,m,i},$$

$$(AIII.47c) \quad \left\| (D_+^t)^k (D_+^x)^j (D_-^x)^m (D_0^x)^i \hat{p}_l^n \right\|^2 \leq I_{k,j,m,i},$$

$$(AIII.47d) \quad \left| (D_+^t)^k (D_+^x)^j (D_-^x)^m (D_0^x)^i \hat{p}_l^n \right|_\infty^2 \leq \tilde{I}_{k,j,m,i}.$$

Proof of Theorem AIII.28:

We derive (AIII.47a), (AIII.47b), (AIII.47c), and (AIII.47d) immediately from lemmas AIII.23, AIII.24, AIII.25, and AIII.26 and the equations \hat{p}_s^n and \hat{p}_l^n satisfy.

What we were initially interested in was to bound all divided differences of \hat{e}_s^n and \hat{e}_l^n both in L_2 and maximum norms.

Theorem AIII.29.

Under the assumptions that T_s, f_s , and their derivatives on $(-\infty, 0] \times [0, T]$, and that g_s and its derivatives on $(-\infty, 0]$, that T_l, f_l , and their derivatives on $[0, \infty) \times [0, T]$, and g_l and its derivatives on $[0, \infty)$ are smooth and bounded, we have

$$(AIII.48a) \quad \left\| (D_+^t)^k (D_+^x)^j (D_-^x)^m (D_0^x)^i \hat{e}_s^n \right\|^2 \leq I_{k,j,m,i},$$

$$(AIII.48b) \quad \left| (D_+^t)^k (D_+^x)^j (D_-^x)^m (D_0^x)^i \hat{e}_s^n \right|_\infty^2 \leq \tilde{I}_{k,j,m,i},$$

$$(AIII.48c) \quad \left\| (D_+^t)^k (D_+^x)^j (D_-^x)^m (D_0^x)^i \hat{e}_l^n \right\|^2 \leq I_{k,j,m,i},$$

$$(AIII.48d) \quad \left| (D_+^t)^k (D_+^x)^j (D_-^x)^m (D_0^x)^i \hat{e}_l^n \right|_\infty^2 \leq \tilde{I}_{k,j,m,i}.$$

Proof of Theorem AIII.29:

We deduce (AIII.48a), (AIII.48b), (AIII.48c), and (AIII.48d) from (AIII.47a), (AIII.47b), (AIII.47c), and (AIII.47d), because the functions \hat{e}_s^n and \hat{e}_l^n are the first components of the vectors \hat{p}_s^n and \hat{p}_l^n .

Then we derive a final result for the nonlinear system, equivalent to theorem I.7.2 of section 7 of chapter I.

Theorem AIII.30.

Under the assumptions that f_s and its derivatives on $(-\infty, 0] \times [0, T]$, that g_s and its derivatives on $(-\infty, 0]$, that f_l and its derivatives on $[0, \infty) \times [0, T]$, and that g_l and its derivatives on $[0, \infty)$ are smooth and bounded, that (AIII.1) is discretized in space with a centered second order finite differences scheme, in time with Crank-Nicholson scheme, then T_s and its derivatives on $(-\infty, 0] \times [0, T]$ and T_l and its derivatives on $[0, \infty) \times [0, T]$ are smooth and bounded, and

$$(AIII.49a) \quad \| T_s - \hat{T}_s - h^2 \hat{e}_s^0 - h^3 \hat{e}_s^1 - h^4 \hat{e}_s^2 \| \leq N h^5,$$

$$(AIII.49b) \quad | T_s - \hat{T}_s - h^2 \hat{e}_s^0 |_\infty \leq \tilde{N} h^3,$$

$$(AIII.49c) \quad \| T_l - \hat{T}_l - h^2 \hat{e}_l^0 - h^3 \hat{e}_l^1 - h^4 \hat{e}_l^2 \| \leq N h^5,$$

$$(AIII.49d) \quad | T_l - \hat{T}_l - h^2 \hat{e}_l^0 |_\infty \leq \tilde{N} h^3,$$

where \hat{T}_s and \hat{T}_l are the solutions of (AIII.1) discretized in space with a centered second order finite difference scheme and in time with Crank-Nicholson scheme, \hat{e}_s^0 , \hat{e}_s^1 , \hat{e}_s^2 , \hat{e}_l^0 , \hat{e}_l^1 , and \hat{e}_l^2 are defined as in section 7 of chapter I.

APPENDIX IV

GENERALIZATION TO A CENTERED FOURTH-ORDER FINITE DIFFERENCE SCHEME IN SPACE

In this appendix, we would like to indicate the differences in obtaining estimates for a discretization with a centered second-order finite difference scheme in space and a centered fourth-order one. At the end of this section, we will present a few remarks concerning the $2m$ th-order scheme because the details of the proof for a fourth-order scheme are similar to those for any $2m$ th-order scheme, $m > 2$. As in appendix II, we will study the heat equation with inhomogeneous Dirichlet boundary conditions and with Neumann boundary conditions because lower order terms do not fundamentally change the final estimates. Nevertheless, we will point out the modifications to the proof required to take into account lower order terms. Then we will apply these results to the system (I.5.3) discretized with a centered fourth-order finite difference scheme in space, the equivalent of (I.5.4) for the two-sided problem. The function \tilde{p} satisfies

$$(AIV.1a) \quad \frac{\partial}{\partial t} \tilde{p}_j(t) = D_{24} \tilde{p}_j(t) + \begin{bmatrix} 0 & \tilde{v}_j(t) \\ 0 & D_{14} \tilde{v}_j(t) \end{bmatrix} A_{04}^* \tilde{p}_0(t) + \begin{bmatrix} \tilde{f}_j(t) \\ D_{14} \tilde{f}_j(t) \end{bmatrix}, \quad j = 1, 2, \dots$$

$$(AIV.1b) \quad \begin{bmatrix} 0 & 0 \\ 0 & 1 \end{bmatrix} D_{14}^* \tilde{p}_0(t) + \begin{bmatrix} 1 & 0 \\ 0 & A_{04}^* \tilde{v}_0(t) \end{bmatrix} A_{04}^* \tilde{p}_0(t) = \begin{bmatrix} 0 \\ A_{04} \tilde{f}_0(t) \end{bmatrix},$$

$$(AIV.1c) \quad \begin{bmatrix} 0 & 0 \\ 0 & 1 \end{bmatrix} D_{32}^* \tilde{p}_0(t) + \begin{bmatrix} 0 & 0 \\ 0 & A_{02} \tilde{v}_0(t) \end{bmatrix} D_{22}^* \tilde{p}_0(t) + \begin{bmatrix} 1 & A_{02} \tilde{v}_0(t) \\ 0 & \frac{d}{dt} A_{02} \tilde{v}_0(t) + A_{02} \tilde{v}_0(t) D_+ \tilde{v}_0(t) \end{bmatrix} A_{02} \tilde{p}_0(t) = \begin{bmatrix} \frac{d}{dt} A_{02} \tilde{f}_0(t) - A_{02} \tilde{f}_0(t) \\ D_+ \tilde{f}_0(t) - D_{22}^* \tilde{f}_0(t) - A_{02} \tilde{v}_0(t) D_+ \tilde{f}_0(t) \end{bmatrix},$$

$$(AIV.1d) \quad \tilde{p}_j(0) = \tilde{g}_j, \quad j = 0, 1, \dots$$

$$(AIV.1e) \quad \tilde{p}_j(t) \rightarrow 0 \quad \text{as } j \rightarrow \infty,$$

where the finite difference operators D_{24} , D_{14} , and A_{02} are those defined in sections

2 and 8 of chapter I. The operators D_{22}^* , D_{32}^* , and A_{04} are

$$\begin{aligned} D_{22}^* v_0 &= D_+ D_0 v_0 \sim v_{xx} (0), \\ D_{32}^* v_0 &= D_+^2 D_- v_0 \sim v_{xxx} (0), \\ A_{04} v_0 &= \frac{1}{16} (-v_2 + 9 v_1 + 9 v_0 - v_{-1}) \sim v (0). \end{aligned}$$

The fourth-order scheme is a five point scheme. So (AIV.1b) does not provide all the boundary conditions or equations needed to solve (AIV.1). We will need another boundary condition. In [18], Kreiss explains different techniques that can be used to derive some extra boundary conditions for ordinary differential equations. These results apply to the case considered here, but won't be useful for the fully discrete system we will consider later on. The way we have decided to supply this extra boundary condition is by taking the boundary condition of the continuous problem, differentiating it with respect to time, replacing time derivatives by space derivatives, by taking into account the partial differential equation, and then discretizing it with a centered second-order scheme. This approach leads to equation (AIV.1c).

We then derive the equivalent of lemma AII.1 of appendix II for the fourth-order case, for the heat equation with Dirichlet boundary conditions, which satisfies

$$\begin{aligned} \text{(AIV.2a)} \quad & \frac{\partial}{\partial t} y_j (t) = D_{24} y_j (t) \quad j = 1, \dots, \\ \text{(AIV.2b)} \quad & A_{04} y_0 (t) = f (t), \\ \text{(AIV.2c)} \quad & D_{22}^* y_0 (t) = \frac{d}{dt} f (t), \\ \text{(AIV.2d)} \quad & y_j (0) = g_j, \quad j = -1, \dots \\ \text{(AIV.2e)} \quad & y_j (t) \rightarrow 0 \quad \text{as } j \rightarrow \infty. \end{aligned}$$

So y satisfies the bound in the L_2 -norm given by

Lemma AIV.1.

Under the assumptions that f and its derivatives are smooth and bounded on $[0, T]$, and that g and its divided differences are bounded, we have

$$\begin{aligned} \text{(AIV.3)} \quad & \| y \|^2 \leq 2 \int_0^t e^{(t-\tau)} \| F(\tau) \|^2 d\tau \\ & + 2 e^t \left(\| k \|^2 + |k_0|^2 + |k_{-1}|^2 \right) + 2 |f(t)|^2 \| \Lambda \|^2, \end{aligned}$$

where

$$\begin{aligned} F_j(t) &= f(t)D_{24} \Lambda_j - f'(t) \Lambda_j \quad j = 1, \dots, \\ \Lambda_j &= e^{-(j-1/2)^2 h^2} \quad j = -1, \dots, \\ k_j &= g_j - f(0) \Lambda_j \quad j = -1, \dots \end{aligned}$$

The scalar product (\cdot, \cdot) and the norm $\| \cdot \|$ are identical to the ones from appendix II. As in chapter I, we have assumed that the functions are real valued.

Proof of Lemma AIV.1:

Because the Dirichlet boundary conditions for (AIV.2) are inhomogeneous, we cannot estimate the function y immediately. Instead we introduce a new function, z , given by $z_j = y_j - f(t) \Lambda_j$, which satisfies fourth-order homogeneous boundary conditions at $x = 0$ and the evolution equation

$$\begin{aligned} \text{(AIV.4a)} \quad & \frac{\partial}{\partial t} z_j(t) = D_{24} z_j(t) + F_j(t) \quad j = 1, \dots, \\ \text{(AIV.4b)} \quad & A_{04} z_0(t) = 0, \\ \text{(AIV.4c)} \quad & D_{22}^* z_0(t) = 0, \\ \text{(AIV.4d)} \quad & z_j(0) = k_j \quad j = -1, \dots, \\ \text{(AIV.4e)} \quad & z_j(t) \rightarrow 0 \quad \text{as } j \rightarrow \infty. \end{aligned}$$

We first take the scalar product of z with (AIV.4a). Then by summing the term $(z, D_{24} z)$ by parts and using the Cauchy-Schwarz inequality, we get

$$\begin{aligned} \frac{d}{dt} \|z\|^2 &\leq -\frac{h^2}{6} \|D_+ D_- z\|^2 - 2 \|D_+ z\|^2 + \|z\|^2 + \|F\|^2 \\ \text{(AIV.5a)} \quad & -\frac{2}{h} z_1(z_1 - z_0) - \frac{1}{6h} (z_{-1} z_1 - z_0 z_2 - z_1^2 + z_0^2), \\ \text{(AIV.5b)} \quad & \leq \|z\|^2 + \|F\|^2. \end{aligned}$$

The summation by parts we carry out in this case is a little more tedious than the one considered in the second-order case, because

$$\begin{aligned} 12(z, D_{24} z) &= \frac{1}{h} \sum_{k=1}^{\infty} z_k (-z_{k+2} + 16 z_{k+1} - 30 z_k + 16 z_{k-1} - z_{k-2}), \\ &= -\frac{2}{h} \sum_{k=1}^{\infty} z_{k-1} z_{k+1} + \frac{1}{h} (z_0 z_2 - z_{-1} z_1) + \frac{28}{h} \sum_{k=1}^{\infty} z_{k+1} z_k \end{aligned}$$

$$\begin{aligned}
 & + \frac{4}{h} \sum_{k=1}^{\infty} z_k z_{k-1} - \frac{12}{h} z_1 (z_1 - z_0) - \frac{13}{h} \sum_{k=1}^{\infty} z_{k+1}^2 \\
 & - \frac{16}{h} \sum_{k=1}^{\infty} z_k^2 - \frac{1}{h} \sum_{k=2}^{\infty} z_{k-1}^2 + \frac{1}{h} (z_1^2 - z_0^2), \\
 & = -\frac{1}{h} \sum_{k=1}^{\infty} (z_{k+1} - 2 z_k + z_{k-1})^2 - \frac{12}{h} \sum_{k=1}^{\infty} (z_{k+1} - z_k)^2 \\
 & + \frac{1}{h} (z_0 z_2 - z_1 z_{-1} - 12 z_1 (z_1 - z_0) + z_1^2 - z_0^2).
 \end{aligned}$$

Then we will bound the term $(z_0 z_2 - z_{-1} z_1 - 12 z_1 (z_1 - z_0) + z_1^2 - z_0^2)/h$ independently of h . The boundary conditions tell

$$\begin{aligned}
 z_{-1} + z_2 &= 0, \\
 z_0 + z_1 &= 0.
 \end{aligned}$$

So the term $(z_0 z_2 - z_{-1} z_1 - 12 z_1 (z_1 - z_0) + z_1^2 - z_0^2)/h = -24 z_1^2/h$. From this, we easily deduce (AIV.5b).

The Gronwall-Bellman inequality applied to (AIV.5b) gives

$$\text{(AIV.6)} \quad \| z \|^2 \leq \int_0^t e^{(t-\tau)} \| F(\tau) \|^2 d\tau + e^t (\| k \|^2 + |k_0|^2 + |k_{-1}|^2).$$

The triangle inequality and the relation

$$(a + b)^2 \leq 2 (a^2 + b^2),$$

lead to (AIV.3).

We want to prove the equivalent of lemma AII.2. So the other system to consider is

$$\text{(AIV.7a)} \quad \frac{\partial}{\partial t} r_j(t) = D_{24} r_j(t) \quad j = 1, \dots,$$

$$\text{(AIV.7b)} \quad D_{14}^* r_0(t) = c(t) A_{04} r_0(t) + f(t),$$

$$\text{(AIV.7c)} \quad D_{32}^* r_0(t) = c(t) D_{22}^* r_0(t) + c'(t) A_{02} r_0(t) + f'(t),$$

$$\text{(AIV.7d)} \quad r_j(0) = g_j \quad j = -1, \dots,$$

$$\text{(AIV.7e)} \quad r_j(t) \rightarrow 0 \quad \text{as } j \rightarrow \infty.$$

This leads to

Lemma AIV.2.

Under the assumptions that f and c and their derivatives are smooth and bounded on $[0, T]$, and that g and its divided differences are bounded, we have

$$(AIV.8) \quad \begin{aligned} \| r \|^2 &\leq \int_0^t e^{M(t-\tau)} \left(C | f(\tau) |^2 + \tilde{C} | f'(\tau) |^2 \right) d\tau \\ &+ e^{Mt} \left(\| g \|^2 + | g_0 |^2 + | g_{-1} |^2 \right). \end{aligned}$$

Proof of Lemma AIV.2:

The computation of (r, r_t) gives, summing the term $(r, D_{24} r)$ by parts

$$(AIV.9) \quad \begin{aligned} \frac{d}{dt} \| r \|^2 &\leq -\frac{h^2}{6} \| D_+ D_- r \|^2 - 2 \| D_+ r \|^2 \\ &+ \frac{1}{6h} (r_0 r_2 - r_1 r_{-1} - 12 r_1 (r_1 - r_0) + r_1^2 - r_0^2). \end{aligned}$$

As in the case of Dirichlet boundary conditions, we will express now the term

$$\frac{r_0 r_2 - r_{-1} r_1 - 12 r_1 (r_1 - r_0) + r_1^2 - r_0^2}{h}$$

independently of h . Using the boundary conditions for r , we deduce that

$$(AIV.10a) \quad \begin{aligned} \frac{1}{3h} (r_2 - r_{-1}) &= \frac{3h^2}{8} c(t) D_{22} r_0 + \frac{3h^2}{8} c'(t) A_{02} r_0 \\ &+ \frac{3h^2}{8} f'(t) + c(t) A_{04} r_0 + f(t), \end{aligned}$$

$$(AIV.10b) \quad \begin{aligned} \frac{1}{h} (r_1 - r_0) &= \frac{h^2}{24} c(t) D_{22} r_0 + \frac{h^2}{24} c'(t) A_{02} r_0 \\ &+ \frac{h^2}{24} f'(t) + c(t) A_{04} r_0 + f(t), \end{aligned}$$

$$(AIV.10c) \quad | r_{-1} | \leq A_1 | r |_\infty + A_2 | f(t) | + A_3 | f'(t) |, \quad \text{and}$$

$$(AIV.10d) \quad | r_0 | \leq B_1 | r |_\infty + B_2 | f(t) | + B_3 | f'(t) |.$$

We get the first two expressions, (AIV.10a) and (AIV.10b) by linear combination of the boundary conditions (AIV.7b) and (AIV.7c). We obtain the last two, (AIV.10c) and (AIV.10d) by eliminating either r_{-1} or r_0 between (AIV.7b) and (AIV.7c), assuming that c and its derivatives are smooth and bounded so that the coefficients in front of r_1 , r_2 , f , and f' , and the fractions in h are bounded on $[0, h_0]$. We then take the absolute value of these expressions and substitute for the coefficients their maxima on $[0, h_0]$. If we use the inequalities $| r_{-1} |$ and $| r_0 |$ satisfy, for $h \leq h_0$, we can estimate $(r_1 - r_0)/h$ and $(r_2 - r_{-1})/h$, in terms of $| r |_\infty$, $| f(t) |$, and $| f'(t) |$

$$(AIV.11a) \quad \left| \frac{1}{h} (r_1 - r_0) \right| \leq C_1 | r |_\infty + C_2 | f(t) | + C_3 | f'(t) |,$$

$$(AIV.11b) \quad \left| \frac{1}{h} (r_2 - r_{-1}) \right| \leq D_1 | r |_\infty + D_2 | f(t) | + D_3 | f'(t) |.$$

We notice that the term $(r_0 r_2 - r_{-1} r_1 - 12 r_1 (r_1 - r_0) + r_1^2 - r_0^2)/h$ can be expressed as

$$\frac{12}{h} r_1 (r_1 - r_0) + \frac{1}{h} (r_1 + r_0) (r_1 - r_0) + \frac{1}{h} r_0 (r_2 - r_{-1}) + \frac{1}{h} r_{-1} (r_1 - r_0),$$

and is bounded in absolute value by

$$(AIV.12) \quad E_1 |r|_{\infty}^2 + E_2 |f(t)|^2 + E_3 |f'(t)|^2.$$

After having substituted it in the inequality (AIV.9), we get the upper bound for the term $(r_0 r_2 - r_{-1} r_1 - 12 r_1 (r_1 - r_0) + r_1^2 - r_0^2)$ where we also take into consideration the discrete Sobolev's inequality (I.5.10)

$$(AIV.13) \quad \begin{aligned} \frac{d}{dt} \|r\|^2 &\leq -\frac{h^2}{6} \|D_+ D_- r\|^2 + (-2 + E_1 \epsilon) \|D_+ r\|^2 \\ &+ \frac{E_1}{\epsilon} \|r\|^2 + C |f(t)|^2 + \tilde{C} |f'(t)|^2. \end{aligned}$$

As in appendix II, we choose ϵ such that $-2 + E_1 \epsilon = 0$. Then the constant M is fixed and we obtain (AIV.8) if we apply the Gronwall-Bellman inequality to

$$(AIV.14) \quad \frac{d}{dt} \|r\|^2 \leq M \|r\|^2 + C |f(t)|^2 + \tilde{C} |f'(t)|^2.$$

If there are lower order terms in (AIV.2a) or (AIV.7a), we add either the terms $(y, b D_{14} y)$ and $(y, c y)$ to $(y, D_{24} y)$ in the scalar product (y, y_t) or the terms $(r, b D_{14} r)$ and $(r, c r)$ to $(r, D_{24} r)$ in the scalar product (r, r_t) . If we assume that c is bounded, brute force estimate provides

$$|(y, c y)| \leq |c|_{\infty} \|y\|^2$$

The term $(y, b D_{14} y)$ is more difficult to bound and we will use the boundary conditions. We again assume that b and its divided differences are bounded.

$$\begin{aligned} (y, b D_{14} y) &= h \sum_{k=1}^{\infty} b_j y_j \frac{-y_{k+2} + 8 y_{k+1} - 8 y_{k-1} + y_{k-2}}{12 h}, \\ &= h \sum_{k=1}^{\infty} \frac{b_{k+2} - b_k}{12 h} y_k y_{k+2} + 2 h \sum_{k=1}^{\infty} \frac{b_k - b_{k+1}}{3 h} y_k y_{k+1} \\ &\quad + \frac{1}{12} (b_1 y_{-1} y_1 + b_2 y_0 y_2) + \frac{2}{3} b_1 y_1 y_0, \end{aligned}$$

$$\begin{aligned}
 &= h \sum_{k=1}^{\infty} \frac{b_{k+2} - b_k}{12 h} y_k^2 + h \sum_{k=1}^{\infty} \frac{b_{k+2} - b_k}{6} y_k \frac{y_{k+2} - y_k}{2 h} \\
 &\quad + 2 h \sum_{k=1}^{\infty} \frac{b_k - b_{k+1}}{3 h} y_k^2 + 2 h \sum_{k=1}^{\infty} \frac{b_k - b_{k+1}}{3} y_k \frac{y_{k+1} - y_k}{h} \\
 &\quad + \frac{1}{12} (b_1 y_{-1} y_1 + b_2 y_0 y_2) + \frac{2}{3} b_1 y_1 y_0, \\
 &\leq \frac{1}{6} |D_0 b|_{\infty} \|y\|^2 + \frac{2}{3} |D_+ b|_{\infty} \|y\|^2 + |b|_{\infty} \|y\| \|D_+ y\| \\
 &\quad + \frac{1}{12} (b_1 y_{-1} y_1 + b_2 y_0 y_2) + \frac{2}{3} b_1 y_1 y_0.
 \end{aligned}$$

If the boundary conditions are of homogeneous Dirichlet type, the term

$$\frac{b_1 y_{-1} y_1 + b_2 y_0 y_2}{12} + 2 \frac{b_1 y_1 y_0}{3}$$

is bounded by

$$|b|_{\infty} |y|_{\infty}^2.$$

If the boundary conditions are of Neumann type, the term

$$\frac{b_1 y_{-1} y_1 + b_2 y_0 y_2}{12} + 2 \frac{b_1 y_1 y_0}{3}$$

is bounded by

$$|b|_{\infty} \left(F_1 |y|_{\infty}^2 + F_2 |f(t)|^2 + F_3 |f'(t)|^2 \right).$$

So

$$(y, D_{14} y) \leq \epsilon F \|D_+ y\|^2 + \tilde{F} \|y\|^2 + G |f(t)|^2 + \tilde{G} |f'(t)|^2,$$

where F , \tilde{F} , G , and \tilde{G} depend on ϵ , $|b|_{\infty}$, $|D_0 b|_{\infty}$, and $|D_+ b|_{\infty}$ and other previously defined constants.

Once we have proven those two basic lemmas, we can show that the results stated in theorems (I.5.8) and (I.5.9) are still valid. The procedure and the proofs are identical to the ones of section 5 in chapter I.

If we choose to discretize an equation with a $2m$ th-order scheme, we will need m discrete boundary conditions. We get the first one by discretizing the continuous boundary condition with a $2m$ th-order scheme, the p th one by differentiating the continuous boundary condition with respect to time $p-1$ times, by replacing the time derivatives by space derivatives if we take into account the original continuous equation evaluated at the boundary points, then by discretizing the transformed boundary condition with a $2(m-p+1)$ th-order scheme. All the rest of the algebra carried out for a fourth-order scheme is still valid provided we deal with m discrete boundary conditions instead of 2.

APPENDIX V

NUMERICAL EXAMPLE: THE STEFAN PROBLEM SOLVED IN A FIXED FRAME OF REFERENCE

In this appendix, we would like to describe the numerical method implemented to solve (I.1.2) with the Collatz Mehrstellenverfahren in space and the Crank-Nicholson scheme in time. This method was suggested by Dr. David Brown. We will show that the numerical results confirm the theory developed in chapter I and generalized to the two-phase problem in appendix III. We have shown that in the continuous case the systems (I.1.2) and (I.1.3) are equivalent but we have no reason to believe that this assumption is still valid when we have discretized them with two different schemes in space, even though the schemes are of the same order. As in section 8 of chapter I, we take the diffusion constants and the specific heat per unit of volume to be 1. This method is faster than the method implemented in section 8, because we do not iterate but we use a direct method.

We choose to work on a bounded domain, and we impose Dirichlet boundary conditions at the end points of the domains. We compute the interface position by discretizing (I.1.2c) with a fourth order one-sided difference scheme and we locate the interface position at a mesh point at each time level. Having chosen to discretize the system with the Crank-Nicholson scheme in time, we need to obtain the solution computed on the grid of the previous time level at the grid points of the new time level. We choose to interpolate the solution on the new grid with at least a fourth-order interpolant. For numerical reasons, the solid and the liquid are two different species and the extrapolated solutions of the solid and the liquid at the new interface position differ. We notice that because the length of the interval on which the solution is extrapolated is of the order of the meshsize, we have introduced no numerical instabilities. The numerical results confirm the theory. We numerically implement the following algorithm

$$(AV.1a) \quad y_{j+1}^{n+1} \left(\frac{1}{12} - \frac{\tau}{2 h_1^2} \right) + y_j^{n+1} \left(\frac{5}{6} + \frac{\tau}{h_1^2} \right) + y_{j-1}^{n+1} \left(\frac{1}{12} - \frac{\tau}{2 h_1^2} \right) \quad 1 \leq j \leq J$$

$$= \tilde{y}_{j+1}^n \left(\frac{1}{12} + \frac{\tau}{2 h_1^2} \right) + \tilde{y}_j^n \left(\frac{5}{6} - \frac{\tau}{h_1^2} \right) + \tilde{y}_{j-1}^n \left(\frac{1}{12} + \frac{\tau}{2 h_1^2} \right),$$

$$(AV.1b) \quad y_0^{n+1} = \Delta,$$

$$(AV.1c) \quad y_{j+1}^{n+1} = f_1((n+1)\tau),$$

$$\begin{aligned}
 & z_{k+1}^{n+1} \left(\frac{1}{12} - \frac{\tau}{2 h_2^2} \right) + z_k^{n+1} \left(\frac{5}{6} + \frac{\tau}{h_2^2} \right) + z_{k+1}^{n+1} \left(\frac{1}{12} - \frac{\tau}{2 h_2^2} \right) \quad 1 \leq k \leq K \\
 \text{(AV.1d)} \quad & = \tilde{z}_{k+1}^n \left(\frac{1}{12} + \frac{\tau}{2 h_2^2} \right) + \tilde{z}_k^n \left(\frac{5}{6} - \frac{\tau}{h_2^2} \right) + \tilde{z}_{k-1}^n \left(\frac{1}{12} + \frac{\tau}{2 h_2^2} \right), \\
 \text{(AV.1e)} \quad & z_0^{n+1} = f_2((n+1) \tau), \\
 \text{(AV.1f)} \quad & z_{K+1} = \Delta, \\
 & \tilde{j}^n = \frac{1}{12 h_1} \left(25 \Delta - 48 y_1^n + 36 y_2^n - 16 y_3^n + 3 y_4^n \right) \\
 \text{(AV.1g)} \quad & + \frac{1}{12 h_2} \left(25 \Delta - 48 z_K^n + 36 z_{K-1}^n - 16 z_{K-2}^n + 3 z_{K-3}^n \right), \\
 \text{(AV.1h)} \quad & \tilde{s}^0 = s_0, \\
 \text{(AV.1i)} \quad & \tilde{s}^{n+1} = \tilde{s}^n + \frac{\tau}{24} \left(55 \tilde{j}^n - 59 \tilde{j}^{n-1} + 37 \tilde{j}^{n-2} - 9 \tilde{j}^{n-3} \right) \quad n \geq 3, \\
 & \tilde{y}_j^n = \text{Int} \left(y_{j-2}^n, \tilde{s}^n + (j-2) h_1^0, y_{j-1}^n, \right. \\
 & \quad \left. \tilde{s}^n + (j-1) h_1^0, y_j^n, \tilde{s}^n + j h_1^0, y_{j+1}^n, \tilde{s}^n + (j+1) h_1^0, y_{j+2}^n, \right. \\
 \text{(AV.1j)} \quad & \left. \tilde{s}^n + (j+2) h_1^0, \tilde{s}^{n+1} + j h_1 \right) \quad 2 \leq j \leq J-1, \\
 & \tilde{y}_0^n = \text{Int} \left(\Delta, \tilde{s}^n, y_1^n, \tilde{s}^n + h_1^0, y_2^n, \tilde{s}^n + 2 h_1^0, \right. \\
 \text{(AV.1k)} \quad & \left. y_3^n, \tilde{s}^n + 3 h_1^0, y_4^n, \tilde{s}^n + 4 h_1^0, \tilde{s}^{n+1} \right), \\
 & \tilde{y}_1^n = \text{Int} \left(\Delta, \tilde{s}^n, y_1^n, \tilde{s}^n + h_1^0, y_2^n, \tilde{s}^n + 2 h_1^0, y_3^n, \right. \\
 \text{(AV.1l)} \quad & \left. \tilde{s}^n + 3 h_1^0, y_4^n, \tilde{s}^n + 4 h_1^0, \tilde{s}^{n+1} + h_1^0 \right), \\
 & \tilde{y}_J^n = \text{Int} \left(y_{J-3}^n, B - 4 h_1^0, y_{J-2}^n, B - 3 h_1^0, \right. \\
 \text{(AV.1m)} \quad & \left. y_{J-1}^n, B - 2 h_1^0, y_J^n, B - h_1^0, f_1(n \tau), B, B - h_1 \right), \\
 & \tilde{z}_k^n = \text{Int} \left(z_{k-2}^n, A + (k-2) h_2^0, z_{k-1}^n, A + (k-1) h_2^0, \right. \\
 & \quad \left. z_k^n, A + k h_2^0, z_{k+1}^n, A + (k+1) h_2^0, z_{k+2}^n, \right. \\
 \text{(AV.1n)} \quad & \left. A + (k+2) h_2^0, A + k h_2 \right) \quad 2 \leq k \leq K-1, \\
 & \tilde{z}_1^n = \text{Int} \left(f_2(n \tau), A, z_1^n, A + h_2^0, z_2^n, A + 2 h_2^0, z_3^n, \right. \\
 \text{(AV.1o)} \quad & \left. A + 3 h_2^0, z_4^n, A + 4 h_2^0, A + h_2 \right), \\
 & \tilde{z}_K^n = \text{Int} \left(z_{K-3}^n, \tilde{s}^n - 4 h_2^0, z_{K-2}^n, \tilde{s}^n - 3 h_2^0, z_{K-1}^n, \tilde{s}^n - 2 h_2^0, \right. \\
 \text{(AV.1p)} \quad & \left. z_K^n, \tilde{s}^n - h_2^0, \Delta, \tilde{s}^n, \tilde{s}^{n+1} - h_2 \right), \\
 & \tilde{z}_{K+1}^n = \text{Int} \left(z_{K-3}^n, \tilde{s}^n - 4 h_2^0, z_{K-2}^n, \tilde{s}^n - 3 h_2^0, z_{K-1}^n, \tilde{s}^n - 2 h_2^0, \right. \\
 \text{(AV.1q)} \quad & \left. z_K^n, \tilde{s}^n - h_2^0, \Delta, \tilde{s}^n, \tilde{s}^{n+1} \right), \\
 \text{(AV.1r)} \quad & y_j^0 = u_0 \left(s_0 + j \tilde{h}_1 \right) \quad 0 \leq j \leq J+1, \\
 \text{(AV.1s)} \quad & z_k^0 = v_0 \left(A + k \tilde{h}_2 \right) \quad 0 \leq k \leq K+1,
 \end{aligned}$$

where \tilde{h}_1 , \tilde{h}_2 , h_1 , h_2 , h_1^0 , and h_2^0 are

$$\begin{aligned}\tilde{h}_1 &= \frac{B - s_0}{J + 1}, \\ \tilde{h}_2 &= \frac{A + s_0}{K + 1}, \\ h_1 &= \frac{B - \tilde{s}^{n+1}}{J + 1}, \\ h_2 &= \frac{A + \tilde{s}^{n+1}}{K + 1}, \\ h_1^0 &= \frac{B - \tilde{s}^n}{J + 1}, \\ h_2^0 &= \frac{A + \tilde{s}^n}{K + 1}.\end{aligned}$$

In this example, we have chosen a fourth-order interpolant. A and B are the end points of the domains of computation and we impose Dirichlet boundary conditions there. Because we can compute an analytical solution for the two-sided Stefan problem on a doubly infinite domain, we have decided to compare the numerical solution to the analytical one. We derive the initial and boundary conditions from this analytical solution. We need to get a few starting values of the jump of the solution at the interface to compute the interface position using Adams's formula. Because we know the exact position of the interface, we will take these values to start the numerical implementation. Otherwise, one would compute those with a special start-up scheme.

n	6	11	21	41
interface error	1.717 d-5	1.118 d-6	6.945 d-8	4.345 d-9
liquid L ₂ error	3.382 d-6	2.153 d-7	1.319 d-8	8.067 d-10
solid L ₂ error	3.884 d-6	2.473 d-7	1.518 d-8	9.479 d-10
liquid max error	4.073 d-7	2.653 d-8	1.647 d-9	1.031 d-10
solid max error	5.105 d-7	3.325 d-8	2.065 d-9	1.292 d-10

Table AV.1 Table of errors at the time $t = 3.5$ for a fixed timestep $\tau = .00001$ and different meshsizes.

The analytical solution is

$$(AV.2a) \quad s(t) = 2 \lambda \sqrt{t},$$

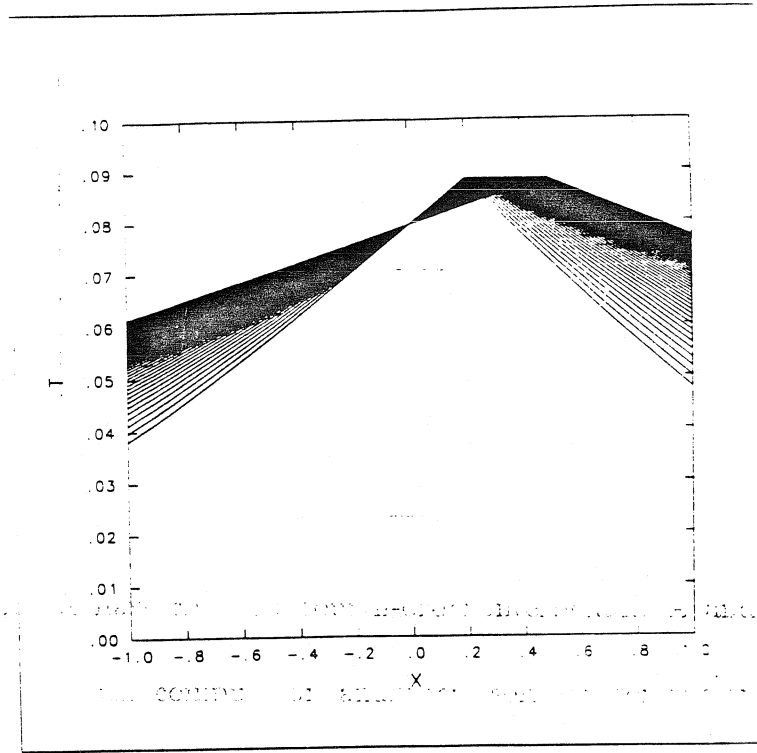


Figure AV.1 Solution of the equation for the solid and the liquid at the times $t = 1 + .1 n$, $n = 0, 1, \dots, 50$. The lowest curve corresponds to the initial condition.

$$(AV.2b) \quad u(x, t) = \frac{\sqrt{\pi}}{2} \lambda e^{\lambda^2} (1 + \operatorname{erf}(\lambda)) \operatorname{erfc}\left(\frac{x}{2\sqrt{t}}\right),$$

$$(AV.2c) \quad v(x, t) = \frac{\sqrt{\pi}}{2} \lambda e^{\lambda^2} \operatorname{erfc}(\lambda) \left(1 + \operatorname{erf}\left(\frac{x}{2\sqrt{t}}\right)\right),$$

with v defined on $(-\infty, s(t)] \times [0, \infty)$, u on $[s(t), \infty) \times [0, \infty)$, where λ is the solution of the algebraic relation

$$(AV.2d) \quad \Delta = \frac{\sqrt{\pi}}{2} \lambda e^{\lambda^2} \operatorname{erfc}(\lambda) (1 + \operatorname{erf}(\lambda)),$$

and erf and erfc are the error function and the complementary error function defined as

$$\operatorname{erfc}(z) = \frac{2}{\sqrt{\pi}} \int_z^\infty e^{-x^2} dx,$$

$$\operatorname{erf}(z) = 1 - \operatorname{erfc}(z) = \frac{2}{\sqrt{\pi}} \int_0^z e^{-x^2} dx.$$

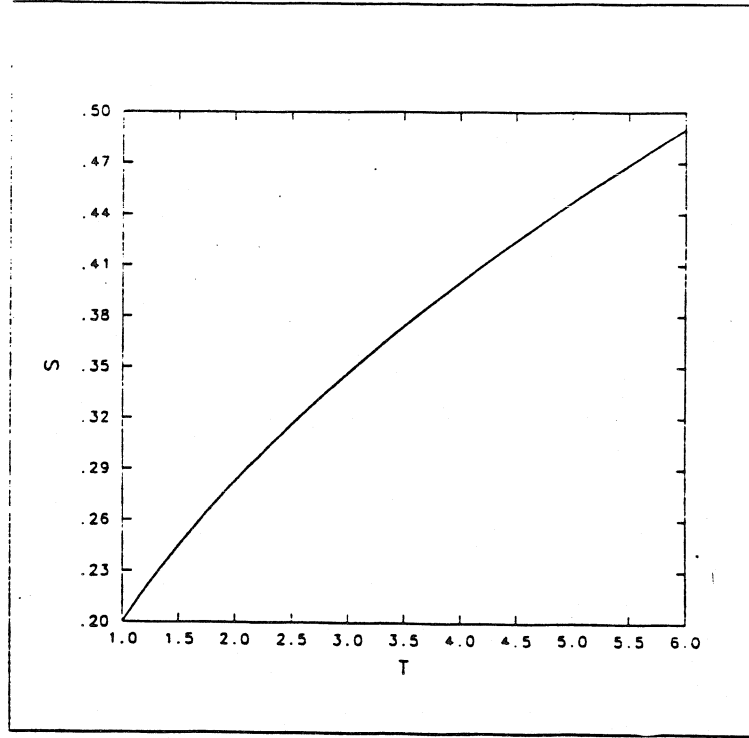


Figure AV.2 Position of the interface between the times $t = 1$ and $t = 6$.

We run the numerical test on the interval $[-1, 1]$, with initial and boundary conditions

$$(AV.3a) \quad y_j^0 = \frac{\sqrt{\pi}}{2} \lambda e^{\lambda^2} (1 + \operatorname{erf}(\lambda)) \operatorname{erfc}\left(\frac{s_0 + j \tilde{h}_1}{2}\right),$$

$$(AV.3b) \quad z_k^0 = \frac{\sqrt{\pi}}{2} \lambda e^{\lambda^2} \operatorname{erfc}(\lambda) \left(1 + \operatorname{erf}\left(\frac{-1 + k \tilde{h}_2}{2}\right)\right),$$

$$(AV.3c) \quad s_0 = 2 \lambda,$$

$$(AV.3d) \quad f_1(n \tau) = \frac{\sqrt{\pi}}{2} \lambda e^{\lambda^2} (1 + \operatorname{erf}(\lambda)) \operatorname{erfc}\left(\frac{1}{2 \sqrt{1 + n \tau}}\right),$$

$$(AV.3e) \quad f_2(n \tau) = \frac{\sqrt{\pi}}{2} \lambda e^{\lambda^2} \operatorname{erfc}(\lambda) \left(1 + \operatorname{erf}\left(\frac{-1}{2 \sqrt{1 + n \tau}}\right)\right),$$

with j taken between 0 and $J+1$ and k between 0 and $K+1$.

We have run the code for different values of τ , h_1 , and h_2 between the times $t = 1$ and $t = 6$, for a value of $\lambda = .1$. For the values of the parameters $\tau = 1.d - 5$,

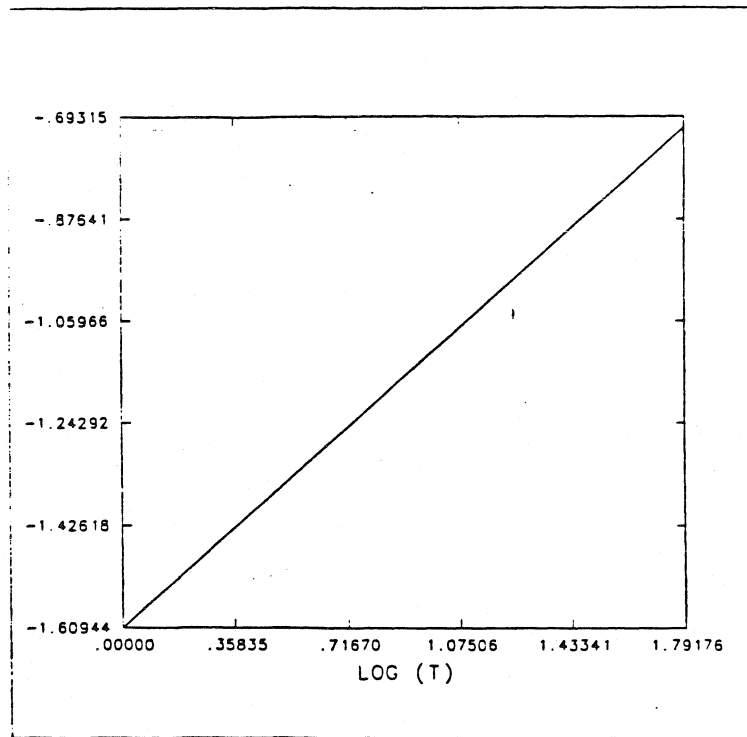


Figure AV.3 Log-Log plot of the position of the interface vs. time.

n_1/n_2	6/11	11/21	21/41
interface error	3.94	4.01	4.00
liquid L_2 error	3.97	4.03	4.03
solid L_2 error	3.97	4.03	4.00
liquid max error	3.94	4.01	4.00
solid max error	3.94	4.01	4.00

Table AV.2 Table of the exponents at the time $t = 3.5$ for a fixed timestep $\tau = .00001$ and different meshsizes.

$h_1 = .025$, and $h_2 = .025$, we have plotted in figure AV.1 the solution of the equation for both solid and liquid and in figure AV.2 the interface position for the time between $t = 1$ and $t = 6$.

We have also plotted in figure AV.3 the logarithm of the position of the interface versus the logarithm of the time. It will show the interface advance as $t^{\frac{1}{2}}$.

First we fix τ and vary the value of h_1 and h_2 . We get the information about the convergence rate of the spatial scheme, because for τ to be sufficiently small,

n	6	11	21	41
interface error	2.116 d-5	1.371 d-6	8.499 d-8	5.298 d-9
liquid L ₂ error	3.094 d-6	1.960 d-7	1.200 d-8	7.458 d-10
solid L ₂ error	3.515 d-6	2.234 d-7	1.363 d-8	8.450 d-10
liquid max error	3.834 d-7	2.483 d-8	1.540 d-9	9.599 d-11
solid max error	4.806 d-7	3.113 d-8	1.930 d-9	1.203 d-10

Table AV.3 Table of errors at the time $t = 6$ for a fixed timestep $\tau = .00001$ and different meshsizes.

n ₁ /n ₂	6/11	11/21	21/41
interface error	3.95	4.01	4.00
liquid L ₂ error	3.98	4.03	4.01
solid L ₂ error	3.98	4.03	4.01
liquid max error	3.95	4.01	4.00
solid max error	3.95	4.01	4.00

Table AV.4 Table of the exponents at the time $t = 6$ for a fixed timestep $\tau = .00001$ and different meshsizes.

τ	2.5 d-3	1.25 d-3	6.25 d-4	3.125 d-4
interface error	3.296 d-9	1.253 d-9	2.874 d-10	4.463 d-11
liquid L ₂ error	1.458 d-9	3.166 d-10	5.95 d-11	9.183 d-12
solid L ₂ error	9.544 d-9	2.447 d-10	6.793 d-11	2.576 d-11
liquid max error	5.941 d-10	2.972 d-11	6.819 d-12	1.059 d-12
solid max error	1.445 d-10	3.72 d-11	8.489 d-12	2.658 d-12

Table AV.5 Table of the errors at the time $t = 3.5$ for a fixed meshsize $h_1 = .005$ and $h_2 = .005$ and different timesteps.

the error due to the time discretization is much smaller than the spatial error.

At the time $t = 3.5$, with $\tau = 1.d - 5$ and $\lambda = .1$, for diverse values of n , with $J = K$ and $n = K + 2$, we have in table AV.1 the table of errors.

If we compare tables I.8.1 and AV.1, we notice that the errors in table I.8.1 are much smaller than the errors in table AV.1. Even if the iterative method is more costly than the direct one, it seems to be more accurate.

In table AV.2, we calculate from table AV.1 the order of the spatial scheme. If the scheme is of order k , we should find that the error behaves like $C h^k$, C a constant

τ_1/τ_2	2.5 d-3/1.25 d-3	1.25 d-3/6.25 d-4	6.25 d-4/3.25 d-4
interface error	1.40	2.12	2.69
liquid L_2 error	2.20	2.41	2.70
solid L_2 error	5.29	1.85	1.40
liquid max error	4.32	2.12	2.69
solid max error	1.96	2.13	1.68

Table AV.6 Table of the exponents at the time $t = 3.5$ for a fixed meshsize $h_1 = .005$ and $h_2 = .005$ and different timesteps.

τ	2.5 d-3	1.25 d-3	6.25 d-4	3.125 d-4
interface error	5.504 d-9	1.349 d-9	2.718 d-10	3.32 d-12
liquid L_2 error	8.23 d-10	1.835 d-10	2.7 d-11	2.023 d-11
solid L_2 error	8.831 d-10	2.198 d-10	5.703 d-11	1.937 d-11
liquid max error	1.333 d-10	2.443 d-11	4.926 d-12	2.097 d-12
solid max error	1.249 d-10	3.016 d-11	6.207 d-12	2.225 d-12

Table AV.7 Table of the errors at the time $t = 6$ for a fixed meshsize $h_1 = .005$ and $h_2 = .005$ and different timesteps.

τ_1/τ_2	2.5 d-3/1.25 d-3	1.25 d-3/6.25 d-4	6.25 d-4/3.25 d-4
interface error	2.03	2.31	6.36
liquid L_2 error	2.17	2.76	0.42
solid L_2 error	2.01	1.95	1.56
liquid max error	2.45	2.31	1.23
solid max error	2.05	2.28	1.48

Table AV.8 Table of the exponents at the time $t = 6$ for a fixed meshsize $h_1 = .005$ and $h_2 = .005$ and different timesteps.

depending on the data, h the meshsize. Because we are unable to evaluate C , we find the value of k by computing the ratio of two consecutive errors corresponding to the number of discretization points $n_1 - 1$ and $n_2 - 1$, taking its logarithm, then dividing it by the logarithm of $(n_1 - 1)/(n_2 - 1)$. This is a good approximation for k .

For the same values of λ , τ , h_1 , and h_2 , we have in table AV.3 the table of errors at $t = 6$.

At $t = 6$, we have in table AV.4 the spatial convergence rate.

So the spatial convergence rate is 4. The theory and the numerical experiment agree.

Then we fix h_1 and h_2 and vary τ . We get the information about the convergence of the temporal scheme, because for h_1 and h_2 sufficiently small, the error due to the space discretization is negligible compared to the temporal error. We choose again $\lambda = .1$ and fixes $K = J = 201$. We have in table AV.5 the table of errors at the time $t = 3.5$ and in table AV.6 the temporal convergence rate.

For the same values of λ , τ , h_1 , and h_2 , we have in table AV.7 the table of errors at $t = 6$ and in table AV.8 the temporal convergence rate.

So the temporal convergence rate is 2, even though for the ratio $6.25 \text{ d-4} / 3.125 \text{ d-4}$, the values are lower than 2. An explanation for this discrepancy may be that the error for $\tau = 3.125 \text{ d-4}$ is already small and in this case the spatial error may no longer be much smaller than the temporal error. So the theory and the numerical experiments agree.

REFERENCES

- [1] E. Ben-Jacob, N. D. Goldenfeld, J. S. Langer, and G. Schon *Dynamics of Interfacial Pattern Formation*. Phys. Rev. Lett. 51, pp 3161-3174 1983.
- [2] E. Ben-Jacob, N. D. Goldenfeld, J. S. Langer, and G. Schon *Boundary-Layer Model of Pattern Formation in Solidification*. Phys. Rev. A 29 pp 330-340 1984.
- [3] R. Bonnerot and P. Jamet *A Second Order Finite Element Method for the One Dimensional Stefan Problem*. International Journal for Numerical Methods in Engineering 8, pp 811-820 1974.
- [4] R. Brower, D. Kessler, J. Koplik, and H. Levine *Geometrical Approach to Moving-Interface Dynamics*. Phys. Rev. Lett. 51, pp 1111-1114 1983.
- [5] R. Brower, D. Kessler, J. Koplik, and H. Levine *Geometrical Models of Interface Evolution*. Phys. Rev. A 29, pp 1335-1342 1984.
- [6] J. Douglas and T. M. Gallie *On the Numerical Integration of a Parabolic Equation Subject to a Moving Boundary Condition*. Duke Math. J. 22, pp 557-571 1955.
- [7] G. W. Evans *A Note on the Existence of a Solution to a Problem of Stefan*. Quart. Appl. Math. 9, pp 185-193 1951.
- [8] A. Fasano and M. Primicerio *General Free Boundary Problems for the Heat Equation I*. J. Math. Anal. Appl. 57, pp 694-723, 1977.
- [9] A. Fasano and M. Primicerio *General Free Boundary Problems for the Heat Equation II*. J. Math. Anal. Appl. 58, pp 202-231 1977.
- [10] A. Fasano and M. Primicerio *General Free Boundary Problems for the Heat Equation III*. J. Math. Anal. Appl. 59 pp 1-14 1977.
- [11] A. Fasano and M. Primicerio *New Results on Some Classical Parabolic Free*

Boundary Problems. Quart. Appl. Math. 38, pp 439-460 1980/1981.

- [12] A. Fasano and M. Primicerio *Classical Solutions of General Two Phase Parabolic Free Boundary Problems in One Dimension. Free Boundary Problems: Theory and Applications Vol. II, Res. Notes in Math.* 79, pp 644-657 1983.
- [13] A. Friedman *Partial Differential Equations of Parabolic Type.* Englewood Cliffs, N.J., Prentice Hall 1964.
- [14] M. E. Glicksman and R. J. Schaefer *Comments on Theoretical Analysis of Isenthalpic Solidification. J. Crystal Growth* 2, pp 239-242 1968.
- [15] S. D. Howinson *Fingering in Hele-Shaw Cells. J. Fluid. Mech.* 167, pp 439-453 1986.
- [16] D. Kessler, J. Koplik, and H. Levine *Geometrical Models of Interface Evolution-II. Numerical Simulations. Phys. Rev. A* 30, pp 3161-3174 1984.
- [17] D. Kessler, J. Koplik, and H. Levine *Geometrical Models of Interface Evolution-III. Theory of Dendritic Growth. Phys. Rev. A* 31, pp 1712-1717 1985.
- [18] H.-O. Kreiss *Difference Approximations for Boundary and Eigenvalue Problems for Ordinary Differential Equations. Mathematics of Computation* 26, pp 605-624 1972.
- [19] H.-O. Kreiss and J. Lorenz *Initial Boundary Value Problems and the Navier Stokes Equations.* Academic Press 1989.
- [20] M. Kruskal and H. Segur *Aeronautical Res. Associates of Princeton Technical Memo*, 85-25.
- [21] J. S. Langer and H. Müller-Krumbhaar *Theory of Dendritic Growth-I. Elements of a Stability Analysis. Acta Metall.* 26, pp 1681-1687 1978.
- [22] J. S. Langer and H. Müller-Krumbhaar *Theory of Dendritic Growth-II. Instabilities in the Limit of Vanishing Surface Tension. Acta Metall.* 26,

pp 1689-1695 1978.

- [23] J. S. Langer *Existence of Needle Crystal in Local Models of Solidification*. Phys. Rev. A 33, pp 435-441 1986.
- [24] J. T. Lin *The Numerical Analysis of a Phase Field Model in Moving Boundary Problems*. SIAM J. Numer. Ana. 25, pp 1015-1031 1988.
- [25] J. Lorenz *Numerical Solution of Partial Differential and Integral Equations*. California Institute of Technology, Course Lecture Notes 1987.
- [26] A. Lorenzi and E. Paparoni *A Continuous Dependence Result for a Parabolic Free Boundary Problem*. Bollettino Un. Mat. Ital. 4-B, pp 191-210 1985.
- [27] H. Müller-Krumbhaar and J. S. Langer *Theory of Dendritic Growth-III. Effects of Surface Tension*. Acta Metall. 26, pp 1697-1708 1978.
- [28] G. E. Nash and M. E. Glicksman *Capillarity-Limited Steady-State Dendritic Growth-I. Theoretical Development*. Acta Metall. 22, pp 1283-1290 1974.
- [29] G. E. Nash and M. E. Glicksman *Capillarity-Limited Steady-State Dendritic Growth-II. Numerical Results*. Acta Metall. 22, pp 1291 -1299 1974.
- [30] A. T. Patera *A Finite Element / Green's Function Embedding Technique Applied to One Dimensional Change of Phase Heat Transfer*. Numerical Heat Transfer 7, pp 241-247 1984.
- [31] P. Pelcé *Dynamics of Curved Fronts*. Perspectives in Physics. Academic Press 1988.
- [32] M. H. Protter and H. F. Weinberger *Maximum Principles in Differential Equations*. Second Edition, Springer-Verlag, New York 1984.
- [33] R. D. Richtmyer and K. W. Morton *Difference Methods for Initial Value Problems*. Second edition, Tracts in Mathematics 4, Interscience 1957.
- [34] R. F. Sekerka, R. G. Seidensticker, D. R. Hamilton, and J. D. Harrison *Investigation of Desalination by Freezing*. Westinghouse Research Lab Re-

port, chapter 3 1967.

- [35] B. I. Shraiman and D. Bensimon *Singularities in Non Local Interface Dynamics*. Phys. Rev. A 30, pp 2840-2842 1984.
- [36] G. Strang *Accurate Partial Difference Methods I: Linear Cauchy Problems*. Arch. Rat. Mech. Anal. 12, pp 392-402 1963.
- [37] G. Strang *Accurate Partial Difference Methods II Non-Linear Problems*. Numerische Mathematik 6, pp 37-46 1964.
- [38] R. Trivedi *Growth of Dendritic Needles from a Supercooled Melt*. Acta Metall. 18, pp 287-296 1970.